COMMUNICATIONS

COMMUNICATIONS

Dear Readers,

The current issue of the Communications - Scientific Letters of the University of Zilina is dedicated to the presentation of results of the research activities of the Faculty of Civil Engineering of the University of Zilina.

It represents an overview of research activities and outputs in productive areas of individual departments which follow the preferred areas as defined in the long-term intention of the Faculty orientation until 2020. These key areas are as follows:

- *theoretical problems of planning, design, building, rehabilitation and restoration of transport infrastructure, including the environmental impacts of transport and its security;*
- *experimental analysis and theoretical problems of diagnostics of engineering structures, transport and land-based buildings and historical and architectural monuments, experimental analysis of building materials and theoretical problems of the determination of residual life assessment of transport and land-based buildings;*
- *development of methods of experimental and numerical analysis, mathematical modeling and dynamic simulation of the theory of evaluation and creation of engineering structures, buildings and land transport;*
- *decision-making processes, strategies for rehabilitations of engineering, transport and construction buildings, maintenance and optimization methods in the management of individual parts of the traffic road;*
- *energy-efficient, environmentally appropriate and building-physical (energy performance, acoustics, aerodynamics, hydrodynamics) proper design of the envelope structures with regard to the sustainable development of society;*
- *geoinformatics systems for design and road restorations, traffic analysis, structure and architecture of intelligent transport systems.*

Apart from contributions of domestic and foreign authors, we have given the opportunity to present the original results of the research activities of our partner faculties with which the Faculty maintains the long-term cooperation.

It is an honor for me to have been able to prepare this issue of the journal. I would like to thank not only the domestic but especially foreign authors who contributed with their publications.

I would like to appeal not only to the readers from the fields of civil engineering and related disciplines, but to provoke their interest in possible cooperation with the Faculty of Civil Engineering of the University of Zilina.

Pavol Durica

Martin Moravcik - Peter Kotes - Miroslav Brodnan - Patrik Kotula *

SOME EXPERIENCE FROM THE ANALYSIS OF EXISTING 40 YEARS OLD PRESTRESSED BRIDGES IN THE NORTH OF SLOVAKIA

The paper deals with the analysis of the chosen short-span bridges from precast prestressed concrete girders. The analysis has been performed at the Department of Structures and Bridges recently. Part of the current technical condition assessment of these structures comprised the load carrying capacity and remaining life time determined by calculation [1, 2 and 3]. The load carrying capacity was calculated in compliance with the previous Slovak standards and new European standards.

Keywords: *Diagnostic, inspections, bridge, prestressed concrete, load carrying capacity, rehabilitation.*

1. Introduction

In cooperation with the Slovak Road Administration, Investment and Construction Management of Roads (Zilina), diagnostic works were conducted on several existing precast prestressed bridges. In this paper, we pay attention to some characteristic features of those structures, e.g., to multi-element beam structures [4, 5 and 6]. The first bridge, No. 018-293 - see Fig. 1, is located on I/18 road and leads over the railway line, rural roads and the nameless creek near the town of Martin. The next one, No. 059-091 - see Fig. 2, is located on E77 road and crosses the river Orava. The third observed bridge, No. 065-086 - see Fig. 3, was built near the village Mosovce on I/65 main road, over the regional road. All the investigated bridges are around 40-50 years old. The main tasks were the assessment of current technical conditions and determination of load carrying capacity influenced by degradation factors due to environmental loading [7, 8 and 9]. On the base of the results gathered from assessment, we made decision in the form of a conceptual design with the aim to eliminate detected deteriorations, to improve the current conditions of the bridges and to increase the load carrying capacity and the serviceability of those bridges.

Fig. 1 The view of bridge No. 018-293 near the town of Martin on I/18 road

Based on the diagnostics and calculation of the current load carrying capacity of the mentioned bridges, it was decided to launch the project of their rehabilitation and structural strengthening.

Fig. 2 The view of bridge No. 059-091 in Nizna over the river Orava

Fig. 3 The view of bridge No. 065-086 near the village Mosovce

* **Martin Moravcik, Peter Kotes, Miroslav Brodnan, Patrik Kotula**
Department of Structures and Bridges, Faculty of Civil Engineering, University of Zilina, Slovakia
E-mail: martin.moravcik@fstav.uniza.sk

2. The description of bridges

The first bridge, No. 018-293, was built in 1964. That bridge crosses the nameless creek, railway line from Vrutky to Martin and two rural roads. The traffic on the railway line is currently not so heavy. Carriageway width on the bridge is 16.335 m with the both sides gadroon 2 x 0.5 m. The bridge consists of 4 simple spans, of post-tensioned concrete girders type of VLOSSAK of 14.40 m. The spans are 2x12.51 + 2x12.91 m. The total length of the bridge is 55.90 m. Vlossak type beams are 0.98 meters wide, the construction height is 0.70 m. The beams are made from the concrete C45/55 (B 600) and post-tensioned by the tendons from the smooth wires f 4.5 mm. The caps and 7 pieces of columns in cross-section were made as precast elements. They have a variable cross-section which changes along the longitudinal direction downward from 1.40 m to 0.90 m near the ground. The column width is constant - 0.25 m. At the time when the bridge was designed, such solutions with non-dilatation contact joints over the internal supports were not common.

The second bridge, No. 059-091, was built in 1957 on the site of a previous steel bridge with the lower deck, suspended on two parabolic curves of the range of 2x35 m. It was destroyed during World War II. The substructure, two abutments and one pier remained preserved. A wooden temporary bridge was built on the site of the original bridge. In the center of the original spans wooden barges were built. The newly built 4-span bridge had a range of one span from 16 to 17 m. The bridge was not insulated against water, which adversely affected the superstructure. Currently, the superstructure in cross-section consists of 10 post-tensioned atypical precast girders of „T“ shape. In the longitudinal section, beams act as 4 simple separate spans, each with a range of 17.175 m and a beam length of 17.875 m with spacing over a support from 20 to 40 mm. The total projected length of the superstructure is 71.64 m. In the longitudinal direction, the beams are not connected. Five cross beams act in the transverse direction. The joints between the beams with a width of about 50 mm are embedded in cement mortar. The superstructure was prestressed by the cross prestressing tendons from the 9 wires of f 4.5 mm. The tendons were placed in the top flange of the beam and in the bottom of the transverse beams.

The third mentioned bridge, No. 065-086, was built in 1972 near the village Mosovce. It is a one span bridge crossing the regional road with 16.0 m long span. The superstructure in cross-section consists of 12 post-tensioned precast girders of the type KA-61 of a box shape with the total length of 15.0 m. The transverse structural behavior acts as a “curtain” slab. The KA-61 girder has a construction width of 0.98 m and height of 0.70 m. The girder was prestressed by 6 tendons from 12 wires of f 4.5 mm and 2 tendons from 6 wires of f 4.5 mm. The tendons are placed at the bottom slab and webs parts of the beam. The girders are made from the concrete C35/45 (B 500).

3. The current technical conditions of bridges

Failures, which have been observed on bridge 018-293, result both from the state of knowledge about bridge building accessible at the time when the bridge was built and also from insufficient maintenance at present. Outer girders, connection joints between the girders and over-supporting parts of the beams are the mostly damaged parts of the superstructure. On outer girders we can see uncovered, exposed, corroded tendons with some ruptured wires. Similar situation can be seen also in Figs. 4 and 5. Loss of cement mortar can be seen mainly in the peripheral connection joints and in over-supporting areas as a result of water leakage through these joints. Precast girders carry all typical features of the first prestressed concrete bridges built in Slovakia. The areas and the edges are rough and broken, the visible surfaces are marked with water leaking through the carriageway and insulation on the superstructure.

Fig. 4 The partial rupture of wires of the prestressing tendon - bridge No. 059-091

Fig. 5 The partial rupture of wires of the prestressing tendon - bridge No. 065-086

The precast superstructure of bridge No. 059-091 carries all the signs of such bridges from the 1st generation of prestressed structures in Slovakia. Consequences of water leakage through the carriageway and insulation can be seen on the superstructure. Anchored areas of the superstructure cross prestressing, particularly in over-supporting sections carry the signs of failures

due to leakage as, for example, removed concrete cover, and corroded anchors. However, the structural system realized in this way is still relatively solid. The girders in the longitudinal direction have still sufficient pressure reserve, which is noticeable in the overhanding. There are some major defects due to technical difficulties connected with cross prestressing and separate spans without linking the neighboring spans by a composite slab.

One of the main deficiencies of the precast superstructure of bridge No. 065-086 from the KA-61 girders is a box shape of the designed girder. The closed shape of the girder cross-section causes the wet environment inside the girder, which affects the rapid reinforcement corrosion. That effect can be seen on many bridges constructed from the KA-61 girders.

4. The results of the diagnostic works

It was found out that the strength of concrete on bridge No. 018-293 corresponds to concrete class C25/30 according to [10], or to concrete class B 330 according to the previous Slovak standard. Strength of concrete was tested in a non-destructive way with the Schmidt hammer type L. Content of chloride ions, especially in the concrete cover, was determined by the tests of RCT instrument. The carbonation depth was determined by a simple indication method by spreading the concrete with phenolphthalein. On the exposed areas of reinforcement incurred by the fall of the concrete cover, the corrosion of prestressed reinforcement was found leading to the rupture of some wires.

On the basis of inspections, the bridge classification according to [11] was replaced by [12] as follows: - The bridge top cover condition: V. = bad, the substructure condition: IV. = satisfactory, the superstructure condition: VI. = very bad, complex bridge condition: V. = bad.

It was found out that the strength of concrete of the precast beams on bridge No. 059-091 was C30/37 (B 400), which corresponds to the designed value. Content of chloride ions Cl-/mc was above the critical value (Fig. 6). The carbonation depth was lower than the concrete cover (Fig. 7). Technical condition

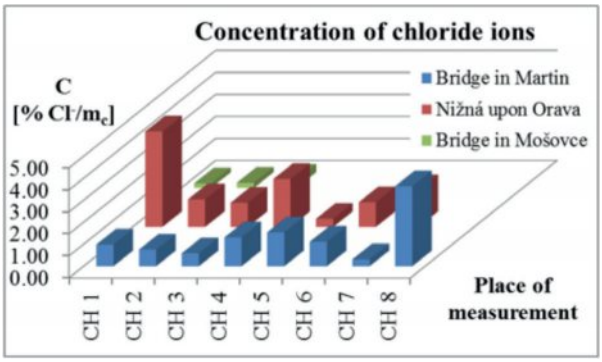

Fig. 6 The concentration of chloride ions- overview

of the bridge, according to [11 and 12] and by visual inspection, can be evaluated as follows:

- The bridge top cover condition: IV. = satisfactory - V. = bad, the substructure condition: V. = bad, the superstructure condition: III. = good - IV. satisfactory, complex bridge condition: V. = bad.

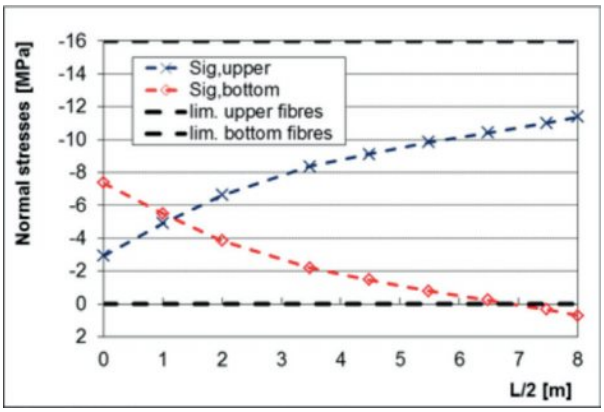

Fig. 7 The carbonation depth - overview

The load carrying capacity showed the following results: Vn = 20 tons (62,5% of required standard value), Vr = 34 tons, (42,5% of required standard value) Ve = 77 tons (39,3% of required standard value), which indicates the insufficient structural capacity. (Vn is the normal load carrying capacity, Vr is the exclusive load carrying capacity and Ve is the exceptional load carrying capacity).

It was found out that the strength of concrete of the precast beams on bridge No. 065-086 was C35/45 (B 500), which corresponds to the designed value similarly as with the above mentioned bridges. Content of chloride ions Cl-/mc exceeds the critical value of content of chloride ions Cl- (Fig. 6). The carbonation depth did not reach the value of the concrete cover

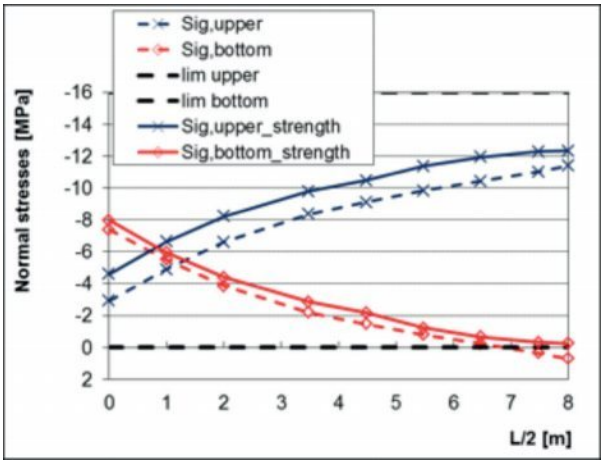

Fig. 8 The normal stresses course along the half span of bridge No. 065-086

(Fig. 7). Technical condition of the bridge, according to [11 and 12] and by visual inspection, can be evaluated as follows:

- The bridge top cover condition: V. = bad, the substructure condition: IV. = satisfactory, the superstructure condition: V. = bad, complex bridge condition: V. = bad. The load carrying capacity calculation showed the following results: Vn = 25 tons, Vr = 59 tons, Ve = 183 tons, which again indicates the insufficient structural capacity, see Fig. 8.

5. Conception design of the bridges rehabilitation

In the case of bridge No. 018-293 it is expected that the reconstruction work will be done with traffic moved over one lane of the bridge. Due to corrosion and subsequent rupture of prestressing tendons of outer girders it was proposed to remove them and replace them with new ones. Increasing the load carrying capacity should be achieved also by new composite slab concreting. The corroded caps have to be strengthened also in several possible ways, for example, by additional prestressing, or by other new reinforcement on the metallic or non-metallic base (FRP materials).

To determine the response of the bearing capacity of bridge No. 059-091, superstructure of the numerical model was used, taking into account the way of creating the connection of additionally prestressed precast beams „T“ in the transverse direction. From the diagnostic survey, it was found that in some places the grout between the beams was broken, and, therefore, there may be rotation of the beam; cross prestress in the model can thus be considered semi-solid.

Despite the high age of the bridge and history of the Orava river bridged in this place, it was recommended to repair this bridge in order to increase its lifetime, and, at the same time, to maintain such capacity which corresponds to the current trends in designing new bridges. We suggest to repair the bridge superstructure by new external prestressing and new composite concrete slab.

In the case of bridge No. 065-086, the numerical model of the “curtain” slab was taken into account. The combination of the strengthening method was used due to the insufficient load carrying capacity. At first, all existing deteriorated elements will be removed from the top of the bridge. The new external prestressing (2 Monostrand tendons on 1 girder) was designed. Then new 150 mm depth of the composite slab concreting on the top of the girders is assumed to be applied. That kind of the structural invasion completely changes behavior of the superstructure from a “curtain” slab to the solid orthotropic slab (Fig. 9). The superstructure being strengthened, similar repair work will be conducted as in the above mentioned cases.

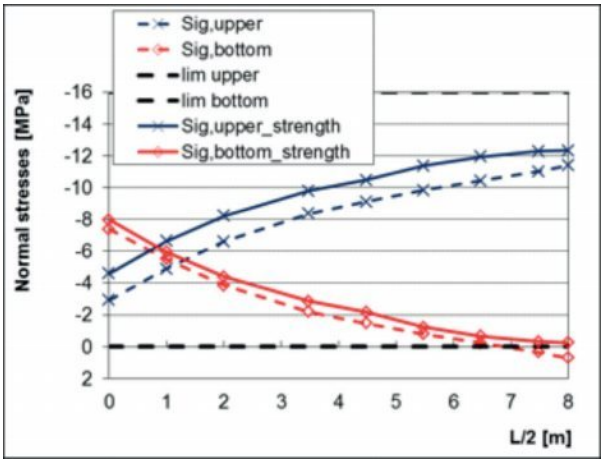

Fig. 9 The course of normal stresses along the half span on strengthened structure of bridge No. 065-086

6. Conclusions

Diagnostics and the load carrying capacity calculations showed that the chosen inspected prestressed concrete bridges built in Slovakia are generally in bad technical conditions after 40 - 50 years of service. It is mostly due to the improper conceptual design at that time and insufficient knowledge about structural behavior, construction detailing and building technology. Another reason of poor technical conditions of the bridges is their insufficient maintenance. But these bridges can be repaired using the modern methods and materials to the level which is required by the current European standards and regulations. The new composite slab concreting, external prestressing or adhesive FRP material base application are examples some methods frequently used for the strengthening of prestressed bridge structures.

This is demonstrated by the example of bridge No. 065-086 where repair work has been successfully done recently. Composite slab concreting and the external prestressing combination method were used for the structural strengthening, as shown in Fig. 10.

Fig. 10 Bridge No. 065-086 after strengthening by external prestressing

Acknowledgement

The research work presented in this paper has been supported by the Slovak Grant Agency VEGA No. 1/0517/12 and supported by the European regional development fund and Slovak state budget by the project "Research centre of University of Zilina", ITMS 26220220183.

References

[1] VICAN, J., GOCAL, J., MELIS, B., KOTES, P., KOTULA, P.: Real Behaviour and Remaining Lifetime of Bridge Structures. *Communications - Scientific Letters of the University of Zilina*, vol. 2, 2008, 30-37. ISSN 1335-4205.

[2] HALVONIK, J., BORZOVIC, V., DOLNAK, J.: *Experience with Design of Prestressed Concrete Bridges According to Eurocode.* Design of concrete structures using EN 1992-1-1: First Inter. Workshop, September 2010. Prague: Czech Technical University, 61-71. ISBN 978-80-01-04581-7.

[3] MORAVCIK, M., BUJNAKOVA, P.: New Precast Bridge Girder with Combined Prestressing. *Communications - Scientific Letters of University of Zilina*, vol. 13, No. 3, 2011, 19-23, ISSN 1335-4205.

[4] KOTES, P., VICAN, J.: Multi-element System Reliability using Markov Chain Model. *Communications - Scientific Letters of the University of Zilina*, vol. 3, 2004, 17-21. ISSN 1335-4205.

[5] BUJNAK, J., ODROBINAK, J.: Behaviour of Steel-concrete Composite Girder. *Communications - Scientific Letters of the University of Zilina*, vol. 5, No. 3, 2003, 48-49. ISSN 1335-4205.

[6] BUJNAK, J., HLINKA, R., ODROBINAK, J., VICAN, J.: Diagnostics and Evaluation of Footbridges. *Procedia Engineering*, vol. 40, 2012, 56-61. ISSN 1877-7058. On-line: http://ac.els-cdn.com/S1877705812024411/1-s2.0-S1877705812024411-main.pdf?_tid= c643ad4e-3482-11e2-8278-00000aab0f26&acdnat=1353574885_b8932ef08b99b234bfc 77d9dbedb0393

[7] KOTES, P., VICAN, J., SLAVIK, J.: Influence of Reinforcement Corrosion on Reliability of Existing Concrete Structures. *Communications - Scientific Letters of the University of Zilina,* vol. 4, 2001, 41-49. ISSN 1335-4205.

[8] VICAN, J., KOTES, P., SLAVIK, J.: Effect of Degradation Factors on Existing Bridge Reliability. *Communications - Scientific Letters of the University of Zilina*, vol. 3, 2003, 62-63.

[9] GAJDOSOVA, K.: *Stress and Crack Width Control According to EN 1992.* Proc. of intern. workshop Design of concrete structures using Eurocodes, September, 2012. Technische Universitat: Wien, 2012, ISBN 978-3-902749-03-1, 199-202.

[10] STN EN 206-1 Concrete, Part 1: *Specification, Performance, Production and Conformity,* SUTN Bratislava, 2002.

[11] TP 04/2008: *Load Carrying Capacity of Bridges on Expressways, Highways, Roads of 1st, 2nd, and 3rd Category and Local Roads + Annexes A, B (in Slovak).* SSC Bratislava, 2008.

[12] Guidance USM 1/2012: *Load Carrying Capacity of Bridges (in Slovak).* SSC Bratislava, 2012.

Libor Izvolt - Janka Sestakova - Michal Smalo - Zuzana Gocalova *

MONITORING OF THE TRACK GEOMETRY QUALITY AROUND THE PORTALS OF NEW TUNNEL CONSTRUCTION TURECKY VRCH - PRELIMINARY RESULTS

At the beginning, the contribution deals with the characteristics of conventional structure (track skeleton placed in the ballast) and unconventional structure (slab track) of railway superstructure. The trial section is characterized in the next part where measurements of relative track geometry are made at regular intervals (spring and autumn) using continuous measuring device (manual measuring trolley KRAB™ - Light). There is made the analysis of measurements made between 2012 - 2013 at the end of the contribution; with a view to assessing the quality of track geometry during particular sections monitored with in-built conventional and unconventional structure of railway superstructure. It also includes transition areas between these structures and an analysis of possible causes of variations in track geometry of modernized railway sections monitored.

Keywords: *Railway track, conventional railway superstructure, slab track, track geometry, diagnostics.*

1. Introduction

Considering the railway operation, a standard structure of railway superstructure has been proven for many decades which is historically also known to be capable of ensuring a relatively long period of operational capacity of the railway line. From a structural point of view, such a railway track with the standard structure of railway superstructure is referred to as a railway track whose track skeleton is stored in railway ballast. In the case of high line tonnage and axle load, increasing track speeds which are associated with the high quality requirements for track geometry, it appears that such a structure has its operational (in terms of guaranteeing the long-term safety and reliability of the track) and economical (in terms of the cost of track maintenance) limits. Standard structure of railway superstructure is characterized by "floating" placement of track skeleton, which causes the growth of dynamic horizontal and vertical forces during each passage of a rail vehicle or a train. They may and usually cause gradual degradation of track geometry which subsequently leads to restless driving of rail vehicles. The elimination of irregularities in track geometry – the quality of the track - forces the operator in a period of time to remove irregularities of track diagnosed by time and costly maintenance works. This phenomenon grows with increasing track speed and thus increases the cost of maintaining and share of track possessions, which reduce the attractiveness of the track for a passenger. It is sufficient, however, if only the weakest structural element of the standard railway superstructure is replaced in railway track, and the track ballast is another, more appropriate structural element which shows no plastic behaviour. Such replacement is a structure in which the track skeleton is concreted (monolithic structure) or placed on a concrete or asphalt substructure (layered structure), thus the design of railway track which is referred to as unconventional superstructure. Currently, thus conceived railway track is referred to as a slab track in which the required flexibility of the railway superstructure system for the wheel/rail is ensured using the flexible structural elements, disposed between the rail and the sleeper and/or under the sleeper.

The term slab track, as defined in [1], refers to such a structure of railway superstructure in which a spread function of railway ballast is replaced by reinforced materials, and which is placed on a concrete or asphalt substructure (slab). The structure of slab track proved to be practical and preferred structural system of railway superstructure in many railway reports, which has led to its spread practically all over the world. The essential reason for building the structure of slab track is the fact that its construction gives high stability of the track which is associated with a smooth movement of vehicles and at the same time with driving comfort for the passenger and the operator with significantly lower maintenance requirements and thus the possessions and finance. This high driving comfort can be obtained, in the case of the application of standard structure of railway superstructure, only with the connection with very high operating costs.

In general, the structure of slab track currently applies mainly to high-speed lines and lines that have high line tonnage where the cost of maintaining the track with the standard structure

* **Libor Izvolt, Janka Sestakova, Michal Smalo, Zuzana Gocalova**
Department of Railway Engineering and Track Management, Faculty of Civil Engineering, University of Zilina, Slovakia,
E-mail: libor.izvolt@fstav.uniza.sk

of railway superstructure grows strongly. At the same time, however, this structure also promotes in the upgraded sections of the standard tracks (track speed up to 160 km.h^{-1}), or tracks for higher speeds (track speed of 160 km.h^{-1} < V ≤ 200 km.h^{-1}) and, in particular, to the tunnel clearance gauge, as there are required properties of the subgrade which do not show settlement of foundation. Furthermore, the use of the slab track structure has a positive impact on the size of the investment costs of tunnel realization, due to the smaller tunnel clearance gauge, in the case of new tunnels, or excluding economically demanding reconstruction of tunnel, in the case of its electrification on the existing tracks. The structures of slab track and bridges offer the application of subgrade without the settlement of foundation, and therefore, the application of this structure is also possible in these track sections.

In connection with the modernization of the trans-European corridor V. Venezia - Trieste / Koper - Ljubljana - Budapest - Chop - Lvov; with a branch Va, passing through the territory of the Slovak Republic in the section of Bratislava - Zilina - Kosice - Cierna nad Tisou - Chop was, under the construction of Railways of the Slovak Republic (ZSR). Modernization of railway track Nove Mesto nad Vahom - Puchov, in track section Nove Mesto nad Vahom - Trencianske Bohuslavice, designed by the construction contractor (REMING Consult, a. s.) and the purchaser (DG Slovak Railways - DG SR) and approved the structure of slab track type RHEDA 2000®. After analyzing alternative solutions of routings around Turecky vrch in the current track of railway line and a new route - tunnel variant – the purchaser decided for the tunnel variant. It is considered that the change of routing of a railway line through the tunnel will increase the current track speed while minimizing adverse impacts on the protected landscape area where the track is led through. Another advantage of the tunnel variant in the decision making process of routing was that the construction of a tunnel did not restrict railway traffic because the tunnel was pierced outside the axes of original track.

In the view of the fact that in the case of necessary maintenance, or future repair and reconstruction works, the implementation of these works in the tunnel is complex. Moreover, due to the reduction of the amount of rock mined from the tunnel profile, which did not have further use, the structure of slab track, which has a lower structural thickness as in the case of using a standard structure of railway superstructure, was the appropriate solution.

2. Characteristics of the test section with the unconventional structure of railway superstructure

Modernization of above track section started in September 2009 and ended in May 2013, while the operation started in October 2012. The railway tunnel Turecky vrch, which is part of the track section, is the first tunnel in Slovakia designed and implemented according to the technical specifications for interoperability for conventional lines. It is convenient to the latest trends in tunnel and railway construction and should become a model for all future tunnels which will be built in Slovakia in terms of the modernization of railway lines. Double-track railway tunnel Turecky vrch is designed to structure gauge UIC C with the track-centre distance 4 200 mm. The total length of the tunnel is 1 775 m, while the tunnel tube of the section excavated has the length of 1 738.5 m and thereon pierced sections of the south portal length of 25 m and northern portal length of 10 m. There is a single cross-section of double-track tunnel with a radius of tunnel tube of 6.1 m throughout the entire length of the tunnel, including portal sections; there are only two chambers in the middle of the tunnel for tensioning mechanism spring for the overhead lines with advanced cross-section. Double-track in the tunnel is designed for the speed of 200 km.h^{-1} with the reverse curves of the radii 2 000 m.

The structure of the slab track was designed, as already mentioned, due to the reduction in the slope area and also due to the durability and fixation of the track geometry and its minimum maintenance in the operation. The structure of the ST of the RHEDA 2000® system applied passes through the different types of subgrade. It starts before the south portal and passes through entire tunnel. Then, the structure of the slab track continues on the bridges and earthworks behind the north portal. The structure of the slab track itself also includes transition areas on both ends which ensure a smooth transition (smooth change of stiffness) from the rigid structure of the slab track o the flexible standard structure of railway superstructure. The total length of the slab track structure is 2 280.145 m (it begins in new km 102.459 825 and ends in new km 104.740 000), while its particular parts: transition area - 45.175 m, tunnel 1 775.000 m, bridges - 34.770 m and earthwork - 425.200 m.

It is clear from the previous text that the structure of the slab track of RHEDA 2000® system applied is not structurally the same on the modernized track section due to differences in the stiffness of the subgrade (tunnel bottom, bridge and railway substructure of earthwork), but is modified, which is reflected in the thickness of the concrete structure and also its reinforcements. The structure of the slab track is divided into 3 basic structural types in the track section in question as follows [2] and [3]:

1. In the tunnel - Figs. 1 and 2: monolithic reinforced concrete slab of variable thickness (according to track superelevation) – concrete class C 35/45 with two-block sleepers B355.3 W60M concreted, lying on the concrete bottom of the tunnel tube.
2. On the earthworks - Figs. 3 and 4: monolithic reinforced concrete slab of constant thickness 240 mm - concrete class C 35/45 with two-block sleepers B355.3 W60M concreted (marked as TCL), lying on a monolithic slab of plain concrete class C 12/15 of constant thickness of 300 mm (marked as

HBL). Track superelevation in curves is made up of sloping plain of sub-ballast surface.

3. On the bridges - Figs. 5 and 6: monolithic reinforced concrete slab of variable thickness (according to track superelevation) – concrete class C 35/45 with two-block sleepers concreted, lying on the separating layer Styrodur + foil on the structure of the bridge.

Fig. 1 View of the slab track structure in the tunnel Turecky vrch

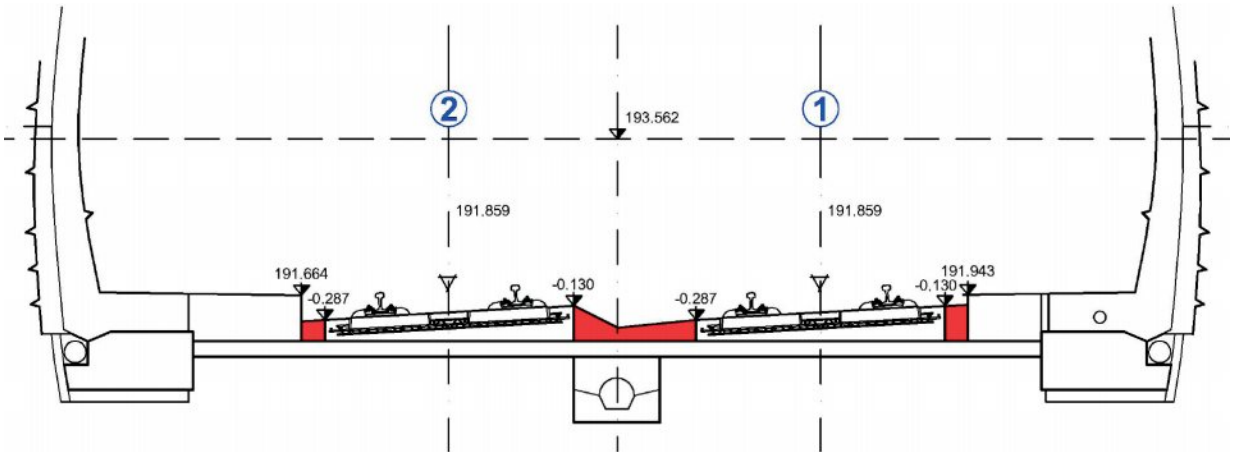

Fig. 2 The structural design of the slab track in the tunnel (concrete filling - marked in red)

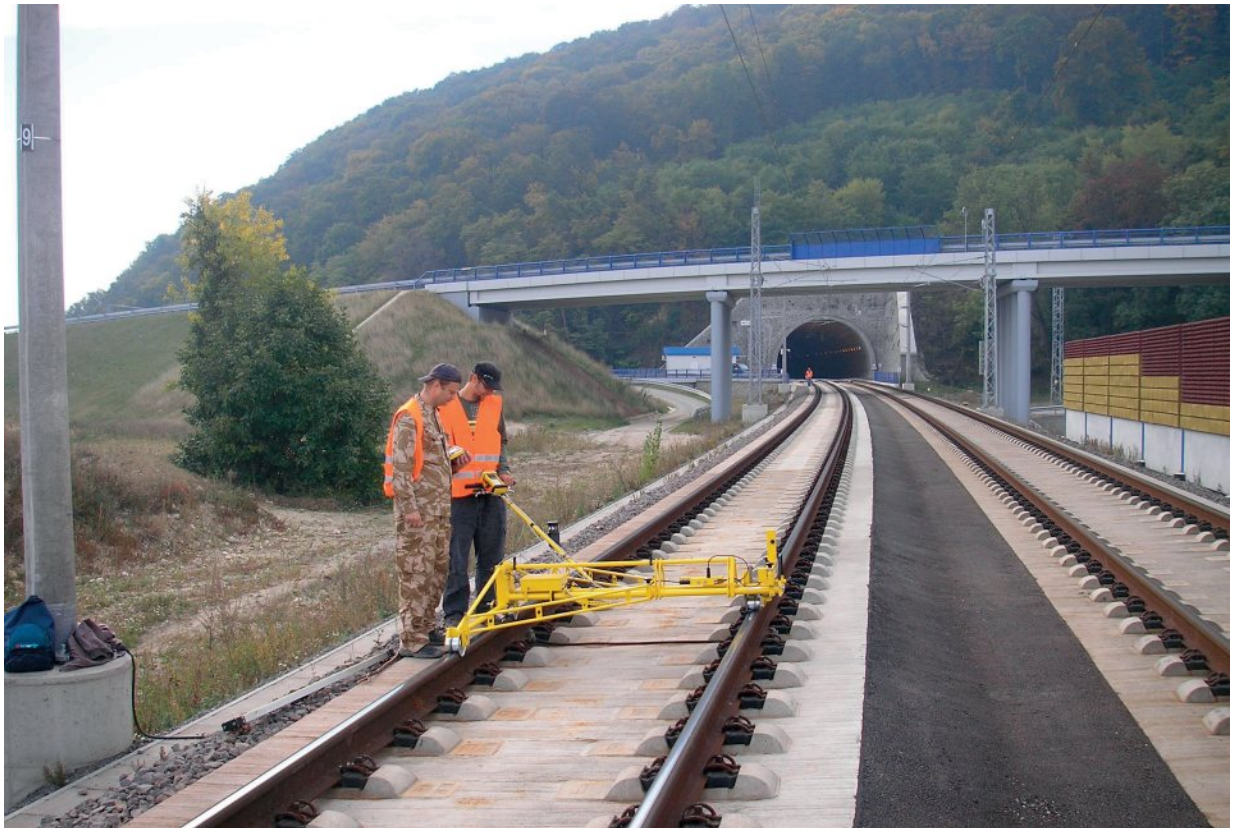

Fig. 3 View of the slab track structure in the area of earthwork (diagnostics of the alignment of track of the track using the KRAB™- Light device)

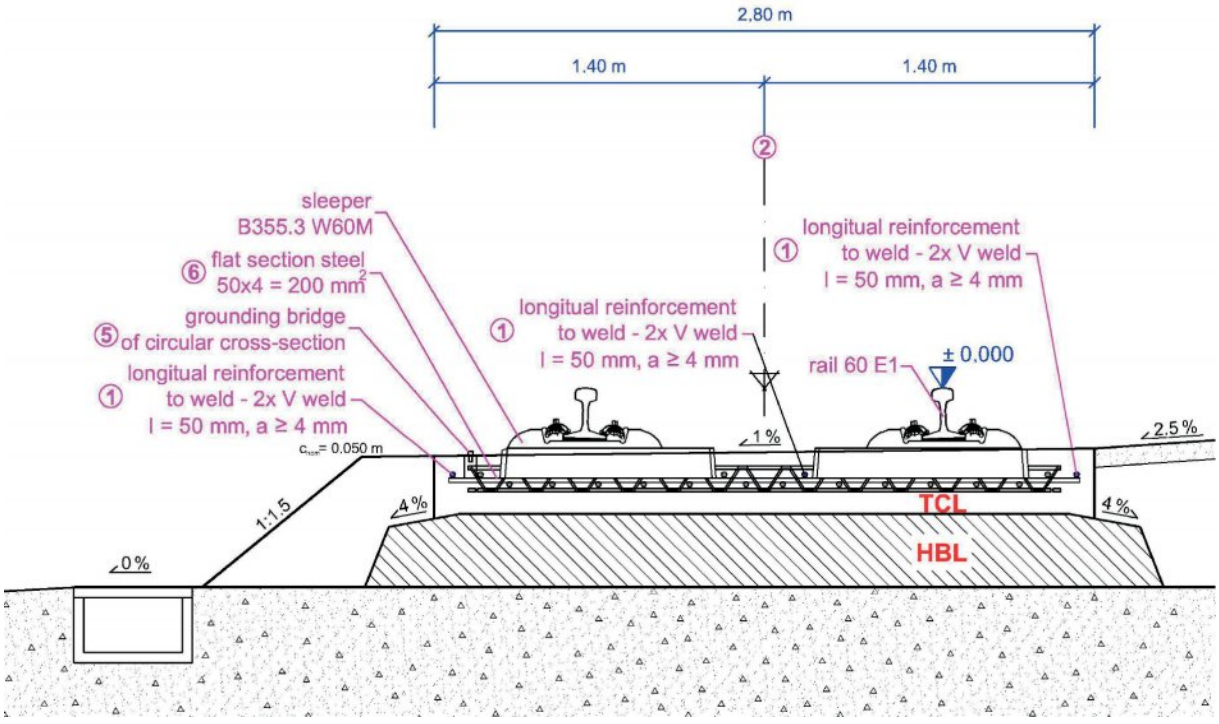

Fig. 4 Cross-section of the slab track structure placed on earthwork

Fig. 5 View of the slab track structure of the railway bridge (diagnostics of actual and relative position of the track realized)

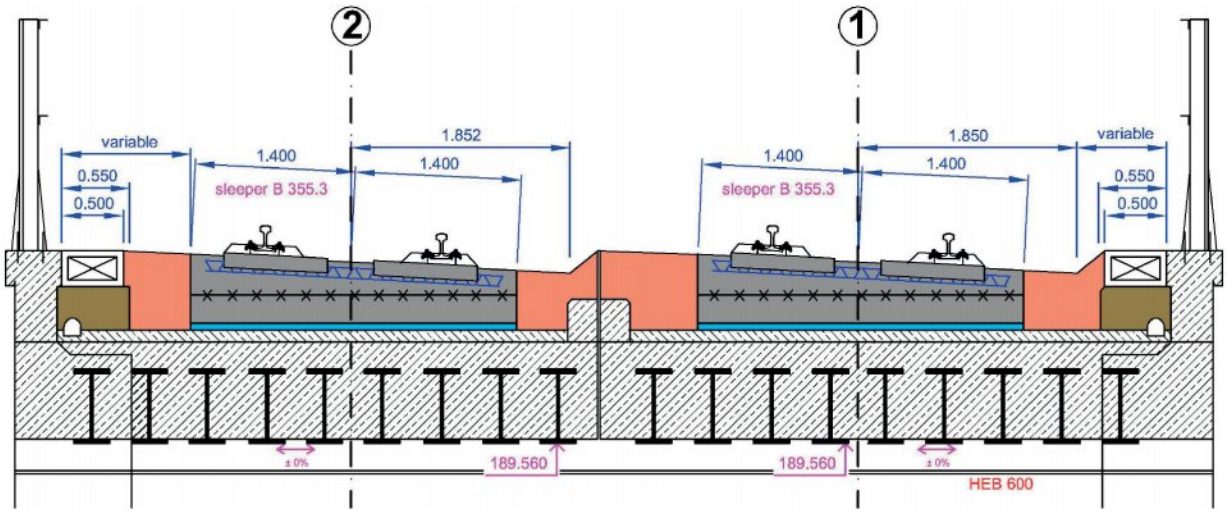

Fig. 6 Cross-section of the slab track structure placed on bridges

The critical point of the slab track structure is its completion and transition to the standard structure of railway superstructure – Figs. 7 and 8. In terms of dynamic effects, this is a place with the change of stiffness and, hence, this place was given special attention. The concrete bed of the length of 20 m was designed and implemented. It was lined with anti-vibration rubber mats of thickness 25 mm stuck on its bottom and sides and then filled with railway ballast material with track skeleton stored identical as in the adjacent track section with the standard structure of railway superstructure.

Fig. 7 View of the transition area built between the structure of the slab track and track section with standard structure of railway superstructure (left in the area of south portal and right in the area of north portal)

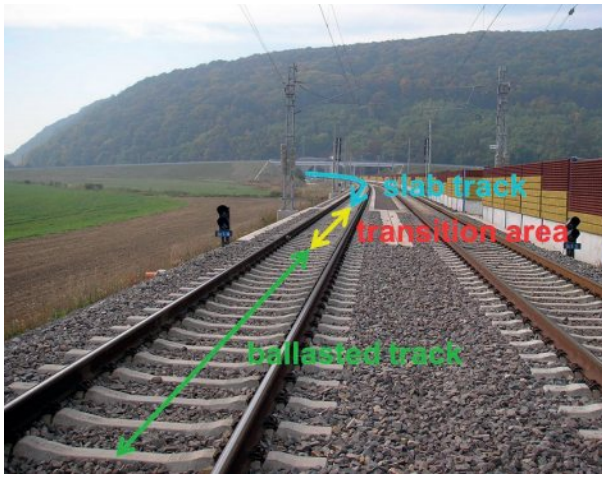

Fig. 8 View of the transition area built between the structure of the slab track and the standard structure of railway superstructure

With regard to the required quality characteristics and service life declared, the structure of the slab track is monitored at regular intervals in the area of both portals, transition sections and adjacent track sections with standard structure of railway superstructure for the purposes of DG ZSR within the scientific and research project from the time of delivering the modernized track section into operation. Input measurements were always made just before putting the tracks into operation (in period 10.07. – 11.07.2012 track No. 2 and 02.10. – 04.10.2012 track No. 1) and they resided, as any other measurements, in the implementation of a comprehensive continuous diagnostics of relative track geometry using manual measuring trolley KRAB™ – Light and also the diagnostics of gauge and elevation in each fastening node using a portable gauge-measurer ROBEL and geodetic positioning of geometric track position, its longitudinal profile as well as the position of the underneath surface of the sleeper – the slab track structures. After these input measurements, there are subsequently carried out operating measurements in the six-month period (every spring and autumn of that year). The monitoring is realized by the Department of Railway Engineering and Track Management in cooperation with the Department of Geodesy of the Faculty of Civil Engineering of the University of Zilina, and in cooperation with the manager of the railway infrastructure – Railways of the Slovak Republic and its Research and Development Institute of Railways (VVUZ) – Figs. 3 and 5. The monitoring on both portals of the tunnel Turecky vrch is focused on a comprehensive diagnostics of the relative and absolute geometric parameters of the track of the slab track in the tunnel (length of 100 m) behind the portal, in the area of transition section of the structure and in the area with the standard structure of railway superstructure (length of 100 m). The track section is monitored in south portal from new km 102.360 to new km 102.535 (length of 175 m) and in the area of south portal from new km 104.200 to new km 104.840 (length of 640 m) in total length of 815 m. The monitoring is planned during the guarantee period for construction works (up to 2016) where it is expected that the relevance of the implementation of the slab track is shown in this track section modernized and, at the same time, the above mentioned advantages of the operation of the structural system of railway superstructure are confirmed in terms of the Railways of the Slovak Republic as well.

4. Preliminary results of the monitoring of track geometry quality - a comprehensive diagnostics of the relative track geometry

In this paper, only the diagnostics results of relative track geometry are presented also in relation to the previously realized diagnostics of structural layers built, which are part of the slab track subgrade, or subgrade structure and which was implemented in the inspection of the quality of the track section built between

2011 and 2012. Diagnostics of relative track geometry of the track section built was implemented three times so far and immediately before putting line tracks into operation in 2012 and then in the spring and, of 2013 [4] and [5]:

1. In track No. 1, section No. 1 (new km 102.360 000 – new km 102.535 000) and section No. 2 (new km 104.200 000 – new km 104.840 000) 03.10.2012 (measurement before putting sections into operation /MSO/), 09.04.2013 (first operational measurement /PO1/) and 08.10.2013 (second operational measurement /PO2/).
2. In track No. 2, section No. 1 and section No. 2 10.07.2012 (MSO), 22.04.2013 (PO1) and 22.10.2013 (PO2).

The sections diagnosed are part of the train section of the railway station Nove Mesto nad Vahom - Railway station. In 2012, the working load was of 7.4435 million tons which corresponds to 4th category of track (source: ZSR).

Within the diagnostics of relative track geometry realized continuously using measuring device (measuring trolley KRAB™ – Light), the following parameters are detected on the base of primarily measured values [6]:

1. Track gauge RK (mm).
2. Change of gauge ZR (mm / m).
3. Track superelevation PK (mm).
4. Track twist, rated above the respective base ZK (mm / m).

Quality of section 1 in track No. 1 — Table 1

Stationing (new km)	Railway superstructure	Directional conditions	MSO (03.10.2012)				PO1 (09.04.2013)				PO2 (08.10.2013)			
			Local errors	MQ	NQ	NQ_{max}	Local errors	MQ	NQ	NQ_{max}	Local errors	MQ	NQ	NQ_{max}
102.360 000	SSRS		9				0				0			
102.460 500	Transition area	Straight section	0	1.15	1.55		0	1.66	2.12		0	1.19	2.10	
102.480 500	Slab track		0			2.3	0			3.6	0			3.6
102.487 250		Transition curve and curve						2.87	1.59			2.19	1.18	
102.535 000														

Quality of section No. 2 in track No. 1 — Table 2

Stationing (new km)	Railway superstructure	Directional conditions	MSO (03.10.2012)				PO1 (09.04.2013)				PO2 (08.10.2013)			
			Local errors	MQ	NQ	NQ_{max}	Local errors	MQ	NQ	NQ_{max}	Local errors	MQ	NQ	NQ_{max}
104.200 000	Slab track	Transition curve and curve	0	0.65	1.21	2.3	0	2.16	1.07	3.6	0	2.23	1.04	3.6
104.716 000														
104.720 000	Transition area	Straight section	0				0	0.75	1.24		0	0.93	1.50	
104.740 000	SSRS		1				0				0			
104.840 000														

5. Longitudinal vertical position of left and right rail VL, VR (mm).
6. Directional position of left and right rail SL, SR (mm).

As already mentioned, first activities were made before putting line tracks No. 1 and No. 2 into operation in 2012 within diagnostics of above characterized track section. The effect of subsequent repair activities (rail grinding, track lining and levelling), implemented under maintenance operations of railway infrastructure manager between the measurements in 2012 and 2013, was not taken into account in the evaluation of relative track geometry, as the working site performing monitoring was not provided with these results of activities.

The development of track geometry (hereinafter referred to as RK) of the monitored sections of southern and northern portal of the tunnel Turecky vrch is shown in Table 1 to Table 4. In the detection of maintenance limits, the quality of the straight section or section in transition curve and curve is specifically evaluated in accordance with [7]. Local errors of the parameters measured are calculated separately for sections with the standard structure of railway superstructure (SSRS), for transition areas and sections with the slab track structure.

The overall superevaluation of test sections (so called "section evaluation") is, in accordance with [1], given by the quality number of the section evaluated (QN), and quality mark (QM) of SP parameters (SL), RK, PK and VR (VL).

The evaluation of section by the number of quality, calculated according to the equation:

$$QN = \sqrt{0,57.SDV_{RK}^2 + 1,6.SDV_{SP,SL}^2 + 1,6.SDV_{PK}^2 + 1,6.SDV_{VP,VL}^2} \quad (1)$$

Quality of section No. 1 in track No. 2 — Table 3

Stationing (new km)	Railway superstructure	Directional conditions	MSO (10.07.2012)				PO1 (22.04.2013)				PO2 (22.10.2013)			
			Local errors	MQ	NQ	NQ_{max}	Local errors	MQ	NQ	NQ_{max}	Local errors	MQ	NQ	NQ_{max}
102.360 000	SSRS		10				0				0			
102.460 500	Transition area	Straight section	1	0.92	1.38		0	1.05	1.53		0	0.81	1.55	
102.480 500	Slab track		0			2.3	0			3.6	0			3.6
102,487 250		Transition curve and curve						2.30	1.29			2.93	1.51	
102.535 000														

Quality of section No. 2 in track No. 2 — Table 4

Stationing (new km)	Railway superstructure	Directional conditions	MSO (10.07.2012)				PO1 (22.04.2013)				PO2 (22.10.2013)			
			Local errors	MQ	NQ	NQ_{max}	Local errors	MQ	NQ	NQ_{max}	Local errors	MQ	NQ	NQ_{max}
104.200 000	Slab track	Transition curve and curve	2				0	2.35	1.19		0	2.35	1.14	
104.716 000				0.71	1.31	2.3				3.6				3.6
104.720 000	Transition area	Straight section	0				0	0.90	1.38		0	0.70	1.46	
104.740 000	SSRS		6				0				0			
104.840 000														

where:

SDV_{RK} - Standard deviation of variable of track gauge,

$SDV_{SP, SL}$ - Standard deviation of variable of direction of the track,

SDV_{PK} - Standard deviation of variable of track superelevation,

$SDV_{VP, VL}$ - Standard deviation of variable of longitudinal track height.

where $SDV = \sqrt{\frac{1}{n-1}\sum_{i=1}^{n} x_i^2}$ (mm) (2)

expresses irregular course of track geometry parameter in the section evaluated where:

n - number of points measured after 0.25 m,

i - marking measuring point,

x_i - dynamic component of the relevant quantity of track geometry (deviation from the center line in the wavelength range 1 m to 25 m).

The evaluation of section according to quality marks shall be carried out according to the equation:

$$QM = \frac{\ln \frac{SDV}{b}}{m} \quad (3)$$

where b and m are numerical constants determined on the basis of the SDV statistics of relevant parameter and speed zone.

The results of quality section evaluation of track according to quality marks are indicative and additional on the railway tracks of the Slovak Republic and are not binding for the evaluation of TG state. Measures, which are set for individual intervals of quality marks, can provide only recommendations:

a) where $0 < QM \leq 2$, state of track geometry is satisfactory in section evaluated,
b) where $2 < QM \leq 3$, it is recommended to design the repair of track geometry in the section evaluated into maintenance work plan,
c) where $3 < QM < 4$, it is recommended to perform the repair of track geometry in the section evaluated to the nearest control,
d) where $4 \leq QM \leq 6$, it is recommended to perform immediate measures in the section evaluated to ensure the safety of operation [1].

5. Comparison of gauge and elevation measurements before putting test section into operation, the first operational measurement and the second operational measurement

The difference of values of gauge deviations found in PO1 and MSO is in the range from 1.27 mm in track No. 2, section No. 1 to -0.74 mm in track No. 1, section No. 2. The difference of values of gauge deviations in PO2 and MSO is in the range from 1.67 mm in track No. 2, section No. 2 to -2.57 mm in track No. 2, section No. 2. The difference of values of gauge deviations in PO2 and PO1 ranges (excluding the section No. 2 in track No. 2) at an average range of about 0.3 mm. There are higher values in all three subsections of section No. 2 of track No. 2: in the section of the structure with the slab track, in the transition area and the section with the standard structure of railway superstructure. The values are in the range from 0.92 mm in track No. 2, section No. 2 to - 3.05 mm in track No. 2, section No. 2.

The difference of values of track elevation found in PO1 and MSO is in the range from 3.36 mm in track No. 1, section No. 2 to -5.27 mm in track No. 2, section No. 2. The difference of values of track elevation found in PO2 and MSO is in the range of 4.35 mm in track No. 2, section No. 2 to -5.19 mm in track No. 1, section No. 1. The difference of values of track elevation measured in PO2 and PO1 ranges at an average range of about 1 mm. Higher values of differences of track elevation occur in all three subsections of the sections: in the section of the structure of slab track, in the transition area as well as the section with the standard structure of railway superstructure. Values are in the range from 3.51 mm in track No. 2, section No. 2 to -1.50 mm in track No. 1, section No. 1.

The ranges of differences of gauge deviation values ΔRK and deviations of track elevation PK are shown in Table 5.

6. Analysis of the possible causes of deviations in track geometric parameters of the track

Static load tests (SLTs) were implemented at the level of subgrade and on the surface of individual structural layers of the track in the sections of the railway track built between 2011 and 2012. Continuous testing of the structural parts in question using SLT has achieved that there have been immediately obtained an overview of the quality of the incorporation of individual rock materials (determining the degree of compaction) and deformation resistance reached in the level of structural layer tested expressed by static module of deformation $E_{s,i}$.

Static load tests were carried out in (Fig. 9) [4] and [5]:

1. Subgrade.
2. Surface of frost-resistant protective layer (in the case of sections with slab track and their adjacent transition section) or sub-ballast layer (in the case of track sections with the standard structure of railway superstructure).
3. Surface layer of railway ballast in the structural thickness of pre-tipped ballast (about the level of loading area of sleepers) in the transition sections and track sections with the standard structure of railway superstructure.

On the basis of comprehensive diagnostics of the relative track geometry it is possible to identify some trends in the growth of deviations in places where the desired values of compaction degrees or deformation resistance were not reached, whose origin may resulted just in the deficiencies in the structure of railway substructure [7].

Differences of values ΔRK and PK measured within MSO, PO1 and PO2 Table 5

Track/section	ΔRK value (mm)						PK value (mm)					
	PO1 – MSO		PO2 – PO1		PO2 – MSO		PO1 – MSO		PO2 – PO1		PO2 – MSO	
	max.	min.	max.	min.	max.	min.	max.	min.	max.	min.	max.	min.
Track No. 1/ section 1	0.72	-0.52	0.17	-0.61	0.63	-0.62	0.22	-4.89	1.92	-1.50	0.85	-5.19
Track No. 1/ section 2	1.27	-0.74	0.11	-0.32	1.06	-0.92	3.36	-4.27	2.12	-0.73	3.97	-3.14
Track No. 2/ section 1	0.67	-0.63	0.02	-0.45	0.44	-0.70	1.20	-4.42	2.61	-0.77	1.76	-3.22
Track No. 2/ section 2	0.95	-0.55	0.92	-3.05	1.67	-2.57	2.96	-5.27	3.51	-1.25	4.35	-4.63

Fig. 9 Implementation of the static loading test in the northern portal (left on the surface of frost-resistant protective layer in the area of slab track, right on the surface of the railway ballast in the area with standard structure of railway superstructure)

The places of origin of negative trends in the values of the track geometry on the basis of the deficiencies in the structure of railway subgrade are shown in Table 6. The places where the desired value of the deformation module was not achieved, or quality of consolidation are marked in red, the parameter values of track geometry which show a negative trend, and it is appropriate to monitor them closely are marked in blue).

It is clear from Table 6 that in some places in which the required value of the static module of changes $E_{s,i}$ or consolidation quality E_{def2}/E_{def1} has not been reached, parameters of track geometry show a negative trend, therefore, it is possible to predict that the worsening trend of parameter deviations of track geometry may have originated in the deficiencies in the deformation resistance or consolidation of the structural layers of slab track, or subgrade structure when operating.

Directional and vertical routing of a railway line does not have a demonstrable impact on the negative tendencies in the deviations of the parameters of track geometry. The parameter values have also been monitored in other places that could be problematic (culverts, slab joints of the slab track structure, transition area wedges), but no clear errors in the track geometry apply to these places.

Complex diagnostics of relative track geometry shows similar deviations as in the sections with the standard structure of railway superstructure and the sections with the slab track structure as well. Significant deviations are not yet recorded in the transition areas between the conventional and unconventional structure of railway superstructure.

7. Conclusions

An essential precondition for the competitiveness of rail transport is the reliable operation of the railway lines, considering the technological understanding, it means a safer and more stable movement of vehicles along the track – rail. The development and validation of a number of technical solutions of slab track in the longer term can ensure the quality of the track geometry parameters, reduce maintenance costs, extend the service life of structure and increase the competitiveness and attractiveness of railway lines. The issue of modernization of the railway infrastructure, which is still very current, is an ideal opportunity to further application of progressive systems and elements of the structure of railway lines, among which the structure of slab track undoubtedly belongs to.

The results of continuous diagnostics of relative track geometry do not show local errors of parameters during operation in any of the diagnosed sections. The total numbers of quality

Analysis of the causes of deviations in RK parameters

Table 6

Stationing (new km)	Structural part	Railway superstructure	Track No.	Value of stat. module of transform. $E_{s,i}$ (MPa)	Degree of consolidation E_{def2}/E_{def1}	Track gauge (PO2)	Track superelevation (PO2)	Track gauge (MSO)	Track superelevation (MSO)	Track superelevation (designed)
Area of southern portal										
102.365	Subgrade	SSRS	2	225.0	4.33	1.84	**-1.43**	1.95	**-0.71**	0
102.375	Subgrade	SSRS	1	250.0	3.50	1.07	**-1.82**	1.09	**0.94**	0
	Earthworks	SSRS		75.0	3.60					
	Railway ballast	SSRS		93.8	3.30					
102.425	Subgrade	SSRS	1	173.1	3.00	1.70	**-2.01**	1.31	**0.49**	0
102.465	Railway ballast	Transition area	1	22.0	1.67	1.10	**-2.24**	0.81	**0.86**	0
Area of northern portal										
104.325	Subgrade	Slab track	1	140.6	2.86	-0.20	**85.15**	-0.12	**83.49**	84
104.335	Subgrade	Slab track	2	132.4	3.29	1.77	**84.67**	1.53	**83.69**	84
104.560	Earthworks	Slab track	2	132.4	3.43	**0.54**	**83.76**	**-0.37**	**82.44**	84
104.585	Earthworks	Bridge wedge	2	102.3	2.50	**0.60**	**84.63**	**-0.03**	**81.19**	82.91
104.600	Earthworks	Bridge wedge	1	375.0	2.33	0.13	**72.95**	0.32	**73.57**	72.31
104.645	Subgrade	Slab track	2	75.0	2.53	1.07	**46.17**	0.71	**43.91**	45.43
104.675	Earthworks	Slab track	1	125.0	2.63	-0.54	**27.27**	-0.20	**25.83**	25.56
104.710	Earthworks	Slab track	2	93.8	2.20	0.91	**6.36**	0.76	**3.58**	0
104.735	Railway ballast	Transition area	2	12.7	1.54	1.00	**-2.48**	0.65	**-1.06**	0
104.810	Railway ballast	SSRS	1	72.6	2.79	0.05	**1.64**	0.08	**1.15**	0

(QN) in diagnosed sections have even slightly improved within the second operating measurement in the four of the eight subsections as opposed to the first operating measurement (maximum improvement is from 1.59 to 1.18) and they slightly deteriorated in the other four partial sections (max. from 1.24 to 1.50).

On the basis of experimental measurements made so far, it is possible to expect that further development of the monitoring of RK in experimental section of the modernized track in the

area of tunnel Turecky vrch confirms the relevance of the application of slab track to the tracks which are standard, not only on the tracks for higher or high speeds. The application on these tracks represents the real benefit and basic precondition for the long-term safe, reliable, and in terms of maintenance cost, economically advantageous track structure.

Acknowledgements

There are partial results of the grant VEGA 1/0597/14 "Analysis of methods used to measure the unconventional railway track construction from the point of view of accuracy and reliability" in the paper.

References

[1] ZSR SR 103-8 (S) *General Requirements for the Design, Construction, Repair, Maintenance and Acceptance of Construction Repair and Maintenance Works on the Slab Track Construction (in Slovak)*, GR ZSR, 2012

[2] IZVOLT, L., SESTAKOVA, J., VILIMEK, P.: *The First Construction of Unconventional Type of Railway Superstructure in the ZSR Infrastructure.* Proc. of 6th intern. conference Concrete and Concrete Structures, Terchova: Vratna dolina, October 2013, 166-175, Procedia Engineering 65 (2013), Elsevier, 1877 - 7058

[3] IZVOLT, L., IZVOLTOVA, J., SESTAKOVA, J.: *Influence of Construction of Railway Super-structure on Railway Quality.* Proc. of the 6th intern. scientific conference on Dynamics of Civil Engineering and Transport Structures and Wind Engineering - DYN-WIND´2014, May 2014, Donovaly, ISBN 978-80-554-0844-6, p. 63-74

[4] IZVOLT, L. et al.: *Monitoring of Sections of Non-conventional Constructions of the Railway Superstructure and the Transition Areas - 3rd Stage. ZSR Modernization of Railway Track Nove Mesto nad Vahom - Puchov, km 100.500 to 159.100, part 24-32-01 Nove Mesto - Trencianske Bohuslavice (in Slovak)*, Zilina : KZSTH : SvF: University of Zilina, 06/2013

[5] IZVOLT, L. et al.: *Monitoring of Sections of Non-conventional Constructions of the Railway Superstructure and the Transition Areas - 4th Stage. ZSR Modernization of Railway Track Nove Mesto nad Vahom - Puchov, km 100.500 to 159.100, part 24-32-01 Nove Mesto - Trencianske Bohuslavice (in Slovak),* Zilina : KZSTH : SvF : University of Zilina, 03/2014

[6] ZSR SR 103-7 (S) *Measurement and Evaluation of Track Geometry by Measuring Trolley KRAB (in Slovak)*, GR ZSR, 2008.

[7] IZVOLTOVA, J., PISCA, P., KOTKA, V., MANCOVIC, M.: 3D Laser Scanning of Railway Line, *Communications - Scientific Letters of the University of Zilina*, vol. 15, No. 4, 2013, 80-84, ISSN 1335-4205.

Ljiljana M. Brajovic - Miodrag Malovic - Zdenka Popovic - Luka Lazarevic *

WIRELESS SYSTEM FOR SLEEPER VIBRATIONS MEASUREMENT

This paper describes testing of a wireless technique for measuring the actual sleeper vibrations and determination of their dynamic deflection based on the experimentally acquired acceleration data. Practical measurements of sleeper vibrations and calculation of displacements (deflections) along the track provide insight into the actual condition of layers below sleepers. The main goal was to develop the equipment for structural health monitoring as a basis for the track maintenance management.

Keywords: *Railways, track geometry deterioration, vibrations, wireless sensor network.*

1. Introduction

The track stiffness is a composite value that represents stiffnesses of different materials involved in layers below running rails which support the wheels of vehicles moving along the track. It is defined by combination of stiffnesses of all layers and components of railway superstructure and substructure as follows: rails, resilient pads in the track structure, sleepers, ballast, sub-ballast and subgrade. It represents the proportion between vertical load and elastic rail deflection (z) at a given moment. Track stiffness has long-term influence on track geometry deterioration, deterioration of all components, rail fatigue, noise and vibrations. Low track stiffness causes large rail displacements and large bending moments. As rail displacements increase, growing number of sleepers shares the load, leading to lower forces being exercised on the sleepers. Too low value of track stiffness causes large track settlement, with considerable stress increase in the rails, whereas high global track stiffness leads to small displacement and small bending moments. Thus, fewer sleepers share the load and forces on each sleeper are higher. In addition, dynamic train/track interaction forces are relatively high and can accelerate the process of track deterioration. Therefore, it is important to determine the optimum track stiffness during track design. Apart from determining the optimum global track stiffness, it is necessary to determine optimum stiffness of every single superstructure and substructure element and to adjust them accordingly.

It is important to emphasize that global stiffness of the track changes along a track during its life cycle. Relationship between the load and the deflection is nonlinear due to nonlinearity of stiffness of rail pads and subgrade, as well as the effect of voids beneath sleepers. This means that the track usually gets stiffer with increased loading. Therefore, measurement and analysis of actual values of the vertical track stiffness is of great importance.

The paper presents a wireless system for measurements of actual sleeper vibrations and determination of their dynamic deflection and train speed. This measurement system was developed at the Faculty of Civil Engineering in Belgrade. The goal was to develop the equipment for structural health monitoring as a basis for the track maintenance management.

2. Characteristics of measuring spot and measuring system

Measurement was conducted on the railway near thermal power plant “Nikola Tesla” in Obrenovac. This railway serves for coal transport from the surface coalmine “Kolubara” (Fig. 1). Coal transport is delegated to the special railway company “Railway transport TENT”. The main purpose of rail transport system is coal transport from surface mine to power plants in Obrenovac and Veliki Crljeni. Railway Obrenovac-Vreoci has 100 km of track and it transports about 100.000 tonnes of coal per day. It means that this railway handles largest volume of freight in Serbia, and it is one of the busiest railways in Europe. Average traffic on this railway is 60 trains per day (empty and loaded). So far, it has transported more than 800 mil. tonnes of coal (over 25 mil. tonnes per year), and large amounts of other freight, such as the equipment, spare parts, consumable materials, etc. The measurement was conducted during passage of several loaded and empty trains. EDF double hopper wagons (Fig. 1) are used

* [1]Ljiljana M. Brajovic, [1]Miodrag Malovic, [2]Zdenka Popovic, [2]Luka Lazarevic
[1]Department of Mathematics, Physics and Descriptive Geometry, Faculty of Civil Engineering, University of Belgrade, Republic of Serbia
[2]Department of Roads, Airports and Railways, Faculty of Civil Engineering, University of Belgrade, Republic of Serbia
E-mail: ljbrajovic126@gmail.com

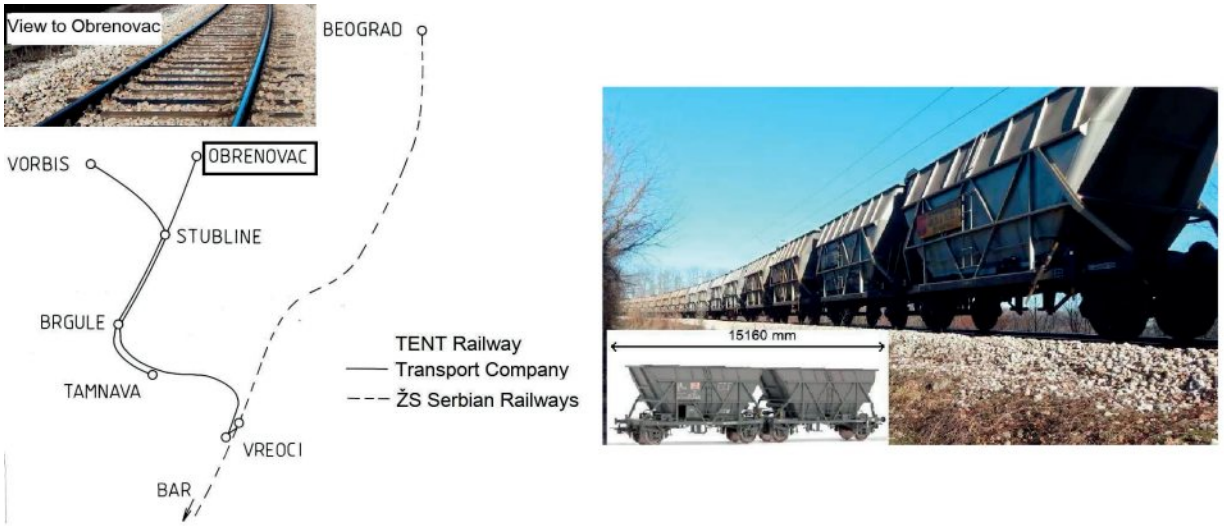

Fig. 1 Rail network Obrenovac-Vreoci and double hopper wagons

for coal transport. Each wagon consists of two hoppers (baskets). Overall wagon length is about 15 m.

Wireless sensor networks are the subject of numerous scientific researches. They are increasingly used in variety of research areas, especially in civil engineering. This paper presents the application of a wireless system for the railway infrastructure measurements. Advantages of wireless sensor networks include cheaper and easier procedures, flexibility and ability to use them in hard to reach places. In addition, there are no expenses for usage of long cables and no practical difficulties that follow their usage. Major advantage of wireless measuring systems is their mobility, and possible relocation of sensor nodes [1].

Need to use wireless technologies is obvious in respect to large areas that railway infrastructure occupies. Condition assessment and monitoring are necessary for all railway infrastructure elements. Large number of infrastructure elements poses a problem that should be investigated, as well as their distribution over a large area [2]. Application of wireless sensor networks for measurements of actual sleeper vibrations and determination of their dynamic deflection is crucial for structural health monitoring. For this purpose, oscillation modes during regular track exploitation, or oscillation modes that are response to artificial excitation are measured and analyzed, or correlation between critical points for given elements is analyzed [3].

A wireless sensor network was developed at the Faculty of Civil Engineering in Belgrade [4] and it consists of wireless sensor nodes and the base station. Sensors are made in surface mount device technology and they use ADuC845 microcontroller produced by Analog Devices [5]. This processor contains multichannel A/D converter, clock, thermometer, and RS232, I2C and SPI interfaces. It can go into sleep mode with insignificant power consumption. In this state, peripheral components are turned off and only circuits that keep processor in regular working condition are powered. In that case, their power consumption is under 0.4 mA and the device can work for more than a month with three NiMH batteries, without additional power source (solar cells that are implemented for the purpose of electric recharge - energy harvesting). If solar cells are applied, the device can work almost indefinitely. This depends on the frequency of device wake ups, number of measurements and data transfers performed number of applied solar cells that are connected in parallel in order to create the solar panel, as well as the exposure of the panel to sun rays. Processor speed and wake up period are programmable. As the main sensor, three-axial MEMS accelerometer LIS3LV02DL [6] was used.

There is possibility to use additional analogue sensors with common or separate power supply, and to replace the accelerometer with other digital sensor. The main board can be connected to a display if needed. It is installed into a separate case with the keyboard. The display is irreplaceable in the development phase, and it can serve for device state diagnostics during regular operation. Sensors communicate with the base station (hub) through a radio (RF) modem Decode PRM4 [7]. This modem operates on 863-867 MHz band, which is relatively low frequency that does not support high data flow rate, but it provides wireless communication indoors and in the presence of obstacles, due to better diffraction on larger wavelengths. If longer range is needed, Yagi-Uda antennae may be used, with omnidirectional antenna at the base station. Small stick antennae are used for short ranges. Range of the device with large antennae is up to 1500 m outdoors. This range can vary a lot depending on whether the device is used in urban environment with high noise level or not. Device block diagram is presented in Fig. 2. As the base station of the system, a PC is used - most commonly a portable laptop.

A software package that runs under MS Windows operating system was developed to operate the base station. Power reserves of the base station are practically infinite, as well as the memory and processing power. In order to conduct modal analysis of vibrations of civil engineering structures, which is the main purpose of this wireless system, it is necessary to collect all unprocessed signals from multiple wireless devices and to compare them mutually.

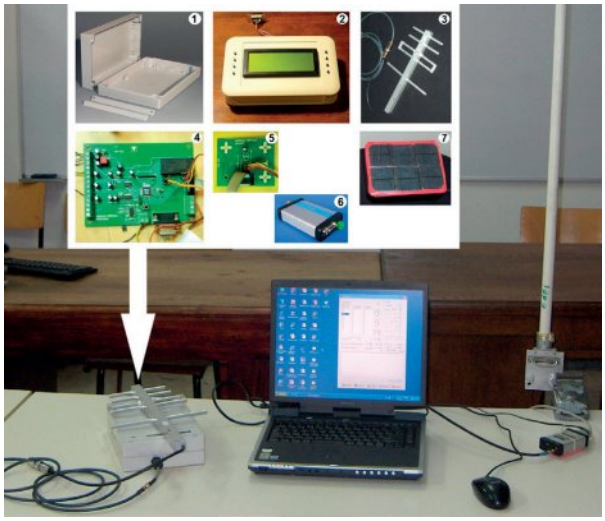

Fig. 2 Sensor node with the hub and device parts: 1) case, 2) display, 3) antenna, 4) main board, 5) accelerometer board, 6) modem and 7) solar cells

The algorithm of system operation implies that sensors are in low power consumption regime most of the time. On the wakeup, sensors spend several seconds checking if there is a signal being broadcasted from the base station. If this signal is detected, sensors remain in stand-by regime for a while expecting a command to begin a measurement, transfer the data, or adjust the parameters. During measurement, 3200 samples of information per axis are collected using variable sampling frequency that ranges from 40 to 2560 Hz. Therefore, time window is between 1.25 and 80 seconds. The data is compressed after the measurement using lossless algorithm of Huffman coding with differential pulse code modulation (DPCM) preprocessor. Since data transfer through a radio connection demands largest power consumption, the goal is to minimize it and to transfer as little bits as possible. The base station conducts data gathering and signal reconstruction. Several methods, including Reference Broadcast Synchronization (RBS), back synchronization [8 and 9], and periodical testing of processors' crystal frequencies and frequency ratios are used to ensure simultaneity of the data collected. Order of magnitude for data synchronization is 0.01 ms and it exceeds possibilities of mechanical sensors with minimum sampling period of 0.4 ms.

The sampling frequency of 160 Hz was used and measurement window was 20 s. Three sensors where fixed on railway sleepers on the outer side of the track. Distance between sensors was 3 m. Signal patterns vary from sleeper to sleeper, which depends on the fact whether the passing train is loaded or empty. For loaded trains oscillation amplitudes were smaller, although static deflections were greater. Amplitude of vertical oscillations was about 0.5 g in case of loaded trains, or about 1 g in case of empty trains. Exact peak values of acceleration were difficult to measure precisely due to insufficient sampling rate of accelerometers, which was not enough to provide reliable recording of short-term impulses of large forces. Accelerations in other directions were typically lower than vertical acceleration, and they were up to 0.25 g in case of empty trains. Two diagrams of vertical acceleration as a function of time (for empty trains) are given in Fig. 3 (example 1: regular diagram recorded on a well tamped sleeper; example 2: irregular diagram recorded on a poorly tamped sleeper).

In the first example, a pattern by which wagons are recognizable can be observed. Therefore, it is possible to calculate speed of the train by dividing the wagon length with passage time. Exact wagon length over buffers can vary a bit (in centimeters) due to wagons coupling. Train speed can be estimated with per mille precision. It was assumed that other uncertainties have negligible influence on this calculation. Relative uncertainty of clock frequency of a sensor is 10^{-4} in the worst case, and it can go as low as 10^{-6} with regular frequency calibrations and application of software correction for temperature changes. Dimension uncertainty due to seasonal variations of temperature and aging is in the order of 10^{-4} relative. Uncertainty of digital accelerometer output based on temperature fluctuations does not influence the calculation, because signal amplitude is not related with speed calculation. Loaded train speed of 70.69 km/h was determined from the example 1 in Fig. 3.

Even in cases when signal is not visually recognizable, as in the example 2 in Fig. 3, time delay estimation (TDE) technique [10] for determination of train speed can be used. Time domain TDE is performed by observing cross-correlation function of a signal with itself shifted in time. Autocorrelation is a powerful mathematical tool for finding patterns in a signal. It can detect the period of a signal masked by noise or identify fundamental frequency in case it is masked by its harmonics and difficult to detect using other methods such as Fourier transform. In our case, autocorrelation function has its maximum at zero shift, but it should also reach notable value when the signal is shifted by the time needed for a wagon to pass over a sleeper. Figure 4 shows correlation derived using TDE technique for two examples presented in Fig. 3. In the first case, with regular signal, peaks that match the passage of entire EDF wagons are obvious. These peaks appear at distances that are easily observable on the original time domain diagram. Mid-peaks are lower and they have smaller intensity, which perfectly corresponds to the wagon shape - it has four axles, with two mid-axles very close to each other. In

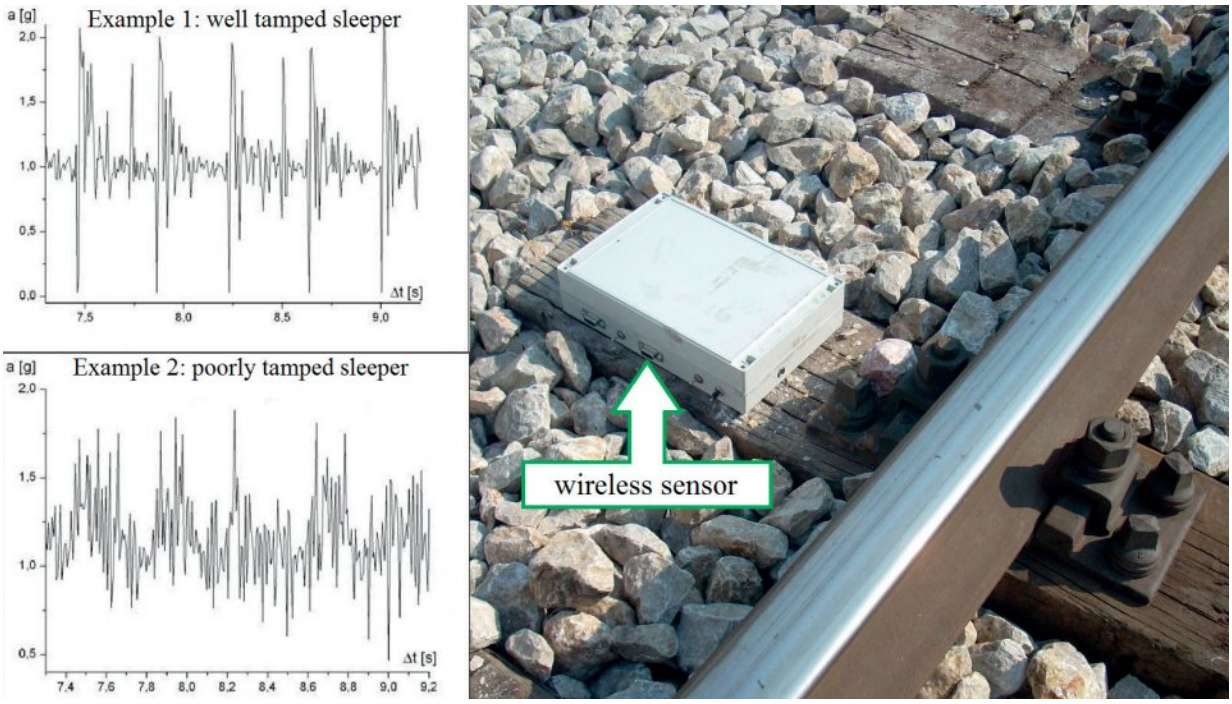

Fig. 3 Vertical acceleration as a function of time on two different sleepers

the second case, with worse quality signal, main peaks and mid-peaks cannot be distinguished by the intensity, but the knowledge gained from the previous case enables identification of real main peaks. Final result is similar to the train speed in the first case - 70.97 km/h. Time delay estimation was performed using 1 ms shift step (and the signal, whose period is 6 ms, was linearly interpolated to fit this). Difference between two calculated speeds corresponds to time offset equal to one third of the sampling period of the accelerometer, or 2 ms.

3. Potential for dynamic deflection measurement

Practical measurements of sleeper displacements (deflections) are followed by many difficulties. The main problem is to

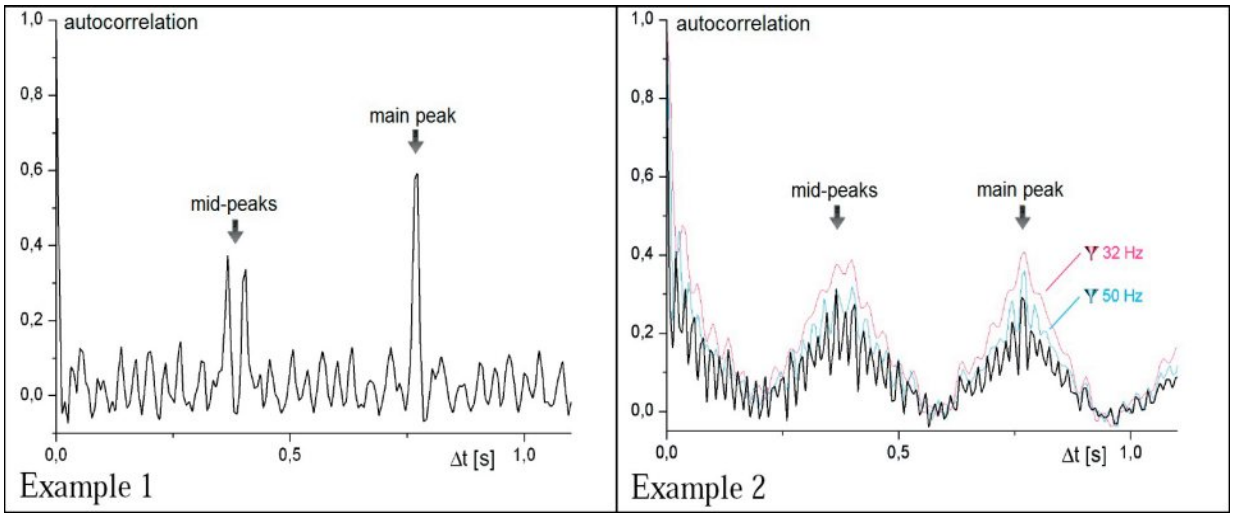

Fig. 4 The result of application of TDE technique on signals from two sleepers

provide a good reference system because all elements of track superstructure are susceptible to vibrations. Vibrations are also transferred to the surrounding ground where elements of the measuring system have to be placed. Some sensors often used for displacement measurements in other engineering areas are not very efficient in applications on sleepers or other track substructure elements.

If accelerometers are used, there is no need for external reference system because they measure inertial acceleration to which they are subjected. Speed and sleeper position can be determined using single and double integration of an acceleration signal over time, although great difficulties have been found in practice [11]. These difficulties include accumulation of noise and random deviation that rise over time, so software correction methods are necessary. Software corrections were applied over periods needed for sleepers to return into their initial states, which correspond to wagon passages.

The calculation of sleeper displacement by double integration of the signal acquired from described wireless system did not provide completely satisfying results. It turned out that higher sampling frequency is needed in order to record sudden impacts with resolution that is good enough for digital integration.

However, approximate estimation of displacement amplitude of the part of the sleeper where sensor is placed (acceleration and displacement are not uniform along the sleeper length and width) is possible using the existing measurement system. It is not important which points in time we consider as the beginning and end of a period if period value is known. Due to measurement imperfections, which include hysteresis, nonlinearity, noise, and other errors, single and double integration over one period, will not yield exactly zero result, although sleeper speed and displacement should return to their initial values. There are also physical reasons for deviations, such as slower oscillation harmonics of the train and the track and differences between wagons. The correction is performed by shifting direct component of the signal (its mid-level) by unique value for each wagon passage period, to ensure that the integration results in nil vertical displacement.

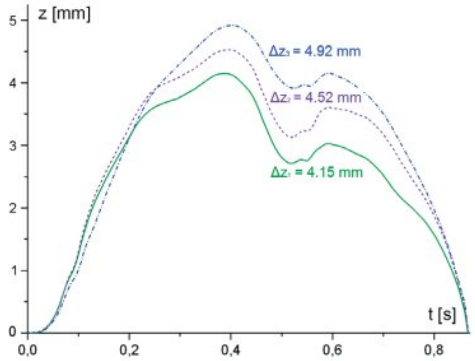

Fig. 5 Examples of calculation of vertical displacement (dynamic deflection) using double integration for the case of regular signal

Figure 5 shows examples of calculation of dynamic vertical displacement (deflection) z of a sleeper using the method of double integration, with correction, for three different periods (wagons). In this case, the train speed was estimated to 62.52 km/h. Values on diagram axes are relative - reference z value was not determined, and time was counted in respect to the beginning of an arbitrary period. Although differences are significant, the pattern is obvious, and deviation of displacement amplitude in the case of loaded train is in the order of 10%. It can be concluded that displacement amplitude is about 2 mm.

Largest deviations occur for passages of empty trains over sleepers with poor quality (example 2 in Fig. 3). A pattern is not recognizable here and amplitudes vary up to 1:2.5. The displacement amplitude is maximum in this case and its value is about 8 mm.

4. Conclusion

A wireless system for vibrations measurement, developed at the Faculty of Civil Engineering in Belgrade, was tested on the railway next to the thermal power plant of Obrenovac. It measured vibrations of track sleepers during passage of empty and loaded trains that transport coal. Train speed was determined with good reliability and dynamic deflection of sleepers was approximately estimated based on the experimentally acquired acceleration data. Autocorrelation of acceleration function can serve as a good criterion to estimate quality of sleeper support. Practical measurements of sleeper vibrations and calculation of displacements (deflections) along the track provide insight into the actual condition of layers below sleepers: ballast (including effect of voids beneath sleepers), sub-ballast and subgrade soil. The effective superstructure maintenance management must include analysis of the substructure [12 and 13]. Data that indicates the state of all layers below the sleepers is obtained by measuring the vibrations of track sleepers during the passage of trains. This method of dynamic deflection measurements of sleepers can be a basis for structural health monitoring and the track maintenance management on railway networks with limited length (such as the railway networks of the TENT Transport Company, Fig. 1).

Acknowledgement

This work was supported by the Ministry of Science and Technological Development of the Republic of Serbia through the research project No. 36012: “Research of technical-technological, staff and organizational capacity of Serbian Railways, from the viewpoint of current and future European Union requirements”.

References

[1] PUCCINELLI, D., HAENGGI, M.: Wireless Sensor Networks: Applications and Challenges of Ubiquitous Sensing, *Circuits and Systems Magazine*, IEEE, 5(3), 2005, 19-31.

[2] KAEWUNRUEN, S., M. REMENNIKOV, A.: *Trends in Vibration-based Structural Health Monitoring of Railway Sleepers*, in R. C. Sapri (ed), Mechanical Vibration: Measurement, Effect and Control, 2009, 3-4.

[3] LYNCH, J. P., LOH, K. J.: A summary Review of Wireless Sensors and Sensor Networks for Structural Health Monitoring, *Shock and Vibration Digest*, 38(2), 2006, 91-130.

[4] MALOVIC, M., BRAJOVIC, LJ., MISKOVIC, Z., TODOROVIC, G.: Vibration Measurement using Wireless Sensor Network, *Tehnika*, 66(6), 2012, 883-889.

[5] Analog Devices, ADuc845 microconverter datasheet, from http://www.analog.com/static/imported-files/data_sheets/ADUC845_847_848.pdf.

[6] ST Microelectronics, LIS3LV02DL accelerometer datasheet, from http://www.st.com/st-web-i/static/active/en/resource/technical/document/datasheet/ CD00091417.pdf.

[7] Decode, PRM-4 radio modem datasheet, from http://www.decode.rs/documentation/ PRM_4-datasheet.pdf

[8] RHEE, I. K., LEE, J., KIM, J., SERPEDIN, E., WU, Y. C.: Clock Synchronization in Wireless Sensor Networks: An Overview, *Sensors*, 9(1), 2009, 56-85.

[9] GAUTAM, G. C., SHARMA, T. P.: A Comparative Study of Time Synchronization Protocols in Wireless Sensor Networks, *Intern. J. of Applied Engineering Research*, 1(4), 2011, 691-705.

[10] CARTER, G. C.: *Coherence and Time Delay Estimation: An Applied Tutorial for Research, Development, Test, and Evaluation Engineers*. IEEE Press, 1993.

[11] COX, S. J.: Deflection of Sleeper in Ballast, *Vehicle System Dynamics Supplement*, vol. 24, 1995, 146-153.

[12] PUZAVAC, L., POPOVIC, Z., LAZAREVIC, L.: Influence of Track Stiffness on Track Behaviour under Vertical Load, *Promet – Traffic & Transportation*, vol. 24, No. 4, 2012, 387-394.

[13] IZVOLT, L., KARDOS, J., LELAK, J., MECAR, M.: Diagnostics of the Track Substructure Model and its Practical use, *Communications - Scientific Letters of the University of Zilina*, vol. 4, 2005, 31-36.

Otto Plasek - Miroslava Hruzikova - Richard Svoboda - Jaroslav Bilek *

UNDER SLEEPER PADS IN RAILWAY TRACK

Under sleeper pads appear to be suitable measure to improve track quality as a consequence of ballast bed protection against extreme stress. The paper comprises experience of under sleeper pads applications in the Czech Republic in two test sections which were built in the Czech Republic in 2007. The tests sections were built with the aim to protect permanent way elements against extremely high dynamic loading. That is why all parameters which could be influenced by the application of USPs are assessed, especially track quality, deflection and vibration of sleepers and bearers. Some positive influence of under sleeper pads on the track quality was observed after six years of monitoring. Extension of the application of under sleeper pads is expected in the Czech Republic especially for switches and crossings.

Keywords: *Under sleeper pads, concrete sleepers, concrete bearers, switches and crossings, track quality.*

1. Introduction

The increase of dynamic effects in railway track structures is connected with the train service speed and axle load increase. An increase of ballast stress is caused not only by the higher dynamic effects but also by the use of concrete sleepers and bearers which are characterized by higher bending stiffness and a relatively small contact area with ballast bed [1]. The dynamic effects occur due to imperfections of a railway track. The dynamic effects cause changes in sleeper or bearer support in ballast bed that unfavourably influence quality development of track geometry parameters.

A progressive deterioration of the track quality characterized by irregular supports of concrete sleepers or even by voiding sleepers which can vibrate in the ballast bed (so called dancing sleepers) as described, e.g., in [2 and 3], is a consequence of the evidence that track imperfections and higher dynamic effects are closely connected together [4] and [5].

Under sleeper pads (USPs) which are fixed on the underneath surface of a sleeper decrease the railway track stiffness. The contact area between sleepers or bearers and ballast is significantly higher. Static and dynamic loads on sleepers and bearers decrease and vehicle–track dynamic system properties are modified. Similarly, furthermore, the transfer of vibrations to a ballast bed is interrupted and damping of vibrations is moved to upper parts of a track [6], [7] and [8].

Two test sections for concrete sleepers and bearers with under sleeper pads were built in the Czech Republic in 2007 [9]. The basic motivation for the construction of the test track sections was an evaluation of the influence of under sleeper pads on improvement of track quality as a consequence of ballast bed protection against extreme stress. The paper comprises experience with applications of under sleeper pads in the Czech Republic from point of view of track settlement. Positive influence of under sleeper pads on track quality and influence on sleepers and bearers deflection and vibration was observed during six years of monitoring.

2. Description of USP test sections

The first test track section was built in the Plana nad Luznici railway station (4th Czech railway corridor: Prague - Ceské Budejovice - Linz) in the Czech Republic in 2007. The test section comprises of a turnout J60-1:12-500-I with USPs and adjacent track. The traffic load of this track ranges from 20 000 to 40 000 gross tons per day.

The assembly of the USPs for the turnout was designed in the finite element model [10] with the aim to reduce abrupt changes of track vertical stiffness. The basic bedding modulus of installed USPs (ballast plate) is 0.25 N.mm^{-3} – Getzner SLB 2210. Softer USPs – Getzner SLS 1010 and SLS 1707 – were used in the crossing panel just behind a frog nose and in the area of long bearers behind the crossing. The softer USPs are only in the middle part of the bearers. The transition zones that allow smooth transition of vertical track stiffness between the track with USPs and the track without USPs were designed. The bedding modulus of USPs in the transition zones is 0.30 N.mm^{-3} – Getzner SLB 3007. The length of the transition zone is 32.4 m, i.e., 54 sleepers. The total length of the track with USPs is 205 m. The pads were

* **Otto Plasek, Miroslava Hruzikova, Richard Svoboda, Jaroslav Bilek**
Department of Railway Structures and Constructions, Faculty of Civil Engineering, University of Technology, Brno, Czech Republic
E-mail: plasek.o@fce.vutbr.cz

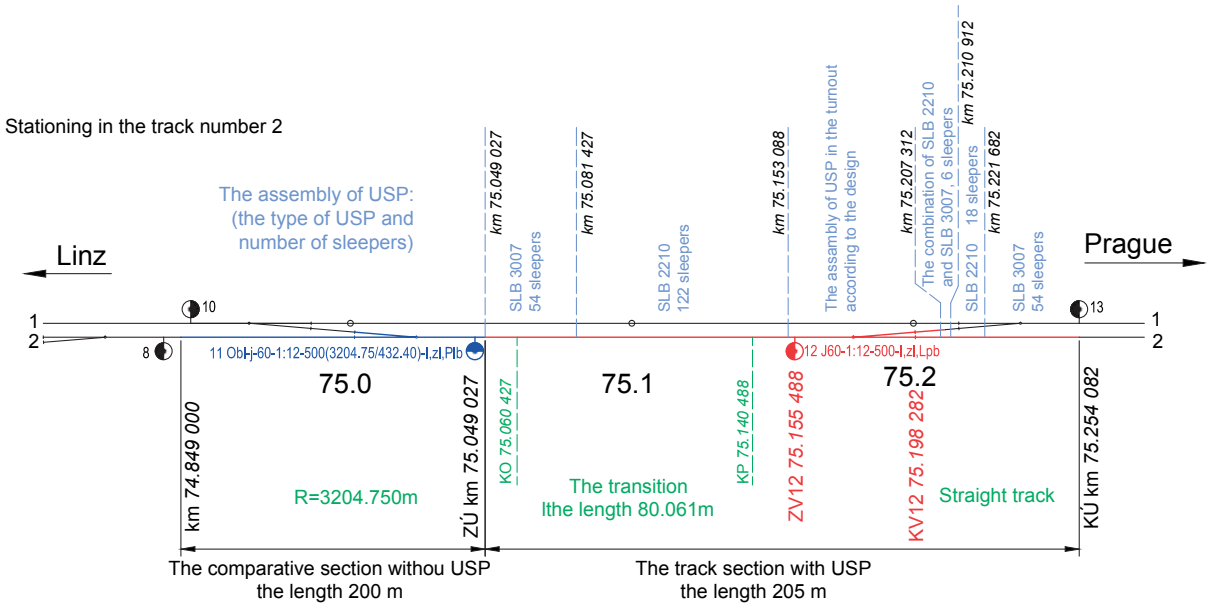

Fig. 1 The scheme of the test track section for USPs in the turnout in Plana nad Luznici railway station

installed on the underneath surface of sleepers and bearers by gluing. The neighbouring turnout and the adjacent track were chosen as a comparative conventional section. Continuous welded rail was constructed in the whole track section including both turnouts. The review of the whole test section is in Fig. 1.

Discrepancies between the assembly design of USPs and its installation (lacking USPs, wrong glued-on USPs) were found out after the turnout had been laid on 9th November 2007. Speed restriction was imposed. The discrepancies reparation was finished on 7th April 2008 and the speed restriction was removed after the tamping of the turnout and the ballast consolidation. The tamping was carried out three times in the test track section: 6th April 2008 (during reparation works, only the turnout with USP), 12th November 2008 (only the turnout with USP) and 23rd July 2009.

In 2007 the second test section in the Czech Republic was constructed in a curve of tight radius with the primary aim to evaluate the influence of USPs on reduction of rail corrugation development and, consequently, on the quality of track geometry parameters worsening. Test section was built in Havlickuv Brod

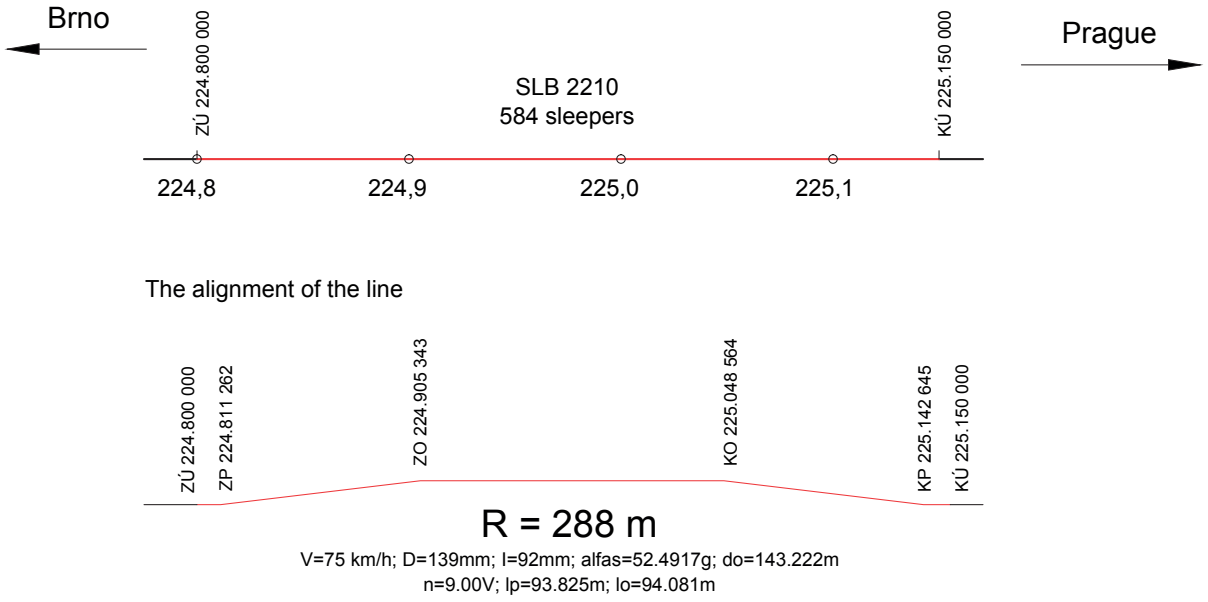

Fig. 2 The scheme of Havlickuv Brod - Okrouhlice test track section for USPs

- Okrouhlice (the second main line Prague - Brno) track section in track No. 1 in length of 350 m. The curve radius is R = 288 m, speed V = 75 km.h^{-1} and cant D = 139 mm, see Fig. 2. The section is partially on an embankment, partially in the cut and includes track on two bridges. Rail 49 E1, fastening Vossloh W 14 and sleepers B 91S (the Czech design and product) were installed in the section. Rail fastening with high elasticity Vossloh E 14 is installed in adjacent track and in track No. 2. The design track vertical stiffness in the case of E 14 fastening and sleepers without USPs is almost the same as the vertical stiffness of track with W 14 rail fastening and sleepers with USP. Therefore, no transition zones were constructed in this test section. The static bedding modulus of USPs (ballast plate) is 0.25 N.mm^{-3} - Getzner SLB 2210.

3. Monitoring of USP test sections

3.1 Review of monitored parameters

The tests sections were built with the aim to protect permanent way elements against extremely high dynamic loading. That is why all parameters that could be influenced by the application of USPs are assessed. The following parameters are being observed:

- quality of track geometry parameters;
- track settlements;
- vertical deflections under a running axle;
- vibrations of railway superstructure elements;
- transfer of vibrations to a track vicinity;
- noise propagation to a track vicinity.

This article deals with the track settlement monitoring by precise levelling. The aim of this assessment is to verify the stability of the support of sleepers and the long bearers with USPs in ballast bed.

3.2 Track level and settlement – precise levelling

The height of running surface of both rails was monitored through a precise levelling. Rail levels, bracket-type datum mark heights and other check points were monitored. Ninety three sections within 74.848 - 75.282 km are being monitored in the Plana nad Luznici track section. The length of sections in the track between the turnouts has the distance of 6 m; the sections in the turnouts have the distance of 3 m. Seventy four sections were established within 224.770 - 225.208 km in the step of 6 m in the Havlickuv Brod – Okrouhlice track section.

The track level is evaluated in a relative altitude system. Relative deviations from the optimized track position, which was

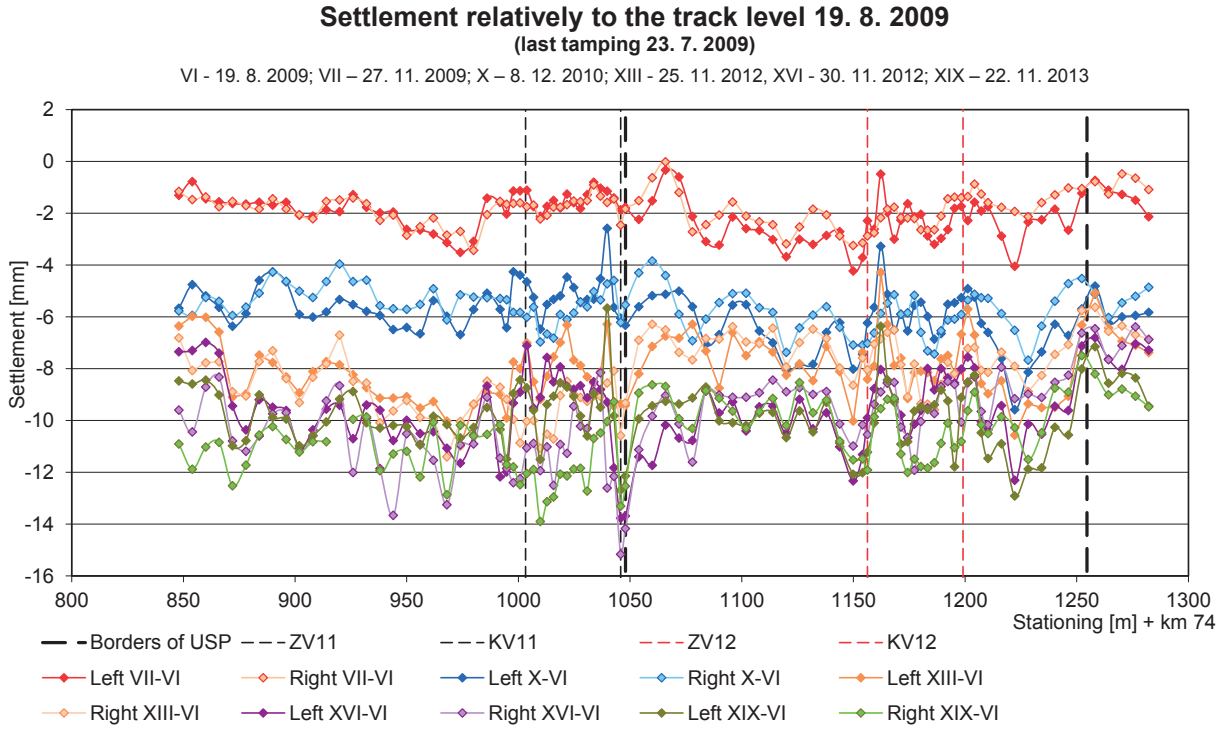

Fig. 3 The track settlement in Plana nad Luznici after track tamping (23 July 2009) relatively to the track level of 19 August 2009 (ZV - front joint of turnout, KV - heel joint)

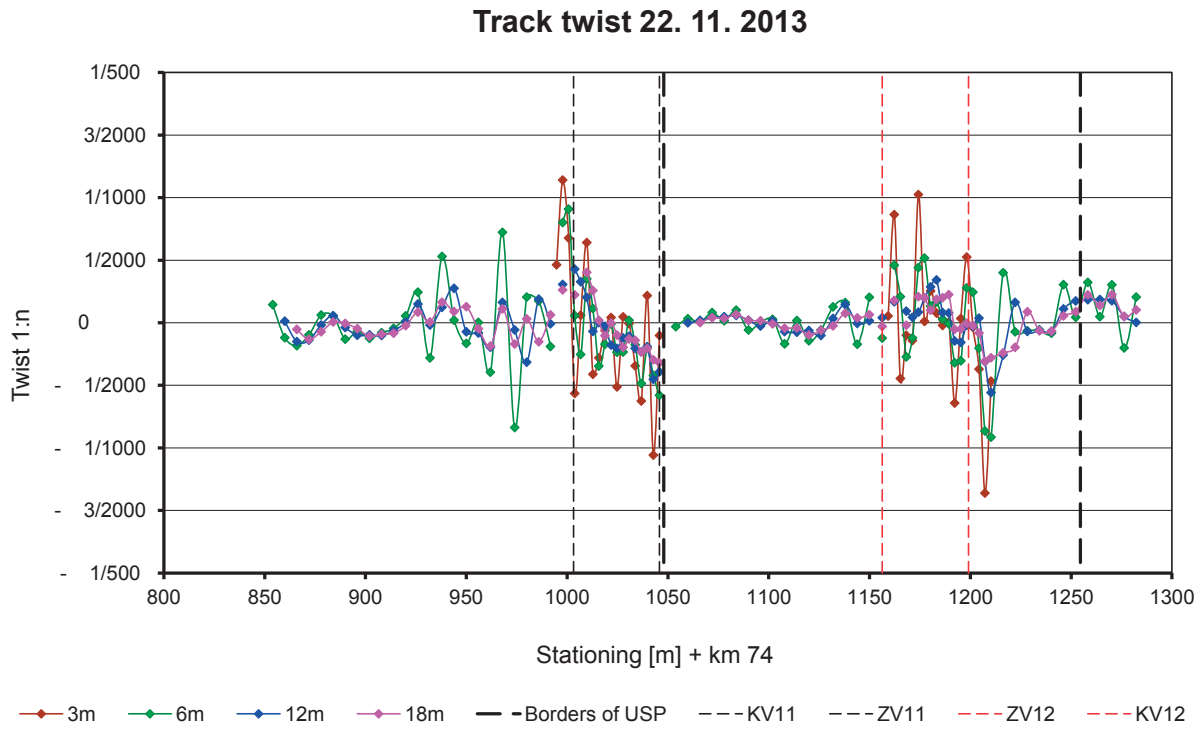

Fig. 4 Track twist in Plana nad Luznici over the length of 3 m, 6 m, 12 m and 18 m; 22 November 2013

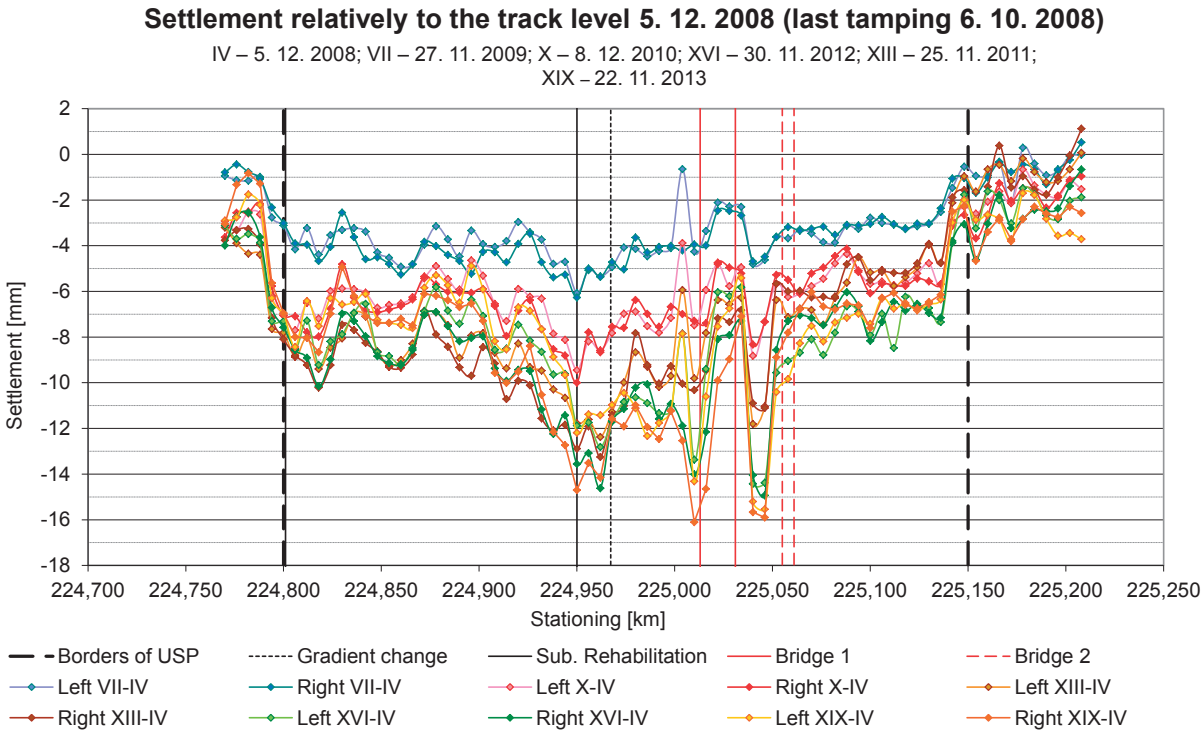

Fig. 5 The track settlement in Havlickuv Brod - Okrouhlice test track section after track tamping relatively to the track level of the 5 December 2008

found out by regression in the initial observation, were calculated. Designed parameters of height curves were taken into account. The evaluation of relative geometry parameters – settlement, track twist – was chosen for two reasons. The first reason is the fact that a printing of absolute track level in a chart doesn't provide an evidence of the track level deviation which is relatively tight to the absolute track level. An expression of the deviation relative to the designed track level is influenced by overall changes of the track level in the whole section - settlement or tamping of the track - which is the second reason. Deviations from relative designed position, track twist in a few wavelengths and a progress of track settlement were calculated.

The longitudinal level of the track in both test track sections was measured three times every year after the test sections had been put into operation. There is an evident local extreme of settlement in the vicinity of heel joint of turnout No. 11 in Plana nad Luznici without USPs in relative stationing of 1050 m, see Fig. 3. The local extreme is caused by unsymmetrical settlement of bearer in the crossing panel and just behind it. The undesirable unsymmetrical settlement is the main reason for the USPs installation on bearers. Such local extreme doesn't appear in the crossing panel in turnout No. 12 with USPs. It can be stated that the installation of USPs in this test track section is a preventive measure improving the track quality.

Next important parameter of track quality is the track twist. The track twist was calculated from computed cant. The distance of the measurement points is either 3 m (in the turnouts) or 6 m (for the points out of the turnouts). Therefore, the twist was calculated for the track length of 3 m (only in turnouts), 6 m, 12 m and 18 m. The twist for the last measurement is to be found in Fig. 4. The influence of USPs is obvious from the results, mainly for the track between turnouts. The track twist for unloaded track in turnouts is roughly the same. Here, the discrepancies during construction of turnout No. 12 with USPs, which are described above, influence the evaluation of track twist.

A significantly higher settlement is evident for the track with USPs in comparison to the track without USPs and elastic fastening Vossloh E 14 in Havlickuv Brod – Okrouhlice test section, see Fig. 5. Both bridges dominantly influence settlement of the track and local extremes of the track settlement occur just in transition zones of the bridges.

3.3 Evaluation of track settlement

The settlement progress analysis in both sections for plain track with and without USPs was carried out. The exponential regression of settlement curves was calculated by least square method following the formula:

$$S(l) = L \cdot \left(1 - e^{-\frac{k}{L} \cdot l}\right) \tag{1}$$

in which symbols mean:

$S_{(l)}$ ... function of settlement [mm];
l ... service load [MGT ... million gross tons];
L ... limit of settlement [mm];
k ... slope of tangent at l = 0 [mm.MGT^{-1}].

The regression functions were determined by least square method to find the minimum of the function:

$$\min\left\{f(x) : x \in X \subset E^2\right\} \tag{2}$$

in which:

x ... vector of parameters of the regression function $[k\ L]^T$;
X ... subset defined by constraints $k > 0$ and $L > 0$ of Euclidean space E^2.

The function $f(x)$ was defined:

$$f(x) = \sum_{i=0}^{n} \left[s_i - S(l_i)\right]^2 = \sum_{i=0}^{n} \left[s_i - L\left(1 - e^{-\frac{k}{L} l_i}\right)\right]^2 \tag{3}$$

in which:

i ... index of track levelling epoch;
n ... number of last epoch;
s_i ... measured track settlement [mm];
l_i ... service load till levelling epoch number i [MGT].

The min $f(x)$ occurs at the point x *:

$$\nabla f(x^*)^T = 0 \tag{4}$$

in which $\nabla f(x)$ is gradient vector:

$$\nabla f(x) = \left[\frac{\partial f}{\partial k} \frac{\partial f}{\partial L}\right] \tag{5}$$

The system of nonlinear algebraic equations was evaluated from the equation (4):

$$\sum_{i=0}^{n} = \left[\left[s_i - L \cdot \left(1 - e^{-\frac{k}{L} l_i}\right)\right] \cdot l_i \cdot e^{-\frac{k}{L} l_i}\right] = 0 \tag{6}$$

$$\sum_{i=0}^{n} = \left[\left[s_i - L \cdot \left(1 - e^{-\frac{k}{L} l_i}\right)\right] \cdot \left(1 + \frac{k}{L} \cdot l_i\right) \cdot e^{-\frac{k}{L} l_i}\right] = 0 \tag{7}$$

The system of nonlinear equations was solved by Newton's method [11]:

$$\mathrm{x}^{k+1} = \mathrm{x}^k - \left(\nabla^2 \mathrm{f}(\mathrm{x}^k)\right)^{-1} \cdot \nabla \mathrm{f}(\mathrm{x}^k) \tag{8}$$

in which $\nabla^2 f(x)$ is the symmetric Hessian matrix:

$$\nabla^2 f(x) = \begin{bmatrix} \frac{\partial^2 f}{\partial k^2} & \frac{\partial^2 f}{\partial k \partial L} \\ \frac{\partial^2 f}{\partial L \partial k} & \frac{\partial^2 f}{\partial L^2} \end{bmatrix} \quad (9)$$

Upper index k means a step number of the numerical iteration. If convergence error was less than tolerance $\varepsilon = 1.10^{-4}$, i.e.:

$$\| \nabla f(x^k) \| \leq \varepsilon, \quad (10)$$

the calculation was stopped and the parameters k, L were determined.

The average operational load is approximately 5.6 MGT per year in Plana nad Luznici section and 9.8 MGT per year in Havlickuv Brod - Okrouhlice section. The settlement progress is roughly the same for plain track with and without USPs in Plana nad Luznici test track section (L = 10.8 mm without USPs, L = 10.7 mm with USPs) and is significantly slower with rather less limit in the track in Havlickuv Brod - Okrouhlice (L = 10.1 mm), see Fig. 6. The difference in the settlement speed could be explained by the fact that in Plana nad Luznici a new subgrade structure was constructed. The settlement limit is not significant and could be omitted regarding other parameters, which influence behaviour of the track sections.

A negative relative settlement is evident for the state of monitoring before last one. This effect has not been explained completely yet. The reason can be either the limited precision of measurement and evaluation methods or influence of isolated maintenance impacts in points of the most deteriorated track level.

The progress of standard deviations of track settlement is also an interesting phenomenon. The standard deviations of settlement values, which correspond to the track quality parameters, were compared only for plain track with or without USPs in both sections, see Fig. 7. The exponential regression is again included into the chart. The significant differences between tracks with USPs and without USPs as well as differences between tracks with USPs in both sections are evident. The worsening of standard deviation in Plana nad Luznici test section almost converge but do not converge in Havlickuv Brod - Okrouhlice section where the value of standard deviation is influenced by the bridges and their transition zones. If plain track with and without USPs are compared in Plana nad Luznici for the same loading better behaviour of the track with USPs is evident.

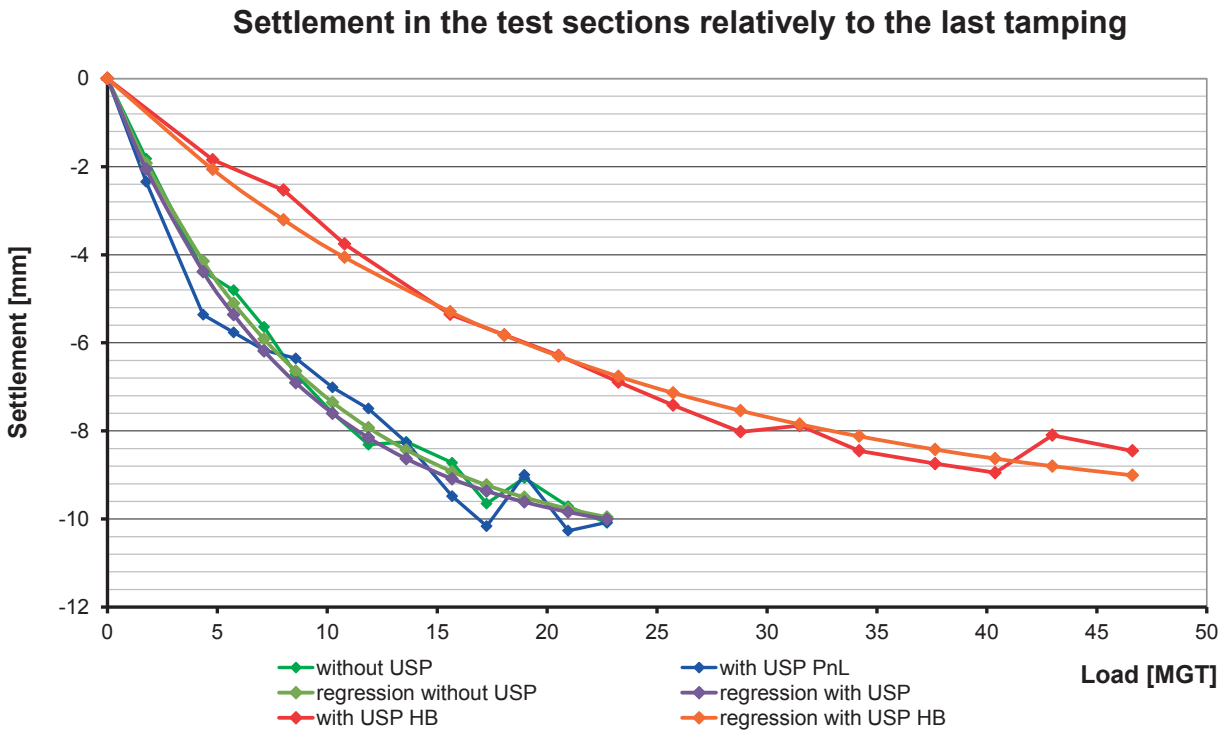

Fig. 6 Progress of settlement (PnL - Plana nad Luznici, HB - Havlickuv Brod – Okrouhlice)

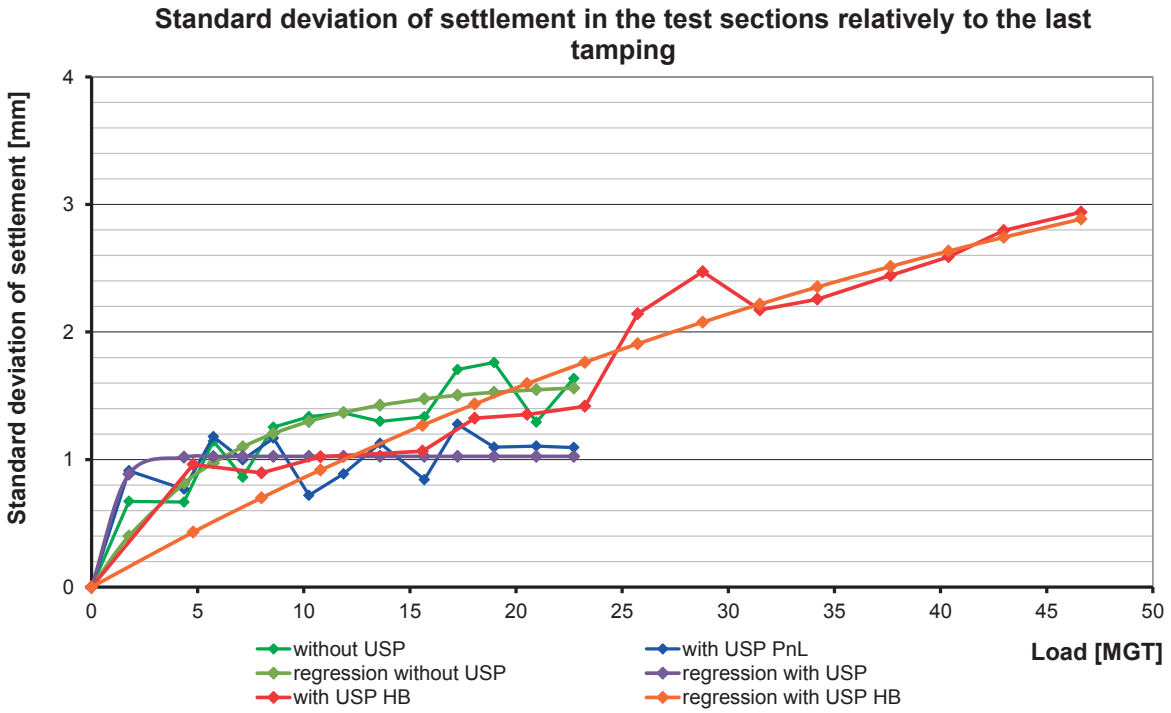

Fig. 7 Standard deviations progress of settlement (PnL: Plana nad Luznici, HB: Havlickuv Brod – Okrouhlice)

4. Conclusion

A summary of results of the evaluations of both track sections are following:

- the deviations of the parameters at the beginning of monitoring were comparable for both sections with and without USPs;
- the deviations in the turnouts are higher than in the plain track in general;
- USPs are efficient regarding to the quality of track geometry parameters in comparison to the track without USPs;
- the most deteriorating factor for track quality occurs on bridges and their transition zones, USPs application does not improve situation significantly;
- USPs reduce an effect of unsymmetrical settlement of long concrete bearers in the crossing panel and adjacent track;
- Vossloh E 14 rail fastening with high elasticity is more effective from the point of view of track settlement, but it needs an extra maintenance effort.

The trial track sections in the Plana nad Luznici railway station and in Havlickuv Brod - Okrouhlice track section were built with the aim to assess a USPs's influence on track geometry quality. The basic conclusions are that the track quality with USPs is better and track geometry deterioration is slower compared to the track quality without USPs. This can be explained by the reduction of stress in ballast bed under a sleeper due to the use of USPs;this phenomenon was analyzed by static and dynamic analyses by FEM [8]. As a consequence the lifetime of ballast bed is extended. The positive influence of USPs is usually evident after longer period of time considering traffic density of a track. The higher track load the sooner influence of USPs is evident and the more investment in USPs would be efficient from the point of view of life cycle costs.

The monitored data show that the influence of USPs had started to be evident two years after the USPs installation. The track settlement and deviations of track geometry parameters are lower in the section with USPs between the turnouts. It is expected that longer time period is required to get evidence of the influence of USPs in the turnout.

Acknowledgement

This outcome has been achieved with the financial support of the project of the Technology Agency of the Czech Republic No. TA01031173 Under Sleeper Pads and the project of Specific research of Brno University of Technology No. FAST-J-14-2534.

References

[1] PLASEK, O.; HRUZIKOVA, M.: *The Use of Under Sleeper Pads as a Protection of Ballast in Plain Track and Turnouts, Akustika, ISSN 1801-9064, Studio Akustika* : Ceske Budejovice, 2007

[2] SCHNEIDER, P.; BOLMSVIK, R.; NIELSEN, J. C. O.: *In Situ Performance of a Ballasted Railway Track with under Sleeper Pads*. Proc. of the Institution of Mechanical Engineers, Part F: J. of Rail and Rapid Transit. 2011, 299-309. Available on WWW: <http://pif.sagepub.com/content/225/3/299.full.pdf+ html>. ISSN 2041-3017 (online), 0954-4097 (print).

[3] USP - *Under Sleeper Pads - Semelles sous traverses - Schwellenbesohlungen. Summarising Report of UIC Project No. I/05/U/440* [online], 4th Edition, Vienna, 2009 [cit. 2011-07-11]. S. 40. Available on WWW: <www.uic.org/IMG/pdf/2009-03-26_Summarising_Report_UIC-USP.pdf>.

[4] IZVOLT, L.; KARDOS, J.: Influence of Parameters of Railway Track Construction on Vertical Dynamic Interaction Vehicle/Track. *Communications - Scientific Letters of the University of Zilina*, No. 3, 2011, 63-70, ISSN 1335-4205

[5] BENCAT, J.; STYPULA, K.: Buildings Structure Response Due to Railway Traffic. *Communication - Scientific Letters of the University of Zilina*, No. 2, 2013, 41-48, ISSN 1335-4205

[6] LEYKAUF, G., STAHL, W.: *Untersuchungen und Erfahrungen mit besohlten Schwellen*. EI - Eisenbahningenieur, 2004, 55, 6. S. 8. ISSN 0013-2810

[7] PETIT, C.: *Experience in the Field of Under Sleeper Pads*, [online], Paris, France, 2006 [cit. 2011-07-11], p. 24, online: <www.uic.org/reunion.php/19039/_23_sateba_petit .pdf>.

[8] POTVIN, R.: *Schieneneinsenkung und Schwellenbesohlungssteifigkeit.* EI - Eisenbahningenieur. 2008, 7. S. 6. ISSN 0013-2810.

[9] HRUZIKOVA, M., PLASEK, O., SMUTNY, J., SVOBODA, R., SALAJKA, V.: *Trial Track Section with Under Sleeper Pads in the Czech Republic*, Proc. of Railway Engineering-2009, ISBN 0-947644-65-2, Engineering Technics Press : Edinburgh, 2009

[10] PLASEK, O., HRUZIKOVA, M.: *Design of Under Sleeper Pads for Turnout.* Archiwum Instytutu Inzynierii Ladowej. Poznan : Archives of Institute of Civil Engineering, 2007, 241-249. ISSN 1897-4007.

[11] DALIK, J.: *Numerical Methods (in Czech).* Brno : CERM, 1997, 145 p. ISBN 80-214-0646-1.

Tereza Pavlu - Luc Boehme - Petr Hajek *

INFLUENCE OF RECYCLED AGGREGATE QUALITY ON THE MECHANICAL PROPERTIES OF CONCRETE

The use of recycled construction and demolition waste - especially recycled concrete - as an aggregate for new concrete mixes, leads to saving of natural resources and helps to reduce the pressure on landfilling sites. Mostly the quality of recycled concrete is lower compared to standard concrete prepared with the same mix design. The reason for the drop in quality is mainly related to the quality of the recycled aggregate. The high water absorption of recycled aggregate has a negative impact of concrete mix workability and influences the water-cement ratio. This paper presents the effect of recycled aggregate quality on the physical and mechanical properties of concrete. Series of concrete with various replacement ratios of natural aggregate by recycled aggregate were prepared for this study. The obtained results confirm the potential use of developed recycling concrete made with local recycled aggregate in some applications in building construction. This can lead to environmental savings, especially reduction of primary resources use, embodied energy and embodied emissions.

Keywords: *Recycled aggregate, recycled concrete, construction and demolition waste, environmental savings.*

1. Introduction

World concrete production has been twelve times increased in the second half of the last century [1]. Nowadays, concrete is after water the second most used material in the world and the production of concrete totally depends on the natural resources. The rapid development in the construction industries leads to the replacement of old existing buildings with new buildings. Consequently, the amount of demolished concrete structures is very high and is gradually increasing. This creates needs and potential for replacement of natural aggregate by recycled aggregated in the new concrete.

Making use of recycled aggregates helps to reduce primary raw materials depletion, pressure on landfilling sites and amount of construction and demolition waste, which reaches up to 31% of all waste in the European Union [2]. After World War II, recycled demolition rubble was used instead of natural aggregate to rebuild roads and houses because there were a lot of demolished buildings in Europe, mainly in Germany [3]. Using of recycled aggregate for the purpose of primary materials savings started in 1980' mainly in countries without natural resources of aggregate. So, the research focused on the use of recycled aggregate (RA) derived from construction and demolition waste (CDW), in recycled concrete started [4].

Lower quality of recycled aggregates compared to natural aggregates negatively influences the mechanical properties of recycled concrete [5]. Four types of RA are defined according to the European Standard EN 206-1 [6] in relationship to their composition. Recycled concrete aggregate mainly from crushed concrete (Type I according to EN 206-1) is often used in production of concrete [7]. RA Type I can also include small amounts (up to 10% in total) of other materials, such as crushed bricks, plasters, ceramic and asphalt particles. Content of these particles depends on a recycling process and origin of waste material [7]. All listed aspects lead to poorer performing properties of RA thaen natural aggregate. On the other hand, it was found that inferior values are not connected with quality of original concrete [8]. Maximum replacement ratio, the percentage of substitution of natural aggregate by RA, was specified by the German Committee for Structural concrete (DAfStb) in 1998 in Germany. Allowed values are based on a 4-years long national research and are published as a supplementary document to DIN 4226-100 [9].

One of the poor properties of RA is the high water absorption capacity [10, 11 and 12], as a result of the attached mortar content and, consequently, higher porosity of aggregate [13 and 14]. Fine fractions of RA contain more cement mortar and impurities such as clay than coarse fractions, which leads to higher absorption and inappropriateness to use it for structural concretes [7, 15 and 16]. High water absorption affects water-cement ratio [4 and 17], workability of concrete mix [13] and physical properties such as water absorption and carbonation [7].

* [1]Tereza Pavlu, [2]Luc Boehme, [1]Petr Hajek
[1]Department of Building Structures, Faculty of Civil Engineering, Czech Technical University in Prague, Czech Republic
[2]Technology Cluster Construction, Faculty of Engineering Technology, KU Leuven, Oostende, Belgium
E-mail: tereza.pavlu@fsv.cvut.cz

The other physical and mechanical properties of aggregate, which are negatively influenced by presence of adhered mortar, are density [8], resistance to degradation and wear [18].

Workability of fresh concrete, which is affected by water absorption capacity and porosity of used aggregate, has impact properties of fresh and hardened concrete such as density, air content and strength [9]. There are certain ways to get better workability of concrete mix either pre-saturating recycled aggregate before adding it to mix [19] or added water-reducing admixtures [4 and 20]. Compressive strength of RA depends on replacement rate, quality and composition of RA [21] and also on effective water-cement ratio [22]. So, the paper presents and discusses experimental results of mechanical properties of recycled concrete. Tested concretes contained different ratios of recycled content and different types of recycled aggregate. All samples were tested under uniaxial compressive stress.

2. Materials and methodology

2.1 Materials

Natural aggregates were extracted from stone quarry in the Czech Republic. Both samples of coarse recycled aggregate came from the same CDW treatment plant in the Czech Republic. Laboratory crushed recycled aggregates from concrete cubes were prepared from several concrete mixes whose properties are described in Table 1.

- Sand (S): grain size 0/4 mm
- Natural aggregate (NA): grain size 4/8 mm and 8/16 mm, from crushed mix gravel
- Laboratory prepared recycled aggregate (LRA): grain size 0/16 mm, from crushing concrete approximately 100 days old, the composition of mixtures is described in Table 1.
- Recycled aggregate from recycling plant (RA1): grain size 4/16 mm, containing 76 % crushed concrete, 18% of masonry, 5% of asphalt and other materials, were defined as type 4 - mixed recycled concrete according to standard [6].
- Recycled aggregate from recycling plant (RA2): grain size 4/16 mm, containing 96% of crushed concrete, 1% of masonry, 1% of asphalt and other, were defined as type 1 - mixed recycled concrete according to standard [6].

One natural aggregate, two samples (RA1 & RA2) of coarse recycled aggregate from recycling plant and three samples (LRA1, LRA2 & LRA3) of laboratory prepared recycled aggregate were tested and used as aggregates for a new concrete.

Figure 1 shows the images and compositions of RA. The geometrical and physical properties of all types of aggregates were determined and shown in Table 2.

Mechanical properties and composition of original concrete cubes used for preparing laboratory made recycled aggregate Table 1

Class of concrete	C 30/37	C60/75	C20/25
	(LRA 1)	(LRA 2)	(LRA 3)
Composition of mixes (kg/m^3)			
Natural sand 0/4 mm	774	820	935
Natural aggregate 4/8 mm	345	350	400
Natural aggregate 8/16 mm	641	750	855
Cement	345	475	275
Water	181	180	165
Water-reducing admixtures	-	4.8	-
Water-cement ratio	0.52	0.38	0.60
Compressive strength (MPa)	42.3	70.8	28.5
Tensile strength (MPa)	4.6	6.8	4.2
Modulus of elasticity (GPa)	27.2	36.2	29.7
Density of hardened concrete (kg/m^3)	2 285	2 580	2 630
Density of aggregate (kg/m^3)	2 446	2 439	2 439
Water absorption of aggregate (%)	3.86	3.71	3.47

Fig. 1 Used recycled aggregates

Physical properties of all used types of aggregate Table 2

Type of aggregate	Grading	Oven-dry particle density	Water absorption
	(mm)	(kg/m^3)	(%)
Natural sand (S) 0/4 mm	0-4	2 603	1.30
Natural aggregate (NA) 4/16 mm	4-8	2 675	1.12
	8-16	2 654	0.79
Laboratory recycled aggregate (LRA) 4/16 mm	4-8	2 284	7.51
	8-16	2 408	3.68
Recycled aggregate (RA1)	4-8	2 181	10.38
	8-16	2 254	7.53
Recycled aggregate (RA2)	4-8	2 147	9.18
	8-16	2 220	7.01

2.2 Concrete mix proportion

The two different ways were adopted in concrete mixtures preparations. For each test series was designed own reference mixture with only natural aggregate for relevant comparison within each test series. The first way was adopted for laboratory prepared aggregate. The amount of water was modified according to water absorption capacity of the RA. In these mixtures fractions 0-16 mm of laboratory prepared recycled aggregate (LRA) were used. The fine fraction was included in the recycled concrete mixture because of high content of cement. Prepared mixtures are listed in Table 3. The second way was adopted for RA from the recycling plant. The amounts of water for these mixtures were calculated according to water absorption capacity of each aggregate to keep the effective water cement ratio constant for all mixtures. Due to the high content of clay, particles of clay bricks and dust in fine fraction of RA from CDW treatment plant, the fraction 0-4 mm was removed. Because of using only the coarse fraction 4-16 mm of aggregate from recycling plant, the percentage of substitution was maximal 63 % of the total amount of used aggregates, but it was 100 % replacementof all coarse aggregate. Prepared concrete mixes are shown in Table 4. All the concrete mixes were designed for different replacements of natural aggregate (NA) by recycled aggregate (RA).

2.3 Testing

Density and water absorption capacity of aggregates were tested by pycnometer method according to EN 1097-6 [23]. Tested concrete specimens were subjected to 28-days wet curing. Tests of compressive strength were carried out on 150 mm cubes.

Mix proportion of concrete mixtures with laboratory prepared recycled aggregate (kg/m^3) Table 3

No.	Replacement percentage	Sand	NA 4/8 mm	NA 8/16 mm	LRA 0/16 mm	cem	w	w/c	w/c$_{eff.}$
NA	0	774	346	641	0	345	180	0.52	0.52
LRA 1- 40	40	438	221	411	688	345	200	0.58	0.50
LRA 1- 50	50	356	188	347	868	345	200	0.58	0.48
LRA 1- 70	70	205	114	211	1234	345	200	0.58	0.43
LRA 2- 50	50	356	188	347	868	345	200	0.58	0.48
LRA 2- 70	70	205	114	211	1234	345	200	0.58	0.43
LRA 3- 40	40	438	221	411	688	345	200	0.58	0.50
LRA 3- 50	50	356	188	347	868	345	200	0.58	0.48
LRA 3- 70	70	205	114	211	1234	345	200	0.58	0.43

Mix proportion of concrete mixtures with aggregate from recycling plant (kg/m^3) Table 4

No.	Replacement percentage	Sand	NA 4/8 mm	NA 8/16 mm	RA 4/16 mm	cem	w	w/c	w/c$_{eff.}$
NA	0	767	458	726	0	320	160	0.50	0.50
RA 1- 50	50	750	0	243	790	320	227	0.71	0.50
RA 1- 63	63	748	0	0	991	320	235	0.73	0.50
RA 2- 31	31	769	192	400	487	320	176	0.55	0.50
RA 2- 50	50	764	0	229	787	320	187	0.58	0.50
RA 2- 63	63	766	0	0	967	320	191	0.60	0.50

For flexural strength tests beams of dimensions 100×100×400 mm were used.

The compressive strength is the peak stress of the test specimens under uniaxial compression. It is the fundamental and important mechanical property of concrete which helps to sort concrete mixes to concrete strength classes. Five 150 mm cubes were prepared for each of tested concrete mixture.

The flexural strength test of the examined concrete was conducted on beams of size 100×100×400 mm^3. Three concrete beams were casted for each concrete mix and cured for 28 days under usual laboratory conditions. The flexural strength was tested by four-point bending test.

3. Results and discussion

3.1 Compressive strength

The average test-results for concrete prepared from laboratory made recycled aggregate are shown in Fig. 2. This graph shows compressive strength of concrete with natural aggregate (NA), reference variant, and three types of recycled concrete prepared from laboratory made recycled aggregate (LRA1, LRA2 & LRA3) with different replacement ratios. The graph shows correlation between replacement ratio and compressive strength. The compressive strength may depend on the composition of the original concrete mixture, but it would need more testing for relevant confirmation. LRA2 includes higher amount of cement than LRA1. Compressive strength of recycled concrete from LRA2 increases and recycled concrete from LRA1 decreases with replacement ratio of RA. But, on the other hand, recycled concrete from LRA3 decreases less than LRA1 regardless the original concrete mixture included the lowest amount of cement. Different results can indicate the problem with using fine fraction with high amount of milled cement. It is not possible to determine how much cement included in fine fraction exactly reacts with water. As a consequence, the amount of unreacted cement in LRA was able to cause higher compressive strength of mixtures included LRA than compressive strength of concrete with only NA.

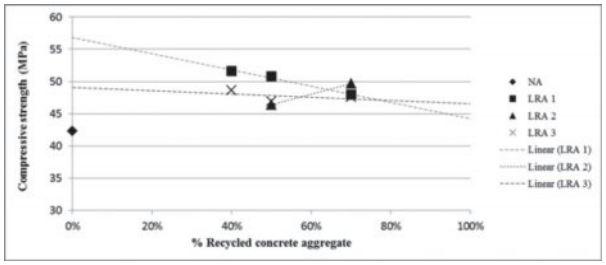

Fig. 2 Correlation between replacement ratio and compressive strength of recycled concrete with laboratory recycled aggregate

Furthermore, correlation between different replacement ratios of recycled aggregate was not proved in this part of investigation. Reference concrete shows lower compressive strength than recycled concretes, which may be due to content of cement in the fine fraction of recycled aggregates.

Correlation between replacement ratio and compressive strength of recycled concrete with recycled aggregate from recycling plant is shown in Fig. 3. This graph convincingly proved approximately linear dependence between mechanical properties of recycled concrete and amount of recycled aggregate in concrete mixture. The effective water cement ratio was kept constant for all mixtures, and there was no cement added to the recycled aggregate.

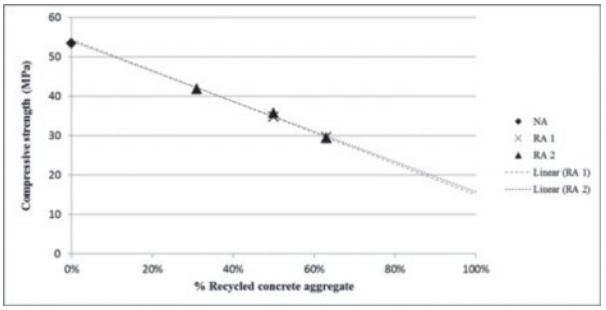

Fig. 3 Correlation between replacement ratio and compressive strength of recycled concrete with recycled aggregate from recycling plant

Generally, the compressive strength of recycled concrete decreased with the increased replacement ratio RA. The highest decline of compressive strength (more than 45 %) was found for concrete samples with 63 % replacement ratio for both recycled aggregate samples from recycling plant (RA 1 and RA 2).

Different impact on mechanical properties of two types of recycled aggregate is caused by their different quality. Recycled aggregate from laboratory included only natural aggregate with adhered mortar. Howerer, recycled aggregate from recycling plant was contaminated with diverse substances, which negatively influenced mechanical properties of concrete.

3.3 Flexural strength

The relation between flexural strength of concrete and replacement ratio was the same as for compressive strength for both types of RA. With the increase of replacement ratio recycled aggregate (RA) the flexural strength of recycled concrete decreases. The highest decline of flexural strength was up to 13 % for concrete samples with 63 % replacement ratio for recycled aggregate (RA 2).

4. Conclusions

The following conclusions can be drawn from this study. In the case of laboratory prepared RA the influence of properties of original concrete on the mechanical properties of recycled concrete was observed but due to a small number of tests it cannot be considered as a relevant confirmation. In the case of the use of RA from recycling plant, the increasing percentage of RA from recycling plant in recycled concrete have negative impact on the mechanical properties of final recycled concrete. The main degradation of properties was observed for compressive strength where 100 % replacement of coarse fraction by recycled aggregate resulted in more than 45 % decline of compressive strength. Important next step of the research is reliability of the reinforced recycled concrete with high percentage of RA concerning corrosion of steel reinforcement [24] and long term durability of recycled concrete in construction applications. Presented results confirm the decease of the mechanical properties of recycled concrete in relation to the quality of recycled aggregate. When the quality of recycled aggregate is known, the properties can meet the requirements of standards [6 and 25].

Acknowledgments

The research was funded by TA03010501 Optimized subtle frame for energy efficient buildings and SGS13/109/OHK1/2T/11 Additional constructions for light-weight concrete frame systems made from natural and recycled materials. All support is gratefully acknowledged.

References

[1] HAJEK, P.: *Integrated Environmental Design and Optimisation of Concrete Slabs*, in proc. Brisbane: CIA, 2003, Sv. Concrete in the 3rd Millenium.

[2] THOMAS, C. et al. Evaluation of the Fatigue behavior of Recycled Aggregate Concrete. *J. of Cleaner Production,* 2013, 397-405.

[3] AKASH, R., KUMAR, N. J., SUDHIR, M.: Use of Aggregates from Recycled Construction. *Resources, Conservation and Recycling,* 2007, Sv. I, 50.

[4] BARDUDO, A., et al.: Influence of Water-reducing Admixtures on the Mechanical Performace of Recycled Concrete. *J. of Cleaner Production,* 2013, 59.

[5] KHATIB, J. M.: Properties of Concrete Incorporating Fine Recycled Aggregate. *Cement and Concrete Research,* April 2005, 763-769.

[6] EN 206-1 Concrete - Part 1: *Specification, Performance, Production and Concrete*, Brussels : European Union : CEN, 2000.

[7] AGRELA, F., et. al: Limiting Properties in the Characterisation of Mixed Recycled Aggregates. *Construction and Building Materials,* 2011, Sv. I, 25.

[8] HANSEN, T. C., NARUD, H.: Strength of Recycled Concrete Made from Crushed Concrete Coarse Aggregate. *Concrete International*, 1, January 1983, 79-83.

[9] DE BRITO, J., SAIKIA, N.: *Recycled Aggregate in Concrete*. London : Springer-Verlag, 2013.

[10] EVANGELISTA, L., DE BRITO, J.: Mechanical behaviour of Concrete Made with Fine Recycled Concrete Aggregates. *Cement and Concrete Composites,* May 2007, 397-401.

[11] XIAO, J., LI, J. A ZHANG, Ch.: Mechanical Properties of Recycled Aggregate Concrete under Uniaxial Loading. *Cement and Concrete Research,* 2005, 1187-1194.

[12] SAGOE-CRENTSIL, K. K., BROUWN, T., TAYLOR, A. H.: Performance of Concrete Made with Commercially Produced Coarse Recycled Concrete Aggregate. *Cement and Concrete Research,* 2001, 707-712.

[13] ETXEBERRIA, M., et al.: Influence of Amount of Recycled Coarse Aggregates and Production Process on Properties of Recycled Aggregate Concrete. *Cement and Concrete Research,* May 2007, 735-742.

[14] SANCHEZ DE JUAN, M.. GUTIERREZ, P. A.: Study on the Influence of Attached Mortar Content on the Properties of Recycled Concrete Aggregate. *Construction and Building Materials,* 23, 2009, 872-877.

[15] NIXON, P. J.: Recycled Concrete as an Aggregate for Concrete a Review. *Material and Structures*, Springer Netherlands, 1978, 371-378.

[16] EVANGELISTA, L., DE BRITO, J.: Durability Performance of Concrete Made with Fine Recycled Concrete Aggregates. *Cement & Concrete Composites* 32, 2010, 9-14.

[17] BOEHME, Luc, et. al.: *ValReCon20 - Valorization of Recycled Concrete Aggregates in Concrete C20/25 & C25/30*, Leuven : ACCO, 2012.

[18] LOPEZ-GAYARRE, F. et al.: Influence of Recycled Aggregate Quality and Proportioning Criteria on Recycled. *Waste Management*, 2009, 3022-3028.
[19] MARTINEZ-LAGE, I. et al.: Properties of Plain Concrete Made with Mixed Recycled Coarse Aggregate. *Construction and Building Materials*, December 2012, 171-176.
[20] BOEHME, L. et al.: *Assessment of Water Reducing Admixture in Concrete with Recycled Aggregates*, Prague : CESB13 - Central Europe towards Sustainable Building, 2013.
[21] TOPCU, I. B.: Physical and Mechanical Properties of Concretes Produced with Waste Concrete. *Cement and Concrete Research*, December 1997, 1817-1823.
[22] RAHAL, K.: Mechanical Properties of Concrete with Recycled Coarse Aggregate. *Building and Environment*, January 2007, 407-415.
[23] EN 1097-6 *Tests for Mechanical and Physical Properties of Aggregates - Part 6: Determination of Particle Density and Water Absorption*, Brussels : European Union : CEN, 2000.
[24] KOTES, P., VICAN, J., SLAVIK, J.: Influence of Reinforcement Corrosion on Reliability of Existing Concrete Structures (in Slovak), *Communications - Scientific Letters of the University of Zilina*, vol. 3, No. 4, 2001, pp. 41-49, ISSN 1335-4205.
[25] CSN EN 12620 + A1. *Aggregate for Concrete (in Czech).* Praha : Cesky normalizacni institut, 2008.

Zuzana Papanova - Daniel Papan - Jan Kortis *

MICROTREMOR VIBRATIONS IN THE SOIL EXPERIMENTAL INVESTIGATION AND FEM SIMULATION

Vibration problems of the building structures caused by technical seismicity are becoming increasingly topical. The aim of this paper is to show FEM simulation of the spreading wave impact, which causes vibration system consisting of subsoil-structure interaction in microtremor. The results of the experiment together with this theoretical analysis and FEM simulation appear to be effective application for engineering experience. They are also used in assessing and predicting the vibration effects induced by technical seismicity due to traffic. [1].

Keywords: *FEM simulation, vibration, response, spectrum, soil, interaction.*

1. Introduction

The *FE* simulations and experimental measurements are used for the purpose of designing and evaluating the structures. However, the experimental measurements are often economically challenging and time-consuming. In the area of structural dynamics, the assessment structure is based on the dynamic response of the structure due to dynamic loading. Each standard has criteria for evaluating the dynamic response. For these purposes appropriate methodology of the *FEM* simulation can be applied. Load of technical seismicity requires precise approach to creating a *FEM* model. During the *FEM* model creation it is necessary to consider the interactive dynamic area. This paper contains a case study of the *FEM* simulation of the dynamic response of the model due to the mechanical impact load. The analytical results are compared with the experimental measurement "in situ". For the purpose of the case study a real single-family house was chosen. It is located close to the railway line, which produces dynamic effects due to technical seismicity. The house of this type was selected as the most frequent building located near the railway line in Slovakia.

2. Description of the analysed object and its locality

The analysed object is a real single-family house located in the city of Zilina, in the area of Strazov. Strazov is situated in the western part of Zilinska Lehota and Dolny Hricov. In the eastern side it is separated from Zilina by the Rajcanka river. In the south it borders on the urban parts of the gardening area. In the northern side of Strazov there is a reservoir called the Hricov dam, city part Povazsky Chlmec and a village named Divinka. The investigated object (Fig. 1) is the house (built in 1962) which has an irregular floor plan and the built-up area is 91.72 square meters.

Fig. 1 The views on the single-family house

Its layout is spread over two floors and the whole surface basement. The attic serves as a storage. Perimeter and interior load bearing walls (the thickness of 450 mm and 300 mm) are built of traditional baked bricks on lime-cement mortar. Non-

* **Zuzana Papanova, Daniel Papan, Jan Kortis**
Department of Structural Mechanics, Faculty of Civil Engineering, University of Zilina, Slovakia
E-mail: zuzana.papanova@fstav.uniza.sk

bearing interior walls are made of bricks. Ceilings are reinforced, thickness 200 mm, reinforcing wreaths are also reinforced concrete, monolithic concrete class C 20/25 and steel 10 505 (R). The building is covered with a saddle-shaped roof with a slope of 40°. The roof load bearing structure is created from a standing stool. The room flooring (ceramic tiles and wood floors) are distributed inside. Access to the ground floor and the basement is provided with a wooden staircase (Fig. 2).

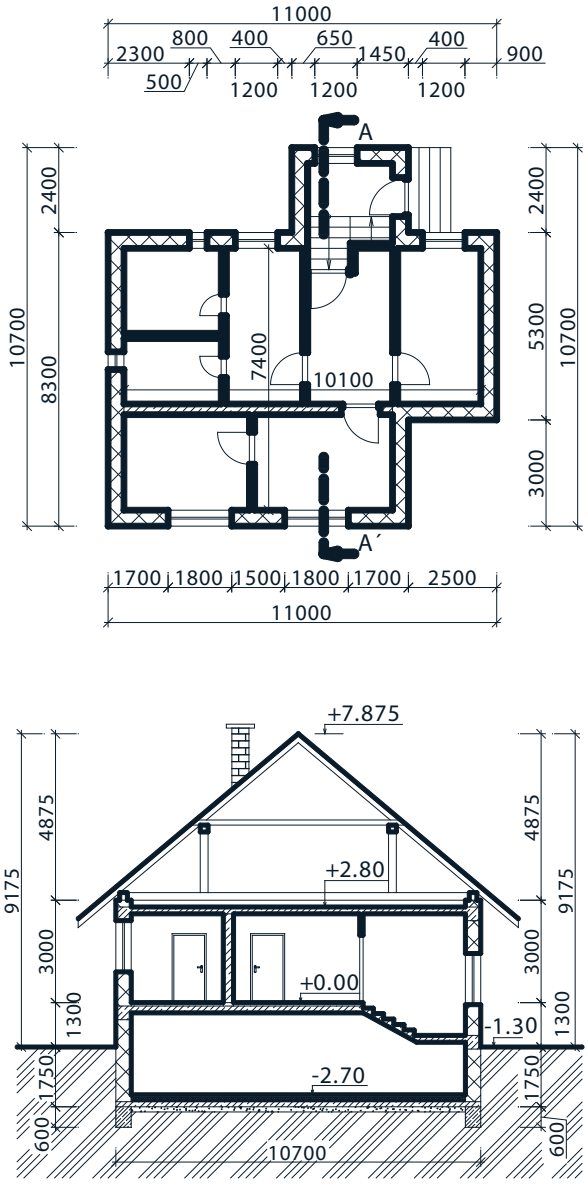

Fig. 2 Plan and cross-section of the single-family house

3. Soil dynamic diagnostics and experimental investigation

The pursued objectives of the measurement were carried out in two phases. The impulse - seismic method (ISM) was applied in the first phase. The ISM is based on the surface wave propagation in the form of pulses from the impact source. The second phase was to carry out an experimental evaluation of the basic soil parameters. Experimental devices used during measurements are shown in Fig. 3.

Dynamic response of real environment (half-space) response loaded by impulse excitation was measured using a set of five accelerometers with a frequency range of 1 ÷ 4000 Hz. (Bruel-Kjaer). The accelerometers were placed in drilled ground holes and on the object (Fig. 4). The accelerometers measured response in the vertical direction. Dynamic response in the observed points were measured in the form of vibration velocities (m/s), in three orthogonal directions *x, y, z*. The measurement was performed using the "off - line" method. The recorded signals are simultaneously saved in two PCs - AMILO and PC FS (NI Compact DAQ software). Evaluation of the measured data was carried out in laboratory conditions of the Department of Structural Mechanics (DSM), Faculty of Civil Engineering (FCE), University of Zilina based on the evaluation of software lines DSM.

The measuring unit consisted of:

- piezoelectric accelerometers BK 8306 (Bruel - Kjaer) - 5pcs,
- integration amplifier BK-2693-014 (Brüel-Kjaer), measuring Notebooks,
- AD converters NI Compact DAQ (NI - National Instrument).

Mechanical movement in the measuring points was transformed by measuring line of accelerometers from an electrical signal after amplification and integration to the vibration acceleration - *a(t)* and vibration velocity - *v(t)*. It was conducted by means of shielded cables to the measuring center near the object. Notebooks were calibrated with NI Compact DAQ AD converters. The analog signal was recorded and saved using NI Lab View software with the sampled frequency f_s = 1000 Hz (the required criteria for sampling signals is $\Delta t < 1/2\, f_{max}$).

Impulse device location and the position of the measured points are schematically shown in Fig. 4. In this case, the experimental finding of soil environment vibration intensity due to impact excitation and its frequency transfer were performed. Excitation signals were propagated as a surface and shear wave from the source. These signals had the stochastic character with the variable performance in time and space. For further analysis the characteristics of an ideal the elastic half space can be used for the soil.

Fig. 3 Accelerometers installed in soil and on structure, ISM procedure

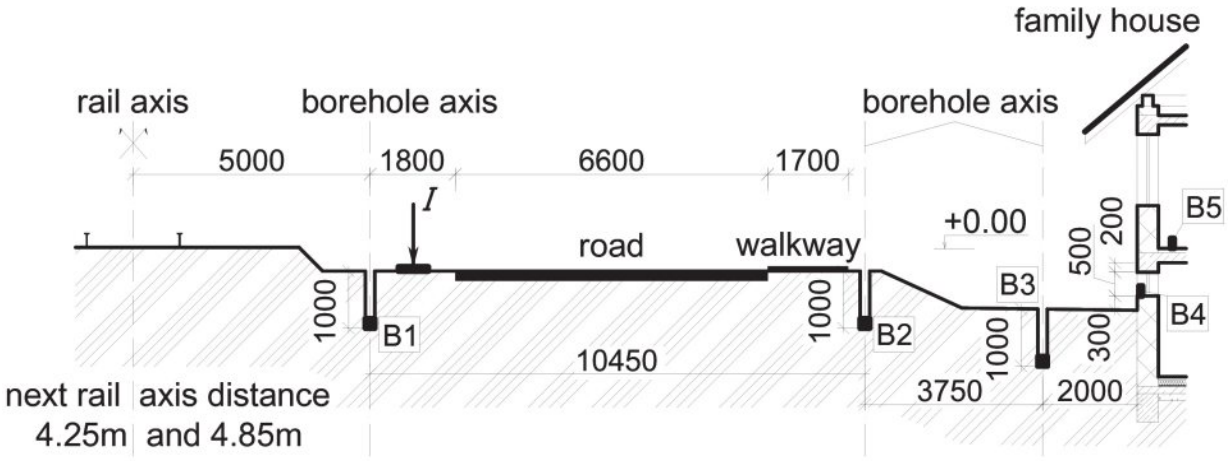

Fig. 4 Experimental measurement scheme

In order to obtain the velocities time histories of vibration in the observed geological location due to impulse, it was necessary to establish the basic soil dynamic parameters. The impulse seismic method (ISM) was used in this case as a simple way to get the basic soil parameters. In the calculations of elastic modulus of the investigated natural environment the following mechanical characteristics were needed:

- $\nu \approx 0.33$ (Poisson ratio),
- unit weight $\rho_{13} \approx 1760$ kg/m^3 (for sandy clays and gravels, point B1 - B3),
- unit weight $\rho_{34} \approx 1600$ kg/m^3 (the sample weight, clays and sandy clays, point B3 - B4).

Velocity of surface waves (C_R) was measured between the points B1-B3 and B3-B4. The corresponding power spectra $Gii(f)$ and cross power spectra $G_{ik}(f)$ together with the coherence function $\gamma_{34}^2(f)$ and transfer characteristic or gain factor $H_{ik}(f)$ calculated from the vibration velocity time histories of pulse load in points $v_3(t)$-$v_4(t)$ are shown in Fig. 6 as an analysis preview. Velocities of Rayleigh surface waves were observed using an analysis of the correlation [2] – cross correlation function $R_{ik}(\tau)$:

the sandy clays and gravels point B1 - B3 compact road subsoil and pavement from 0.0 to 4.0 m level below the surface (Impulses) $C_R \approx 128$ - 132 m/s,

for clays and sandy clays point B3 - B4, subsoil at 1.0 to 5.0 m level below the surface (Impulses) $C_R \approx 92$ - 98 m/s.

For investigated soil environment ($\nu \approx 0.33$) the correlation between Rayleigh surface and shear wave velocity [3] can be evaluated in the equation (1).

$$C_S = \frac{C_R}{0.93} \cdot [\mathrm{m/s}] \tag{1}$$

Seismic modulus of elasticity in shear strength-pressure is then calculated from the equation (2):

$$G_0 = C_S^2 \rho, \quad E_0 = 2G_0(1+\nu) \quad [\mathrm{MPa}]. \tag{2}$$

Substituting the average value of wave velocity to (2) the elastic modulus parameter [4] was calculated for:

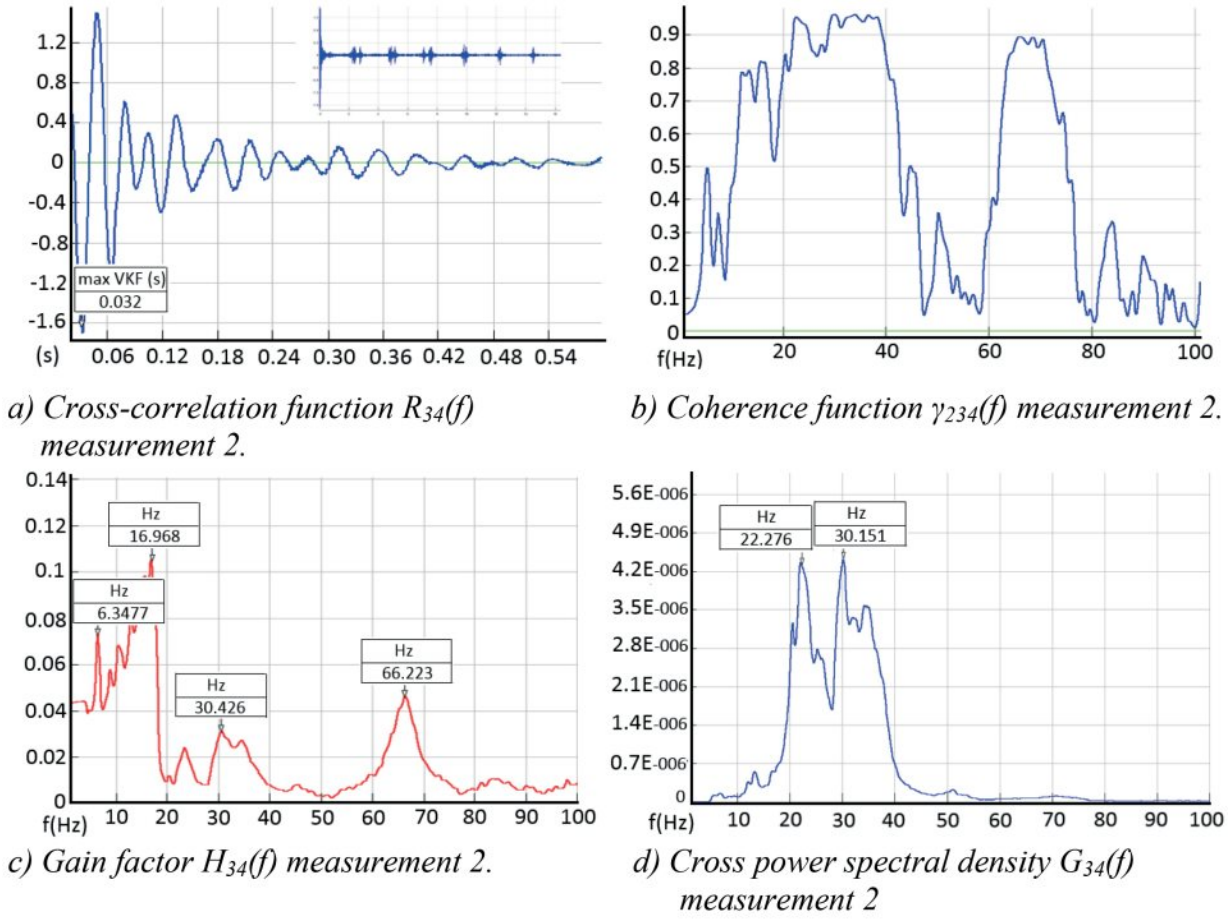

a) Cross-correlation function $R_{34}(f)$ measurement 2.

b) Coherence function $\gamma_{234}(f)$ measurement 2.

c) Gain factor $H_{34}(f)$ measurement 2.

d) Cross power spectral density $G_{34}(f)$ measurement 2

Fig. 5 The ISM- Analysis of impulses in the time and frequency domains in points B3, B4

- subsoil (points B1-B3, ρ_{13} = 1760 kg/m^3)
  $E_0 \approx 77.33$ [MPa], $G_0 \approx 29.74$ [MPa],
- subsoil – foundation of the house (points B3-B4, ρ_{34} = 1600 kg/m^3)
  $E_0 \approx 39.42$ [MPa], $G_0 \approx 14.40$ [MPa].

Attenuation parameter α_R, according to material and geometric characteristics of the soil environment damping in frequency range (0-100 Hz) had the following averaged values: $\alpha_R \approx 0.286$ m^{-1} (measurement series 1 and 2).

Frequency response characterized by cross power spectral density $G_{ik}(f)$ or gain factor $H_i(f)$ can determine the most suitable impulse excitation. A wide range of excitation frequencies from passing trains is not included in this transmission. The subsoil has a dominant band of transmission frequencies: f_{DI} = 20 ÷ 52 Hz. The example of ISM procedure analysis functions is shown in Fig. 5.

4. FEM simulation of the vibrations transmission in the soil

The finite element method as the most widely used numerical method for finding approximate solution is used for modelling the wave propagation in the elastic subgrade. This phenomenon is governed by the following equation

$$\mathrm{M}\ \ddot{\mathrm{U}} + \mathrm{C}\ \dot{\mathrm{U}} + \mathrm{K}\ \mathrm{U} = \mathrm{R} \tag{3}$$

Solution of the equation is reached by the central difference method which assumed that the first derivative is

$${}^{t}\dot{\mathrm{U}} = \frac{1}{2\Delta t}\left(-{}^{t-\Delta t}\mathrm{U} + {}^{t+\Delta t}\mathrm{U}\right) \tag{4}$$

and second derivative is

$${}^{t}\ddot{\mathrm{U}} = \frac{1}{\Delta t^2}\left({}^{t-\Delta t}\mathrm{U} - 2{}^{t}\mathrm{U} + {}^{t+\Delta t}\mathrm{U}\right) \tag{5}$$

The governing equation is given in the following form

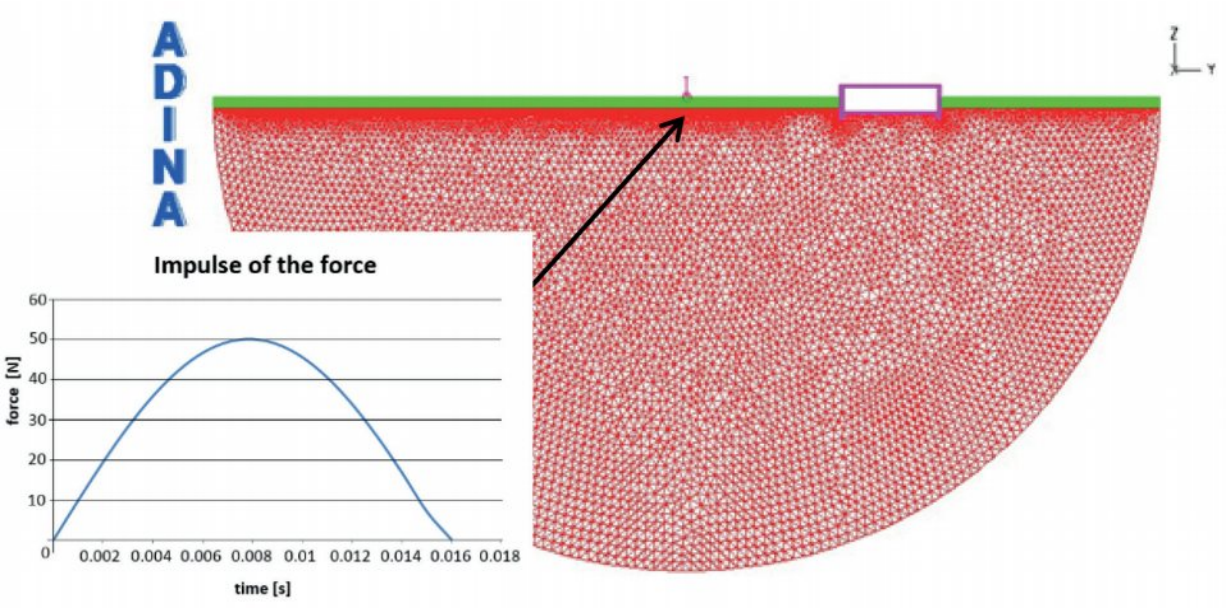

Fig. 6 The model for numerical simulation with dynamic load

$$M\,{}^{t}\ddot{U} + C\,{}^{t}\dot{U} = {}^{t}R + {}^{t}F \tag{6}$$

Substituting for ${}^{t}\dot{U}$ ${}^{t}\ddot{U}$ we obtain

$$\left(\frac{1}{\Delta t^2}M + \frac{1}{2\Delta 1}C\right)^{t+\Delta t}\ddot{U} = {}^{t}R + {}^{t}F + \frac{2}{\Delta t^2}M\,{}^{t}U - \left(\frac{1}{\Delta t^2}M + \frac{1}{2\Delta 1}C\right)^{t+\Delta t}U \tag{7}$$

It can be used to solve the value ${}^{t+\Delta t}U$.

The ADINA software was used for the soil vibration simulation. This software is used to do the numerical simulation because it offers the explicit dynamic analysis which is based on the central difference method. This method is appropriate for the solution of wave propagation. The geometry of the model is defined in a plane. It means that the spacious character of the wave propagation is neglected. The result is that the amount of equations is lower and there is no problem with solution of the simulation by using a common computer. The shape of a half-circle with a diameter of 50 meters is used to define the subgrade. The zero displacements are prescribed at the edge of the model (Fig. 6). This can be done because the width of the model is longer than the wave can pass during the time of the simulation. It means that the wave does not bounce back from the edge of the model.

The defined material characteristics of the subgrade are comparable with the values obtained from experimental analysis. The walls of the house are made as brick structures and the flooring plate is made of concrete. Results in the time domain for whole *FE* field in several time steps are shown in Fig. 7. (*FE* displacement)

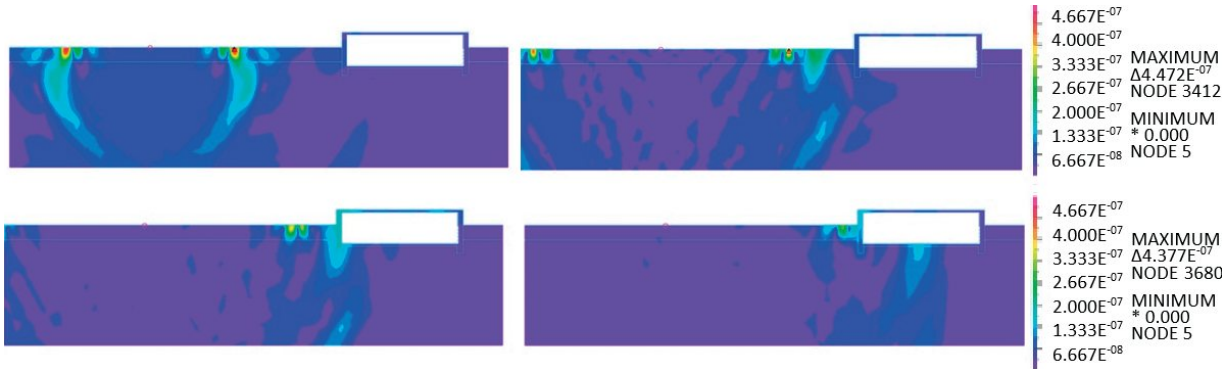

Fig. 7 Displacement magnitude in time t (sec)

5. Experimentand comparison of FEM results

FEM simulation was performed in the time domain. The measured power pulse was used as load. For dynamic load the pulse shape divided into time steps 0.001 sec. was considered in order to compare the results with experiment. The time duration of the pulse load 0.016 sec was determined experimentally. Force amplitude reached the value of 50 N. These values were statistically evaluated as the average parameters. The results of *FEM* simulation in time and frequency domains are shown in Fig. 8. The time histories from experimental measurements are in relatively good accordance with the time histories obtained from *FE* simulation in points B1-B5. Time shifts between Rayleigh and shear waves propagation are identical. Particle velocities are not so identical due to inhomogeneity of the soil [5].

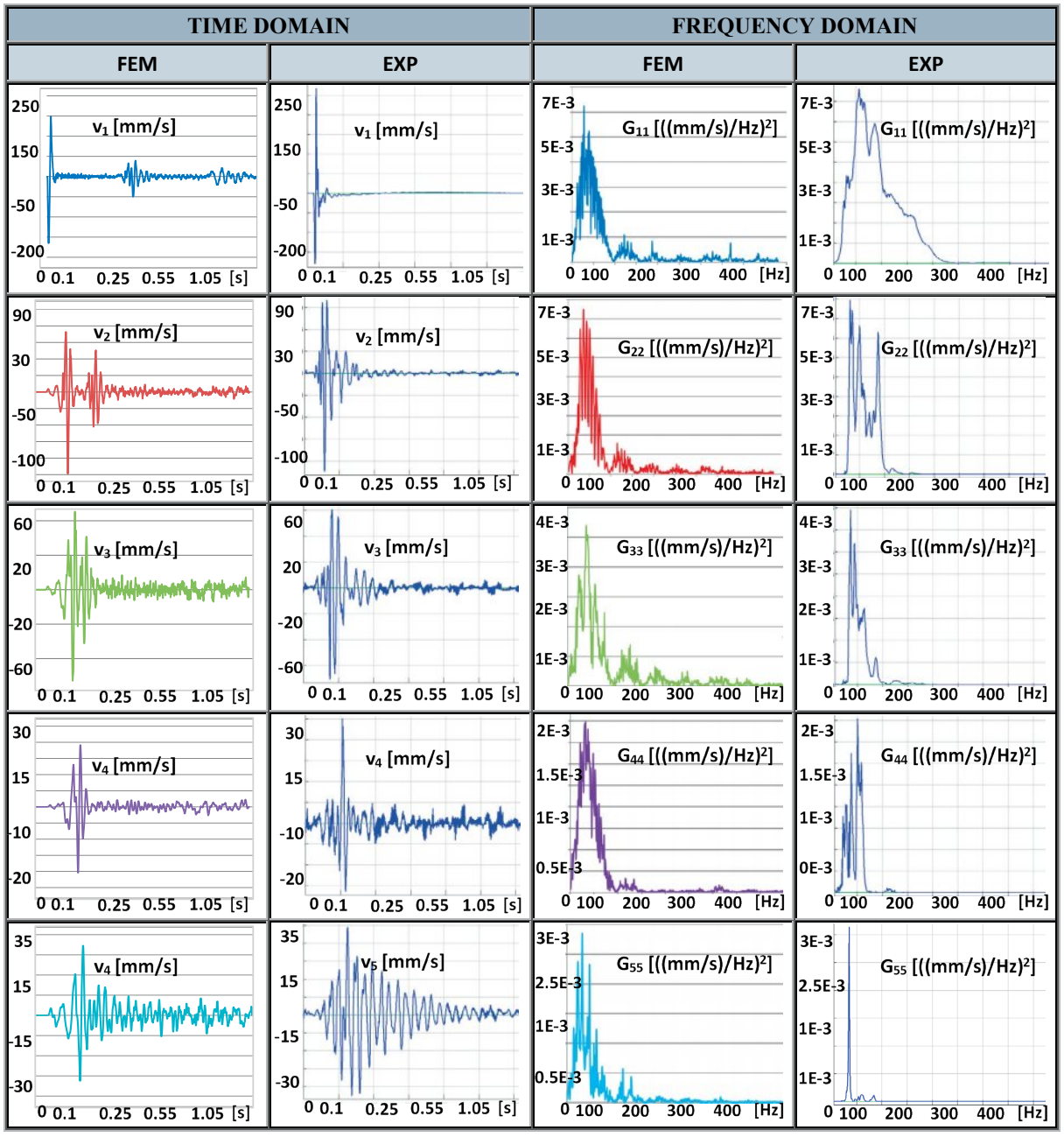

Fig. 8 FE and experimental comparison in time and frequency domains (points B1 - B5)

6. Conclusions

Problems with the vibrations of civil structures due to technical seismicity resources are current. Soil-borne vibrations and their effects on civil structures can be solved theoretically (using *FEM* simulations) and can also be detected experimentally [6]. Experimentally obtained dynamic response of the structure is an objective basis for the structure evaluation loaded by technical seismicity effects. Measurements are not possible in the case of new buildings (designed near technical seismicity sources). In this case it is possible to measure the dynamic response in the reference points for future civil structure. These measured records can be used as a dynamic load for *FE* model. In such simulation, however, the soil-structure interaction can not to be considered. The case study shows the possibility of using complex modeling layered soil with structure interaction. The results obtained by *FEM* simulation are in good accordance with the experiment. It is necessary to know the basic parameters of the soil for the complex computing model. These parameters can be easily detected using the ISM method. The most effective method to estimate the effects of the technical seismicity on structures can be the combination of theoretical - *FEM* simulation and experimental measurements [7] .

Acknowledgement

This paper was created with the support of the OP Education for the project "Education quality support and research for the transport sector as the engine of the economy" (ITMS: 26110230076), which is co-financed by the European Social Fund.

Modern education for the knowledge society / Project co-financed from EU sources.

References

[1] JUHASOVA, E.: *Action of Seismic Motions on Building Structures.* Veda, Bratislava, 1985

[2] BENDAT, J. S., PIERSOL, A. G.: *Engineering Applications of Correlation and Spectral Analysis*. Wiley : New York, 1980

[3] RAYLEIGH, J. W.: *On Waves Propagation along the plane Surface on Elastic Solid.* Proc. Math. Soc., London, 1885

[4] DECKY, M., DRUSA, M., PEPUCHA, L., ZGUTOVA, K.: *Earth Structures of Transport Constructions.* Pearson Education Limited, 2013, Edinburg Gate : Harlow : Essex CM20 2JE. Edited by Martin Decky, p. 180, ISBN 978-1-78399-925-5.

[5] POLAK, M., PLACHY, T., ROTTER, T.: *Vibration Monitoring of the Bridge Loaded by Heavy Vehicle Traffic*, 5th WSEAS intern. Conference on Applied and Theoretical Mechanics Location, Puerto de la Cruz, 2009, 120-123.

[6] BENCAT, J., STYPULA, K.: Buildings Structure Response Due to Railway Traffic. *Communications - Scientific Letters of the University of Zilina,* vol. 15, No. 2, 2013, 41-48. ISSN 1335-4205.

[7] COULIER, P., FRANCOIS, S., DEGRANDE, G., et al.: Subgrade Stiffening Next to the Track as a Wave Impeding Barrier for Railway Induced Vibrations. *Soil Dynamics and Earthquake Engineering*, vol. 48, 2013, 119-131. ISSN 0267-7261.

Izabela Major *

THE ACCELERATION WAVE IN A THIN TWO-MATERIAL AND THREE-SEGMENTAL ROD WITH SLOWLY CHANGING CROSS-SECTION MADE OF MURNAGHAN MATERIAL

The paper presents propagation of acceleration waves in a thin rod with slowly changing cross-section made of hyperelastic Murnaghan material. Analytical calculations were made based on the models obtained for the intensity of the transmitted and reflected wave. Numerical analysis of the velocity of wave propagation in the three-segmental rod made of two compressible elastic materials (steel and aluminum) has been made.

Keywords: *Murnaghan material, acceleration wave, compressible material, FEM.*

1. Introduction

A mathematical model of continuum is used for investigations in numerous fields of science, whereas the results obtained are used in practice in different aspects of technological solutions. However, finding a relatively simple constitutive relationship, which contains small number of constants and can be used in modelling of material properties in the full range of deformation, remains the subject of many studies and analyses.

Constitutive equations have the nature of phenomenological relations determined usually by means of experimental studies and represent a specific link that connects deformation of the material caused by the stress. These equations describe the relationships between deformations and stresses or between deformations and energy for hyperelastic materials are obtained based on the equations of mechanical energy balance. The model of material is adopted depending on the factors that are of essential importance to behaviour of the specific medium. The most frequently used constitutive relationship for compressible materials is Murnaghan elastic potential.

In terms of the theory of elasticity and in broadly understood mechanical problems, including continuum mechanics, elastic bodies are considered as material continuum with internal bonds and without them. For the elastic bodies without bonds, the properties of such a medium are given if the function W can be defined, which, for any deformation d of this medium, determines the corresponding elastic energy $W=W(d)$ accumulated in the unit of volume with respect to the reference configuration B_R.

Function W is typically defined as a function of deformation energy. For uniform isotropic elastic bodies, the constitutive equations can be written as

$$W = W(I_1, I_2, I_3) \tag{1}$$

where I_1, I_2, I_3 are invariants of the deformation tensor.

2. The acceleration wave in a thin segmental rod with slowly varying cross-section

The basic equations of propagation for the rod discussed originate from the study [1]. According to this study, in the case of propagation of the acceleration wave in a hyperelastic rod with variable cross-section (Fig. 1), the equation of transport for the wave intensity is a generalized Riccati equation. A supplementation of the above publication is the study [2] where authors demonstrated that the intensity of the acceleration wave that propagates in a rod with variable cross-section, with elastic potential $\Sigma(p)$ meeting the condition $\partial^3\sum/\partial p^3 \neq 0$, is represented by the Bernouli equation (p denotes displacement gradient).

We consider a homogeneous isotropic elastic material with elastic potential Σ and constant density ρ_R. An axially-symmetric, semi-infinite thin rod is assumed, with its cross-section varying slowly with the distance. A Cartesian system of material coordinates $\{X_\alpha\}$ in the reference configuration B_R and Cartesian system of spatial coordinates $\{x_i\}$ in the current configuration B are also assumed for $(i, \alpha = 1,2,3)$, which parameterize the same space and are mutually covered. The deformation of the rod is (see [1])

$$x = u(X,t) + X \quad \text{for} \quad x_1 = x \tag{2}$$

* **Izabela Major**
Department of Technical Mechanics, Faculty of Civil Engineering, Czestochowa University of Technology, Poland
E-mail: admin@major.strefa.pl

where *u(X,t)* is a displacement of the points of continuum in the direction of the rod axis.

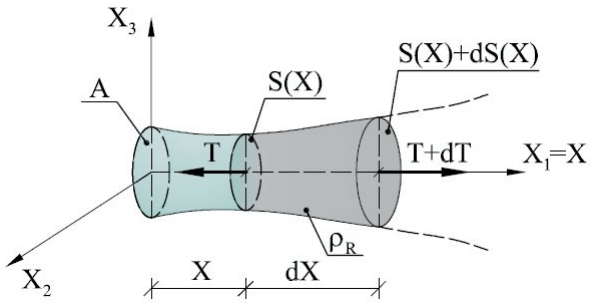

Fig. 1 Axially-symmetric rod with slowly varying cross-section

For the deformation (2), the equation of motion is (see [1])

$$\frac{\partial v}{\partial t} - c^2 \frac{\partial p}{\partial X} - \frac{T}{\rho_R} - \frac{d}{dX} \ln S(X) = 0 \tag{3}$$

where $c = c(p) = \left(\frac{1}{\rho_R} \frac{\partial^2 \Sigma}{\partial p^2} \right)^{\frac{1}{2}}$ (4)

The above term Σ means elastic energy accumulated per unit of surface. For the case of the rod considered, the condition (3) represents basic equations of single-dimensional propagation of the acceleration wave.

2.1 Propagation of the acceleration wave

We assume that the propagation of disturbance occurs along the rod axis in the direction of the axis *X*. The area before the front remains undisturbed and is subjected to the deformation $p_o(X)$. Functions *p* and *v* are continuous, the discontinuity jump occurs for their first and second derivatives.

We assume an exponential change in the rod cross-section $S(X) = A_o e^{\gamma \cdot x}$ for $\sigma_1(X)$ and $S(X) = A_o e^{-\gamma \cdot x}$ for $\sigma_2(X)$. Therefore, the acceleration wave intensity $\sigma(X)$ is (see [2] and [3])

$$\sigma_{1,2}(X) = \sigma(0) \frac{e^{\pm \frac{Q(X) \cdot X \cdot \gamma}{2}}}{1 \mp \sigma(0) \left[2 \left(e^{\pm \frac{Q(X) \cdot X \cdot \gamma}{2}} \right) \frac{\beta(X)}{Q(X) \cdot \gamma} \right]} \tag{5}$$

where $Q(X) = \left[1 - \frac{T_0}{2\rho_R^2 c_o^4} \left(\frac{\partial^3 \Sigma}{\partial p^3} \right) \right]$ (6)

$\sigma(0)$ is an initial value of the acceleration wave intensity for *X=0*, whereas

$$\mu(X) = \frac{1}{2} \left[1 - \frac{T_0}{2\rho_R^2 c_o^4} \left(\frac{\partial^3 \Sigma}{\partial p^3} \right) \right] \left[\frac{d}{dX} \ln S(X) \right]$$

and $\beta(X) = -\frac{1}{4\rho_R c_o^4} \left(\frac{\partial^3 \Sigma}{\partial p^3} \right)$ (7)

The above term c_o represents the velocity of propagation of the front of acceleration wave [2].

2.2 Acceleration wave for Murnaghan material

We assume that the acceleration wave propagates in a compressible elastic material determined by Murnaghan potential [4]

$$W(I_1, I_2, I_3) = \rho_R \Sigma(I_1, I_2, I_3) = \frac{l + 2m}{24} (I_1 - 3)^3 + \\ + \frac{\lambda + 2\mu + 4m}{8} (I_1 - 3)^2 + \frac{8\mu + n}{8} (I_1 - 3) - \frac{m}{4} \\ (I_1 - 3)(I_2 - 3) - \frac{4\mu + n}{8} (I_2 - 3) + \frac{n}{8} (I_1 - 1), \tag{8}$$

where λ and μ are Lame's constants, *l,m,n* - elastic constants of the second order. We assume these constants according to Table 1 (see [5]).

Elastic constants for steel and aluminum [5] Table 1

Material	λ [GPa]	μ [GPa]	*l* [GPa]	*m* [GPa]	*n* [GPa]
Steel	108.854	80.513	-452.087	-623.703	-694.311
Aluminum	55.898	27.066	-304.987	-393.247	-400.111

3. Calculations for two-material and three-segmental rod

For the analysis of propagation of the surface of discontinuities, modelled as a flat acceleration wave, we assumed a thin, axially-symmetric three-segmental rod with slowly varying cross-section. Each of the three segments, at the lengths of l_i, for *i=1,2,3* (Fig. 2), were made of homogeneous hyperelastic materials with isotropic properties. c_i and ρ_i denote velocity of propagation of the longitudinal waves and the density of the material. It was assumed that the cross section *S(X)* changes with the distance. We assume that, at the instant *t=0* for *X=0*, propagation of the surface of discontinuities occurs along the increasing values of the axis *X*, whereas the area before the wave front remains undisturbed $v(X,t)=0$. The functions of the velocity of propagation ν and gradient of displacement *p*, are according to [3].

3.1 Intensity of the acceleration wave for the cases of the rod analysed

It was assumed that σ(X) is the intensity of the wave at the point *X* of the rod studied. For γ>0 and γ<0, intensity of the

acceleration wave is given by (5). For analytical calculations, we assume a static velocity of deformation of the order of 10 s^{-1}.

It was assumed that the shape of the rod is described, for the first segment and the half of the second segment by $S(X) = A_o e^{-\gamma \cdot x}$, and, from the half of the segment 2 and in the third segment, by the function $S(X) = A_o e^{\gamma \cdot x - 0.3}$.

Based on the conditions on the division plane, we assume that

$$\left.\frac{\sigma^{T2}(X^+)}{\sigma_1(X^-)}\right|_{X=l_1} = \frac{2\rho_{R1}c_1}{\rho_{R1}c_1 + \rho_{R2}c_2}, \qquad \left.\frac{\sigma^{T3}(X^+)}{\sigma 2(X^-)}\right|_{X=l2} = \frac{2\rho_{R2}c2}{\rho_{R2}c_2 + \rho_{R3}c_3} \tag{9}$$

$$\left.\frac{\sigma^{R1}(X^-)}{\sigma_1(X^-)}\right|_{X=l_1} = \frac{\rho_{R1}c_1 - \rho_{R2}c_2}{\rho_{R1}c_1 + \rho_{R2}c_2}, \qquad \left.\frac{\sigma^{R2}(X^-)}{\sigma 2(X^-)}\right|_{X=l2} = \frac{\rho_{R2}c_2 - \rho_{R3}c_3}{\rho_{R2}c_2 + \rho_{R3}c_3} \tag{10}$$

X^+ is a coordinate on the surface Λ before the front of the acceleration wave, whereas X^- is the coordinate on the same surface Λ behind the front of the acceleration wave.

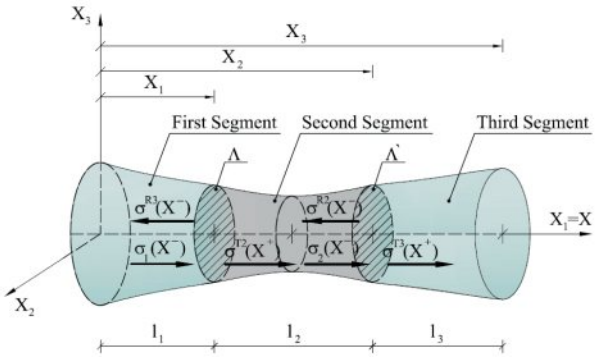

Fig. 2 Flat acceleration wave (falling σ(X), reflected σ^R(X) and transmitted σ^T(X)) that propagates in two-material three-segmental rod with varying cross-section

We assumed two non-linear compressible elastic materials described with Murnaghan potential [6]. Cross-section of the rod changes exponentially, and this change is described by the function $S(X) = A_o e^{-\gamma \cdot x}$. It was assumed that in the second segment, the change in the cross-section of the rod occurs from decreasing into increasing (see Fig. 2)

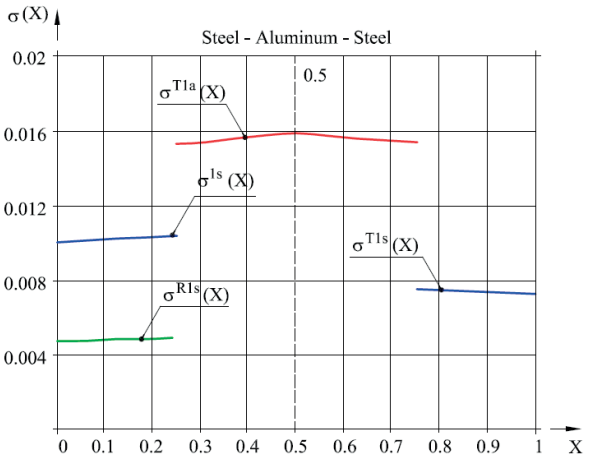

a) Case one

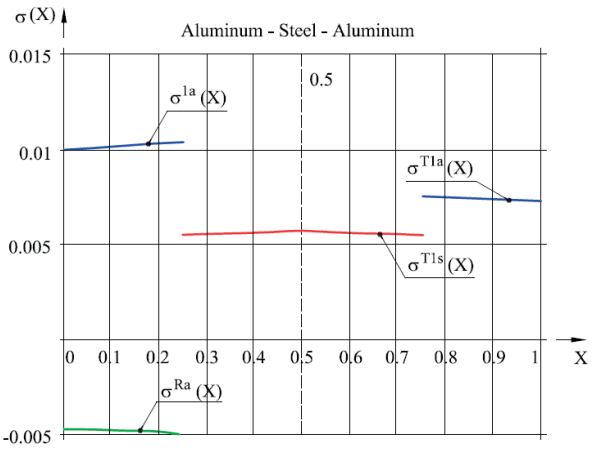

b) Case two

Fig. 3 Intensities [m/s²] of the acceleration wave (falling σ(X), transmitted σ_T(X) and reflected σ_R(X)) for three-segmental two-material rod with the length of $X \in \langle 0;1 \rangle$ m. Superscripts s and a correspond to steel and aluminum, respectively

The calculations for the three-segmental and two-material rod showed that the change in the cross-section of the rod causes the change in the intensity of the propagating acceleration wave. This is particularly noticeable in the second segment of the rod where the increasing and decreasing function is observed. Due to different density of the materials at the sections l_1, l_2, l_3, which are 0.25 m, 0.5 m and 0.25 m, respectively, the intensity jumps are observed in the surface of contact of individual segments for the propagating acceleration wave. The charts presented in Fig. 3a show that the intensity of the acceleration wave that goes through aluminum to the steel decreases. After transition from the steel to aluminum, it increases. This causes that the intensity of the acceleration wave that propagates in the hyperelastic material that moves from the material with lower density to the material with

higher density is decreasing, whereas in the case of moving from the material with higher density towards the material with lower density, the intensity increases. The initial value of the intensity of the acceleration wave of 0.01 m/s^2 after moving through the first segment of the rod has at the beginning of the second segment the value higher in aluminum ~0.01526 m/s^2 and lower in steel ~0.0055 m/s^2. This leads to the conclusion that the intensity of the wave transmitted in aluminum increases by ca. 50% compared to the intensity of the wave propagating in steel and decreases in steel also by ca. 50% compared to the wave propagating in aluminum.

3.2 Numerical example

In order to carry out the numerical modelling of the course of wave (disturbance) propagation in an isotropic, two-material and three-segmental rod with slowly changing cross-section, we adopted two 2D objects which are the cross-section of the rod with the length of 1m (see Fig. 4). The initial and final diameters of the rod are 10 cm, whereas the middle diameter in 9.2 cm and, at the contact of segments (the first with the second and the second with the third), it is 9.6 cm. Discretization of the object discussed was carried out by means of 4 nodes. Due to the variety of rod diameters in the frontal and middle planes and at the surface of the contact of materials, generation of the grid forced, in several points, creation of 3 node objects. In order, for the rod analysed, we obtained 1000 elements 2D. The load of the objects analysed was represented by forced linear dislocation of the edges L11 towards the y axis. The value of the forced displacement amounted to 1cm for the time t=0.01 s. On the opposite (with respect to the load) L1 edge, the bonds were imposed to prevent from displacement towards y and z axes. These are bonds {B}, see Fig. 4.

The aim of the numerical calculations was to model the propagation of the wave (disturbance) for the three-segmental rod made of two compressible elastic materials (steel and aluminum). ADINA software was used to present the problems referring to analytical computations performed in this paper (see also [7]). ADINA is a program often used for stress and velocity analysis [8]. Calculations were made for the above boundary conditions and the assumed deformation. The declared load in the object occurred at the instant t=0.01 s, and then the effect was removed. The process of propagation of the disturbance in the model could be observed in 100 other steps. The dynamic implicit method was used. Therefore, we obtained information about generation of the velocity of disturbance propagation in two-material and three-segmental compressible rods with slowly varying cross-section.

For the given boundary conditions and external effects (displacements), Figs. 5 and 6 show the course of propagation of disturbance in two-material and three-segmental rod for selected time steps.

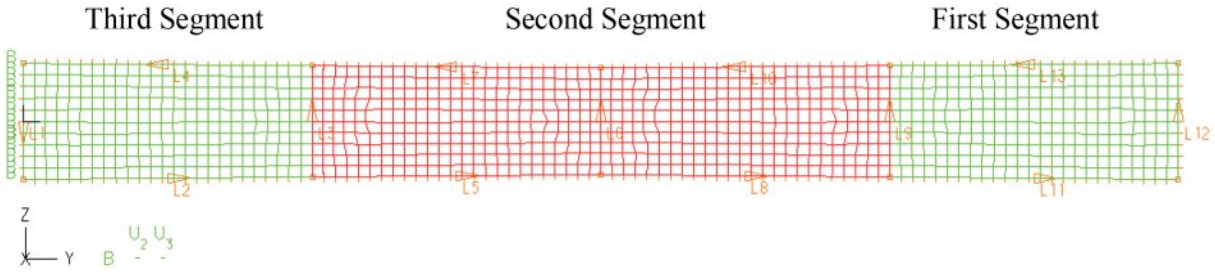

Fig. 4 2D model of a rod: grid, load and boundary conditions

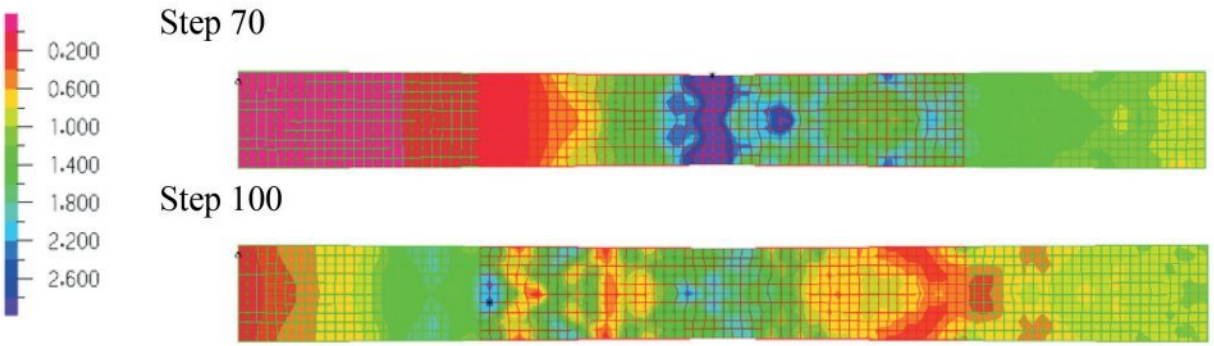

Fig. 5 The velocity of wave propagation [m/s] in steel (on the right), aluminum (in the middle) and steel (on the left), respectively

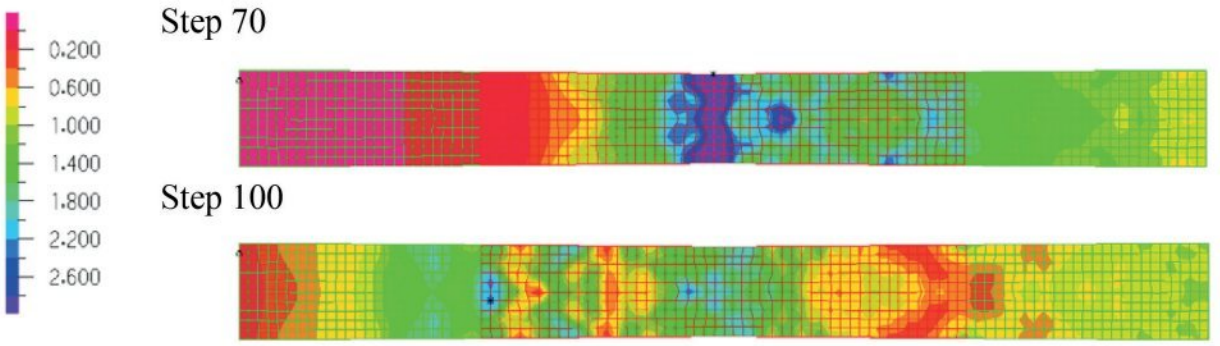

Fig. 6 The velocity of wave propagation [m/s] in aluminum (on the right), steel (in the middle) and aluminum (on the left), respectively

4. Conclusions

The comparative analysis carried out for the velocity of propagation of the wave (disturbance) in the rod with increasing and decreasing cross-section obtained using the adopted numerical model reveals that there are differences in the course of wave propagation in steel and aluminum. The results obtained confirm the results obtained through analytical investigations. It can be noticed that the wave velocity varies depending on the cross-section for the rod configurations analysed. The propagating wave, moving from the material with lower density (aluminum – 2700 kg/m^3) to the material with the greater density (steel – 7859 kg/m^3) decreases the velocity of propagation, see Fig. 5, step 100, and Fig. 6, step 70. At the moment of transition from the segment 1 to 2 a change in the velocity of the propagating transmitted wave can be observed (i.e. during transition from steel to aluminum, see Fig. 5 and from aluminum to steel, see Fig. 6). With transition from steel to aluminum, the velocity increases from ˜1.4 m/s to ˜2.6 m/s, whereas with transition from aluminum to steel, it decreases from ˜1.625 m/s to ˜0.875 m/s. Similar pattern is observed for the velocity of the transmitted wave for the transition from the segment 2 to segment 3. With transition from steel to aluminum, the velocity of the propagated wave increases (Fig. 6, step 100), whereas with transition from aluminum to steel, it decreases (Fig. 5, step 100). At the moment of transition from the material I to the material II and the material II to the material III, the wave propagating in the rod divides the energy into the transmitted and reflected waves. The reflected wave can be observed in both figures above (Fig. 5, step 70 and Fig. 6, step 70).

References

[1] JEFFREY, A.: Acceleration Wave Propagation in Hyperelastic Rods of Variable Cross-Section, *Wave motion*, No. 4, 173-180, 1982
[2] JEFFREY, A., GILBERT, R. P.: On the Approximation of Acceleration Waves in Rods, *Int. J. Non-Linear Mechanics*, vol. 22, No. 3, 209-215, 1987
[3] MAJOR, I.: Propagation of Acceleration Wave in the Rod with Changing Cross-section (in Polish), *Zeszyty Naukowe Politechniki Slaskiej*, No. 1559, 379-386, 2002, ISSN 0434-0779
[4] MURNAGHAN, F. D.: Finite Deformations of an Elastic Solid, *Amer. J. Math.*, 59, 235-260, 1937
[5] KOSINSKI, S.: *Reflection and Evolution of the Shock Wave in the Selected Hyperelastic Materials (in Polish)*, Wydawnictwo IPPT PAN : Warszawa, 1995, ISSN 0208-5658
[6] MAJOR, M.: Acceleration Wave in the Pre-deformed Murnaghan Material (in Polish), Z. Nauk. P. Sl., No. 1514, *Budownictwo*, z. 93, 305-314, Gliwice 2001, ISSN 0434-0779
[7] MAJOR, M.: *Modeling of Wave Phenomena in Hyperelastic Zahorski Material* (in Polish), p. 188, 2013, Wyd. P. Czest. : Czestochowa, ISBN 978-83-7193-600-5
[8] VASKO, M., GURAN, A., JAKUBOVICOVA, L., KOPAS, P.: Determination the Contact Stress Depending on the Load Rate of the NU220 Roller Bearing, *Communications - Scientific Letters of the University of Zilina*, No. 2, 2013, 88-94, ISSN 1335–4205.

Jan Mikolaj - Lubos Remek - Lubomir Pepucha *

OVERVIEW OF THE ROAD NETWORK MANAGEMENT SYSTEM

The long-term high standard research in civil engineering at the Department of Construction Management contributed to the fact that Slovakia succeeded to create its own pavement management system called Road Network Management System, which was accepted by international financial institutions on providing investment credits for rehabilitation of road network. At present, when the system has been in operation for more than 15 years, we can assess and analyse the results achieved in practice. This article presents a concise overview of the Road Network Management System. Computational details of pavement distress assessment and pavement structure evaluation are omitted, the focus lays on the decision making procedures for selection of appropriate repair action and process or priorization and optimization.

Keywords: *Road Network Management System, Pavement Management System, Decision making, Prioritization, Optimization.*

1. Introduction

The Road Network Management System (RNMS) emerged in the early '90s when the first structure of the system including individual modules was established based on the integrated Pavement Management Systems [1]. These modules were created to describe elements, processes and the creation of regulations in areas of Pavement Evaluation, Repair Method Selection, Life Cycle Cost Analysis (LCCA), and Funding Allocation. The outputs of RNMS development are the different sophistication levels of operational funding allocation, with the main aim to maintain the road network at the required technical and operational level. At various stages, optimization of the funding allocation process was achieved through the implementation of probabilistic methods and exact methods. The system started as a probabilistic empiric-intuitive decision making tool (a.k.a. Expert System) in which technical considerations and expert estimates were the decisive factor, concurrently with the application of Markov chain model. The system performed well and it produced valid Maintenance Repair & Rehabilitation (MR&R) action schedules. However, the Expert System was very influenceable by subjective judgement of evaluators in charge. Therefore, further development in this direction was abandoned and efforts commenced to rework the system to operate on the basis of exact methods [2].

2. Road Inventory and Pavement Distress Assessment & Pavement Structure Evaluation

Main part of this module is a database aggregating data regarding the road network. In addition to data on traffic volume and physical characteristics of road sections, as well as physical characteristics of other road network assets such as bridges and culverts, substantial part of the database consists of data regarding surface characteristics of pavements, i.e. pavement distress data. The RNMS differentiates among these types of pavement distresses: Roughness, Rut depth, Skid resistance and Surface distress.

Within the RNMS, evaluation of pavement structure is used for the calculation of residual service life, overlay thickness and optimization of performed repairs [3]. These calculations are based on measurements of deflection bowl induced by the dynamic deflectometer *FWD KUAB 150* [4]. The calculations are, for the needs of RNMS, incorporated into software called *Comprehensive Analysis of the Pavement Bearing Capacity – CANUV* [4].

- Pavement Structure - Residual Service Life Calculation - uses the elastic modulus of asphalt layers,
- Overlay Thickness Design - is based on pavement design method; the method utilizes the characteristics of surfacing, sub-base and subgrade of particular pavement.

* **Jan Mikolaj, Lubos Remek, Lubomir Pepucha**
Department of Construction Management, Faculty of Civil Engineering, University of Zilina, Slovakia
E-mail: jan.mikolaj@fstav.uniza.sk

3. MR&R Method Selection

This module is necessary due to the fact that various MR&R actions can be performed using several methods. The decision whether it is sufficient or insufficient to apply surface dressing, microsurfacing thin overlay, thick 40 - 80 mm overlay, or undertake complete reconstruction which would include subgrade or sub-base rejuvenation, depends primarily on evaluation of pavement structure. The MR&R methods are arranged into algorithm through which appropriate method can be selected, this selection algorithm is shown in Fig. 1.

The decision making algorithm itself is based on the outputs of pavement evaluation and evaluation of pavement structure, i.e. outputs of the first two RNMS modules, and consecutively, the calculation of required overlay thickness. Depending on Pavement Condition – the level of surface damage and rutting depth – it may not be necessary to reinforce the pavement; instead, a thin overlay technology can be selected for rejuvenation of pavement surface including a milling and replacement of upper part of the surfacing layer. Thickness of the overlay is chosen according to calculated reinforcement thickness provided that reinforcement of the

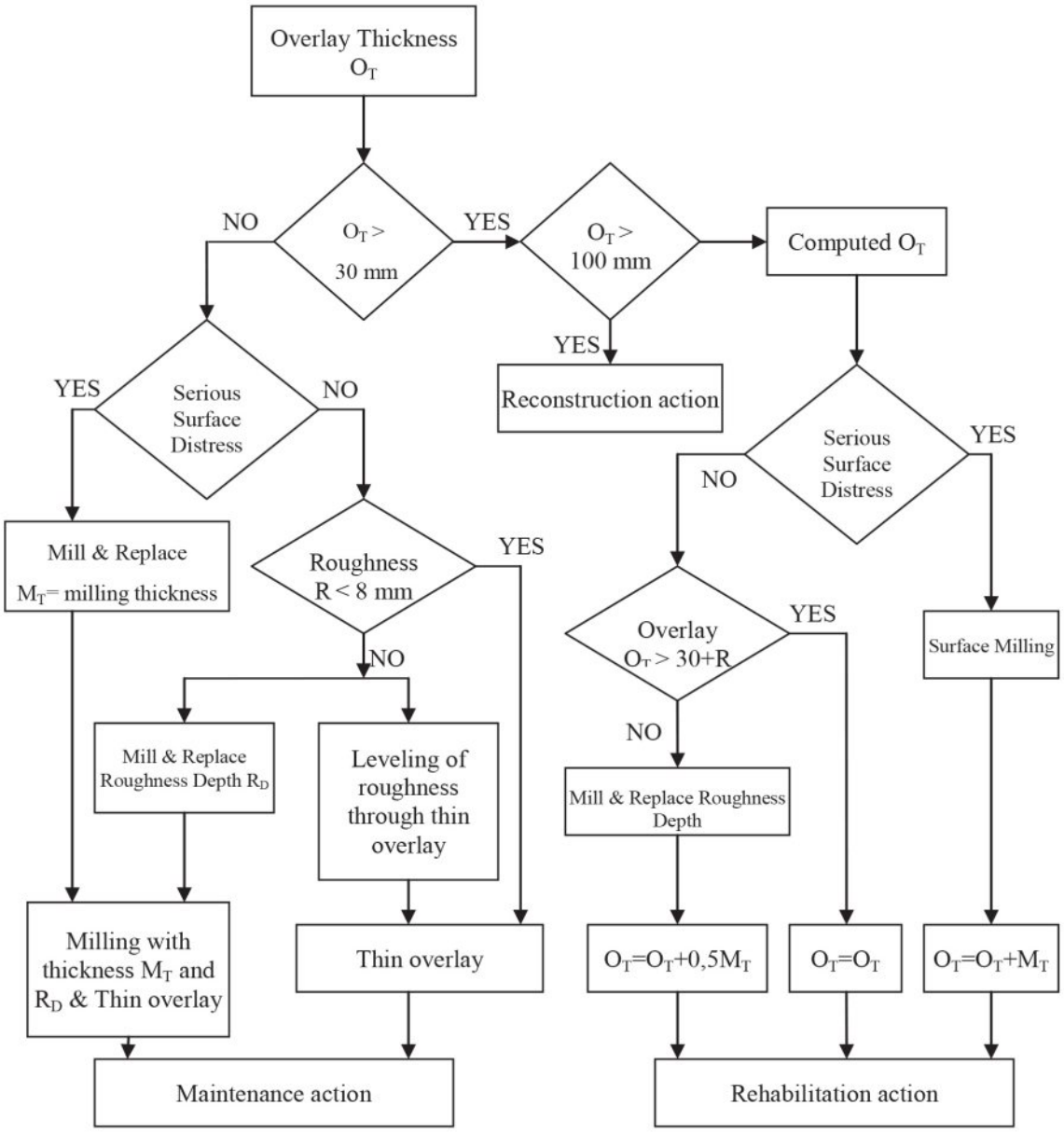

Fig. 1 Repair method selection algorithm

pavement is necessary. A detailed rehabilitation project has to be prepared in case that reconstruction of the pavement is necessary.

The MR&R methods, be it dressings, thin overlays, mill and replace, recycling or overlays are chosen by individual road administrators themselves. Their decision is based on their Library of Technologies, created according to their individual technological resources or according to resources of their public sector subcontractors.

4. RNMS as a Decision Making Tool

In terms of decision-making procedures, RNMS uses the prioritization and optimization approach. For the RNMS, a number of separate modules were established. These sub-modules consist of database containing road network parameters, algorithms for pavement distress and pavement structure evaluation, algorithm for selection of appropriate MR&R method and methodology for Life-Cycle Cost Analysis. In terms of pavement analysis, in addition to pavement serviceability, the emphasis lies on evaluation of pavement structure.

The RNMS operates at:

- Road Network Level - prioritization and optimization of MR&R actions and optimization of MR&R strategies.
- Project Level - optimization of Rehabilitation and Reconstruction (R&R) actions and assessment of new infrastructure investments.

At network level, in contrast to the well-established standards, RNMS includes much more detailed data regarding pavement structure evaluation such as residual service life and overlay thickness which are the base for decision whether maintenance, rehabilitation or reconstruction actions is appropriate. This decision, if done properly, will allow for considerably more realistic MR&R policies, programming, and schedules.

Operations on project level are based mainly on the diagnostics and evaluation of the pavement structure. Data from the trailer mounted dynamic impulse loading device KUAB FWD – falling weight defelectometer – are supplemented by measurements of complex modulus of elasticity on samples extracted from asphalt layers of the analyzed pavement section. Subsequently, local influences are assessed in relation to the repair technologies and their durability, as well as regional pricing specifications, e.g., market prices charged by contractors of the repair actions. The output is an exactly defined list of appropriate MR&R actions, according to this schedule, road network administrators can prepare contract for suppliers of MR&R works.

The main decision making criterion is economic efficiency, which enables us to create incisive outputs like strategy for allocation of limited funds between particular road sections, or the total funding amount necessary for preserving the road network in serviceable condition. In principle, economic efficiency assessment evaluates the impact of all MR&R actions. The positive effect – improvement of current state – of these actions has to overweigh their construction costs. Identification and calculation of benefits generated through repaired pavements is a key factor for economic efficiency calculation. Road user benefits are calculated as savings, i.e., difference between higher road user costs prior to the MR&R action and road user costs after the MR&R action. Each MR&R method has its expected serviceability defined by its pavement performance functions - equation (1).

$$RUB = \sum_{t=1}^{z} \left[\left(RUC_{DS} - RUC_{DN} \right) \cdot k_{DEG} \cdot k_{ATG} \right] \quad (1)$$

$$k_{DEG} = 1 - \left(\frac{t}{z} \right)^{B} \quad (2)$$

where:

RUB = road user benefits,
RUC_{DS} = road user costs in "do something" variant,
RUC_{DN} = road user costs in "do nothing" variant,
k_{DEG} = coefficient of function predicting condition of the pavement,
k_{ATG} = annual transportation growth coefficient,
t = years 1 – z,
z = service life of MR&R action,
B = pavement structure parameter.

The coefficient of degradation k_{DEG} calculated according to equation (2) is a mathematical expression for degradation of surface characteristics. This coefficient is a parameter of a fundamental importance for the accuracy and validity of economic efficiency calculation. For the needs of the RNMS, the trend lines for degradation of skid resistance, longitudinal and transverse roughness and surface distress were derived according to outputs of Circular Test Track which is an outdoor accelerated pavement testing facility - Fig. 2.

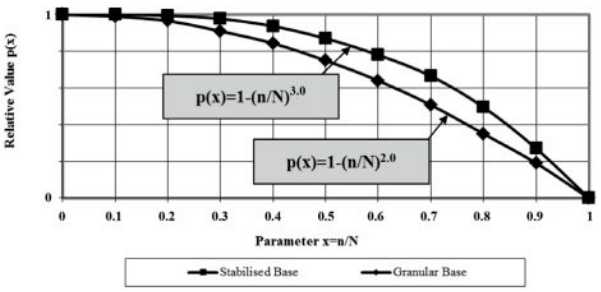

Fig. 2 Degradation functions of IRI for flexible pavements B=2.0 and semi-rigid pavements B=3.0 [5]

Fig. 3 Experimental pavement testing facility

Currently, the CCT is not in service anymore, mainly due to energy costs of its operation. At present, the trend lines of degradation are being verified using results of measurements carried out for the needs of Slovak Road Inventory (Research Institute of Engineering Constructions, 1993). However, given the large number of input variables and conditions, and thus the large dispersion of the results, construction of a new experimental test facility started at the University of Zilina. This facility will simulate traffic load, and subsequently, scrutinize inducted pavement response on a 1:1 model - Fig. 3.

4.1 Prioritization

Prioritization program is a necessity, as it is required by road administrators; road administrators are obliged to deal with insufficient funding, they are also responsible for maintaining the road network in satisfactory condition. Therefore, priorities have been established; these priorities include: functional categorization of road communications, blackspots, extreme traffic volume, extent, severity of pavement distresses and cost effectiveness.

RNMS provides a full set of outputs for network and project level assessment. In particular, the prioritization of fund expenditures allocated for MR&R policies and creation of site specific plans for MR&R actions, i.e., plans for meeting the performance objective. For network level assessment, the final output is a cumulative table which includes a final list of selected road sections and corresponding repair types - Table 1. The table shows all necessary data required for final decision. In addition, several other outputs are generated, for instance, pavement distress data and traffic related data, data regarding the results of the evaluation – IPSV, IRI, selected MR&R technology, their costs, traffic load and internal rate of return. Price for the repair is only an estimated value; the real value will be based on competition process where contractor for the construction works will be selected.

4.2 Optimization

Optimization program, in addition to establishment of general options for optimal treatment for each possible combination of performance variables, deals with optimization of timing of R&R actions. The program is based on a mathematical model for calculation of optimal repair time. This model consists of cost optimization, namely, calculation of construction costs and subsequent sum of annual maintenance costs for the duration of residual service life. However, the requirement of this calculation is the application of an analytical calculation of the residual service life and calculation of the overlay thickness in each year of the residual service life. Subsequently, user costs are calculated for each R&R variant and each year of its possible implementation. The optimal variant and year is the one with the lowest sum of construction, maintenance and user costs [1].

The calculation consists of two procedures. Firstly, calculation of pavement performance trend line. Secondly, subsequent calculation of overlay thickness for each year, until the end of pavement's residual life. The overlay thickness of the structure is related to point in time at which the action will take place – it grows over time. Overlay extends service life of the pavement and reduces user costs. Optimal time is calculated as the sum of construction costs for the reinforcement, user costs before reinforcement and user costs after the action. This sum of costs is divided by the number of years of newly extended

Example of road works prioritization- MR&R action plan — Table 1

No.	Road	Road Section	Lenght [m]	Price [€]	Cumm. price [€]	IRI [m/km]	Kpo [mm]	Pavement operating condition index	Repair Works	IRR	AADT	AADT of Trucks	Price €/1km
1.	I/50	Rimavska Sobota	2 746	296 500	296 500	5.14	19.44	1.21	o, z	77.6	6830	1299	107 975
2.	I/61	Dubnica n. V.	703	161 428	457 928	4.55	20.23	3.11	o	55.3	17093	1329	229 628
3.	I/66	Cifer	1 000	154 518	612 446	4.59	10.12	1.95	z	49.7	11200	1495	154 518
4.	I/50	Krivan	1 962	586 600	1 199 046	5.77	21.84	0.11	z	49.4	9535	2349	298 981
5.	I/18	Liskova	3 797	961 359	2 160 405	3.67	16.68	1.05	z	48.7	14078	1857	253 189

service life. This is shown in equation (3). The model shows that the later we carry out the reinforcement, the more expensive the reinforcement will be in terms of construction and user costs. Reinforcement prior to the optimal time will produce little change to the user cost and small extension of service life. Even greater precision of this optimal life calculation is attained if we take into account the maintenance costs for variants with, and without the reinforcement.

$$OI = \frac{(CC + UC_{BR} + UC_{AR})}{Tt} \quad (3)$$

where

OI = optimization index;
CC = construction costs;
UC_{BR} = sum of user cost before reinforcement;
UC_{AR} = sum of user cost after reinforcement;
Tt = number of years of extended service life.

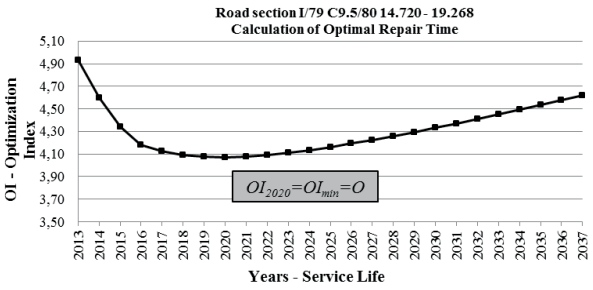

Fig. 4 Calculation of Optimal Repair Time for road section I/79 C9.5/80 14.720 - 19.268

Optimization index is computed for each year of the whole service life. As seen in graph shown in Fig. 4, the lowest point on the OI curve – OImin – represents the optimal time for the R&R action. At this point in time, the R&R action will be preventive instead of reactive and will yield largest amount of benefits.

5. Conclusion

RNMS, despite its theoretical character, has been exhibiting practical application for nearly 18 years. The application of the system resulted in the fact that the resources are allocated to road sections which have the highest demand for repairs, thus financial funds are used effectively. The saved funds are in turn used as additional resources for more repairs. Also important is the fact that this systematic approach increased the discipline of subcontractors of repair works which are being employed by road administrators. All potential deficiencies are revealed by means of diagnostics. The road network administrator has, by means of the new system, a huge number of results which are enabling him to optimize his activities; for example, the trend lines of roughness, skid resistance or surface damage. On the 1st class road network – unlimited access trunk road network – average rutting depth was reduced as a result of the RNMS which diversifies between different causes of the rutting and recommends appropriate repair technology. The results of the RNMS application proved that it is possible to optimize resources by this sophisticated decision making process. Based on calculations of the residual service life and overlay thickness it is possible to select more economical MR&R methods like dressings and thin overlays.

RNMS application has allowed us to spend resources more effectively, which was a requirement for other methods of financing, for instance financing through European Investment Bank loans or Public Private Partnerships.

Acknowledgement

The research is supported by the European Regional Development Fund and the Slovak state budget for the project "Research Centre of University of Zilina", ITMS 26220220183.

References

[1] MIKOLAJ, J.: The Road Network Management System in Slovakia. *Transport Reviews*, vol. 16, No. 4, 1996, 313-321, Taylor and Francis Ltd.: London.

[1] MIKOLAJ, J.: Research report: N 05 514 907 E 03 IDU 3: *Enhancement of Performance and Serviceability of Roads.* Road Maintenance and Rehabilitation Planning System. University of Zilina, 1992, SCHLOSSER, F., SRAMEKOVA, E., SRAMEK, J.: Rheology, Deformational Properties and Fatigue of the Asphalt Mixtures, Advanced Materials Research, vol. 875-877, 2014.

[2] Engineering & Research Int. Inc., 2013. KUAB Falling Weight Deflectometer [online]. Available from: http://www.erikuab.com/kuab.htm [Accessed 10 April 2013].

[3] KOMACKA, J., CELKO, J.: CANUV - Computer Program for Analysis of the Bearing Capacity on the Deflection Bowl Basis. *Communications - Scientific Letters of the University of Zilina*, 19, 1996, 63-70.

[4] VUIS CESTY, s.r.o: *Evaluation of Functional Serviceability of Pavements*, Research task N 05-514-904, Report 1993, Bratislava 1993.

Andrea Segalini - Luca Chiapponi - Marian Drusa - Benedetta Pastarini *

NEW INCLINOMETER DEVICE FOR MONITORING OF UNDERGROUND DISPLACEMENTS AND LANDSLIDE ACTIVITY

The paper illustrates the theoretical basis of a new device called MUMS – Modular Underground Monitoring System – and one of its applications. MUMS has been designed for monitoring of underground displacements through a continuous and automated data acquisition system. MUMS instrumentation can be used to monitor the deformation of natural and artificial slopes as well as geotechnical structures. The device consists of a series of nodes located at known distances along a connecting rope and is installed within a vertical borehole. Each node measures its local rotation relative to the vertical axis by means of a 3D micro electro-mechanical acceleration sensor (MEMS). The direction cosines of each node are calculated in order to determine the 3D shape and deformation of the entire borehole. The paper illustrates an interesting application of MUMS in natural slopes and points out the benefits of the system.

Keywords: *Landslide and geotechnical monitoring, early warning systems, MEMS technology.*

1. Description of MUMS instrumentation

The MUMS instrumentation [1] consists of a 'chain' of nodes which are located at known distances from each other and which are connected by an aramid fibre rope. Each node is equipped with both a 3D micro electro-mechanical acceleration sensor (MEMS) and a 3D digital magnetic sensor. The first sensor measures its orientation relative to the vertical (gravitational acceleration direction, Fig. 1 a), while the second one enables to determine the heading (azimuth) of each node related to the magnetic North, (Fig. 1 b).

Raw data are affected by several errors principally related to sensor limitations and accuracy, to instrument assembly, as well as to local magnetic anomalies that may be present.

Instrumental errors (due to sensor technology and assembly) can be reduced through the calibration procedure [2] which is carried out at the production laboratory. Errors related to local magnetic anomalies can be corrected once the vertical axis direction is known from accelerometer measurement since the node is supposed to be still at each reading and gravity is the only acceleration being present.

Each node is also equipped with a temperature sensor particularly useful on sites characterized by severe and changing environmental conditions.

Thanks to the three previously exanimated sensors, each node returns at least 7 data sets. Increasing the complexity of nodes, the amount of data to be transferred increases as well; therefore, an innovative connecting system has been applied. This system uses a supply cable of 4 poles with serial queries and transmits data of each node.

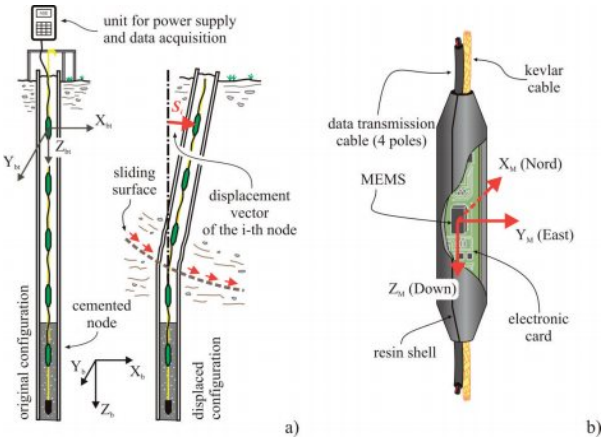

Fig. 1 Modular Underground Monitoring System a) Schematic representation. Xb, Yb and Zb are the global reference system axes (as further defined) while Xbt, Ybt and Zbt are the local reference systems at each node centre; b) Schematic representation of the single MUMS orientation node

* [1]Andrea Segalini, [1]Luca Chiapponi, [2]Marian Drusa, [1]Benedetta Pastarini
[1]Department of Civil and Environmental Engineering and Architecture, University of Parma, Italy
[2]Department of Geotechnics, Faculty of Civil Engineering, University of Zilina, Slovakia
E-mail: andrea.segalini@unipr.it

It is possible to equip each node with different sensors in order to measure other physical entities (i.e. pore pressure, resistivity, etc.).

The chain is pre-assembled in laboratory and its design is customized to the needs of each installation. During the pre-assembly, all the nodes are manufactured, connected and tested for a correct response; they are then molded in resin along an aramid fibre rope and cable at known distances (usually 0.5 m).

Each node is waterproof tested up to 2 MPa. Once the MUMS chain is complete, it is wrapped around an appropriate coil for transport. Nodes are calibrated simultaneously by moving the coil in several positions at a constant temperature. Calibration values obtained for each node are stored on the data logger memory (SD card).

The on-site installation is carried out through a simple procedure, analogous to the one of a standard inclinometer casing. The only difference is that the MUMS chain has a maximum diameter of 3 cm. This feature and the flexibility of the instrument allow installation of the chain either in small boreholes or inside old inclinometer casing that were partially broken by previous landslide movements.

Once the installation site is reached, the chain is unwrapped from the coil and lowered inside the borehole. The deeper part of the chain must be placed in a stable portion of the slope and the lower portion (1–2 m) has to be cemented within the borehole, through the injection of appropriate fast hardening grout. In this way it is possible to create a stable benchmark to which the displacements measured along the chain refer. The remaining portion of the borehole is then filled with clean gravel having diameter of 3 to 4 mm.

Subsequently, the chain is connected to the data acquisition system placed at the surface near the borehole. This proprietary system is characterized by a data logger that manages the readings, the local storage and the remote communication of data (using GPRS, UMTS or HDSPA technology).

2. Data collection and error handling

2.1 Raw data structure and sources of uncertainty

Each node returns the three components of gravitational acceleration, measured along the sensor axes (Fig. 1b), linearized and normalized to g. This implies that an axis aligned (direction and orientation) with the gravitational acceleration returns a value equal to 1 and, vice versa, an axis perpendicular to the gravitational acceleration returns a value equal to 0. Likewise, the magnetometer returns the three magnetic field components within the same coordinate system. These values are expressed in Gauss and not normalized. Each node returns its temperature too. The raw data are saved in a file structured as a matrix where each row corresponds to a specific instant (date and time) recorded in column one. The second column of the file (the first after date and time) contains the power supply level at the reading time. Each MUMS node generates seven column of data, reported sequentially starting from node 1 (bottom of the chain). The data order for each node is: 1. three components of gravitational acceleration; 2. three components of the magnetic field; 3. temperature. An example of the output file - limited to the first node of the chain - is shown in Table 1.

The readings (recovered from each node) are poorly dispersed because of the precision limits of the MEMS [2]. In addition, a drift affects the output dataset over time, a part of which is typical of this kind of sensors (characteristic of static applications and not related to any external input) and the remaining part is related to temperature variations. In order to accurately describe and compensate these errors, it is useful to analyse the output signal related to the first group of (3-4) nodes. Such nodes are installed and cemented within the lower (and stable) portion of the slope and they should not move at all. Therefore, the variation of the output signal (for these nodes) can be related exclusively to the intrinsic noise and drift of the sensor. Fig. 2a shows the raw data series and the typical drift of a 'stable' node. By subtracting

Example of the output file limited to the first node of the MUMS chain — Table 1

Date and Time	Battery Level (V)	Node 1						
		a_x	a_y	a_z	m_x	m_y	m_z	T [° Celsius]
13/12/12 2:03	13.6	0.9323	0.3082	0.1895	-0.4606	-0.0274	-0.0404	15.00
13/12/12 4:03	13.6	0.9286	0.3155	0.1954	-0.4624	-0.0283	-0.0404	15.25
13/12/12 6:03	13.6	0.9307	0.3126	0.1899	-0.4634	-0.0274	-0.0394	15.00
13/12/12 8:03	13.5	0.9310	0.3130	0.1880	-0.4624	-0.0310	-0.0413	14.75
13/12/12 10:03	13.6	0.9305	0.3148	0.1870	-0.4643	-0.0310	-0.0404	15.25
13/12/12 12:03	13.6	0.9304	0.3135	0.1898	-0.4596	-0.0274	-0.0384	15.00
13/12/12 14:03	13.6	0.9323	0.3098	0.1864	-0.4624	-0.0310	-0.0413	15.00
13/12/12 16:03	13.6	0.9311	0.3104	0.1918	-0.4624	-0.0292	-0.0394	14.50

the measured trend from the data series we can obtain the signal dispersion whose distribution is reported in Fig. 2b. The type of this distribution is Gaussian, proving that the dispersion of the data is due to electronic noise (and thus to the acquisition system). Any "step" (intended as an abrupt change of the output signal), detected by a single node at a well-defined point, will univocally identify a slope movement occurred in the close proximity of the examined node. Such circumstance will indicate a kinematics which took place at a well-defined time.

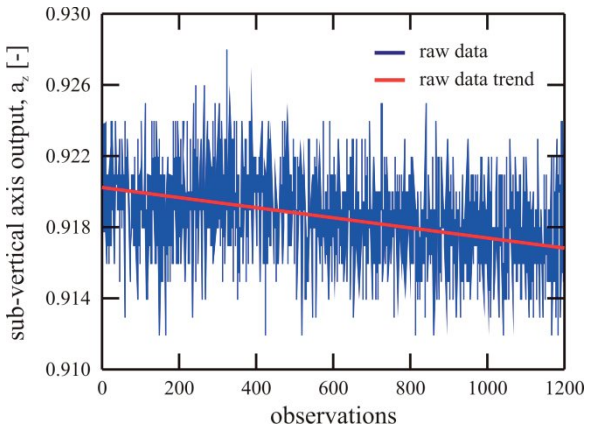

a)

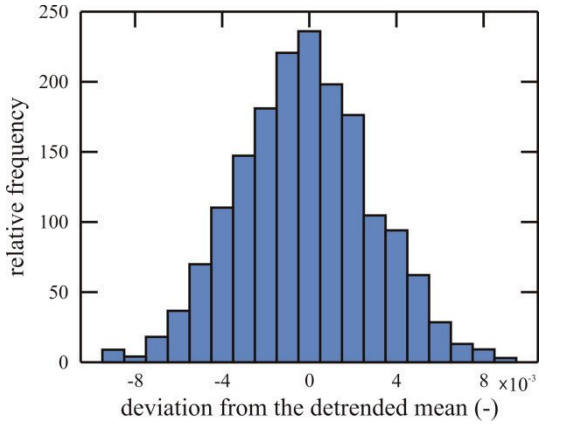

b)

Fig. 2 Measured data

a) Raw data series and extracted data trend of the z axis of one node; b) Distribution of the signal dispersion around the average value

The analysis of the data trend of the first nodes is used to quantify and correct the drift error affecting the whole chain. This method is based (a) on the high similarity between MEMS belonging to the same lot – therefore characterized by similar behaviour – and (b) on the assumption that nodes in a chain are exposed to the same environmental conditions. Each node will present a drift not dissimilar to the representative one (estimated as explained above).

It is important to point out that a variation of few thousandths in the acceleration components might induce the reconstruction of significant displacements. Such phenomenon is partly related to the initial inclination of the sensor, and it is explained by the non-linearity of the trigonometric functions used to calculate the displacement of the i-th node, S_i. In general, neglecting the information related to the direction of the displacements, the module of S_i can be calculated from the sub-vertical component of the gravitational acceleration, a_z, as:

$$S_i = L\left[\sin\cos^{-1}a_z - \sin\cos^{-1}\left(a_z + \Delta a_z\right)\right] \quad (1)$$

where L is the length of the chain portion referring to the particular node and Da_z is the variation of the a_z value from the first reading (zero reading). Depending on the original inclination of the MEMS sensor, the same variation Da_z can generate large differences in the calculated values of S. This explains why (a) it is necessary to process a data in order to reduce the dispersion of the signal and why (b) the initial lying posture of the sensor could reduce the sensitivity to the described noise.

When it is not possible to distinguish the instrumentation drift from a slow and continuous deformation of the slope, it is necessary to introduce the concept of instrumental resolution, intended as the threshold below which the variation of the output data must be ascribed to interferences and spurious effects other than to a real displacement of the installed MUMS node.

2.2 Software filtering

As described above, the data can be downloaded when necessary (either remotely or on site) and elaborated in order to evaluate slope deformations.

It is possible to transform the gravitational and magnetic field components into the displacement vector components only after filtering the data. Data have to be filtered in order to reduce their dispersion and to resolve the drift phenomena described above. At first, the data dispersion can be reduced using a moving average operator, with an amplitude window level to be evaluated as a function of both the frequency of acquisition and amplitude of the dispersion (noise level). This procedure would significantly reduce the noise of the dataset. However it also induces a loss of information. That implies the impossibility of precisely identifying the time instant in which a "small discrete" displacement of the node (and therefore of the slope) has taken place. The data elaboration is carried out by a MATLAB® script, developed using specific average functions (e.g., "smooth" with the "rlowess" option, which executes a local regression of the data using weighted linear least squares and a 1st degree polynomial model. The function also assigns lower weight to outliers in the regression). About the amplitude of the mobile window, two values have been compared: 12 and 84 samples; in fact, for the examined

case, the data were acquired every two hours and, therefore, the amplitude of the mobile window corresponds to one day or one week, respectively. In the first case, the correlation between the filtered and the original signal is higher, while in the second, data stability is higher and the determination of node displacement becomes more reliable. In order to correct the instrumental drift it is possible to execute the "detrend" of data, as above mentioned, remembering that such operation could prevent recognizing a prolonged, and constant and slow, and small slope movement.

To confirm the obtained results, it is possible to conduct a second type of analysis. The calculation of nodes displacements at regular time intervals (i.e. daily displacements) makes it possible to build an output statistics and to determine the movement threshold beyond which a displacement should be considered real (generated by a slope movement) and it is not to be considered dependent on the instrumental errors. To do this the dimension of the sample has to be evaluated and a corresponding value of the Student's t must be chosen, accordingly to a predefined reliability level. The displacements will be considered reliable only when they are higher than a certain number of standard deviations added to the local mean value. The average value of the displacements should, once again, be subtracted from the determined reliable displacement, in order to account for the instrumental drift.

3. An interesting application of MUMS instrumentation

Various test installations of MUMS instruments have been placed in natural slopes affected by instability phenomena [3] and [4]. Nowadays, the area of future installation is highly demanded for monitoring of transport constructions in difficult geological conditions, e.g. embankments of railway line for high-speed on soft soils [5]. Accurate information from innovative monitoring methods allows calibration of the results of new numerical methods [6] on real transport structures. Underground displacements measured by MUMS show that the great amount of information – collected by an automated and continuous monitoring – gives an evaluation of the ongoing physical process which is more detailed than the one obtained by traditional inclinometers. Those data may be elaborated and analysed for various purposes in order to highlight different relations between the physical entities involved. The main objective of data analysis concerning slope instability is to relate the displacement values with other natural phenomena that can be considered as triggering events (rainfalls and related increase of pore pressure, seismic loading etc.).

The detailed and frequent recording of data allows to determine how the variation in underground displacement is related to other physical entities (whose effects are considered one by one). The analysis may be also focused on appropriately chosen time intervals (e.g. seasonal period).

A MUMS device was installed in late spring of 2013 in Boschetto (Parma river valley, Parma, Italy). On April 2013, Boschetto village was affected by a landslide (Fig. 3) which involved a thick debris accumulation already defined as dormant landslide deposits of a complex landslide [7]. The debris is composed by weathered arenaceous and marly rock particles in a clay and silty matrix. The deep and stable portion of the slope is characterized by the rock formation named Pink Tizzano marl – Castelmozzano member [8] and [9].

Fig. 3 Boschetto landslide's crown area. The provincial road that crossed the slope just in front of the depicted house was completely destroyed by the landslide, causing the seclusion of the inhabited upper Parma river valley

The borehole instrumented with MUMS is located in the upper portion of the colluvium deposit, about 20 m above the landslide crown. That MUMS device is a 20.5 m long inclinometer chain equipped with a piezometer positioned 1 m above the presumed sliding surface.

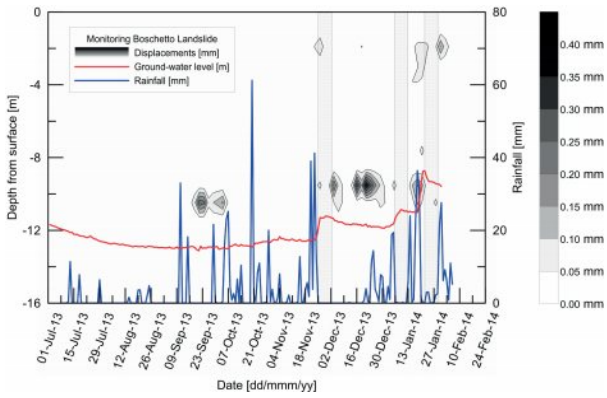

Fig. 4 Combined representation of the recorded and elaborated data. The plotted contours are indicating the amount of daily displacement recorded at each depth (left axis) while the dotted rectangles are indicating one week time span. The water table level variation is related to the left axis as well while the daily cumulated rainfall is related to the right axis.

Underground displacements data and ground-water level have been recorded every two hours and cumulated at daily intervals. Cumulated daily rainfalls have been obtained from the Regione Emilia-Romagna website [10]. Data collected from June 2013 to February 2014 are shown in Fig. 4. Daily underground deformations are represented in a contour plot where different (and darker) colours correspond to different (and greater) values of displacement. It is possible to recognize a main shear band located about 10 m under the surface, as shown in Fig. 4. The displacements occurring in the recognized shear band are related to the variations of the ground-water level (i.e. pore pressure). The ground-water level trend shows three different steps. Those steps correspond to a rapid increase of the pore pressure and they are followed by a subsequent increase in the displacement values. Such landslide movements take place approximately one week later than the corresponding variation in underground-water level. The dotted rectangles highlight the time interval occurring between ground-water level steps and increasing velocity of underground displacements.

4. Conclusion

The recent evolution of electronic micro-sensors provides invaluable support for the development of innovative monitoring systems which are accurate and cost-efficient. The electronic components provide digital outputs that require appropriate analysis and treatment in order to obtain reliable, repeatable and accurate physical responses.

Once the appropriate data analysis is carried out, the obtained results lead to a completely new interpretation of the investigated physical phenomena, offering the basis for an independent validation of previous theoretical assumptions and for the introduction of new and original interpretations.

An application of a novel instrumentation for landslide monitoring (based on MEMS and developed around a completely new concept of diffuse and continuous monitoring) is presented in this paper. The basic concepts regarding the sensor application and the analysis of some data are illustrated. Such results lead to an original interpretation of the relation between other natural phenomena (like rainfalls and related increase of pore pressure) and landslide behaviour.

References

[1] SEGALINI, A, CARINI, C.: Underground Landslide Displacement Monitoring: A New MMES Based Device, *Landslide Science and Practice*, vol. 2, 2013, Early Warning, Instrumentation and Monitoring - Margottini, Canuti & Sassa Eds. : Springer London, pp. 87-93 - doi: 10.1007/978-3-642-31445-2

[2] SEGALINI, A., CHIAPPONI, L., CARINI, C.: Evaluation of a Novel Inclinometer Device Based on MMES Technology through Comparison with Traditional Inclinometers in Landslide Applications. *Geophysical Research Abstracts,* vol. 15, EGU2013-1993, 2013. EGU General Assembly 2013

[3] SEGALINI, A., CHIAPPONI, L., PASTARINI, B., CARINI, C.: *Automated Inclinometer Monitoring Based on MEMS Technology: Applications and Verifications* - accepted for publication in the proc. of the III World Landslide Forum 3, June, 2014, Beijing

[4] SEGALINI, A., CHIAPPONI, L., PASTARINI, B.: Application of Modular Underground Monitoring System (MUMS) to Landslides Monitoring: *Evaluation and New Insights* - accepted for publication in the proc. of the XII IAEG Congress, September 2014, Turin

[5] VLCEK, J. et al.: *Analysis of Earth Pressure at Retaining Walls Reinforced with Geosynthetics,* Proc. of SGEM 2014, ISSN 1314-2704, vol. II., pp. 33-40

[6] MUZIK, J., KOVARIK, K., SITANYIOVA, D.: Meshless Analysis of an Embankment Using Local Galerkin Radial Point Interpolation Method (LGRPIM), *Communications - Scientific Letters of the University of Zilina*, vol. 15, No. 2, 2013, pp. 34-40, ISSN:1335-4205

[7] Cartografia del Dissesto Idrogeologico, 2010: Regione Emilia Romagna URL: http://ambiente.regione.emilia-romagna.it/geologia/cartografia/webgis-banchedati/cartografia-dissesto-idrogeologico

[8] CERRINA, FERONI, A., FONTANESI, G., MARTINELLI, P., OTTRIA, G.: Elements of Stratigraphic Correlation between the Bersatico Member (Tizzano Val Parma Pink Marl Formation) and the Poviago Member (Val Luretta Formation) within the Northern Italian Appennine (in Italian). *Atti Tic. Sc. della Terra*, vol. Sp., 1: 117-122, 1994, Pavia

[9] IACCARINO, S., FOLLINI, M. P.: Calcareous Nanoplankton of the Cretaceous M. Caio Flysch Formation and of the Tizzano Val Parma Paleocene "Pink Marl" Formation (Northern Italian Appenine) - in Italian, *Italian J. of Paleontology,* 76 (4): 579-618, Milano, 1970.

[10] Sistema Dexter - Servizio Idro-Meteo-Clima - ArpaER - Regione Emilia Romagna URL: http:// www.arpa.emr.it/sim/?osservazioni_e_dati/dexter.

Jana Izvoltova - Peter Pisca - Andrej Villim - Marian Mancovic *

PRECISION ANALYSIS OF HEIGHT MEASUREMENTS REALIZED ON BALLASTLESS TRACK

The ballastless track is a relatively new track construction built in Slovak Railways. The Department of Geodesy and the Department of Railway Building and Track Management of the University of Zilina have been involved in the research project aimed to monitor such an unconventional track construction. The periodical diagnostics of the vertical and positional geometrical track parameters is realized by absolute and relative methods to determine the construction conditions under traffic loading. Precision analysis of the observation is necessary to define confidential interval of measurements errors.

Keywords: *Reference network, digital levelling, Gauss-Markov model, outlier, standard deviation.*

1. Introduction

Railway modernization in Slovakia brings apart from the social-economic and environmental advantages also technological innovations of construction layers of railway body, which will eventually contribute to the increase of the railway safety and passengers comfort. Such a technological innovation of railway body was realized in the tunnel *Turecky vrch* built at the railway corridor *Nove Mesto nad Vahom - Puchov* where the traditional railway construction was replaced by the ballastless one. The University of Zilina has been involved inthe research project aimed to monitor the behaviour of the ballastless track because it is a relatively new construction in Slovak conditions. Specifically, the Department of Railway Building and Track Management has great experience with diagnostics of the railway surface and subgrade and the Department of Geodesy monitors the geometric track position in its absolute position.

The great advantage of using geodetic methods in precise measurement of a construction is the determination of its spatial position relative to global or local reference system. Disadvantage of geodetic observations can be in the fact that precision of the measured construction depends also on the interior precision of the used reference system.

The main task of this paper is to present the geodetic measurements realized on the track ballastless construction, to demonstrate the process of precision analysis of periodical height measurements from the point of view of its conformity with the prescribed tolerances involved in the technical standards [1], [2] and [3].

2. Observation requirements

Present experience with using the ballastless track construction RHEDA 2000 (Fig. 1) which has been implemented into the railway body in some European countries (Germany, Spain, Netherland, etc.) shows that the great advantage of such a construction is in its positional and vertical stability, which demands less maintenance [4] and [5]. For these reasons, it is highly important to apply very precise methods to monitor the potential vertical changes of geometrical track position which can be caused by the traffic loading.

Technical norm [3] oriented on the control measurement of line constructions recommends the basic standard deviation $\overline{\sigma}_{met}$ with the following ratio:

$$\overline{\sigma}_{met} = 0.5\,\varepsilon_{\alpha}, \tag{1}$$

where ε_{α} is the boundary measurement error which depends on the control parameter tolerance Δx:

$$\varepsilon_{\alpha} = 0.2\,\Delta x \tag{2}$$

* [1]Jana Izvoltova, [1]Peter Pisca, [1]Andrej Villim, [2]Marian Mancovic
[1]Department of Geodesy, Faculty of Civil Engineering, University of Zilina, Slovakia
[2]The Institute of Foreign Languages, University of Zilina, Slovakia
E-mail: jana.izvoltova@fstav.uniza.sk


Fig. 1 Type of Ballastless Track Construction RHEDA 2000

For monitoring the ballastless track, the digital precise levelling was applied in both measurements to control the vertical stability of the reference network and track construction.

3. Precision analysis of vertical reference network

The precision analysis of the reference network consists both of definition of the reference network vertical stability and determination of a unit standard deviation which involves the levelling precision criteria.

The vertical stability of the reference network starts with the parameter estimation of a regression line constructed on the base of determining the elevation differences (superelevations) between all pairs of the reference points:

$$\Delta^{j}_{i,i+1} = \sum_{k=i}^{n-1} \Delta h^{j}_{k,k+1}. \tag{3}$$

The elevation differences are calculated as the levelling differences between reference points of a periodical measurement and the reference points of the first mesurement as follows:

$$\Delta h^{j}_{k,k+1} = h^{j}_{k,k+1} - h^{1}_{k,k+1}, \tag{4}$$

where the upper index j = 1,2 represents the series of periodical measurements, lower index i = 1,2...,n - 1 means the number of calculated elevations and n = 10 is the number of reference points (benchmarks). Providing the superelevations are normally distributed, the position of the regression line can be estimated by the least square method [6] and [7], otherwise a robust regression can be used [8] and [9].

The process of controlling the reference network stability comes to an outlier diagnostics procedure which consists in testing the extreme difference between the superelevation and the regression line. Most of the outlier detection methods belong to the statistical hypothesis testing and are based on postulate of null hypothesis:

$$H_0 : x_{ex} > x(\alpha)_{crit} \tag{5}$$

where the testing value x_{ex} is compared with the critical value $x(\alpha)_{crit}$ both from the same probability distribution.

For the reason of outlier detection of the vertical reference network, a robust outlier detection method was applied to test the studentized (jackknifed) residuals which are the secondary products of estimation theory applied on Gauss-Markov model. The parameter estimation primary brings a vector of unknown parameters $\hat{\beta}$, residuals $\hat{e}$ which represents the vertical displacements of superelevations from the regression line and their covariance matrices $D(\hat{\beta})$, $D(\hat{e})$ with their appropriate variance and covariance components [10]:

$$\begin{aligned} \hat{\boldsymbol{\beta}} &= (A^T A)^{-1} A^T y \\ \hat{e} &= y - A\hat{\boldsymbol{\beta}} = (I - A(A^T A)^{-1} A^T) y \\ D(\hat{\boldsymbol{\beta}}) &= \sigma^2 (A^T A)^{-1} \\ D(\hat{e}) &= \sigma^2_e = \sigma^2 (I - A(A^T A)^{-1} A^T) \end{aligned} \tag{6a, b, c, d}$$

where y represents $n \times 1$ vector of dependent observations, A is an $n \times k$ design matrix and σ^2 is an estimation of variance calculated as follows:

$$\sigma^2 = \frac{\hat{e}^T \hat{e}}{n-k} \tag{7}$$

The estimation of studentized residuals anticipates the calculation of the standardized residuals e_{si}. Suppose, the residuals $\hat{e} \in N(0, \sigma^2_e)$ are normally distributed, the standardized residuals are evaluated by their transforming into standard normal distribution $e_{si} \in N(0,1)$:

$$e_{si} = \frac{\hat{e}_i - 0}{\sigma_e} = \frac{\hat{e}}{\sigma_e}, \tag{8}$$

In the conformity with the formula (6d) the particular standardized residual of *i-th* value can be evaluated from the identical equation

Fig. 2 Benchmarks of Vertical Reference Network

$$e_{si} = \frac{\hat{e}_i}{\sigma\sqrt{1 - r_{ii}}}, \tag{9}$$

where r_{ii} is the diagonal element of a projection matrix:

$$R = A\left(A^T A\right)^{-1} A^T. \tag{10}$$

Analogous to the idea of computation of the standardized residuals, the studentized residuals are estimated as follows:

$$e_{ji} = \frac{\hat{e}_i}{\sigma_{-1}\sqrt{1 - r_{ii}}}, \tag{11}$$

where σ_{-i} is the estimation of the unit standard deviation calculated without the extreme *i-th* observation. Studentized residual of *i-th* value belongs to the Student distribution with the parameter $t(\alpha)_{n-u-1}$ which represents a quantil of Student distribution with $n - u - 1$ degrees of freedom and the defined probability $P = 1 - \alpha$. Using studentized residual as the testing value and the appropriate student parameter as a critical value, the null hypothesis can be postulated as follows:

$$H_0 : \left| e_{ji} \right| > t(\alpha)_{n-u-1} \tag{12}$$

Reference network used for the diagnostics of vertical changes of ballastless track construction was based on ten reference points fixed bored to the concrete of the poles bottom (Fig. 2). The elevation differences (superelevations) between the benchmarks expressed in formula (3), were arranged into observed vector of the functional Gauss-Markov model which was analysed by the least square method to estimate the regression line parameters and their accuracy.

The projection matrix R is calculated according to the formula (10) with the dimension 9×9:

$$R = \begin{pmatrix} 0.3975 & 0.3206 & 0.2432 & 0.1719 & 0.1030 & 0.0391 & -0.0189 & -0.0920 & -0.1644 \\ & 0.2644 & 0.2077 & 0.1556 & 0.1052 & 0.0584 & 0.0160 & -0.0375 & -0.0905 \\ & & 0.1720 & 0.1392 & 0.1074 & 0.0779 & 0.0511 & 0.0175 & -0.0159 \\ & & & 0.1240 & 0.1094 & 0.0958 & 0.0835 & 0.0680 & 0.0526 \\ & & & & 0.1113 & 0.1131 & 0.1148 & 0.1168 & 0.1189 \\ & & & & & 0.1292 & 0.1438 & 0.1622 & 0.1804 \\ & & & & & & 0.1702 & 0.2033 & 0.2362 \\ & & & & & & & 0.2551 & 0.3065 \\ & & & & & & & & 0.3762 \end{pmatrix}, \tag{13}$$

Diagonal components of the projection matrix r_{ii} are needed to evaluate vector of residuals $\hat{e}$, standardized residuals $\hat{e}_s$ and the studentized residuals $\hat{e}_j$:

$$\hat{e} = \begin{pmatrix} 0.1828 \\ 0.1540 \\ -0.1740 \\ 0.3393 \\ -0.6183 \\ -0.4903 \\ 0.1317 \\ 0.3499 \\ 0.1249 \end{pmatrix}, \hat{e}_s = \begin{pmatrix} 0.6292 \\ 0.4797 \\ -0.5108 \\ 0.9685 \\ -1.7523 \\ -1.4040 \\ 0.3862 \\ 1.0833 \\ 0.4226 \end{pmatrix}, \hat{e}_j = \begin{pmatrix} 0.8019 \\ 0.6109 \\ -0.6505 \\ 1.2334 \\ -2.2317 \\ -1.7880 \\ 0.4919 \\ 1.3796 \\ 0.5382 \end{pmatrix}. \quad (14a, b, c)$$

The value of standard deviation σ estimated from the full residual vector and unit of standard deviation σ_{-5} estimated without the extreme value of residuals are following:

$$\sigma = 0.37 \text{ mm}$$
$$\sigma_{-5} = 0.29 \text{ mm} \quad (15a, b)$$

The estimated vector of residuals (14a) was indicative of the fifth extreme value $e_5 = -0.6183$ and so the appropriate value of studentized residual $e_{j5} = -2.2317$ had to be exposed to null hypothesis as follows:

$$H_0 : |-2.2317| > t(\alpha)_{n-u-1} \quad (16)$$

Suppose that the model redundancy is $n-u-1$ and the Student coefficient is $t(0.05)_{n-u-1} = 1.9432$, the fifth superelevation in the reference network is considered to be outlier with probability P = 95%. Owing to the fact that null hypothesis is confirmed, measurements and evaluations proceed without this extreme superelevation.

4. Precision analysis of track measurement

The main output of the precision analysis of vertical reference network consists in defining its vertical stability which is important for additional monitoring of the track construction and in estimation of levelling precision represented by the value σ_h.

The precision of height differences of the measured track construction is estimated according to the equation:

$$\sigma_h = \sigma_0 \sqrt{L} = 0.41 \text{ mm} \quad (17)$$

The vertical displacement of an observed point is evident if it exceeds the tolerance boundaries which are determined as a double value of standard deviation σ_h:

$$\bar{x} - 2\sigma_h \leq \Delta \leq \bar{x} + 2\sigma_h \quad (18)$$

The observed results and the analysis of precision are graphically demonstrated in Fig. 3. The measured vertical

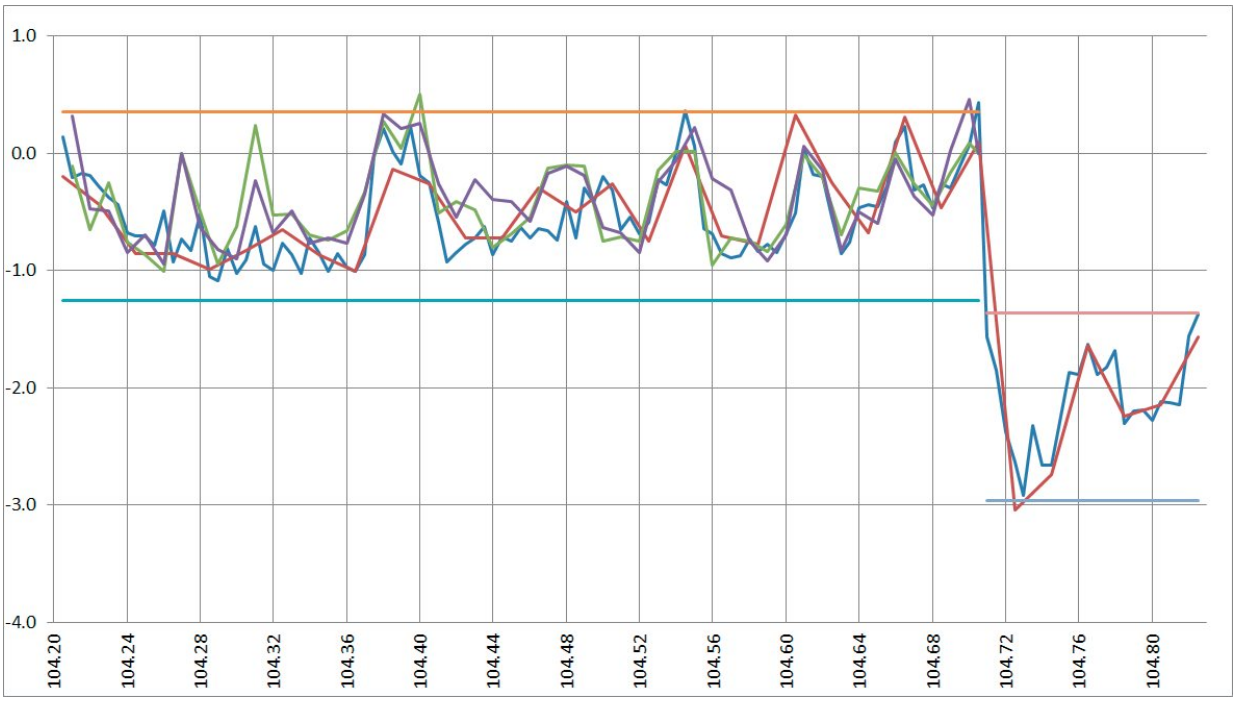

Fig. 3 Analysis of vertical stability of track 1

changes of the ballastless track construction did not exceed the confidential interval and so the vertical displacements of the track construction are not confirmed. Another situation occurs in the railway part in km 104.705 – 104.820, built on the traditional track construction where the track construction decreased by more than two millimetres (see Fig. 3).

5. Contributions

Precision analysis of height measurements realized on the ballastless track consists both of analysis of vertical reference network and precision analysis of the track measurements. The first one brought the view on stability of the reference system and standard deviation as the main characteristic of the used levelling method (15). Precision analysis of track measurements consists of defining the standard deviation of height differences (17) and the confidential interval (18) which qualifies the evident vertical displacements of track construction.

The precision analysis of geodetic observations realized on the ballastless track construction was performed in the conformity with the appropriate technical standards. Precision of used digital levelling satisfies the demands defined for observation of such an unconventional track construction. Since the vertical stability of the ballastless track construction has been confirmed by both measurements, the vertical changes of traditional track construction have been registered.

Acknowledgement

This article is the result of the implementation of the project: "Innovation and internationalization of education – the means to increase the quality of the University of Zilina in the European educational space (ITMS: 26110230079) supported by the Research & Development Operational Programme funded by the ERDF.

This article is the result of the implementation of the project VEGA No. 1/0597/14 "Analysis of methods used to measure the unconventional railway track construction from the point of view of accuracy and reliability" supported by the Scientific Grant Agency of the Ministry of Education, science, research and sport of the Slovak Republic and the Slovak Academy of Sciences.

References

[1] STN 73 0202 *Precision of Geometric Parameters in the Construction (in Slovak)*. General requirement, Bratislava 1985

[2] STN 73 0212-6 *Precision of Geometric Parameters in the Construction (in Slovak)*. Precision control, Bratislava 1993

[3] STN 73 0275 *Precision of Geometric Parameters in the Construction (in Slovak)*. Control measurement of line structures, Bratislava 1985

[4] RHEDA 2000® Ballast-less Track System. http://www.railone.com/en/main-nav/products/railways-and-commuter-traffic/ballastless-track-systems.html

[5] IZVOLT, L., HODAS, S.: *Modernisation of Railway Infrastructure in the Slovak Republic*. COMPRAIL XIII. intern. Conference on Design and Operation in Railway Engineering, WIT Press Southampton : Boston, ISBN 978-1-84564-616-5

[6] MARCAK, P., KUBACEK. L.: The Problem of the System of Height Reference in Determining the Settling of Foundations and Buildings. *Studia Geophysica et Geodaetica*, 18, 33-46, 1974

[7] SIMA, J., KOTKA, V., PISCA, P., SEIDLOVA, A.: *Geodetic Work for Reconstruction and Building of Narrow-gauge Railway*. XIII. intern. Slovak-Poland-Russian geodetic days : Liptovsky Jan, 84-88, 2007, ISBN 978-80-969692-0-3

[8] CEBECAUER, D.: Reference System used for Measurement of Vertical Shifts in Line Buildings (in Slovak). *Geodeticky a kartograficky obzor*, vol. 12, No. 36/78, 300-303, 1990

[9] ROUSSEEUW, P. J., LEROY, A. M.: *Robust Regression and Outlier Detection*, Wiley & Sons : New Jersey 2003, 329 p., ISBN 0-471-48855-0

[10] MUZIK, J., KOVARIK, K., SITANYOVA, D.: Meshless Analysis of an Embankment Using Local Galerkin Radial Point Interpolation Method (LGRPIM). *Communications - Scientific Letters of the University of Zilina*, No. 2, 34-40, 2013, ISSN 1335-4205.

Dana Sitanyiova, Sona Masarovicova *

ADVANCE AUDIT - PRACTICAL AUDIT TOOL FOR IMPROVING URBAN MOBILITY PLANS

This paper presents the methodology and the results of the ADVANCE project. ADVANCE supports cities and municipalities on their way towards a more sustainable urban mobility, thus assisting them to set up and improve the quality of Sustainable Urban Mobility Plans (SUMPs) and policies. ADVANCE has developed an audit scheme designed by an interdisciplinary team of mobility experts, to assess the quality of the cities' mobility plans. Thereby, it contributes to the take-up of Sustainable Urban Mobility Plans in Europe.

Keywords: *Audit, assessment, mobility, plan, SUMP.*

1. Introducing ADVANCE and SUMP

ADVANCE was an international project funded by Intelligent Energy Europe programme, which ran from 2011 to 2014. It aimed to develop, test and apply the ADVANCE Audit – a tool that analyses the strengths and weaknesses in the current sustainable mobility planning of a city and gives clear indications for improvement. Measures and areas of actions to improve the sustainable mobility planning in the city can be derived directly from the action plan that results from the audit process. The action plan can be used as a basis for the development of a new or updated Sustainable Urban Mobility Plan.

Sustainable Urban Mobility Plans (SUMPs) define a set of interrelated measures designed to satisfy the mobility needs of people and businesses today and tomorrow. They are the result of an integrated planning approach and address all modes and forms of transport in cities and their surrounding area. Different approaches to sustainable urban mobility planning exist throughout Europe. While some countries, such as France and the UK, may be considered forerunners, Sustainable Urban Mobility Plans are a new or yet unknown planning tool in other parts of the EU including Slovakia. Sustainable Urban Mobility Plans mean "Planning for People". The European ELTIS plus project has highlighted the benefits of SUMPs in comparison to traditional transport plans. SUMPs take due consideration of integration, participation, and evaluation principles with the aim to create a sustainable urban transport system by addressing - at least - the following objectives:

- Ensure the accessibility offered by the transport system is available to all;
- Improve safety and security;
- Reduce air and noise pollution, greenhouse gas emissions and energy consumption;
- Improve the efficiency and cost-effectiveness of the transportation of persons and goods;
- Contribute to enhancing the attractiveness and quality of the urban environment and urban design.

A Sustainable Urban Mobility Plan is a way of tackling transport-related problems in urban areas more efficiently. Building on existing practices and regulatory frameworks, its basic characteristics are:

- A participatory approach: involving citizens and stakeholders from the outset and throughout the process in decision making, implementation and evaluation, building local capacity for handling complex planning issues;
- A pledge for sustainability: balancing economic development, social equity and environmental quality;
- An integrated approach: mixing practices and policies between policy sectors (e.g. transport, land-use, environment, economic development, social inclusion, gender equity, health, safety), between authority levels (e.g. district, municipality, agglomeration, region, nation, EU), and between neighbouring authorities (inter-municipal, inter-regional, transnational, etc.);
- A focus on achieving measurable targets derived from short term objectives;
- A review of transport costs and benefits, taking into account wider societal costs and benefits, also across policy sectors.

Based on the methodology developed within the ELTIS plus project, an "ideal" planning cycle for a sustainable urban mobility plans was defined (Fig. 1). The ADVANCE Audit process, which

* **Dana Sitanyiova, Sona Masarovicova**
Department of Geotechnics, Faculty of Civil Engineering, University of Zilina, Slovakia
E-mail: dana.sitanyiova@fstav.uniza.sk

Fig. 1 SUMP cycle in relation to the Mission Fields of ADVANCE
Source: Guidelines SUMP - ELTISplus, 2011 [1]

is based on this SUMP development cycle, distinguishes between 5 Mission Fields, related to the process of setting up a SUMP (Precondition, Vision & Strategy, Organisation, Implementation of action fields, Monitoring & Evaluation) and 8 Action Fields related to the implementation of measures defined in a SUMP (Parking management, Street design, Walking, Cycling, Public transport, Car related measures, Mobility management, Freight management) that compose the main elements of a SUMP. The Action fields and Mission Fields are assessment basis for the ADVANCE Audit scheme:

- **Action Fields** are actions and measures described in a SUMP;
- **Mission Fields** are related to the process of a SUMP.

2. Total quality management in sustainable mobility planning

According to the principles of Total Quality Management, excellent quality is the result of continuous improvement achieved by applying the repetitive cycle of success with a view to fulfil the city's needs [1]. Based on this, ADVANCE considers sustainable mobility planning as a dynamic process that can be depicted with the ADVANCE Audit Scheme (Fig. 2).

There were three categories defined in the project to identify the status of a SUMP and sustainable urban mobility policy in a city:

1. **Starting cities**: These cities do not have a SUMP or a sustainable mobility strategy at all. The city takes ad hoc

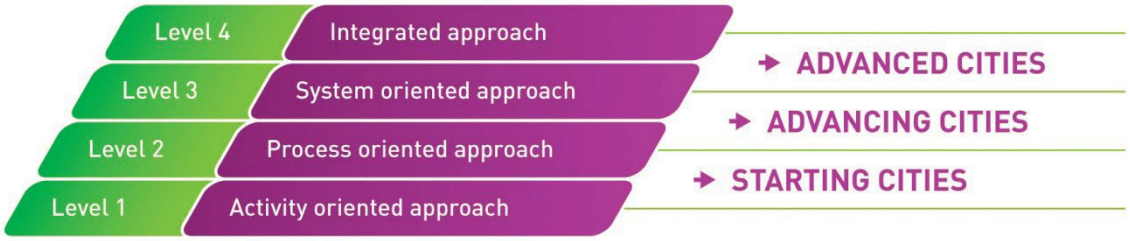

Fig. 2 Quality management ladder of development; Source [2]

measures in case of an urgent mobility problem and will only give short term and purely technical solutions towards mobility problems.

2. **Advancing cities**: The city has a SUMP and there is a common vision on which mobility strategy to follow. There is a systematic approach towards actual or expected mobility problems. The city takes first steps in evaluating the current mobility policy to find out in which fields improvements are possible.
3. **Advanced cities**: The city has a SUMP and a clear mobility strategy. The mobility policy is constantly evaluated and quality indicators are being used. The city anticipates expected mobility problems via monitoring. The mobility policy is oriented to the future and innovative solutions are implemented.

The important element to consider is the iterative process of elaboration of a SUMP: the elaboration of a SUMP should not be the summative result of successive stages of studies, but an integrative process allowing a shared diagnosis of the situation, a progressive definition of objectives and the consistency of means.

The ADVANCE Audit can be conducted in small, medium and large sized cities. The size of the partner cities, which tested and applied the ADVANCE Audit, varied from about 35.000 inhabitants (Agioi-Anargyroi, Greece) to more than 400.000 inhabitants (Szczecin, Poland). But the ADVANCE Audit is also suitable for larger cities. The ADVANCE Audit Scheme intends to systemize the mobility planning process by:

- Assessing the city's sustainable urban mobility plan and policy;
- Describing the strengths and weaknesses in the different planning elements;
- Prioritising improvement actions together with relevant stakeholders;
- Editing an ADVANCE action plan which can be a basis for a new or updated SUMP.

The audit scheme has not only the aim to improve the quality of the SUMP as a paperwork of the mobility planning and policy in the city, but it has also the aim to analyse, systemize and improve the whole process of the development of the SUMP (involvement of citizens and stakeholders, presence of a clear vision, collaboration between different departments - urban planning, traffic, etc.). The cities are guided through the audit-process with the help of a trained ADVANCE Auditor (See www.eu-advance.eu for the list of certified auditors). Cities that pass the ADVANCE Audit successfully receive a certification. Repeating the ADVANCE Audit regularly every 5 years will indicate progress in the sustainable mobility planning of the city.

3. Audit methodology

The ADVANCE Audit Scheme is not a theoretical model, but it has already been applied in practice during its development phase. The final ADVANCE Audit Scheme is based on discussions within the consortium (including the University of Zilina), a first test-run in 3 cities, the feedback from the EUROCITIES network, the feedback from the QUEST scientific board and a second-test-run in 6 cities (including Zilina) and 7 Brussels Municipalities. The ADVANCE Audit Scheme guides cities in 5 steps through the audit during a period of maximum 6 months (Fig. 3).

Fig. 3 ADVANCE Audit Scheme
Source [2]

		not applicable	level 1 We have done this sporadically or ad-hoc. We have some anecdotal information. Very little performance. Fire principle: we take action if necessary, as long as necessary and only when necessary.	level 2 We are implementing this and/or have done this a couple of times or at a small number of sites. We have information related to some areas. Some performance.	level 3 We have implemented this and have done this regularly or at many sites. We have good information. Rather strong performance. There are indeed structural initiatives, but there is still room for improvement.	level 4 We have implemented this ar regularly reviewing this i systematic way. We work systematic and innovative Strong performance. In this we score excellent.
M4 - Implementation Implementation refers to how the mobility policy is implemented. The goal must be to enumerate all the strategy elements and measures taken within the city in relation to the vision described in the policy document.						
M4.1 Proper management	**Degree to which the implementation of the policy document is carried out according to an agreement on management procedures and responsibilities with all stakeholders involved in implementing the measures.**	☐	☐	☑	☐	
M4.2 Sustainable measures	The sustainable urban mobility planning has to find a balance between various objectives, considering 4 fundamental issues:					
M4.2.1 - Right for mobility for everyone	**Degree to which the implemented measures are compatible with the right for mobility for everyone, including for people with disabilities.**	☐	☑	☐	☐	
M4.2.2 - Protection for environment and health	**Degree to which the implemented measures are compatible with the Protection for environment and health.**	☐	☐	☑	☐	
M4.2.3 - Articulation between land use and transportation	**Degree to which the implemented measures are compatible with the articulation between land use and transportation.**	☐	☐	☑	☐	
M4.2.4 - Road safety	**Degree to which the implemented measures are compatible with the road safety.**	☐	☑	☐	☐	
M4.3 Communication	**Degree to which the implementation of the SUMP is communicated to the citizens on a regular basis, in order to encourage their participation.**	☐	☐	☑	☐	

Fig. 4 Assessment of Mission Field - Implementation

Step 1

A meeting between the auditor and the city is organized. The auditor explains the ADVANCE Audit process including the commitment needed from the city. He/she describes the necessary capabilities and resources that are required to compose the ADVANCE working group. Special emphasis is put by the auditor on the involvement of relevant stakeholders. The city and the auditor agree on the definitive composition of the working group. The auditor collects some context indicators that will help the auditor to set up the baseline situation of the city. The context indicators are organized in two main groups. On the one hand, those indicators that will help the auditor set up the baseline situation of the city and, on the other hand, those indicators that will help the auditor to evaluate changes in the local mobility policies. These data are also important to evaluate the effects of the application of the ADVANCE Audit in future. The auditor has to collect these data and include them in the assessment report.

Step 2

The auditor researches the relevant documents (SUMP, mobility plans, transport plan etc.) and carries out a site visit that can be combined with the first working group meeting where the auditor explains all the details of the ADVANCE Audit process. Special attention is given to the role and expectations towards all participants. The working group needs to be composed of the main internal and external players on urban transport and mobility planning. It is important that the group's composition reflects the departments within the city and the relevant stakeholders that are responsible for the functions covered by the mission and action fields. It is also important to find out about the political level's interest in the ADVANCE Audit before the actual start of the audit process. The auditor distributes the ADVANCE questionnaire which will be used to assess the quality of mobility planning in the city.

ADVANCE questionnaire

The ADVANCE questionnaire is the main instrument to perform the assessment of the current situation. This assessment is crucial in helping to define appropriate policies and provides the necessary baseline against which progress can be measured. The analysis should be as comprehensive as possible, but also needs to be manageable with the given resources. The ADVANCE evaluation questionnaire covers all the Mission and Action Fields. It is an excel document that provides an interactive tool to score and visualise the results. The Mission Fields and Action Fields are assessed by scoring the statements. All statements are to be assessed on a scale from level 1 to 4. Level 4 indicates the highest level of performance or implementation and level 1 the lowest (Fig. 4). The ADVANCE working group members complete the ADVANCE questionnaire individually. The scoring for the different mission and action fields is presented using cobweb diagrams. This is illustrated for the Action Fields (Fig. 5).

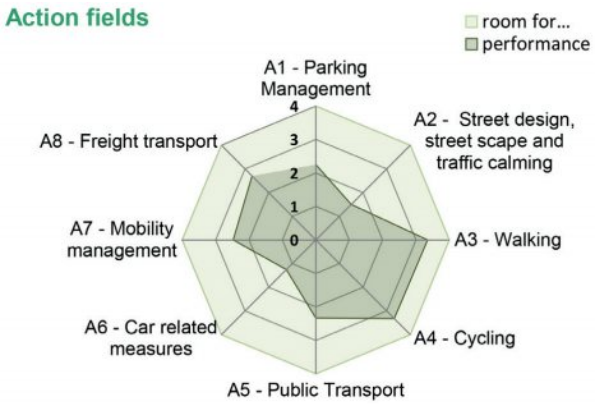

Fig. 5 Cobweb Action Fields

In the example in Fig. 5 the strength of the city lies within the Action Fields A3 and A4. The weakness lies within the Action Fields A2 and A6. The scoring for the individual statements per

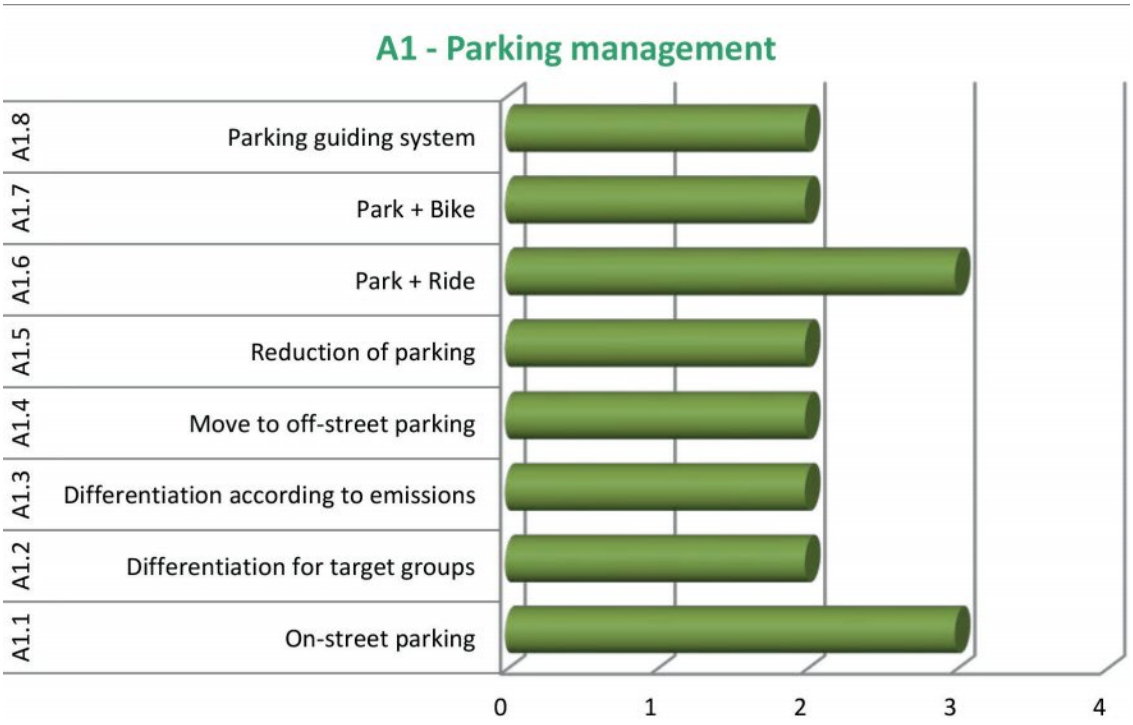

Fig. 6 Bar diagram for Action filed A1 – Parking management

mission and action fields in questionnaire is presented in bar diagrams (Fig. 6 – example for parking management).

All individual questionnaires are collected, summarised and analysed by the auditor with the help of excel summary tool. During the consensus meeting, it is important for the auditor to facilitate the discussion about strengths and weaknesses. At the end of the meeting a consensus on the score for every field has to be reached. Several options to achieve a consensus are available: keeping the arithmetic average, up- or down grading based on arguments of individual group members, voting for average score. The city is evaluated as Advanced if it reaches the total score >75 %, as Advancing if the score is > 50 %, and as Starting if it is < 50 %.

Step 3

After the consensus meeting all members of the working group representing different organisations, stakeholders and municipality are asked to compile their list of priorities. The auditor drafts an action plan (AP) based on the list of possible improvement actions. In the AP concrete objectives and actions are set out in a timetable with specific budgets and responsible persons or departments. During prioritisation meeting a discussion takes place on the priorities in the list of actions mentioned in the draft AP. The discussion is done in a plenary session or in different working groups. The working group discusses and agrees on which (other) stakeholders need to be consulted before drawing the final AP.

Step 4

Based on the previous steps the final ADVANCE Action Plan is edited by the auditor. This is a final output of the ADVANCE Audit process with concrete actions to improve the local urban mobility plan and policy. The AP needs to reflect the commitment of the key actors and implementation actors and will be presented to the political representatives of the city. In order to apply for the ADVANCE-certificate the AP needs to be accepted by the political decision takers. The AP is no SUMP in itself, but can be the basis for the development (in starting cities without a SUMP) or the upgrade (in advancing or advanced cities) of the local SUMP. While the time horizon for the implementation of a whole SUMP might take more than five years, the proposed actions in the AP should be able to get implemented within the next five 5 years.

Step 5

The auditor writes the Audit Report including the notes of the working group meetings and recommendation for certification. The final and approved AP is added as an annex to the Audit Report. If the city meets the criteria for certification, it receives the ADVANCE certificate.

4. Conclusions

The progress of the implementation of the Action Plan is checked by the ADVANCE Committee after a period of 3 years based on an update of the Action Plan. The city is informed about the time of the Action Plan update. The ADVANCE certificate must be confirmed every 5 years by the ADVANCE Committee. A city can do a re-audit if it meets the following procedural steps:

- The City has sent a follow-up of the Action Plan after a 3 years period to the ADVANCE Secretariat;
- The City has fulfilled at least 50% of the actions during the time-frame of the certificate since it was certified.

For the re-audit the audit and the certification process will be similar to the initial certification. This approach ensures the sustainability of actions to improve the Sustainable Urban Mobility in the city.

ADVANCE project developed a methodology for multi-criterion evaluation. The audit provides an honest and clear picture on the strengths, weaknesses and opportunities of current planning practices with regard to developing a Sustainable Urban Mobility Plan in the local context. The evaluation methodology is very efficient for obtaining conclusions in a minimum period of time. The crucial aspect of the methodology is involvement of all different types of stakeholders throughout the planning process, addressing their specific requirements. There were different approaches to assess the quality of a city's entire sustainable mobility policy being developed in the three IEE STEER projects: Ecomobility SHIFT (www.ecomobility.org/shift/), QUEST (www.quest-project.eu/) and ADVANCE (eu-advance.eu/). Final ADVANCE Audit Scheme and Guidelines with comprehensive description of the methodology and the whole audit process is available at: http://eu-advance.eu/docs/file/d2_5_final_advance_audit_scheme_including_guidelines_en.pdf. European Commission should decide for common procedure to assess the quality of SUMPs in near future.

Legal disclaimer

Co-funded by the Intelligent Energy Europe Programme of the European Union

References

[1] Mobilityplans.eu: *Guidelines on the development and implementation of a Sustainable Urban Mobility* Plan (online http://www.mobilityplans.eu/docs/file/guidelines-developing-and-implementing-a-sump_final_web_jan2014b.pdf).

[2] ADVANCE consortium: *Final ADVANCE Audit Scheme and Guidelines*, 2014.

Peter Juras - Pavol Durica *

INFLUENCE OF WIND-DRIVEN RAIN ON THE THERMAL CONDUCTIVITY OF BUILDING ENVELOPES WITH DIFFERENT CEMENT-LIME COATINGS

This paper deals with influence of the wind-driven rain on the building envelopes in terms of thermal conductivity. Low rise building was simulated in Computational fluid dynamics CFD software OpenFOAM using Eulerian multiphase model for rain phase and determined rain load was used as an input for Heat-Air-Moisture HAM simulation in WUFI. Two different wall constructions which were used differ in the core layer and also in exterior coatings. The influence of wind-driven rain load on the thermal conductivity for aerated concrete and aerated clay brick was established.

Keywords: *Wind-driven rain, CFD, precipitation, rainfall, Eulerian multiphase model, TRY, heat-air moisture simulation, HAM, cement-lime coating.*

1. Introduction

Wind-driven rain (WDR) can be an important moisture source for building facades and therefore is of great concern in civil engineering. Wind-driven rain or driving rain is rain that is given a horizontal velocity component by wind. WDR intensity depends on several parameters such as building geometry, surroundings, terrain topography, position on the facade, wind velocity, wind direction, rainfall intensity and raindrop-size distribution. Wind-driven rain research is important within a number of research areas including Earth sciences, meteorology and building science. As one of the most important moisture sources, it affects the hydrothermal performance and durability of facades. Consequences of its destructive effect can take many forms. Moisture accumulation in porous materials can lead to water penetration, frost damage, moisture induced salt migration, discoloration by efflorescence, structural cracking due to thermal and moisture gradients, increased thermal lost due to the raised thermal conductivity, aesthetics etc. [1 and 2].

Computational Fluid Dynamics (CFD) simulations can be a valuable alternative to measurements and semi-empirical methods. According to the STN EN 15 026 [3], WDR load should be involved in building envelope heat-air-moisture (HAM) simulation. This leads to the need for accurate information on the spatial distribution of surface wetting and, therefore, CFD simulations with their high resolution are very useful.

The use of various simulation programs has increased with development of computers. Programs for simulation of heat-air and moisture transport in building envelope uses non-steady boundary condition – outdoor climate data sets – test reference years (TRY) [4]. Test reference years are used in building science for many purposes. Generally, there are two types of test reference years: energy TRY (to calculate the energy consumption) and moisture reference year (to analyze the moisture problems in building envelopes). The methodology for creation of moisture TRY from long term observation is analyzed and described by Sanders [4].

This paper deals with influence of WDR on the building envelope in terms of thermal conductivity. Low rise building was simulated in CFD software OpenFOAM using Eulerian multiphase model for rain phase and determined rain load was used as an input for HAM simulation in WUFI. Two different wall constructions which were used differ in the core layer and also in exterior coatings. The influence of wind-driven rain load on the thermal conductivity for the aerated concrete and aerated clay brick was established.

2. Computational domain

The computational domain for the simulated building with dimensions 775 x 1600 x 420 m is shown in Fig. 1 and consists of 4,876,875 tetrahedral cells. The blockage ratio of the domain is 0.1 % and the distances of the modelled building between the domain boundaries are according to the guidelines of Franke et al. [5].

* [1]Peter Juras, [2]Pavol Durica
[1]Research Centre, University of Zilina, Slovakia
[2]Department of Building Engineering and Urban Planning,, Faculty of Civil Engineering, University of Zilina, Slovakia
E-mail: peter.juras@rc.uniza.sk

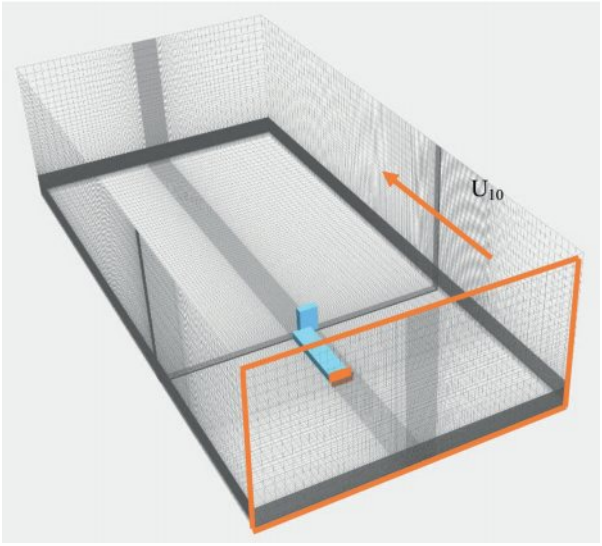

Fig. 1 Computational domain with dimension 775 x 1600 x 420 m and marked investigated windward facade, inlet plane with flow direction and wind velocity U_{10} = 10 m/s

3. Reference wall constructions

Two walls with two different traditional coatings (totally four variants) from Baumit were used for the heat-air and moisture simulation (HAM) - see Table 1. The basic difference between EdelPutz and FeinPutz is the final surface of the coating. The material base is more or less the same. FeinPutz has smooth and EdelPutz scraped surface. The material parameters are summarized in Table 2. The measured properties from previous research [6 and 7] are highlighted. The rest of properties are from the WUFI software database, mostly measured by Fraunhofer Institute for Building Physics.

4. Wind and rain phase

Computer code OpenFOAM was used for numerical simulation. It is an open-source, implicit, segregated and double precision solver. Eulerian multiphase model [8] was used for the rain phase instead of commonly used and more time consuming Langrangian particle tracking model. This model enables to reduce the computational expense to model a long rain event which is discretised into 1 min or 10 min time steps. CFD simulations are made for a limited number of horizontal rainfall intensity and wind velocity couples. The wind-flow field in the domain is solved for wind velocity U_{10} = 10 m/s and wind-flow fields for other reference wind velocities (1, 2, 3 and 10 m/s) are obtained by linear scaling.

In Fig. 2, we can see a wind flow field showing the mean wind velocity on the vertical mid-plane through both buildings. The wind flow on the high building is clearly influenced by the lower building. Typical flow features as the standing vortex, the down-flow from the stagnation point, large vortices behind the building, and flow restoration behind the building are visible.

Detailed construction of the reference walls — Table 1

Aerated clay brick wall	**TSF**	FeinPutz - smooth coating th. 5 mm	GrobPutz th. 20 mm	Aerated clay brick (ACB) th. 365 mm	Gypsum plaster th. 15 mm
Aerated clay brick wall	**TSE**	EdelPutz - scraped coating th. 10 mm	MVR Uni th. 15 mm	Aerated clay brick (ACB) th. 365 mm	Gypsum plaster th. 15 mm
Aerated concrete wall	**PSF**	FeinPutz - smooth coating th. 5 mm	GrobPutz th. 20 mm	Aerated concrete (ACC) th. 365 mm	Gypsum plaster th. 15 mm
Aerated concrete wall	**PSE**	EdelPutz - scraped coating th. 10 mm	MVR Uni th. 15 mm	Aerated concrete (ACC) th. 365 mm	Gypsum plaster th. 15 mm

Material properties of used materials — Table 2

Name	Bulk density (kg/m^3)	Porosity (-)	Thermal conductivity (dry state) λ (W/(m.K)	Diffusion resistance factor μ (-)	Water absorption coefficient A ($kg/m^2s^{0.5}$)	Capillary water content w_{cap} (kg/m^3)
EdelPutz	**1303**	**0.11**	0.8	15	**0.0123**	**71.31**
FeinPutz	**1361**	**0.17**	0.5	20	**0.0261**	**110.24**
Grobputz	**1568**	**0.22**	0.9	20	**0.1583**	**203.36**
MVR Uni	**1015**	**0.18**	0.5	20	**0.0154**	**109.55**
ACB	600	0.77	0.12	16	-	188
ACC	400	0.81	0.1	7.9	-	380
gypsum plaster	850	0.65	0.2	8.3	-	400

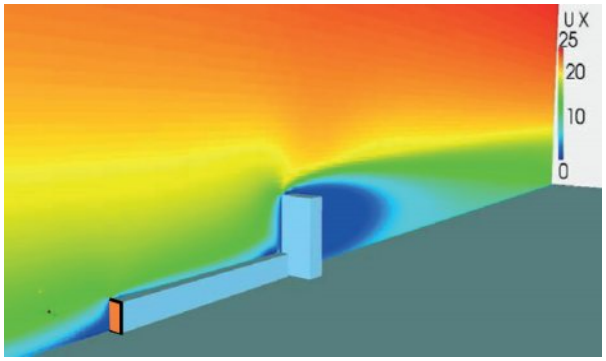

Fig. 2 Wind flow field through vertical plane. Reference wind velocity U_{10} = 10 m/s; marked windward`s north-west facade of investigated low-rise building

The inlet profile of the mean wind velocity is defined by the typical log-law expression [9]:

$$U(y) = \frac{u^{*}ABL}{k} \ln\left(\frac{y + y_0}{y_0}\right) \quad (1)$$

where $U(y)$ is the mean streamwise wind velocity at height y above the ground plane, u^{*}_{ABL} the ABL friction velocity, k the von Karman constant (used 0.41 in the present study), and y_0 the aerodynamic roughness length. In the paper, an aerodynamic roughness length of 0.5 is chosen which represents a landscape totally and quite regularly covered with similar-size large objects according to the Davenport roughness classification [10 and 11]. The Aerodynamic boundary layer (ABL) friction velocity, u^{*}_{ABL}, is chosen to obtain the desired reference wind speed, U_{10}, at a height of 10 m (in this study 10 m/s).

In Fig. 3 we can see the difference of raindrop trajectories with different wind velocity and raindrop diameter. The higher the wind velocity, the more inclined the trajectories are. Behind the obstruction the turbulent flow occurs which influences the

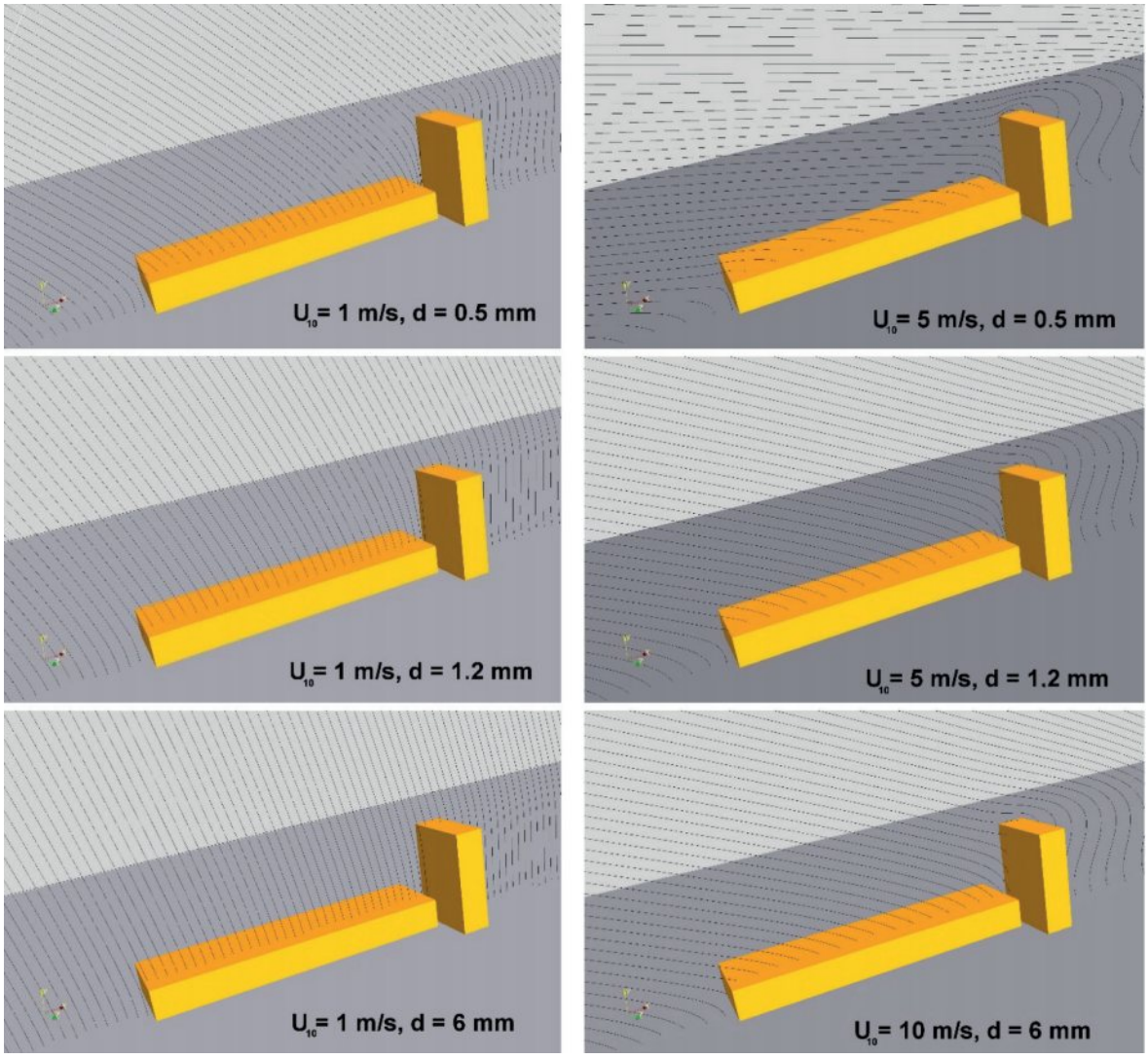

Fig. 3 Raindrop trajectories for selected wind velocity and raindrop diameter

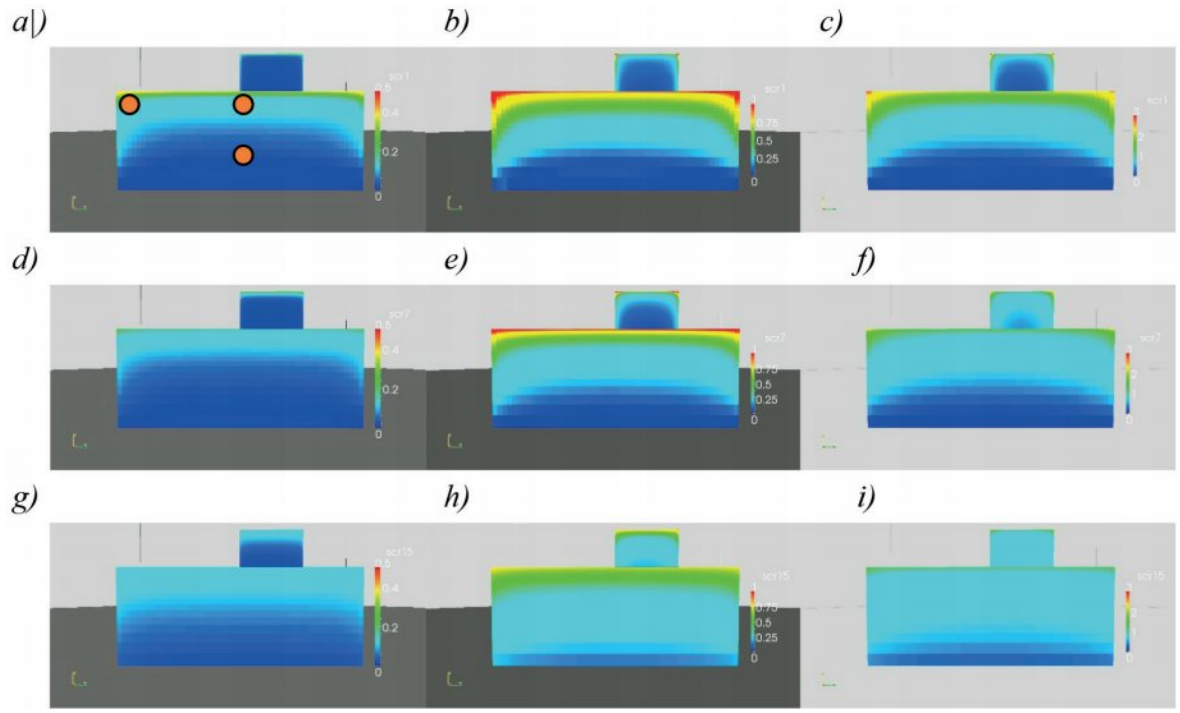

Fig. 4 Specific catch ratio η_d on the low rise building facade for the selected wind velocity and raindrop diameter: a) U10 = 1 m/s, d = 0.5 mm; b) U10 = 5 m/s, d = 0.5 mm; c) U10 = 10 m/s, d = 0.5 mm; d) U10 = 1 m/s, d = 1.2 mm; e) U10 = 5 m/s, d = 1.2 mm; f) U10 = 10 m/s, d = 1.2 mm; g) U10 = 1 m/s, d = 6 mm; h) U10 = 5 m/s, d = 6 mm; i) U10 = 10 m/s, d = 6 mm

trajectories. With using each reference wind-flow field, specific catch ratio distributions are calculated for various diameters (Fig. 4) of raindrops (diameters from 0.5 to 1 mm in steps of 0.1 mm, from 1 to 2 in steps of 0.2 and from 2 to 6 in steps of 1 mm). Catch ratio distributions are obtained for a list of reference horizontal rainfall intensities R_h (0, 0.1, 0.5, 1, 2, 3, 4, 5, 6, 8, 10, 12, 15, 20, 25, and 30 mm/h, catch ratio chart in Fig. 5) using the droplet size distribution as input [12]. The global catch ratio for selected rain event is obtained by summation over all the time steps in the rain event (inputs are wind velocity, wind direction and rainfall on the horizontal plane) [8 and 13].

5. Determination of wind-driven rain load

The global catch ratios for six positions on the facade (Fig. 5) are summarized in Table 3. It was obtained through the numerical model for the measured rain event on 4-5 November 2012 [12].

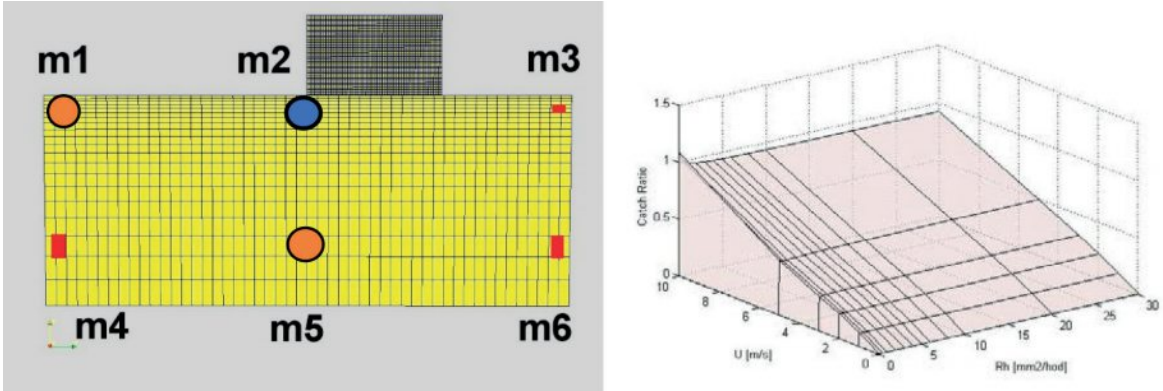

Fig. 5 Position of selected cells on low-rise building facade from Table 3 and catch ratio chart for the position m2; the charts represent R_{wdr}/R_h as function from rain intensity and wind velocity

Catch ratio and proportion factor for the selected locations in Fig. 5 Table 3

Position on facade	Cell number	catch ratio $\eta = R_{wdr}/R_h$	proportion factor *a*	height above the terrain (m)
m1	**1236**	**0.784**	**0.238**	**18**
m2	**1694**	**0.558**	**0.169**	**18**
m3	6575	0.711	0.216	18
m4	1222	0.227	0.069	5
m5	**1683**	**0.170**	**0.052**	**5**
m6	6562	0.203	0.062	5

More detailed information about the rain event is stated in [12]. The rain lasted for 9 hours with cumulative horizontal rainfall 44.5 mm/m^2 .

From Fig. 4, which represents specific catch ratios, we can clearly see the difference of WDR load on the facade which is highest in the upper part and especially in the top corners. For the determination of WDR load on the facade, three positions on the facade were selected (Fig. 5), concretely *m1* with the highest catch ratio, *m2* with overall value for the upper part and *m5* for the lower part of the building. Catch ratio chart for the position *m2* is shown in Fig. 5 and it depends on the wind velocity and rain intensity. The catch ratios from the numerical model are transformed to the proportion factor (Table 3). The proportion factor in the HAM simulation program WUFI defines the position on the facade.

6. HAM simulation in WUFI

For simulation in WUFI software, two different wall types with different coatings were used. According to the previous research [14], climatic year 2010 for Bratislava (mean temperature 9.5°C, horizontal rain sum 1012 mm/m^2) were used as the outer boundary condition. As input for the numerical model was used only rainfall with corresponding wind direction (wind-driven rain which affects the facade -raindrops hit the windward north-west facade). The initial moisture for used materials was typical built-in moisture according to the WUFI database. The inner boundary condition was derived from outer according to the STN EN 15026:2007. Figs. 6 and 7 represent the average annual course of water content in the core layer (ACB and ACC) in the 5th year after the construction of building. Table 4 shows the annual averages of water content for selected positions.

Mean annual water content in the core layer of simulated walls Table 4

[kg/m^3]	TSE	TSF	PSE	PSF
***m1* a = 0.238**	45.86	49.76	78.54	38.26
***m2* a = 0.169**	42.04	42.20	69.28	28.39
***m5* a = 0.052**	27.06	15.06	31.76	8.86

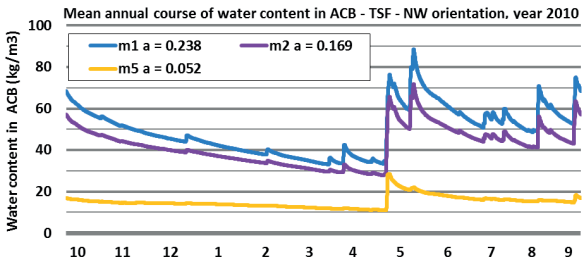

Fig. 6 Mean annual course of water content in aerated clay brick (ACB) wall TSF for the three selected positions on facade with exterior smooth coating FeinPutz

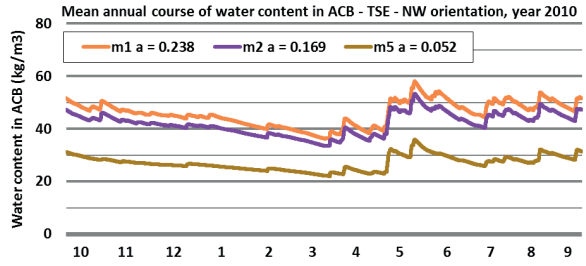

Fig. 7 Mean annual course of water content in aerated clay brick (ACB) wall TSE for the three selected positions on facade with exterior scraped coating EdelPutz

7. Results and discussions

From Figs. 6 and 7 we can clearly see the difference between the WDR load and its influence on the water content in the aerated clay brick. In Tables 5 and 6 we can see how the increased water content is reflected in thermal conductivity (Fig. 8), especially in the upper positions and the aerated clay brick wall where the difference is very big. The thermal resistance decreases up to 45 % for the aerated clay brick wall (TSF) with smooth FeinPutz coatings. With the aerated concrete wall, the values are not so high. In the bottom part of the building (*m5*), the values of thermal conductivity are significantly lower.

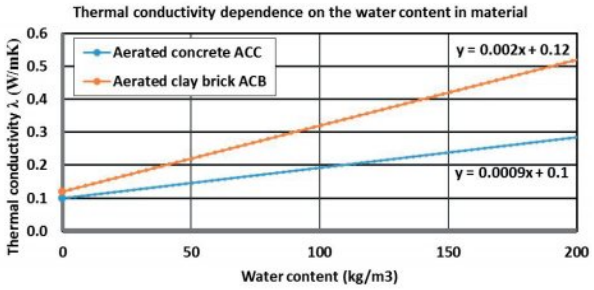

Fig. 8 Thermal conductivity dependence on water content in material
Source: WUFI database

Difference between dry values and values according to the average water content for position *m1* Table 5

m1 a = 0.238	λ (dry)	λ (wet, from Fig. 8)	R (dry)	R (wet)	Difference (%)
TSE	0.12	0.21	3.04	1.72	43.4
TSF	0.12	0.22	3.04	1.66	45.4
PSE	0.1	0.17	3.65	2.15	35.8
PSF	0.1	0.13	3.65	2.81	23.0

Difference between dry values and values according to the average water content for position *m5* Table 6

m5 a = 0.052	λ (dry)	λ (wet, from Fig. 8)	R (dry)	R (wet)	Difference (%)
TSE	0.12	0.17	3.04	2.15	29.4
TSF	0.12	0.15	3.04	2.43	20.0
PSE	0.1	0.12	3.65	3.04	16.6
PSF	0.1	0.11	3.65	3.32	9.1

8. Conclusion

It was demonstrated that the wind-driven rain load has crucial influence on the water content in the wall for the windward oriented facades with exterior coatings based on the traditionally cement-lime material base. The water content values, especially for the aerated clay brick, can be different for different producers because they differ in the shape of the cavities, clay etc. Moreover, the water transport model in WUFI is not ideal considering the materials with cavities (all materials in WUFI are treated as porous material). Also the difference for other manufactures of cement-lime coatings can be different. Each producer has his own manufacturing secrets and different ingredients and mixing ratios.

In the end, we offer a recommendation based on the results of the research. For the windward facades of buildings higher than 10 meters, the usage of cement-lime coatings is not recommended without any other protection (e.g. water repellent paint) because the thermal resistance will be significantly decreased.

Acknowledgement

The research is supported by the European Regional Development Fund and the Slovak state budget for the project "Research Centre of University of Zilina", ITMS 26220220183 and VEGA No. 1/0729/13.

References

[1] BLOCKEN, B., CARMELIET, J.: A Review of Wind-driven Rain Research in Building Science. *J. of Wind Engineering and Industrial Aerodynamics* [online] 13/2004. pp. 1079-1130. [cit. 2010-01-10].

[2] DURICA, P., VERTAL, M.: Verification of the Water Transport Parameter - moisture Storage Function of Autoclaved Aerated Concrete - Approximately Calculated from a Small Set of Measured Characteristic Values. *Communications - Scientific Letters of the University of Zilina,* No. 4, 2011, pp. 35-42, ISSN 1335-4205.

[3] STN EN 15026:2007 *Hygrothermal Performance of Building Components and Building Elements - Assessment of Moisture Transfer by Numerical Simulation (in Slovak).*

[4] SANDERS, C.: *IEA ANNEX 24, Final report, vol. 2, Task 2: Environmental conditions.* Leuven, 1996. ISBN 90-75741-03-0.

[5] FRANKE, J. et al.: The Cost 732 Best Practice Guideline for CFD Simulation of Flows in the Urban Environment: A Summary. *Intern. J. of Environment and Pollution* [online], vol. 44, No. 1-4, 2011, pp. 419-427.

[6] JURAS. P., ZILINSKY, J.: *Measurements of Wind-driven Rain Absorptivity of Various Coatings in Rain Chamber.* Proc. of ATF 2013: 2nd Conference on Acoustics, Light and Thermal Physics in Architecture and Building Structures. Leuven, Belgium 2.-3.5.2013. Katholieke Universiteit Leuven, 2013, pp. 78-84. ISBN 978-90-8649-637-2.

[7] JURAS, P. et al.: *Determination of Rain Reduction Factor of Coatings.* Proc. of ATF 2014: 3rd Conference on Building Physics and Applied Technology in Architecture and Building Structures. Vienna, May, 2014.

[8] KUBILAY, A. et al.: CFD Simulation and Validation of Wind-driven Rain on a Building Facade with an Eulerian Multiphase Model. *Building and Environment*. [online] 61/2013, pp. 69-81 [cit. 2013-04-20].

[9] BLOCKEN, B. et al.: CFD Simulation of the Atmospheric Boundary Layer: Wall Function Problem. *Atmospheric Environment* [online] 41/2007, pp. 238-252 [cit. 2013-04-20].

[10] WIERINGA, J.: Updating the Davenport Roughness Classification. *J. of Wind Engineering and Industrial Aerodynamics* [online], 41-44/1992, pp. 357-368 [cit. 2013-04-20].

[11] HLADIK, O. et al.: Complex Effects of Free Stream Turbulence and Surface Roughness on the Transition Intermittency. *Communications - Scientific Letters of the University of Zilina,* No. 4A, 2012, pp. 47-52, ISSN 1335-4205.

[12] BEST, A. C.: The Size Distribution of Raindrops. *QJR Meteorological Society*, [online] 76/1950, p. 16-36, [cit. 2013-04-20].

[13] JURAS, P., CHVILA, B.: Experimental Measurements of Wind-driven Rain and Validation with CFD (in Slovak), *Meteorologicky casopis / Meteorological J.,* vol. 16, No. 1, 2013, p. 33-40, Bratislava : SHMU, 2013. ISSN 1335-339X.

[14] JURAS, P. et al.: Analysis of Climate Data for Developing TRY for Bratislava. *Meteorologicky casopis / Meteorological J.,* vol. 16, No. 1, 2013, pp. 19-23, Bratislava : SHMU, 2013. ISSN 1335-339X.

Andrea Kocianova *

THE CAPACITY LIMITS OF ROUNDABOUTS

According to the manuals for the capacity calculation and evaluation of roundabouts it is possible to calculate and evaluate the capacity of roundabout entries only under particular traffic conditions. However, it is not possible to simply determine the total capacity of roundabouts. For this reason, custom software tool, which allows total capacity calculation for different models of roundabouts under different traffic conditions, has been created. Results of the maximum capacity limits for some of the analyzed roundabouts at the most influencing traffic conditions settings are shown in the article. For better illustration, the results are compared with maximum capacity limits of simple unsignalized intersection.

Keywords: *Roundabout, capacity, traffic load, critical gap.*

1. Introduction

Modern roundabouts which were developed in the United Kingdom have started to be built in Slovakia after 1999. Concurrently, mainly in urban and rural areas, single-lane roundabouts are widely used. The reasons for their use are mostly:

- enhancement of safety in comparison with other forms of at-grade intersections;
- speed reduction, as one of significant reductions of fatal and injury accidents;
- noise reduction [1];
- aesthetic improvement; and
- higher traffic capacity in comparison with unsignalized intersections [2] and, in some cases, also with signalized intersections [3].

Higher traffic capacity of roundabouts in comparison with unsignalized intersections is related to several factors. One of them is that traffic operation at roundabouts is much easier than traffic operation at unsignalized intersections. At roundabouts, vehicles travel clockwise around a raised centre island, with entering traffic yielding the right-of-way to circulating traffic. This fact results not only in reduction of conflicting points in comparison with unsignalized intersections – from 32 conflicting points at four leg unsignalized intersections to 8 conflicting points at single-lane roundabouts. Moreover, it results in reduction of the number of conflicting traffic streams and hierarchical levels of priorities – from 4 to 2 ranks. Further important factor is the low speed of conflicting traffic flows at the circulating lane – usually 20-25 km/h [4]. At lower speeds of conflicting traffic flows, the critical gaps and follow-up headways are lower, which means more acceptable gaps for safe entrance of vehicles to the circulating lane and also higher capacity.

The aim of the article is to present the capacity limits for selected types of roundabouts under the most influencing traffic conditions settings – proportion of left-turning vehicles and ratio of traffic volume on the major and minor streets. For better illustration they are compared with capacity limits of simple unsignalized intersection – intersection with shared lanes on all legs.

2. Types of roundabouts in Slovakia

Concurrently, mainly compact ***small single-lane roundabouts*** are built in Slovakia. They are roundabouts with diameter between 26 m and 40 m and with single-lane entry at all legs, and one circulating lane (Fig. 1).

Under larger traffic volume ***large double-lane roundabouts*** with diameter more than 40 m (usually up to 60 m) are built. These roundabouts are designed with single- or double-lane entries and two circulating lanes. They are built occasionally because of lower safety on the circulating lane when vehicles need to weave [5]. For the same reason, capacity of the internal lane at double-lanes entries is not much efficient [6 and 7].

Due to deficiency of free space in urban area ***mini-roundabouts*** with diameter between 14 m and 22 m and with traversable island for larger vehicles are built (Fig. 1).

In recent years, ***turbo-roundabouts*** with the spiral arrangement of the circulating lane are designed and built in some European countries. Due to absence of standards and regulations to support

* **Andrea Kocianova**
Department of Highway Engineering, Faculty of Civil Engineering, University of Zilina, Slovakia
E-mail: andrea.kocianova@fstav.uniza.sk

this type of roundabouts, they are not built in Slovakia, but it is only a question of a short time until this trend changes.

Fig. 1 Typical Slovak single-lane roundabout (up) and mini-roundabout (down)

3. Capacity calculation of roundabouts

Capacity manuals are used for capacity calculation but only the capacity of the roundabout entries under particular traffic conditions is possible to calculate and evaluate. However, the total capacity of roundabout as the maximum hourly rate at which vehicles can enter a roundabout under specific geometric and traffic conditions is required. For this reason, the custom software tool was created. By using this software tool the total capacity of various models of roundabouts under various combinations of traffic loads can be calculated in an iteractive fashion. It is possible to determine the maximum total capacity of roundabouts when the degree of saturation of any entry is equal to 1.0 – the reserve of capacity, as a difference between the entry capacity and entry traffic volume, is zero. In addition, it is possible to determine the total capacity of roundabouts for other levels of service. These levels of service depend on an average waiting time. The total capacity of roundabout, as the sum of traffic volumes on all entries of the roundabout, is reached if required limit of any entry is achieved.

As the basis for capacity calculation, the procedure in Czech capacity manual TP 234 [8] was used. Calculation method described in this manual is related to gap acceptance procedure. For the calculation of basic capacity of roundabout entry equation designed by Wu [9] is used (modified the basic idea of Tanner, 1962):

$$G = 3600 \cdot \left(1 - \frac{t_{\min} \cdot q_k}{3600 \cdot n_c}\right)^{n_c} \cdot \frac{n_e}{t_f} \cdot e^{-\frac{q_k}{3600}\left(t_c - \frac{t_f}{2} - t_{\min}\right)} \qquad (1)$$

where:

G - basic capacity of a roundabout entry [pcu/h],
q_k - circulating traffic flow in front of the entry [pcu/h],
n_c - the number of circulating lanes [-],
n_e - parameter taking into account the number of entry lanes [-], n_e=*1.0* for single-lane entry; n_e=*1.5* for double-lane entry,
t_c - critical gap [s],
t_f - follow-up headway [s],
t_{min} - minimum headway between the vehicles circulating in the circulating lane [s].

According to formula (1), the entry capacity of roundabout depends on circulating traffic flow, the number of circulating lanes, the number of entry lanes and on the driver gap acceptance behaviour. This driver gap acceptance behaviour is represented by the critical gap t_c, follow-up headway t_f and minimum headway between circulating vehicles t_{min}. Critical gap is the minimum gap between the vehicles on circulating lane which an entering driver is ready to accept to enter the roundabout. Follow-up headway is the time difference between two consecutive vehicles using the same gap to enter the roundabout.

The values of gap times t_c, t_f and t_{min} specified in TP 234 were derived from experimental data on Czech roundabouts – Table 1. They depend on type and size of roundabouts. For single-lane roundabouts the gap times are also dependent on their geometry - distance between the exiting and entering conflicting points and entry radius. For capacity calculation, the Slovak capacity manual TP 10/2010 [10] has not been used. The reason is that the values of gap times have been taken from HBS (2001) and they are based on the initial experimental data on German roundabouts (observations of Stuwe, 1992). These values have not been verified under Slovak conditions and they are used regardless of the type and geometry of roundabouts (Table 1). Although the values of gap times in Germany have been updated [11], Czech parameters were used, because the traffic rules and a typical behaviour of drivers is very similar as Slovak and Czech Republic are neighbouring countries.

For minimum and maximum geometry parameters of single-lane roundabout, dependence of basic capacity of roundabout entry according to TP 234 is shown in Fig. 2. The chart also shows measurements of 5-minutes interval of saturation flows measured for several single-lane entries at roundabouts in Zilina (some of them are presented in [12]). In some cases, the measured capacity exceeds the value of the theoretical capacity according to TP 234 for minimum geometry parameters of roundabout (*TP 234 min*), but only in a few cases, the measured maximum capacity is higher than theoretical capacity for maximum geometry parameters (*TP 234 max*).

Values of gap times on roundabouts according to TP 234 and TP10/2010 Table 1

TP 234	t_c *[s]*	t_f *[s]*	t_{min} *[s]*
Mini-roundabouts (Mini)	$t_c = 4.5$	$t_f = 3.1$	$13\,m \le D \le 23\,m$ $t_{min} = 3.45\text{-}0.05 \cdot D$
Single-lane roundabouts (1/1)	$11\,m \le b \le 20\,m$ $t_c = 5.6\text{-}0.1 \cdot b$	$8\,m \le R \le 16\,m$ $t_f = 3.6\text{-}0.0625 \cdot R$	*2.1*
Double-lane roundabouts (1/2, 2/2)	*3.7*	*2.6*	*2.1*
TP 10/2010	t_c *[s]*	t_f *[s]*	t_{min} *[s]*
Mini, 1/1, 1/2, 2/2	*4.1*	*2.9*	*2.1*
D – external diameter of roundabouts *R – entry radius* *b – distance between the exiting and entering conflicting points*			

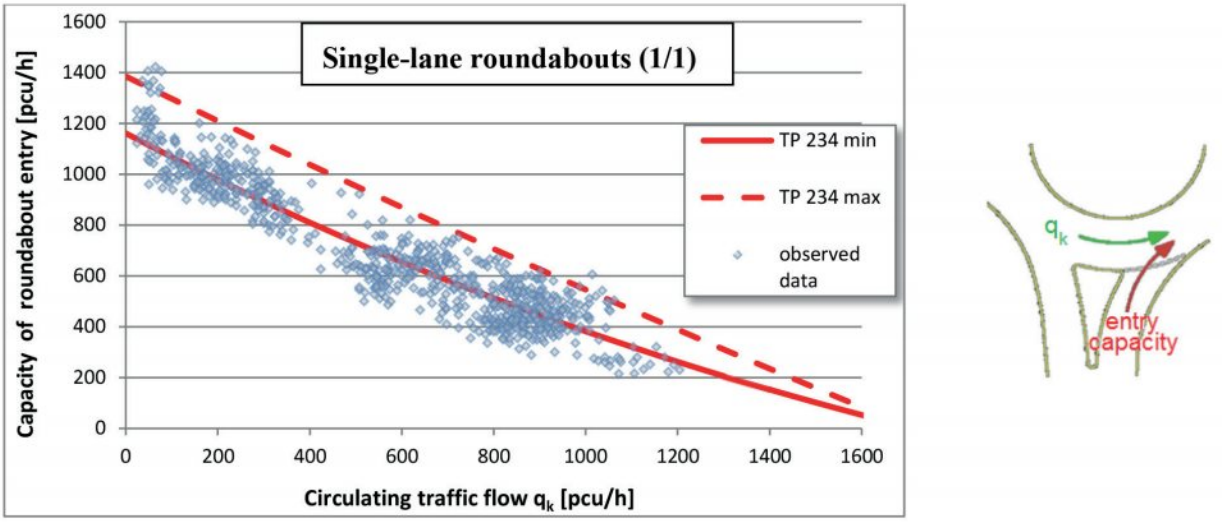

Fig. 2 Comparison of basic entry capacity of single-lane roundabouts according to TP 234 with measurements for single-lane roundabouts in Žilina

4. Capacity limits of roundabouts

Maximum capacity of roundabouts with various geometry parameters (type and size of roundabout, the number of entry lanes and circulating lanes) were evaluated within the analysis. Some of them were selected for the presentation of capacity results in the article. The analyzed roundabouts are listed in Table 2. Moreover, capacity limits of simple unsignalized intersection – with shared lanes on all legs – are also provided for comparison purposes.

In the calculation, it is considered that main and minor streets are crossed in the roundabout location. Two opposite roundabout entries at a major street are in the article referred to as the major entries and two opposite roundabout entries at a minor street are referred to as the minor entries.

Types of analyzed roundabouts – basic parameters Table 2

Type of roundabout	Mini-roundabouts	Small single-lane roundabouts		Large double-lane roundabouts
	One lane on all entry, exit and circulatory roadways	One lane on all entry, exit and circulatory roadways		Double-lane on all entry, exit and circulatory roadways
Labeling	***Mini***	***1/1 min***	***1/1 max***	***2/2***
D	14 m	26 m - 40 m		40 m - 60 m
b	-	11 m	20 m	-
R	-	8 m	16 m	-

The results of the analysis have shown that proportion of traffic volume on the major street and proportion of left-turn vehicles (left-turn percentage) have a significant influence on the intersection capacity from the traffic conditions. For this reason, the following presented dependences are focused only on these two factors. In addition to the maximum total capacity of roundabouts, dependence of the minor entries capacity on the traffic volume on the major entries is shown.

Figure 3, for selected roundabouts and for simple unsignalized intersection, shows graphical dependencies of the minor entries capacity on the major entries traffic volume. The flow pattern is chosen as follows: proportion of left-turn vehicles and right-turn vehicles is 30% and 10% separately for all entries, a ratio of directions is the same on the major street and also on the minor street.

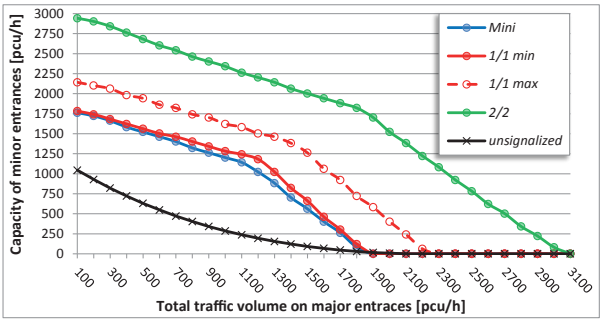

Fig. 3 Graphical dependence of the minor entries capacity on the major traffic volume

We can observe a significant decrease in the minor entries capacity depending on the increasing major entries traffic volume at all of intersections. Capacity of the single-lane roundabout with minimal parameters (*1/1 min*) is only slightly higher than capacity of the mini-roundabout (*Mini*). More significantly, the capacity increase can be achieved by single-lane roundabout with higher parameters (*1/1 max*) – larger entry radius and wider splitter islands, which obviously assumes larger external diameter of roundabout. Higher traffic capacity can be achieved by large double-lane roundabout (*2/2*). However, it should be noted that they are less safe in comparison with single-lane roundabouts because of Slovak roundabout design method for this particular type of roundabout – vehicles must interweave on the circulating lane. All types of roundabouts achieve a significantly higher minor entries capacity in comparison with unsignalized intersection.

The chart in Fig. 3 also clarifies that the total capacity of all types of roundabouts rises when the traffic volumes of the all entries are closer to each other. The highest total capacity is not achieved at very high traffic volume on the major street, as it is for unsignalized intersection. The largest capacity of roundabouts is achieved in the point where the traffic volume at all entries to the roundabout is uniform.

On the charts shown in Figs. 4 and 5, we can observe influence of traffic volume proportion on the major entries (major entries percentage) and the left-turn percentage (*L*) to the total capacity of roundabouts. While the total capacity of roundabouts is increased by reducing of proportion of the traffic volume on the major entries – about 15% - 25% in dependence on left-turn percentage, conversely, the total capacity of unsignalized intersection is reduced to about 30%.

Figure 4 shows the total capacity of single-lane roundabout with minimum parameters (*1/1 min*) which achieve about 1700 pcu/h - 2150 pcu/h at high traffic volumes on the major street – major entries percentage is 90%. The total capacity of simple unsignalized intersection at the same flow pattern is about 1400 pcu/h – 1600 pcu/h. If the traffic loads on the major and minor streets are uniform – major entries percentage is 50%, the total capacity of *1/1 min* roundabout is about 2200 pcu/h - 2500 pcu/h and the total capacity of unsignalized intersection is only about 1000 pcu/h – 1200 pcu/h.

On this chart, the total capacity is shown for following flow pattern: 10% right-turn percentage and the same ratio of directions on the major and minor streets. At higher proportion of right-turn vehicles, the total capacity of roundabouts is increased. At different load ratio of directions on the major and minor streets, the total capacity is reduced.

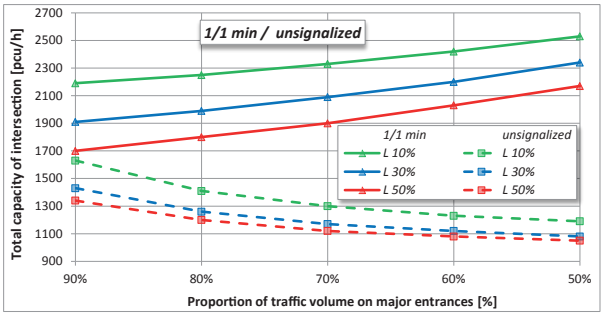

Fig. 4 Traffic volumes on major street influence the total capacity of single-lane roundabout and unsignalized intersection

Figure 5 shows an influence of left-turn percentage to the roundabouts capacity. Increase of left-turn percentage from 10% to 40% leads to a reduction of roundabout capacity by about 10% to 20% depending on traffic volume of the major entries. In higher traffic volumes of the major street the influence of left-turn percentage is more significant. For the given traffic conditions, the capacity were found at intervals: 1750 pcu/h - 2400 pcu/h for the mini-roundabout, 1800 pcu/h - 2500 pcu/h for single-lane roundabout with minimum parameters (*1/1 min*), 2100 pcu/h - 3000 pcu/h for single-lane roundabout *1/1 max*, 2800 pcu/h - 3900 pcu/h for double-lane roundabouts. Mini-roundabout thus can achieve capacity values of 30% - 100% higher than capacity of simple unsignalized intersection. Single-lane roundabout with maximum parameters have 50% - 150% higher traffic capacity

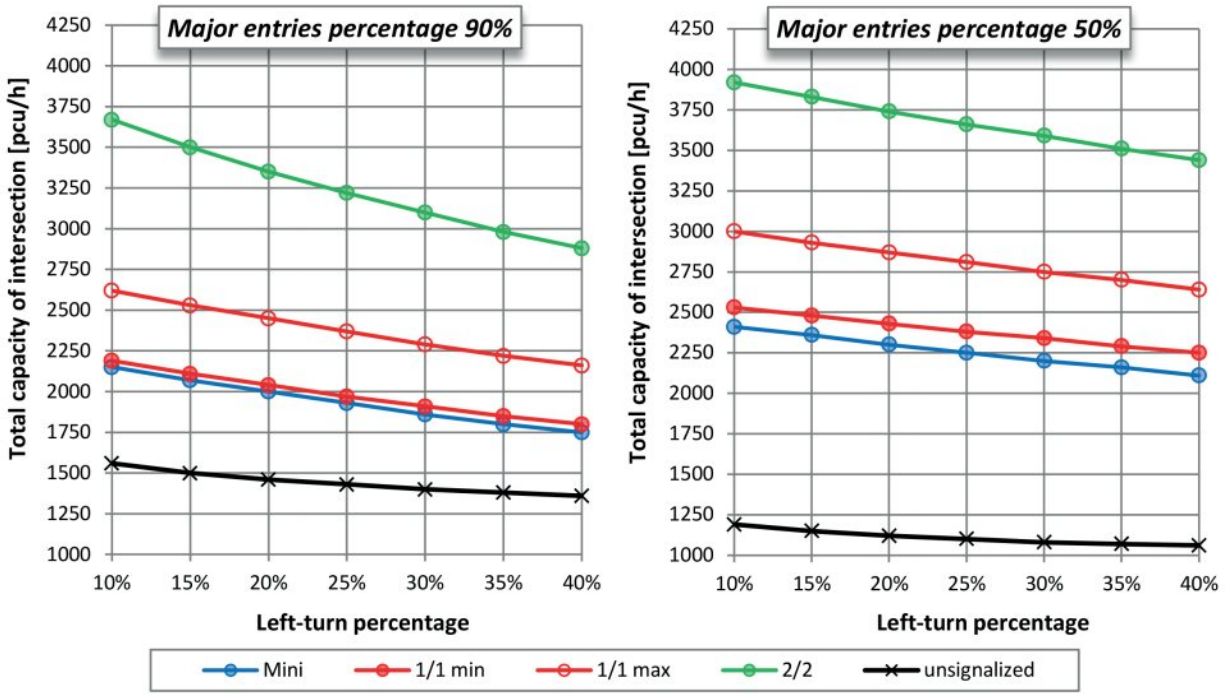

Fig. 5 Total capacities of roundabouts and unsignalized intersection depending on proportion of left-turn vehicles

than simple unsignalized intersection, and large double-lane roundabout have the capacity even two or three times higher.

Maximum capacity limits for roundabouts and simple unsignalized intersection for the whole spectrum of observed combinations of traffic loads are shown in Fig. 6. The lower limit corresponds to the total capacity at unfavourable traffic conditions. When the maximum total traffic load of roundabout is less than this limit, roundabout will be always satisfactory. The upper limit indicates the maximum value of total capacity at favourable traffic conditions. When the maximum total traffic load of roundabout is greater than this limit, roundabout will be always unsatisfactory. Between these borders, it is necessary that the roundabout capacity is verified according to capacity regulations.

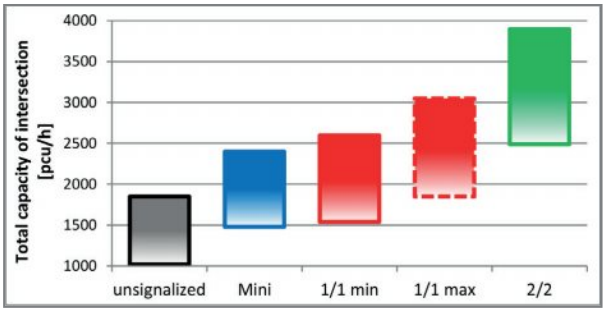

Fig. 6 Maximum capacity limits of roundabouts and simple unsignalized intersection

In Fig. 6, the maximum capacity limits for roundabouts are shown. These capacity levels can be reached, however, this will result in longer waiting times which will be around 100 to 150 seconds at the busiest roundabout entry. If we want to ensure a higher level of service, capacity limits of roundabouts will be lower. For example, level of service ”D” – average waiting time at the busiest roundabout entry is equal to 45 seconds – this will be achieved at reduced maximum total capacity of roundabout, reduced by about 150 pcu/h.

For comparison, following maximum traffic volumes during peak hours were measured at many overloaded intersections of two-lane roads in Zilina: in the range 1300 pcu/h - 1600 pcu/h at simple unsignalized intersections; in the range 2200 pcu/h - 2400 pcu/h at a mini-roundabout; in the range 2500 pcu/h - 2700 pcu/h at single-lane roundabouts, and in the range 2000 pcu/h - 2300 pcu/h at signalized simple intersections. These values do not necessarily mean a maximum total capacity of intersections.

5. Conclusion

Roundabouts are unsignalized intersections which can provide increased traffic safety as well as higher efficiency. Maximal capacity limits for different types of roundabouts, in different traffic conditions are presented in the article. The analysis showed a significant influence of traffic volume of the major street and proportion of left-turn vehicles to the total capacity of roundabouts. The influence of these factors can mean

up to 40% difference in the total capacity of the same roundabout type. By suitable design of roundabouts significantly higher total capacity can be achieved in comparison with unsignalized intersections. Depending on roundabout geometry, and on traffic condition, maximum capacity limits for conventional single-lane roundabout can exceed simple unsignalized intersection capacity by 50% -150%. Moreover, this will provide shorter waiting times on entries.

Presented maximum capacity limits of roundabouts can be exceeded. Additional efficiency can be achieved by addition of separate by-passes for right-turn vehicles, or by designing of modern roundabouts – turbo roundabouts – with spiral arranged circulating lanes, which are more efficient and also safer than conventional Slovak double-lane roundabouts.

Acknowledgements

This contribution/publication is the result of the project implementation:

Centre of excellence for systems and services of intelligent transport, ITMS 26220120028 supported by the Research & Development Operational Programme funded by the ERDF.

„Podporujeme vyskumne aktivity na Slovensku/Projekt je spolufinancovany zo zdrojov EU“

References

[1] DECKY, M., TROJANOVA, M., REMEK, L., JATY, L.: *Noise Pollution from Roundabout Traffic in the outer Environment of Built-up Areas of Towns,* 12th Multidisciplinary scientific geoconference SGEM 2012, June, 2012, Albena, ISSN 1314-2704, pp. 927-934.

[2] SLABY, P., KOUKAL, M.: Capacity of At-grade Intersections in Relation to the Quality of Service (in Czech), *Silnicni obzor*, No. 9, pp. 234-238, 2005, ISSN 0322-7154 47 320.

[3] *Transport Research Board: Roundabouts: An Informational Guide.* NCHRP Report 672 – 2nd ed., Washington D.C., 2010.

[4] REZAC, M., CIHLAROVA, D., SEIDLER, T., SIMONIK, P.: *Options to Mitigate Congestion on Roads,* Proc. of Intern. Conference on Civil Engineering, Architecture and Building Materials, CEABM 2013. Jinan, May, 2013, vols. 361-363, pp. 2049-2052, ISSN 1660-9336, ISBN 978-3-03785-777-9.

[5] KRIVDA, V: Video-Analysis of Conflict Situations on Selected Roundabouts in the Czech Republic. *Communications - Scientific Letters of the University of Zilina*, vol. 13, No. 3, 2011, pp. 77-82, ISSN 1335-4205.

[6] BRILON, W.: Roundabouts: *A State of the Art in Germany*. National Roundabout Conference, Vail : Colorado, May, 2005

[7] SMELY, M., RADIMSKY, M., APELTAUER, T.: Capacity of Roundabouts with Multi-lane Entrances (in Czech), *Dopravni inzenyrstvi*, No. 1, pp. 20-21, 2011, ISSN 1801-8890.

[8] TP 234 *Capacity Evaluation of Roundabouts (in Czech)*, EDIP, 2011, ISBN 978-80-87394-02-01.

[9] BRILON, W., BONDZIO, L., WU, N.: *Unsignalized Intersections in Germany - a State of the Art*, 2nd Intern. Symposium for Unsignalized Intersections, Portland : Oregon, 1997.

[10] TP 10/2010 *Capacity Calculation of Roads (in Slovak)*, MDPaT SR, 2010.

[11] BRILON, W.: *Studies on Roundabouts in Germany: Lessons Learned*, 3rd Intern. TRB-roundabout Conference, Carmel : Indiana, May, 2011.

[12] GAVULOVA, A., DRLICIAK, M.: Capacity Evaluation of Roundabouts in Slovakia. *Transport and Telecommunication*, vol. 13, No. 1, 2012, Riga, ISSN 1407-6160 (e-ISSN 1407-6179), pp.1-10.

Josef Vican - Peter Janik - Ruzica Nikolic *

EXPERIMENTAL AND NUMERICAL ANALYSIS OF ECCENTRICALLY LOADED BEAM-COLUMNS

The beam-column subjected to the combination of the axial force and the bending moments is an example of the very complicated task from the viewpoint of the design resistance verification. The general theoretical solution of the resistance assessment of that beam-column is not suitable for practical use due to complicated and non-general form. Then, the standard simplified approach is used. Therefore, the paper deals with the experimental and numerical analyses of the resistances of eccentrically loaded beam-columns and their comparison with the standard approaches. Discussion of results and conclusions related to further research direction are also presented in this paper.

Keywords: *Eccentrically loaded beam-column, beam-column resistance, experimental analysis, numerical study.*

1. Introduction

The verification of the beam-column resistance subjected to the axial force in combination with the bending moments is a very complex task from the viewpoint of design practice. Therefore, the standard approach [1] to beam-column resistance assessment is based on the simplified model of substitute member whose accuracy and suitability is controversial in the special cases of member load effects and member boundary conditions. Then, the determination of the beam-column resistance and its verification need necessarily to be more precise and complex, supported by the numerical calculations or experimental analyses. From this point of view, the paper presents results of experimental and numerical analyses of the determination of the beam-column resistance and its verification compared to the standard approaches [1].

2. Theoretical background

In general, the bending and torsional moments' equilibrium of the pin-ended beam-column with the double symmetric constant cross-section, initially imperfect about both axes subjected to the constant compressive axial force and bending moments, could be described by means of the system of differential equations presented, e.g., in [2] and [3]. Generally, the system of differential equations represents system with non-constant coefficients whose solution cannot be found in an analytical form. In the case when only the axial force is acting eccentrically with respect to both cross-sectional axes and the eccentricities are constant within the length of the beam-column, the bending moments M_y and M_z have constant shapes. Then, the exact solution in the analytical form should only be found. The system of equations becomes more inhomogeneous when the initial equivalent geometric imperfections in the form of initial bows about axes y-y and z-z, and initial cross-sectional rotation are implemented into the system. Thus, buckling resistance of the initially imperfect beam-column with double symmetric constant cross-section, subjected to eccentrically axial compressive force N, causing bi-axial bending moments M_y and M_z in the two principal cross-section planes of loading, can be described by the system of differential equations in the following forms

$$\begin{aligned} &EI_z v^{IV} + N\left(v + v_o\right)^{II} + M_y\left(\theta + \theta_o\right)^{II} = 0 \\ &EI_y w^{IV} + N\left(w + w_o\right)^{II} + M_z\left(\theta + \theta\right)^{II} = 0 \\ &EI_w \theta^{IV} - GI_t \theta^{II} + i_s^2 N\left(\theta + \theta_o\right)^{II} + M_y\left(v + v_o\right)^{II} + \\ &+ M_y\left(w + w_o\right)^{II} = 0 \end{aligned} \tag{1}$$

where:

E	is the Young's modulus of elasticity,
G	is the shear modulus,
I_y, I_z	is the second moment of area about the y-y or z-z axis, respectively,
I_t	is the St. Venant's torsional constant,
I_w	is the warping torsional constant,
N	is the normal compressive force,
M_y, M_z	are the bending moments about the y-y and z-z axis, respectively, induced due to eccentrically acting axial force; $M_y = Ne_z$, $M_z = Ne_y$

* [1]Josef Vican, [1]Peter Janik, [2]Ruzica Nikolic
[1]Department of Structures and Bridges, Faculty of Civil Engineering, University of Zilina, Slovakia
[2]University of Kragujevac, Faculty of Mechanical Engineering, Kragujevac, Serbia
E-mail: josef.vican@fstav.uniza.sk

i_s is the cross-sectional polar radius of gyration around to the centre of shear,
v_o is the initial deflection of a member in the y-y axis direction,
v is the deflection increment of a member in the y-y axis direction,
w is the deflection increment of a member in the z-z axis direction,
w_o is the initial deflection of a member in the z-z axis direction,
q_o is the angle of the initial cross-sectional rotation of a member about the x-x axis,
q is the angle increment of cross-sectional rotation of a member about the x-x axis.

The analytical solution of the above described system of differential equations was presented, e. g., in [4] together with the comparison of the results experimentally obtained by Chuvikin [5] and results determined using numerical analyses by means of software ANSYS. A great attention was paid to the problem of the beam-column resistance verification in the frame of preparation of the European standard [1]. Conclusions and results of many numerical and experimental analyses and studies, worked up in the field of the above mentioned area, were summarized in [6] and [7] in comparison to the approach proposed in standard [1]. There is more information related to theoretical background of the beam-column resistance verification and solved examples according to rules for reliability verification of beam-column recommended in [1] using the method of substitute member based on the interaction formulas respecting the second-order theory.

3. Experimental analysis

3.1 Test samples and testing description

The formulas for verification of the beam-column resistances in standard [1] are based on the behavior of the single-span isolated members with simply supported end conditions. Therefore, the maximum bending moments in the two principal cross-section planes of loading are situated within the beam-column span. In the cases of other end conditions, the application of standard formulas for substitute members is rather complicated and extreme care should by taken when applying them to members integrated in frames. Accordingly, the experimental analyses supported by the numerical calculations were proposed to verify this general case approximated in both types of analyses, by the model of pinned-fixed beam-column. The main objective of the experimental investigation was to determine the actual ultimate resistances of tested beam-columns subjected to compressive axial force in combination with the applied end bending moments due to the axial force eccentricity and also to verify the suitability and correctness of standard approaches to the assessment of beam-column resistance in accordance with [1]. Consequently, four sets of beam-column samples, designated as A, B, C and D according to the type and eccentricity magnitude, were investigated in laboratory of the Department of structures and bridges. Each set of samples comprised three beam-columns made of IPE 120. Due to laboratory space and testing device arrangement, all samples had equal length of 1400 mm introducing beam-column relative slenderness of $\bar{\lambda} = 0.82$ respecting the model of pinned-fixed beam-column. Beam-columns of set A were tested with the zero eccentricity of axial force (centrically loaded beam-columns), samples of set B had the preliminary measured eccentricity of the axial force of e_y = 32.2 mm in the y-axis direction, samples of set C had the eccentricity of e_z = 52.2 mm measured in the z-axis direction and beam-columns of set D had the both type of eccentricities of axial force, i.e. e_y = 32.2 mm and e_z = 55.2 mm measured before experimental testing. The fixed edges were situated at the bottom ends of the vertically tested samples while the hinged boundary conditions were simulated at the tops of samples using the specially adjusted device. Both beam-columns ends were equipped with the end-plates of 30 mm (at the bottom) or 20 mm (at the top) thick ensuring the zero warping deformations of beam-column edges.

Before testing, the actual geometrical and material characteristics of the beam-columns were determined and evaluated statistically. Concurrently, the initial bow imperfections in direction of both axes were measured by means of geodetic method and its measured amplitudes reached values of $L/3860$ in the z-axis direction and $L/5250$ in the y-axis direction. Using the obtained average material and geometric characteristics of tested beam-column (the yield strength f_y = 300 MPa, the cross-section area A = 1382.86 mm^2, the second moments of cross-section area I_y = 3.308 .10^6 mm^4, I_z = 2.86.10^5 mm^4) and taking into account the measured actual initial member eccentricities and bow imperfections, the resistance verifications of all the tested samples were performed according to [1], to prepare the testing program.

The strains and lateral deflections in chosen beam-columns locations (see Fig. 1) were monitored using gauges 6/120 LY11 (HBM) and potentiometer sensors of deformations TR50 recorded by means of Spider 8, also enabling recording of the actual value of compressive force monitored by dynamometer situated at the top end of the tested beam-column. As it can be seen in Fig. 1, the measurement devices were located at distance of 50 mm (gauges) or 40 mm (deformation sensors), respectively from the end-plates to avoid local effects of test load. Test loading was organized in two stages. In the first stage, the loading force increments were chosen gradually by 20 kN up to limit value of 100 kN ensuring the elastic state of maximum stressed beam-column cross-section. After the limit loading force had been reached, the unloading of the tested beam-column followed. In the second testing stage, the loading force increments were added gradually by 20 kN up to the limit value of 200 kN when the test has continued by means of deformation increments by constant

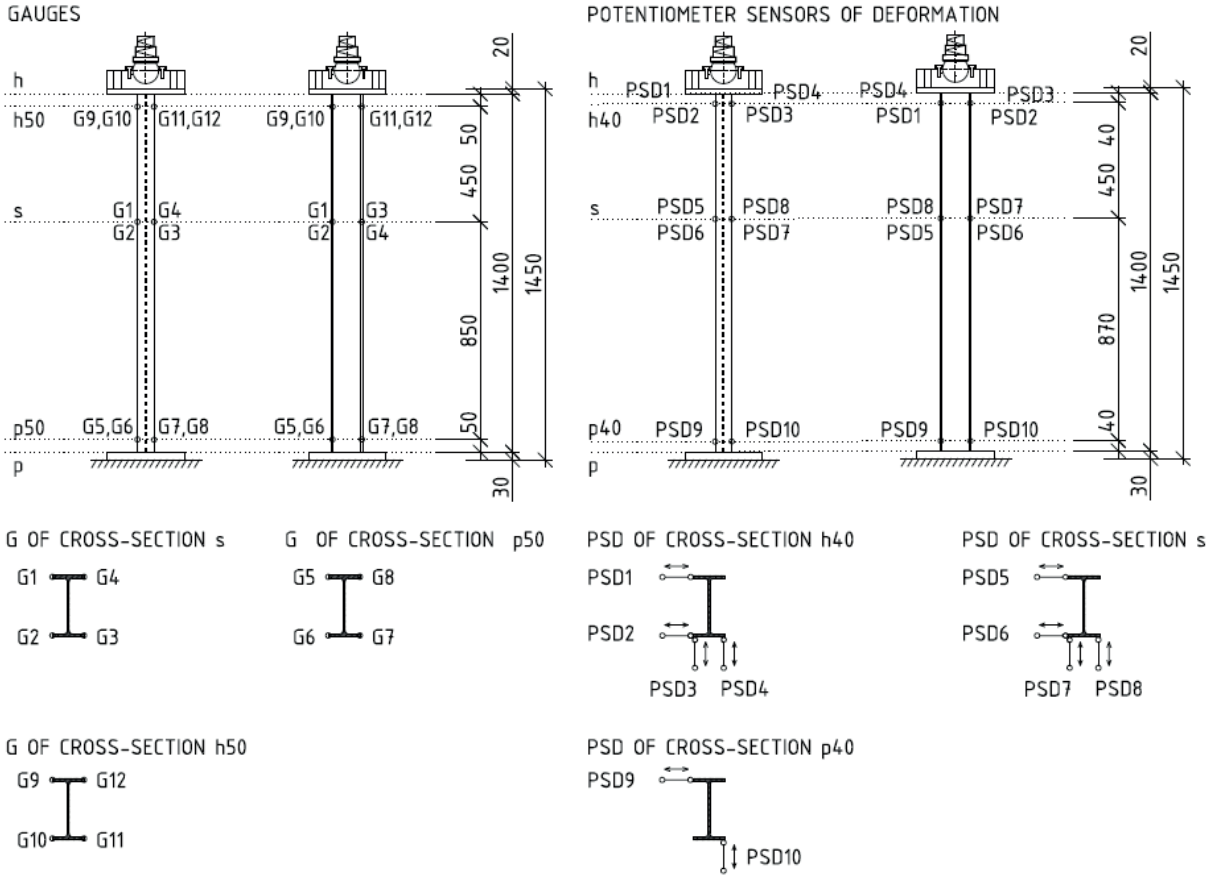

Fig. 1 Laboratory samples of beam-columns with designated locations of measured strains and lateral deflections; G - gauges locations; PSD - locations of deformation sensors

adding of 0.1 mm, up to the beam-column collapse. The above described testing program was applied to all laboratory tested beam-columns. More information related to the voluminous experimental analysis can be found in [8].

3.2 Results of experimental analysis

The beam-column behavior was observed within the loading tests to identify the decisive steps of the member cross-section resistance. In the case of sample set A, the first plasticization occurred in the cross-section *p50* (see Fig. 1). Then the plasticization of cross-section *s* followed and the plasticization of the cross-section *h50* was the last, very close to member collapse. In the case of sample set B, the first plasticization occurred in the cross-section *h50* (see Fig. 1).

Then the plasticization of the cross-section *p50* followed and the plasticization of the cross-section *s* was the last. Results of tested samples of set C and D showed that the first plasticization occurred in the cross-section *h50*, then the plasticization of the cross-section *s* followed and the plasticization of the cross-section *p50* was the last. Due to bending moment effects, the greater plastic reserves were indicated in the case of all tested beam-columns compared to the centrically loaded samples of set A. Experimentally investigated ultimate resistances defined by the member collapses are presented in Table 1.

Ultimate resistances N_u of tested members — Table 1

Designation	N_u [kN]	Designation	N_u [kN]	Designation	N_u [kN]	Designation	N_u [kN]
A1	346.0	**B1**	133.0	**C1**	221.0	**D1**	107.0
A2	345.0	**B2**	149.0	**C2**	220.0	**D2**	114.0
A3	341.0	**B3**	148.0	**C3**	211.0	**D3**	112.0
Average	**344.0**	**Average**	**143.3**	**Average**	**217.3**	**Average**	**111.0**

Results of the experimental analyses were also used for evaluation of the actual force eccentricities and member bow imperfections. As it was mentioned above, the real imperfections of tested members were measured before testing to calculate more precisely the resistances of tested members. The evaluation of measured strains in the chosen locations gives more correct information related to the actual member imperfections including actual eccentricities of applied forces. From the view point of correct comparison of experimentally obtained resistances of tested samples to the numerically determined ones, the application of by these means evaluated imperfections into the numerical calculations is needed.

4. Numerical analysis

4.1 Numerical modeling and results

Generally, nine numerical models were created to simulate behavior of member samples A up to D. To plan the testing program, four numerical models were developed in the preparation stage before experimental testing. After experimental analysis, other five models were created taking into account real geometry and actual imperfections of tested members obtained by evaluating experimental tests. Due to large difference between the ultimate resistances of samples B1 and B2, B3 (see Table 1), the sample behavior of set B were modeled by means of two models respecting the mentioned differences.

Numerical models of tested members were developed in the working environment of the software Ansys -Workbench using actual geometric characteristics of tested members. The actual eccentricities, evaluated from the strain measurements were also implemented into the numerical models. Effects of residual stress were taken into account by means of equivalent geometric imperfection whose amplitude e_{0e} was calculated using standard expression for Perry factor in accordance with [1].

The bilinear material model with actual yield strength f_y = 300 MPa obtained from material tests and the nominal value of the Young's elasticity modulus E = 210 GPa was used to simulate material behavior. Effect of material strengthening was neglected because real beginning of material hardening reached almost 5 % of measured strains while the strain corresponding to the actual material yield strength was 0.14 %. The numerical model was developed using the 3D finite elements Solid 186 and Solid 187, enabling geometrically and materially nonlinear analysis with imperfections included (GMNIA), [9]. Contacts were modeled using finite elements of Conta174, Targe170 Surf154 and Combin14. An example of the applied numerical model created in working environment of the software Ansys -Workbench is shown in Fig. 2 for the case of tested sample set C.

Results of experimentally determined ultimate resistances of tested members A1, B1, C1 and D1 compared to numerically calculated ones using above described numerical models are presented in Table 2.

Ultimate resistances of tested members compared to numerically determined ones — Table 2

Designation	Experimental analysis [kN]	Numerical analysis [kN]	Difference [%]
A1	346.0	346.16	0.05
B1	133.0	133.81	0.6
C1	221.0	226.88	2.6
D1	107.0	111.4	4.1

It can be seen that the numerically obtained ultimate resistances of members are a little higher than experimentally achieved ones. That is probably caused due to applications of standard equivalent imperfections determined by means of standard expression for Perry factor in [1] which have the larger effects than real member's imperfections obtained from the measurements. Fig. 3 shows the deformation states of numerically analyzed members in the stage closely before member collapses (see Fig. 3).

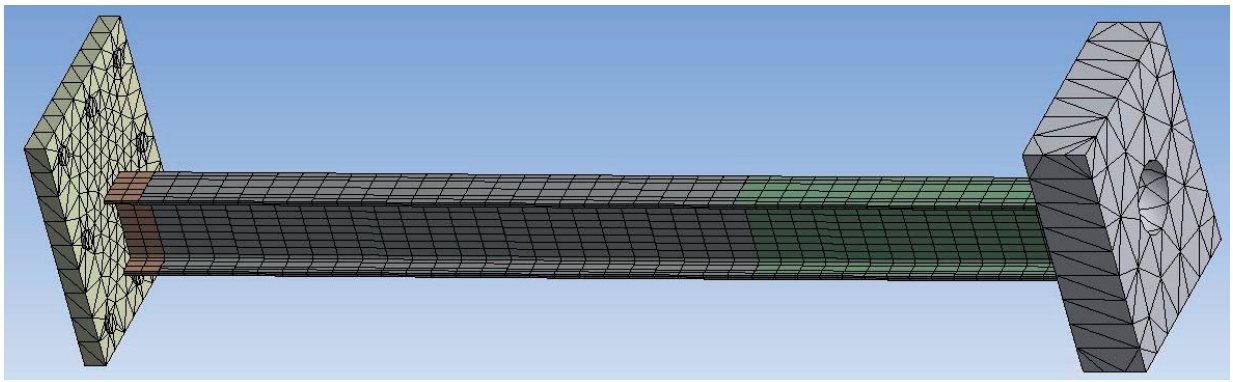

Fig 2 An example of the developed numerical model

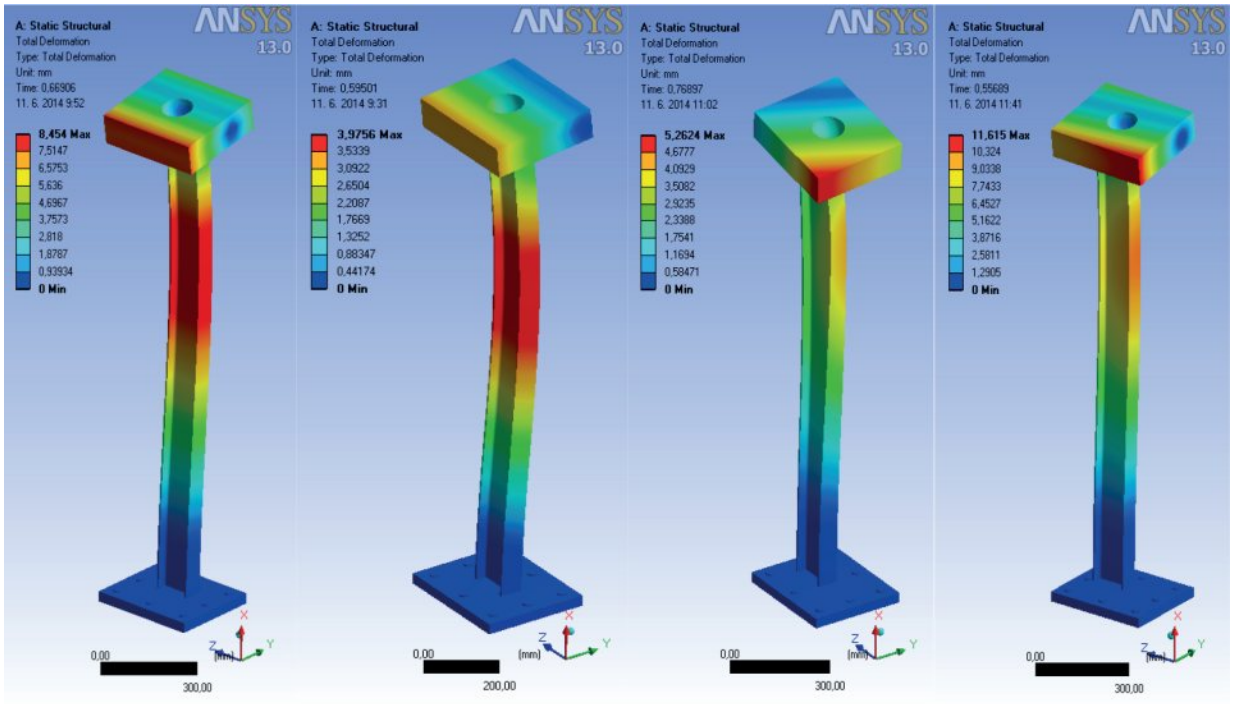

Fig. 3 Deformation states of numerically tested members in collapse stage (from A to D - from left to right)

4.2 Comparison of horizontal deflections

Values of recorded horizontal deflections of tested samples are compared to the numerically determined ones in Figs. 4 to 7.

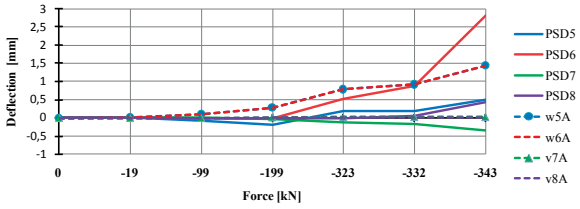

Fig. 4 Comparison of horizontal deflections in the cross-section s of sample A1

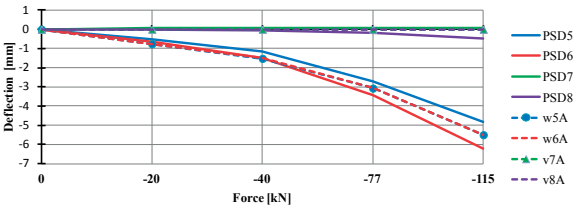

Fig. 5 Comparison of horizontal deflections in the cross-section s of sample B1

Values of deflections calculated by means of above described numerical models are marked in Figs. 4 to 7 as w5A, w6A, v7A, v8A and are corresponding with the values measured using deformation sensors designated as PSD5 up to PSD8 (see Figs. 4 to 7).

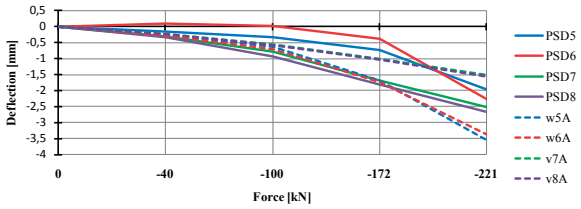

Fig. 6 Comparison of horizontal deflections in the cross-section s of sample C1

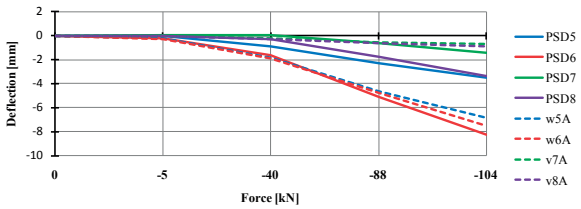

Fig. 7 Comparison of horizontal deflections in the cross-section s of sample D1

From Figs. 4 to 7, the relative good accordance of measured deflections with the numerically determined ones is evident.

4.3 Comparison of strains

Values of strains, measured within the experimental tests, were compared to the values of strains obtained using numerical calculations, respecting the elastic or elastic-plastic states of the member's cross - sections defined by means of the appropriate material model. Values of strains marked in Figs. 8 to 11 as ε1-ε4 are strains measured during experimental tests using gauges. Designations of ε1A - ε 4A correspond to values of strains obtained by means of the numerical calculations.

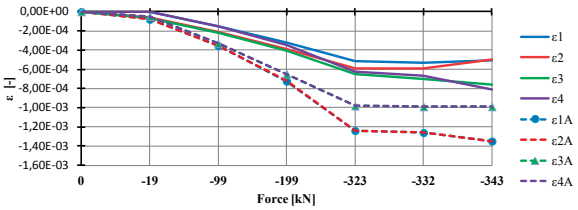

Fig. 8 Comparison of strains in cross-section s of member A1

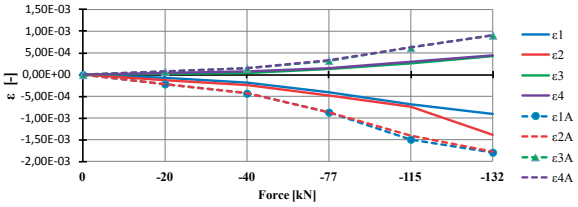

Fig. 9 Comparison of strains in cross-section s of member B1

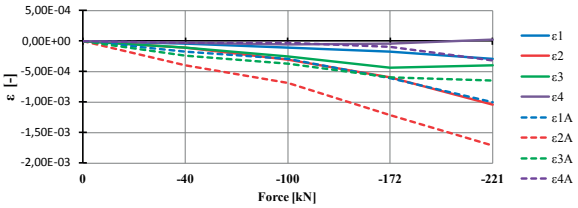

Fig. 10 Comparison of strains in cross-section s of member C1

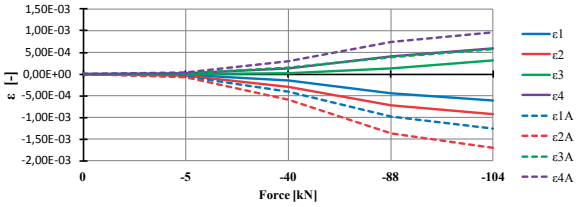

Fig. 11 Comparison of strains in cross-section s of member D1

Increase of strains showed similar trend in both analyses but measured values of strains are lower than numerically calculated ones (see Figs. 8 to 11). Difference of values could be caused by the greater effects of the second-order theory, considered in the numerical calculations compared to actual ones in the experimental analysis. This greater effect of the second - order theory in numerical calculations proved that the standard equivalent geometric imperfection has a greater influence than the real member imperfections and eccentricities measured within testing.

4.4 Comparison of experimental resistances to the standard ones

The experimentally determined resistances of the tested samples were also compared to resistances defined using the standard approach according to [1]. In this standard two methods A and B for verification of the beam-column resistance are recommended. The resistances of the tested samples were determined from appropriate formulas valid for beam-column resistance verification under following assumptions:

- the buckling resistance only of the type A samples was assessed;
- the resistance of the B samples was determined without respecting the effects of lateral-torsional buckling;
- the assessment of the buckling resistances of the C and D samples was carried out with respecting the effects of the lateral-torsional buckling;
- the average value of the material yield strength f_y = 300 MPa was considered,
- the nominal values of the Young's elasticity modulus E = 210 GPa and shear modulus G = 81 GPa were taken into account in calculations;
- the actual geometric characteristics of the tested samples obtained from the measurements were considered to calculate the standard resistances;
- the buckling lengths of the tested samples C and D were taken as $L_y = L_z$ = 980 mm;
- the imperfection factors α_l = 0.21 for buckling in the z-axis direction and α_1 = 0.34 for buckling in the y-axis direction were considered for calculation of initial bow amplitudes in the both member cross-section directions.

The obtained results of the resistances calculated according to methods A and B from the standard [1] are presented in Table 3 together with the resistances determined experimentally. The following designations are used in Table 3:

e_y is the eccentricity of the axial force in the y-axis direction;
e_z is the eccentricity of the axial force in the z-axis direction;
N_{exp} is the experimentally determined ultimate resistance of tested members;
N_A is the resistance of the tested members calculated by means of method A in accordance with [1];
N_B is the resistance of the tested members calculated by means of method B in accordance with [1].

Comparison of experimentally determined resistances to the standard ones Table 3

Designation	e_z	e_y	$N_{exp.}$	N_A	N_B	N_A/N	N_B/N
	[mm]	[mm]	[kN]	[kN]	[kN]	[%]	[%]
A1	0.00	0.00	323.00	295.5	295.5	91.5	91.5
B1	0.00	13.00	133.00	126.00	131.00	98.5	89.5
C1	22.65	2.36	221.00	214.00	196.00	96.8	88.7
D1	36.50	18.34	106.60	122.00	110.00	114.4	103.2

Besides the sample of type D1, the comparison of the member resistances presented in Table 3 proves very good compliance of experimentally determined resistances with those calculated according to approaches recommended in [1] (see Table 3). The member resistances calculated by means of method A are closer to the experimental results than resistances determined according to method B. This conclusion corresponds to the theoretical background of both methods whereas the method A is generally considered as the more precise approach to the beam-column resistance verification.

5. Conclusions

The paper presents the results of voluminous experimental analysis of resistances of the pinned-fixed beam-columns subjected to centrically (samples of set A) and eccentrically (samples of sets B to D) acting axial force and their comparison to the numerically determined ones using GMNIA. Results of comparison proved very good correspondence of numerical calculations with the experimental tests; thus the developed numerical models could be used for further parametric studies to obtain more information about actual behavior of those complicated structural members. The standard approach designated as method A [1] also proved relatively good compliance due to its more precise but also more complicated formulation. Moreover, the experimental analysis confirmed the correctness of theory related to importance of the point with the maximum effect of the second-order theory [8].

Acknowledgements

This work was supported by the Slovak Research and Development Agency under contract APVV-0106-11 and by Research Project No. 1/0364/12 of Slovak Grant Agency. Moreover, the research presented here was supported by the European Regional Development Fund and the Slovak state budget for the project “Research Centre of University of Zilina”, ITMS 26220220183.

References

[1] STN EN 1993-1-1. *Eurocode 3: Design of Steel Structures - Part 1-1: General Rules and Rules for Buildings*, CEN Brussels, May 2005.
[2] VLASOV, V.Z.: *Thin-walled Elastic Members*, SNTL, Prague, 1962.
[3] BREZINA, V.: *Buckling Resistance of Metal Members and Beams*, Czechoslovak academy of sciences : Prague, 1962.
[4] VICAN, J., JANIK, P.: Beam-column Resistance According to Slovak Standard and Eurocodes, *Communications - Scientific Letters of the University of Zilina*, 15 (2013), pp. 21-27.
[5] GALAMBOS, T. V.: *Review of Tests on Biaxially Loaded Steel Wide-Flange Beam-Columns*. Lehigh University, April, 1963.
[6] BOISSONNADE, N. et al.: *Rules for Member Stability in EN 1993-1-1*, *Background Documentation and Design Guidelines*, ECCS 2006.
[7] SIMOES DA SILVA, L., SIMOES, R., GERVASIO, H.: *Design of Steel Structures – Eurocode 3: Design of Steel Structures Part 1-1: General Rules and Rules for Buildings*. Mem Martins : Multicomp Lda, 2010.
[8] JANIK, P.: *Resistance of Beam-column Subjected to Transversal Load and Axial Force*, PhD. Thesis, University of Zilina, 2014.
[9] KALA, Z., KALA, J.: *Respecting the Influence of Geometrical and Material Imperfections of Steel Beam when Calculating their Load-carrying Capacity*, Stability and Ductility of Steel Structures, Budapest : Akademiai Kiado, 2002, pp. 103-110.

Marian Drusa - Jozef Vlcek *

NUMERICAL APPROACH TO PILE LOAD TEST USING 3D FINITE ELEMENT METHOD

Despite the various design approaches, the design of the pile foundations is still to be verified by the in-situ load tests to check the design stage assumptions. This paper presents the results of the study aimed at the soil properties and interaction between piles and soil. Calibration of the numerical model is based on the in-situ pile load test. It represents the case study, how variation of soil characteristics acting in interaction with pile and numerical technics can attain the coinciding results with tested outputs. Moreover, this study is contribution to the effort of designing the pile foundations more accurately with limiting occurrence of potential risks.

Keywords: *Pile test, displacement piles, 3D FEM, pile interaction*

1. Introduction

Confirmation of the pile design by the in-situ tests is a common approach to achieve safe and economic design. The static pile load test is the best method of verifying the bearing capacity of a pile [1]. Mechanisms involved in pressing or pulling of the pile are complicated to describe by the analytical methods. Difference between analytical solutions and real state is represented by the empirical coefficients [2]. On the other hand, numerical modelling allows taking into account the boundary conditions and factors, such as limit settlement of the pile, shear surface propagation around the pile and stress distribution around the pile bottom. However, numerical modelling places more demands on the quality and volume of input data. Accurate model of soil-pile interaction and appropriate soil parameters [3], [4] are the goals of the numerical modelling. The data were optimized through the model calibration until numerical model results reached the outputs of the pile load test.

2. Static pile load test

Static pile load test realized on a single massive circular pile offered a basic set of results such as settlement and corresponding load, which were used as a comparable output for numerical model. Static load test carried out on the vertically loaded bored pile [5], with diameter 880 mm and 5.5 m length, made by classical method with casing support. The pile is a part of bearing system of a new production hall. The maximum vertical force was set to 870 kN according to the design load determined by the calculation. The pile load test was arranged to measure the ultimate limit state.

Geological profile was explored by the dynamic penetration test (DP), which is suitable in case of deep foundation, especially in case of piles. Penetration of the rod is similar to the pressing of the pile, [6]. For the reason of possible occurrence of large boulders in the top layer consisting of antropogenous soils, a dynamic test method was chosen with weight of the hammer 50 kg. Determined soil properties were verified by the macroscopic evaluation of the borehole core [7], [8].

3. Numerical model

Numerical modelling was performed by software Plaxis 3D Foundation using finite element 3D code, (Fig. 1). Numerical model data were taken by the geological survey [7] and had been required a set of soil parameters used by Mohr-Coulomb material model (Table 1.). For the concrete pile material, a linear elastic non-porous model was chosen with unit weight 24 kN.m^{-3}, reference modulus of elasticity E_{ref} = 31 GPa and Poisson's ratio ν = 0.17.

The first step of model series was used to determine the appropriate value of reduction factor R_{inter} as the parameter of soil-pile interaction [1]. Reduction factors, as well as drain conditions were varied. Only undrained conditions (soil fully saturated in terms of short-term condition) with effective shear strength parameters and reduction factor R_{inter} = 1.0 were able to achieve closest results in the final settlement of pile head in comparison to test data (Fig. 2). This first approach using only data from

* **Marian Drusa, Jozef Vlcek**
Department of Geotechnics, Faculty of Civil Engineering, University of Zilina, Slovakia
E-mail: drusa@fstav.uniza.sk

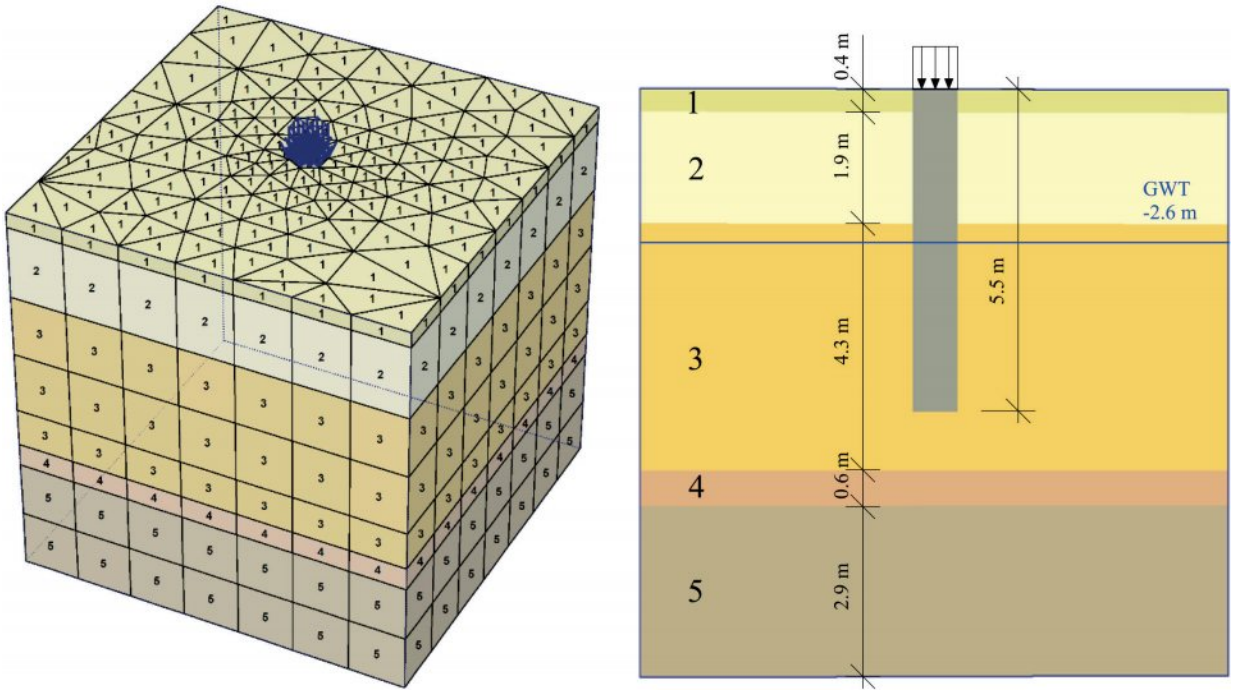

Fig. 1 Numerical model of the tested pile – overall view (left), profile of the model (right)

Soil characteristics for Mohr-Coulomb model — Table 1.

Mohr-Coulomb model		1 F4=CS firm	2 F4=CS stiff	3 S5=SC medium	4 S5=SC loose	5 S5=SC medium
Type		Un/Drained	Un/Drained	Un/Drained	Un/Drained	Un/Drained
γ_{unsat}	(kN/m³)	18.5	18.5	18.5	18.0	18.5
γ_{sat}	(kN/m³)	19.0	19.0	19.5	19.0	19.5
E_{ref}	(kN/m²)	11 700	25 800	23 000	7 500	28 300
ν	(-)	0.35	0.35	0.35	0.35	0.35
c_{ref}	(kN/m²)	18	44	5	3	7
φ	(°)	24	27	26	24	28
ψ	(°)	0	0	0	0	0
$R_{inter.}$	(-)	0.7 – 1.0	0.7 – 1.0	0.7 – 1.0	0.7 – 1.0	0.7 – 1.0
Groundwater table (GWT) 2.6 m below the top of the surface of the FEM model.						

geological survey brought final vertical settlement 5.17 mm, which correlates with experimental settlement of 3.14 mm obtained from the pile load test [5].

A model simulating the loading process during the pile load test was created based on the results of first approach. Each loading stage was chosen according to the load test protocol (Fig. 3).

In order to achieve the expected results, it is necessary to change the properties of soil below the pile bottom. The soil properties indicate an increase of density and other parameters such as deformation modulus, angle of internal friction and cohesion. This is caused by the compression of the soil under the pile during the test. Along with this, bearing capacity of the movable "floating" pile strongly depends on the bearing capacity of the pile toe. To examine the influence of the modulus and shear strength properties on the overall settlement of the pile, a sensitivity analysis was performed. Chosen parameters were varied in certain steps and an overall settlement was determined for each step, (Fig. 4, 5 and 6). Variation of the values was applied only for layer of clayey sand (cluster No. 3), because the pile toe and main part of the pile body was situated in this soil layer.

Range, in which the values were changed, was set according to the normalized soil properties from large compilation of in-situ tests.

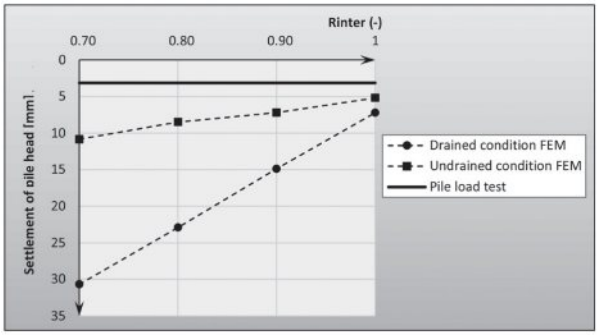

Fig. 2 Settlement of the pile head from FEM analysis and load test

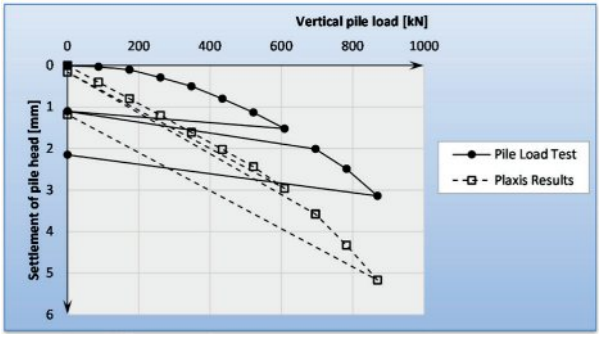

Fig. 3 Work diagram for pile load test and numerical model

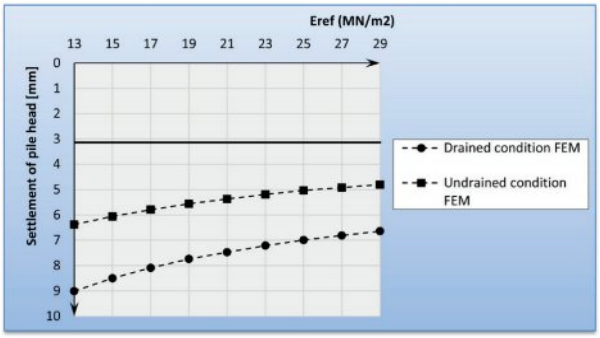

Fig. 4 Influence of the change of modulus on the pile head settlement

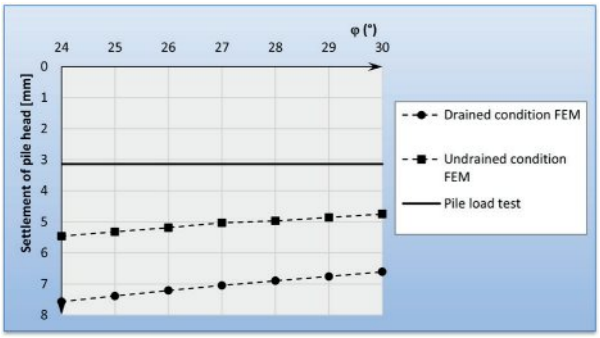

Fig. 5 Influence of the change of internal friction angle on the pile head settlement

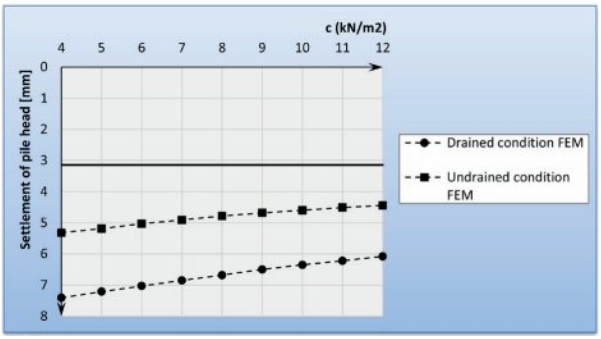

Fig. 6 Influence of the change of cohesion on the pile head settlement

Change of the values of modulus influences the settlement, but only if a wide range of values is taken into account. Within the small range, the difference in the settlement is negligible. (Fig. 4). Different shear strength parameters cause small variations in overall pile head settlement (Fig. 5 and 6). However, change of cohesion brings the results closer to the real measured data.

It should be noted that the use of Mohr-Coulomb material model leads to strictly linear results of settlement development and quite-constant difference between drained and undrained conditions in the particular graphs [9]. This is caused by the linear definition of Mohr-Coulomb material model.

4. Results of the modelling

Mentioned analysis is a contribution to the pile design in terms of second limit state considering practical restrictions in input data from the geological survey. Lack of sufficient data sets for soil environment usually restricts the selection

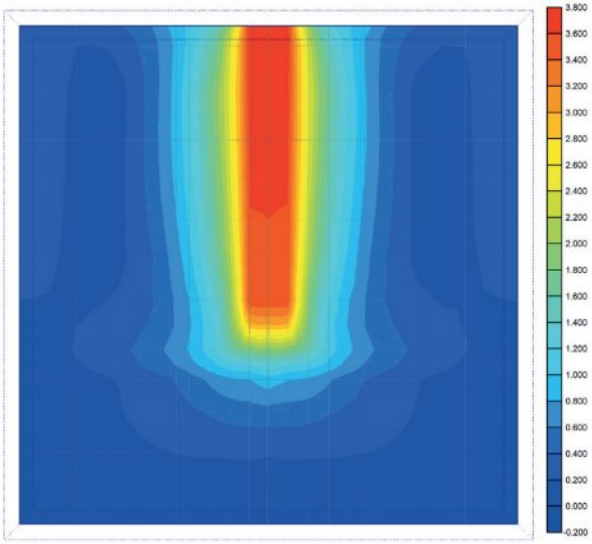

Fig. 7 Overall displacements in the numerical model in mm

of appropriate material model to Mohr-Coulomb model. Only in-situ tests were adopted as a basis for numerical model. The results of the modelling indicate that even small improvements in calculation procedure produce outputs with sufficient accuracy in comparison to the measured data.

Variation of selected parameters does not considerably affect the overall settlement, However, using a maximum values of properties for clayey sand layer from sensitivity analysis (E_{ref} = 29 MN/m^2, ϕ = 30°, c = 12 kN/m^2) led to pile head settlement of 3.73 mm, which is only 19% deviation from the measured value of 3.14 mm (Fig. 7). This reverse calculation procedure determines only assumed parameters of the soil near the pile toe. In order to verify the effect of soil improvement due to the pile settlement, compaction and lateral spreading, it is necessary to perform additional in-situ tests and tests with taken samples.

In the case of additional laboratory tests, using of advanced material models such as Hardening soil model or Soft soil creep model can provide more realistic results and predictions.

5. Conclusions

Analysis discussed in this paper represents the contribution to the design of piled foundations in terms of second limit state and overall stability. Settlement of the pile is only an auxiliary value at the pile load test, which checks the bearing capacity of the pile, thus first limit state. This study showed that utilization of undemanding material model and appropriate terrain surveying method can bring similarly accurate results for pile foundation design. Mohr-Coulomb model does not place high demands on input data, which provides an opportunity for practical and economical design of pile foundation. Use of advanced material model requires wider range of input data from terrain sampling and related laboratory tests [9] and [10]. Additional data are more time-consuming and less cost-effective, but usually geotechnical survey is only a minor part of the overall budget of the project. Therefore, basic material models, such as Mohr-Coulomb model, are still capable of providing suitable engineering output. Despite these results, another research in the field of data collection for advanced material models and numerical models calibration is necessary [11]. The research should consider variable geological conditions and numerous structure and load scheme conditions.

References

[1] BOWLES, J. E.: *Foundation Analysis and Design*, Fifth Edition: McGraw-Hill, 1996.

[2] BRINKREVE, R. B. J.: *PLAXIS 3D v 1.5 Manuals*, 2005.

[3] BENCAT J., CIBULKA, M., HRVOL, M.: Evaluation of the Soil Elastic Modules by Means of Box Tests, *Communications - Scientific Letters of University of Zilina*, pp. 5-9, ISSN 1335-4205.

[4] DECKY, M., et. al.: Non-Destructive Determining CBR Values of Ground Structures of Engineering Constructions. *J. of Intern. Scientific Publications: Ecology & Safety.* vol. 7, part 2, pp. 122-129, 2013, ISSN 1313-2563.

[5] VRABEL, B.: *Report - Pile Load Test, Production Hall "F" Slovaktual Pravenec, SO 101 – Production Monoblock - pile No. A20 (in Slovak),* 2014.

[6] DRUSA M.: Estimation of Strength and Deformation Characteristics of Soils (Nitra, South Slovakia) by using Cone Penetration Test, *Cumhuriyet Earth Sciences J. ,* vol. 30, No. 2, 2013, pp. 63-70, e-ISSN:1300-1949.

[7] OBERT, L.: *Final Report 462/2013. Production Hall "F" Slovaktual Pravenec. (in Slovak),* 2013.

[8] MUZIK, J., SITANYIOVA, D.: *Creation of 3D Geological Models using Unterpolation Methods for Nnumerical Modelling Needs,* Modelling and visualization of spatial data: 19.11.2008 Bratislava: Abstracts proceedings - STU Bratislava, p. 7, 2008, ISBN 978-80-227-2988-8.

[9] DECKY, M., DRUSA, M., PEPUCHA, L., ZGUTOVA, K.: *Earth Structures of Transport Constructions.* Harlow : Essex : Pearson, pp.180, 2013, ISBN 978-1-78399-925-5.

[10] BISWAS, S., MANNA, B.: *Three Dimensional Finite Element Nonlinear Dynamic Analysis of Full-scale Piles under Vertical Excitations.* Proc. of the 18th Intern. Conference on Soil Mechanics and Geotechnical Engineering, Paper No. 1691, 2013.

[11] DRUSA, M., MORAVCIK, M.: *Foundation Structures*, ISBN 978-80-554-0068-6, English textbook, EDIS : University of Zilina 2008, pp. 118.

Rudolf Kampf - Milos Hitka - Marek Potkany *

INTERANNUAL DIFFERENCES IN EMPLOYEE MOTIVATION IN MANUFACTURING ENTERPRISES IN SLOVAKIA

Differences in employee motivation in Slovak manufacturing enterprises during the years 2013 and 2014 are analysed in the paper. Independent samples t-test is used to compare the equality of averages and to calculate the significance level p for individual motivation factors. Definition of the significant increase or decrease of the average level of motivation factors and the comparison of an order of the importance of motivation factors in the year 2013 and 2014 are the findings of the paper. Despite no significant change in various motivation factors they need to be included in the motivation programme of enterprises owing to their importance. Statement that the enterprise management should pay adequate attention to motivation programmes updating because of the interannual changes in employee needs is the research finding. Future development of the level of employee motivation can be predicted following the findings.

Keywords: *Motivation programme, employee motivation, two-sample t-test.*

1. Introduction

Current financial crisis affecting the global economy started in the USA in early 2007. It became evident in Slovakia in the second half of 2008. Hardly anybody expected such a high impact of the financial crisis on the global economy. Subsequent problems of many financial institutions and uncertainty and risk in the financial markets caused mainly American but also European economy to slow down [1]. Interconnection among countries and globalisation in relations caused a domino effect. Global economy went down and will go down until the crisis hits the rock bottom. On the other hand, economic crisis can initiate also cleansing and structural processes in enterprises. Several enterprises experience the problem how to motivate staff remaining in the enterprise after restructuring and downsizing the workforce, without having to increase financial resources. An ideal way how to do it is to start using other forms of motivation and to invest in the development of remaining staff. The objective of our paper is to compare interannual differences in the level of motivation in Slovakia, to define potential significant interannual change and to mention a need to adapt employee motivation.

2. Strategies of employee motivation and motivation programmes

The process of employee motivation should mainly include basic needs of employees. Their economic conditions are poor, especially at the present time when there is no job security and they reassess their individual needs. Therefore, the role of managers is to update motivation programmes to motivate and stimulate employees in the right way and not to take advantage of the situation [2 and 3]. One of the most important factors of employee motivation is to show an interest in them, employees need to feel valued and important for the enterprise [4 and 5]. Good workplace relations are another way how to support staff motivation. Managers show adequate appreciation to their employees more often. On the other hand, managers can lose their employees' respect by showing much appreciation. The right or effective style of management includes also information about performance results of employees whereby managers highlight positive results and discuss strengths and weaknesses affecting the job performance [6]. Some other methods can be used to manage the period of crisis by means of non-monetary rewards of employees - to restructure teams, arrange educational activities in the enterprise, train employees, offer language and IT courses, management training, professional courses, seminars and trainings furthermore to benefit by several outsourcing tools of the market

* [1]**Rudolf Kampf,** [2]**Milos Hitka,** [2]**Marek Potkany**
[1]Institute of Technology and Business in Ceske Budejovice, Czech Republic
[2]Faculty of Wood Sciences and Technology, Technical University in Zvolen, Slovakia
E-mail: kampf@mail.vstecb.cz

[7]. Many sports activities and various corporate events can be carried out by the enterprise to improve interpersonal skills, too. It is also important to encourage corporate communication especially towards subordinates [8]. Selection of non-monetary rewards should be made by employees. Other way of employee motivation is self-actualization, which means delegation of some competences and responsibilities. However, employees can be motivated also by changes in management system in enterprise. Benefits and motivation programmes which can meet employee needs of self-actualization or their economic requirements can be effective for employees. Effective tools for employers are those which can help them, with low cost, start their employee potential [9].

Motivation programme is, in general, a written document of the enterprise, (mostly internal) the role of which is to recruit new employees or to keep employees in required job positions and to create overall working conditions and work environment for them; to set goals and to define methods and tools of work management relating to them; to define ways of influencing negotiation at work and employee behaviour aimed at achieving the setting goals and the schedule of gradually creating conditions to carry out the programme [10]. Motivation programme can be considered a strategic corporate document dealing with:

- measuring motivation level in order to identify areas necessary to improve the motivation,
- creating the environment where employees feel respected and rewarded by the enterprise,
- designing responsible and engaged employee behaviour in the enterprise,
- creating an empowering motivational climate in the enterprise,
- improving skills in the area of human resource management,
- creating operational tasks and new workplaces,
- managing employee performance,
- managing the performance-based rewarding [11].

Forasmuch as goal setting and a set of tools (business operations) to ensure that particular goals will be achieved represent the corporate strategy, its implementation involves creating particular strategies to specify goals of corporate strategy in individual areas (e.g. marketing, investment, product development, finances) [12]. The role of motivation strategies is to create a work environment and to develop policy for improving employee performance [13].

3. Aim and methodology

The objective of the paper was to identify changes in employee motivation in manufacturing enterprises in Slovakia during the years 2013 and 2014. A questionnaire was used to determine the level of motivation and to analyse motivation factors in the studied enterprises. The questionnaire consisted of 30 closed questions [10]. It was divided into 2 parts. Socio-demographic and qualification characteristics of employees were searched in the first part of the questionnaire. Basic data about respondents related to their age, sex, seniority, completed education and job position were obtained in this part. The second part consisted of individual motivation factors through which information about work environment, working conditions, applied appraisal and reward system, about personnel management, health and social care system and system of employee benefits as well as information about employee satisfaction or dissatisfaction, value orientation, relation to work and the enterprise or co-workers' relationship in the enterprise can be found out. Motivation factors were in alphabetical order not to affect respondents's decision. Respondents evaluated individual motivation factors by one of the five levels of importance from a pre-defined 5-point rating scale, 5 - the most important and 1 – unimportant. The inquiry survey ran during the years 2013 and 2014. Questionnaires were sent to the respondents via e-mail, mail or were completed in a form of personal interview. Representative sampling unit consisted of 11,263 respondents. At first, obtained values were evaluated on the basis of mean values of individual motivation factors using average [14]:

$$\bar{x} = \frac{x_1 + x_2 + x_3 + \cdots + x_n}{n} = \frac{1}{n}\Sigma_{i=1}^{n} x_i \qquad (1)$$

where: n = the size of the sample (number of questionnaires)
x_i = the value of variable ith statistical unit.

Subsequently the questionnaires were evaluated using the programme STATISTICA 7. Descriptive statistics was used to describe the primary sampling unit. Statistical characteristics, which compressed information about studied primary sampling units into smaller number of numerical characteristics and made mutual comparison of sampling units easier (years 2013 and 2014), were computed for each motivation factor (real, required). Each motivation factor was described in summary by basic characteristics of size and variability of quantitative features - averages $\bar{x}$, standard deviations s_x and coefficients of variation. Subsequently, the results were compared by inductive statistics. Besides simple comparison of descriptive characteristic values, considering the selected type of obtained data, testing the equality of averages and standard deviations of primary sampling units was carried out. The purpose of testing was to verify statistical significance of differences in averages and standard deviations of individual motivation factors in the studied enterprises so that the fact that detected differences of descriptive characteristics at the selected level of significance α were not caused only by the mistake made by representative sampling, was eliminated. The null hypothesis vs. the alternative hypothesis was tested, they were as follows:

$H_0: \mu_1 = \mu_2$ vs. $H_1: \mu_1 \neq \mu_2$

H_0: we suppose that the averages of studied motivation factors (required, real) in the studied period are equal and at the same

time we suppose that the difference between them, if any, is owing to the random variation of results.
H_1: we suppose that the averages of studied motivation factors (required, real) in the studied period are not equal and at the same time we suppose that the difference between them, if any, is not caused only by the random variation of results.

The random variable t was used as a test criterion. The Student's t distribution was as follows [14]:

if $\sigma_1^2 = \sigma_2^2$; X_1 a X_2 are homogenous

$$t = \frac{\bar{x}_1 - \bar{x}_2}{\sqrt{\frac{n_1 \cdot s_1^2 + n_2 \cdot s_2^2}{n_1 + n_2 - 2} \cdot \frac{n_1 + n_2}{n_1 \cdot n_2}}} \quad (2)$$

if $\sigma_1^2 \neq \sigma_2^2$; X_1 a X_2 are non-homogenous

$$t = \frac{\bar{x}_1 - \bar{x}_2}{\sqrt{\frac{s_1^2}{n_1 - 1} + \frac{s_2^2}{n_2 - 1}}} \quad (3)$$

In the end of the test we compared t to $t_{\alpha/2;f}$, in a case of $t \leq t_{\alpha/2;f}$, H_0 was not rejected and the difference was not considered significant but in a case of $t > t_{\alpha/2;f}$, H_0 was rejected at the level of significance of 5% and the alternative hypothesis $H_1$was accepted.

4. Results

Analyses of motivation in manufacturing enterprises were focused on the manufacturing enterprises in Slovakia all along. They were carried out in almost all regions of Slovakia using random selection method and the structured questionnaire. 7,009 employees of the manufacturing enterprises in Slovakia were analysed by the end of the year 2013. Other 4,254 employees of Slovak manufacturing enterprises were analysed in the year 2014. Respondents evaluated individual motivation factors in the questionnaire by one of the five levels of importance from a pre-defined 5-point rating scale Questionnaire evaluation was carried out from the data matrix with *number of employees x number of motivation factors*. Stated matrix is a data entry form for carrying out the statistical analysis of motivation factors.

Considering the independence of representative sampling units and their big sizes a two-sample t-test for independent samples at the same or different variances was used. The null hypotheses about the equality of two averages of representative sampling units were tested. The null hypothesis about the equality of mean values of individual motivation factors was tested at the significance level α = 0.05. Results are shown in Table 1. Motivation factors with significant change are in bold. A line graph (Fig. 1) was created following the results. During the financial crisis motivation factors like *atmosphere in the workplace, job security, supervisor's approach, fair appraisal system, basic salary* are the most important for the employees. The less interesting motivation factors for employees are *physical effort at work, name of the company, prestige, region's development.* Despite a visual form of the level of motivation in 2013 and 2014 we tested the significance level p for individual motivation factors using t-test. Results of the analysis are shown in Table 1.

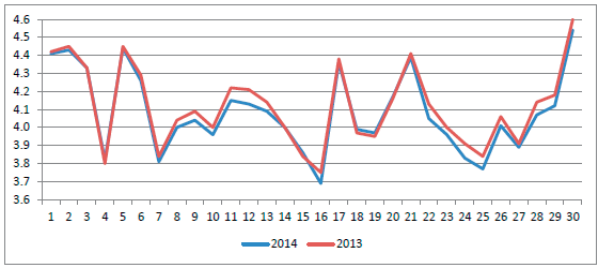

Fig 1 Comparison of averages of motivation factors
Source: Own data processing

On the basis of the results we can draw following conclusions. The most important motivation factors are: *atmosphere in the workplace, job security, supervisor's approach, fair appraisal system, basic salary.* From all of them only basic salary shows a significant increase. Significant difference (requirement raise) was determined in 14 motivation factors: *opportunity to apply one's own ability, workload and type of work, information about performance results, working time, work environment, job performance, prestige, stress, mental effort, mission of the company, region's development, education and personal growth, free time, recognition.* Even though, there were no significant differences in other motivation factors we consider them important from a long-term point of view. Considering their importance it is necessary to implement them in the motivation programmes of enterprises.

Other important findings of our survey are following statements:

- in principle, employees do not change motivation requirements interannaully,
- employees are motivated by motivation factors not important for them until now.

Following the mentioned facts we can suggest giving adequate attention to motivation programme updating because motivation needs of employees can change interannually.

5. Conclusion

At the present time many enterprises do not want or do not consider important to develop and to train staff. Later on, it can affect the performance of enterprise because of the staff performance decrease, a subsequent fall in profits and an increase

Averages and significance level *p* of individual motivation factors Table 1

	∅ 2013	∅ 2014	t	p variances	F	p variances
Atmosphere in the workplace	4.41	4.42	-0.56	0.579	1.02	0.391
Good work team	4.43	4.45	-1.09	0.276	1.05	0.090
Further financial reward	4.33	4.33	-0.27	0.790	1.00	0.958
Physical effort at work	3.82	3.80	0.79	0.431	1.05	0.108
Job security	4.44	4.45	-0.14	0.889	1.02	0.471
Communication in the workplace	4.26	4.29	-1.71	0.087	1.02	0.427
Name of the company	3.81	3.84	-1.29	0.198	1.32	0.000
Opportunity to apply one's own ability	4.00	4.04	-2.42	0.015	1.09	0.003
Workload and type of work	4.04	4.09	-2.78	0.006	1.00	0.941
Information about performance results	3.96	4.00	-2.28	0.023	1.01	0.710
Working time	4.15	4.22	-4.18	0.000	1.03	0.236
Work environment	4.13	4.21	-4.71	0.000	1.06	0.039
Job performance	4.09	4.14	-3.09	0.002	1.05	0.083
Moving up corporate ladder	4.00	4.00	-0.32	0.753	1.00	0.856
Competences	3.86	3.84	1.18	0.240	1.03	0.224
Prestige	3.69	3.75	-2.83	0.005	1.02	0.395
Supervisor's approach	4.36	4.38	-1.72	0.085	1.04	0.137
Individual decision making	3.99	3.97	0.95	0.344	1.05	0.068
Self/actualization	3.97	3.95	1.36	0.173	1.08	0.004
Social benefits	4.17	4.16	0.64	0.523	1.17	0.000
Fair appraisal system	4.39	4.41	-1.52	0.128	1.04	0.160
Stress/limitation of stress in the workplace/	4.05	4.13	-4.07	0.000	1.24	0.000
Mental effort	3.96	4.00	-2.05	0.040	1.11	0.000
Mission of the company	3.83	3.91	-2.95	0.003	3.25	0.000
Region's development	3.77	3.84	-2.83	0.005	1.93	0.000
Education and personal growth	4.01	4.06	-3.18	0.001	1.04	0.207
Relation to the environment	3.89	3.91	-1.25	0.213	1.08	0.006
Free time	4.07	4.14	-4.18	0.000	1.03	0.316
Recognition	4.12	4.18	-3.55	0.000	1.13	0.000
Basic salary	4.54	4.60	-3.68	0.000	1.08	0.007

Source: Own data processing

in expenses. Enterprises have to be aware of expenses relating to education in comparison to business start-up costs. Teplicka [15] incorporated all motivation factors into possibilities to reduce costs whilst the most important factor during the ongoing financial crisis is to preserve good name of the company and brand, and to improve performance and product or service quality as well. From the point of view of employees an enterprise cannot work when employer does not respect employment contract or promises made to staff. Fulfilling the tasks as well as the behaviour in the workplace, correct communication and openness belong among corporate values [16].

We can also state that during recession employees are fully aware of the importance of *job security* and moreover, of the fact that employers are not able to provide *financial reward* to them. Therefore, enterprises should focus on the motivation through developing motivation factors based on interpersonal relationship and job security. During recession employers tend to enhance motivation thereby to increase job satisfaction what is in accordance with individual factors defined in Maslow's hierarchy of needs [17]. Detailed analysis of individual motivation factors allows us to assume that at the present time:

– impact of motivation factors increases and employees consider them more motivating,

- success as well as recognition, personal growth and a job itself become the most important motivation factor,
- employee dissatisfaction with a work control and subsequent variability of financial reward increase,
- number of factors considered neutral by employees decreases and they accept an opinion that supervisors should not concentrate on the areas like private life and relationship with subordinates.

During recession it is very important to provide job security and create reliable mutual relationships to employees. It can be achieved through effective communication. However, employers do not give adequate attention to this need. Research studies show that employers only rarely allow their staff to meet this need. Motivation factor - reward, recognition, and delegating tasks to employees can be seen as effective motivation factors as well.

Acknowledgement

This paper has been supported by the project VEGA No. 1/0268/13 "Perspectives of facility management application for the increasing of competitiveness within the woodprocessing and forestry companies in the context of outsourcing principles".

References

[1] BLASKOVA, M.: Creative Proactive-concluding Theory of Motivating. *Business: Theory and Practice,* vol. 11, No. 1, 2010, 39-48. ISSN 1648-0627

[2] BLASKOVA, M., HITKA, M.: Model *of Employee Motivation Management in Manufacturing Enterprises (in Slovak),* Technicka univerzita : Zvolen, 2011, 171 p., ISBN 978-80-228-2296-1.

[3] HERZKA, P., FUKSOVA, N.: Process of Employee Motivation in Manufacturing Enterprise *(in Slovak), J. of Management and Economics,* vol. 1, No. 2, 2009, 126-138, ISSN 1337-9488.

[4] POTKANY, M.: Personnel Outsourcing Processes, Economics and Management: *Scientific Economic J. (in Czech),* vol. 11, No. 4, 2008, TU Liberec, 2008, 53-62, ISSN 1212-3609.

[5] HITKA, M.: *Model of Employee Motivation Analysis in Manufacturing Enterprises (in Slovak),* Technicka univerzita : Zvolen, 2009, 150 p., ISBN 978-80-228-1998-5.

[6] STACHOVA, K., STACHO, Z.: Employee Allocation in Slovak Companies. *Business: Theory and Practice,* vol. 14, No. 4, 2013, 332-336, Vilnius, ISSN 1648-0627 (doi: 10.3846/btp.2013.35)

[7] STACHO, Z, URBANCOVA, H., STACHOVA, K.: Organisational Arrangement of Human Resources Management in Organisations Operating in Slovakia and Czech Republic. *Acta Universitatis Agriculturae et Silviculturae Mendelianae Brunensis,* vol. LXI, No. 7, 2787-2799, 2013, ISSN 1211-8516. (doi: org/10.11118/actaun 201361072787)

[8] RIMARCIK, M.: *Statistics in Practice (in Slovak),* 2007, 200 p., ISBN 978-80-969813-1-1.

[9] SCHEER, L.: *Biometrics (in Slovak),* Vysokoskolska ucebnica, Technicka univerzita vo Zvolene, 2007. ISBN 978-80228-17233.

[10] StatSoft. Inc. 2004. *STATISTICA* (data analysis software system), version 7. www.statsoft.com.

[11] SULGAN, M., SOSEDOVA, J.: Procurement of Materials and Components for Manufacturing Activity, *Communications - Scientific Letters of the University,* 16 (2), 58-62, 2014, ISSN 1335-4205.

[12] ZAVADSKA, Z., ZAVADSKY, J., SIROTIAKOVA, M.: Process Model and its Real Application in the Selected Management Areas. *E a M: Ekonomie a Management,* vol. 16, No. 1, 2013, 113-127, ISSN 1212-3609.

[13] TEPLICKA, K.: Progressive Management Trends in Manufacturing Enterprises *(in Slovak), Ekonomie a management,* vol. 7, No. 4, 2004, 26-31, ISSN 1212-3609.

[14] VETRAKOVA, M. et al.: *Human Resources and Their Management (in Slovak),* EF UMB Banska Bystrica: Bratia Sabovci, s. r. o. Zvolen, 2011, 206 p., ISBN 978-80-557-0149-3.

[15] ROLKOVA, M.: Participative Management Style and its Relation to Employee Willingness to Accept Job offer in the Same Company Once Again, *Communications - Scientific Letters of the University of Zilina,* 15 (4), 2013, 96-99, ISSN 1335-4205.

[16] VODAK, J., SOVIAR, J., LENDEL, V.: Identification of the Main Problems in Using Cooperative Management in Slovak Enterprises and the Proposal of Convenient Recommendations, *Communications - Scientific Letters of the University of Zilina,* 15 (4), 2013, 63-67, ISSN 1335-4205.

[17] KROPIVSEK, J., JELACIC, D., GROSELJ, P.: Motivating Employees of Slovenian and Croatian Wood Industry Companies in Times of Economic Downturn, *Drvna industrija,* vol. 62, No. 2, 2011, Zagreb, 97-103, ISSN 0012-6772 (doi: 10.5552/drind.2011.1040).

Martin Lopusniak - Dusan Katunsky *

PEOPLE MOVEMENT CHARACTERISTICS BASED ON AN EVACUATION TEST

Modelling of the evacuation of people is the only method leading to a proper design of emergency escape routes from buildings. The background details necessary for modelling can only be obtained from actual incidents or evacuation tests. The paper presents the results of an evacuation test carried out in a university environment with respect to an announced evacuation. The introduction of the paper describes the scope of the test, physiological characteristics of the participants, the geometry and the environment. The analysis of the evacuation test focuses on the movement of people and the flow. The analysis of the results showed that the values recorded in the test are identical to those used in evacuation models; nevertheless, they differ from the calculation model and values used in the national prescriptive code.

Keywords: *Evacuation test, movement, flow, fire safety.*

1. Introduction

Details of human behaviour in various situations have been the subject of research since the 1950s [1], [2], [3] and [4]. Data collection is carried out using evacuation tests [5], [6] and [7] based on observations of current situations or actual incidents [8] and [9]. Only data from an actual incident allows creating a real view of human behaviour, but this is rare and practically non-repeatable. It is less risky to carry out an evacuation test from which a number of relevant data can be obtained. The range of information depends on the approach and scope of the observations during the test. Only one pre-selected value or set of values can be obtained from an evacuation test. According to Gwynne [10], human behaviour is influenced by the environment, procedures and geometry. This means that every situation is in fact genuine and, therefore, the implementation of evacuation tests, their monitoring and the analysis of the results are always beneficial.

2. Scope, objectives and the methods of work

The scope of the paper is an evacuation test. The results of an evacuation test could be expressed as "time travel" in terms of fire engineering. The following objectives are defined in accordance with the scope of this paper: to obtain data for analysing the movement of people; to obtain information on evacuation times and routes including selected sections of evacuation routes; to quantify the movement of people during an evacuation test; to compare the results with available and generally accepted values for behaviour and movement.

The basic method of work is itself an evacuation test. The test was carried out by evacuating volunteers from a building to a protected area. The evacuation was then repeated six times. Individual evacuations are referred to as Run 1, Run 2, Run 3, Run 4, Run 5 and Run 6. In terms of movement, we focus on movement mainly at checkpoints, for example stairs, doorways, fire barriers, etc. The test was monitored using hand-held video cameras (CAM designation 1-7) scattered throughout the evacuation route (Fig. 1). The total evacuation time was recorded directly during the evacuation test. Evacuation times, as well as the behaviour of people and other data, were obtained from a video analysis.

2.1 Participants

The test was conducted in a university environment. The evacuation test was conducted with the participation of fifty-four student volunteers, of 36 men and 18 women. The average age of volunteers was 22.7 years. The average height of men was 181 cm. The average height of women was 168 cm. The average weight of males was 79.9 kg. The average weight of women was 58.2 kg.

The volunteers were randomly divided into three basic groups labelled A, B, and C. Volunteers 53 and 54 arrived late, so they were only included in Runs 2-6. Three modifications to groups designated A1, A2, B1, B2, C1, C2 were made according to Table 1 due to this discrepancy. The groups were divided into three

* **Martin Lopusniak, Dusan Katunsky**
Department of Building Physics, Faculty of Civil Engineering, Technical University of Kosice, Slovakia
E-mail: dusan.katunsky@tuke.sk

classrooms R1, R2, and R3 (Fig. 1). Each group started a run in a different room. Distribution of people in groups is shown also in Table 1.

The students who were quasi-studying started the evacuation immediately after being notified. Subsequently all persons were evacuated without further instruction using the fire escape stairs which led to the nearest building exit (Runs 1-4). In the case of Runs 5-6, participants were evacuated to the protected area R5 using only flat spaces.

Distribution of participants into groups during an evacuation test — Table 1

Group	Persons	Number of persons in the group	Run
A1	1 – 17	17	run 1, 3, 6
A2	1 – 17; 53	18	run 2, 4, 5
B1	18 – 36; 40	20	run 1, 2, 4, 5
B2	18 – 36; 40; 53	21	run 3, 6
C1	37 – 39; 41 – 52	15	run 1, 2
C2	37 – 39; 41 – 52; 54	16	run 3, 4, 5, 6

Volunteers were instructed to move as quickly as possible but in a manner to avoid unwanted and unnecessary injuries.

2.2 Environment

The test was performed in a five storey building. All of the sample rooms were situated on the fifth floor and designated as R1, R2 and R3. Runs 5 and 6 were directed to a protected area designated R5, which is also situated on the fifth floor. The fire escape designated R4 contained a total of eighty-one stairs. During the test, areas were illuminated only by natural light. The floor plan dimensions, designation of rooms, doors, technical data rooms, hallways and stairs are shown in Fig. 1. The area of a standard flight of stairs is 3.6 m^2. The length of one flight is 3.2 m. The evacuation test did not include any artificial barriers. All volunteers were familiar with their surroundings.

During Runs 1 to 4, participants completed a route from rooms R1, R2, R3 through door D1, D2, and D3 (width 800 mm, standard handle, opening against the direction of escape) to a corridor. It was followed by movement through door D4 (double door - fire door, wing width 2 x 800 mm, standard handle on the main wing, latch on the other wing, opening in the direction of escape) towards the staircase (R4). The descent to door D6 which led to the exit (width 900 mm, standard handle, opening against the direction of escape) was completed in a short amount of time. The start of Runs 5 and 6 were identical to Runs 1-4, but the level movement (the corridor) led in the opposite direction to door D5 (same as D4).

3. Results

The results obtained from the evacuation test present two sets of data. The first set lists evacuation times. The second set contains parameters describing people's movement and flows.

3.1 Evacuation times

The first set of results presents total and partial evacuation times. Each designated evacuation time is associated with figures indicating the number of runs, for example $t_{2,3}$ (t_2 evacuation time for Run 3). The total and partial evacuation times of runs are listed in Table 2.

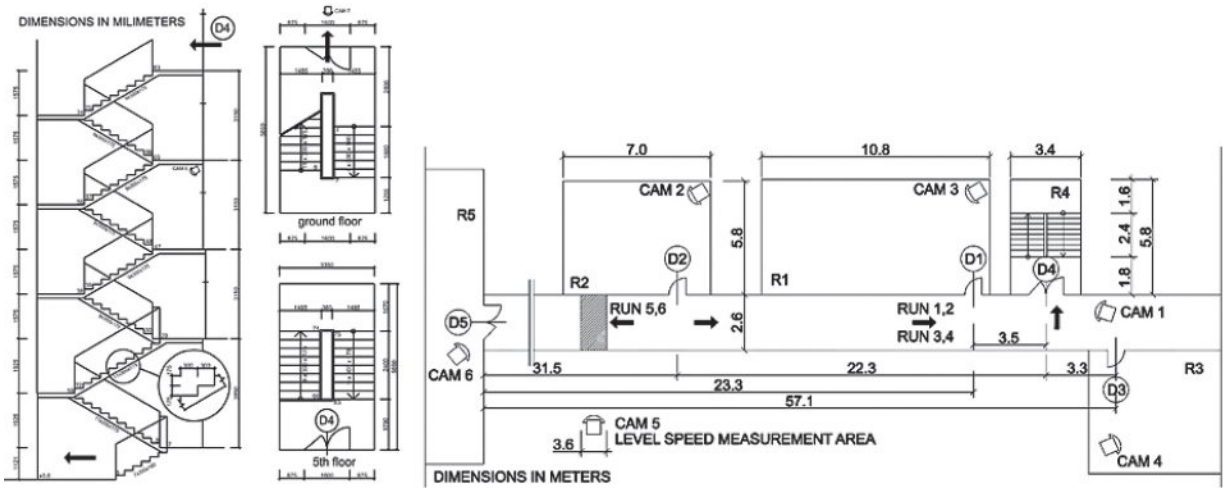

Fig. 1 Overall schematic view of space on the fifth floor and cameras' positions and cross section of the stairwell

Results of the evacuation test

Table 2

Run number	Room R1	Room R2	Room R3	Evacuation time	Run number	Room R1	Room R2	Room R3	Evacuation time
The total evacuation time (ET), t_1, (s)					ET leaving room R1, t_2 (s)				
Run 1	C1	B1	A1	84	Run 1	C1			16.5
Run 2	A2	C1	B1	89	Run 2	A2			15.4
Run 3	B2	A1	C2	87	Run 3	B2			21.9
Run 4	C2	B1	A2	95	Run 4	C2			15.6
Run 5	A2	C2	B1	53	Run 5	A2			14.8
Run 6	B2	A1	C2	55	Run 6	B2			18.8
ET for the last person to enter the door D4 to the staircase (space R4), t_3 (s)					ET for the first person to enter the door D4 to the staircase (space R4), t_4 (s)				
Run 1	C1	B1	A1	37	Run 1	C1	B1	A1	3
Run 2	A2	C1	B1	38	Run 2	A2	C1	B1	4.5
Run 3	B2	A1	C2	35	Run 3	B2	A1	C2	5.2
Run 4	C2	B1	A2	37	Run 4	C2	B1	A2	5
ET to pass door D4 by all people, t_5 (s)					ET to pass a flight of stairs by all people, t_8 (s)				
Run 1	C1	B1	A1	34.7	Run 1	C1	B1	A1	42.6
Run 2	A2	C1	B1	32.3	Run 2	A2	C1	B1	40.0
Run 3	B2	A1	C2	32.3	Run 3	B2	A1	C2	35.3
Run 4	C2	B1	A2	34.3	Run 4	C2	B1	A2	45.6
ET of the first person from R2 to enter the door D5, t_7 (s)					ET to pass door D5 by all people, t_6 (s)				
Run 6	B2	A1	C2	11.3	Run 5	A2	C2	B1	33.8
					Run 6	B2	A1	C2	40.2
Evacuation time leaving room R3, t_9 (s)					ET to pass door D3 by all people from R3, t_{10} (s)				
Run 5	A2	C2	B1	15.2	Run 5	A2	C2	B1	13.8
Run 6	B2	A1	C2	11.3	Run 6	B2	A1	C2	10.0
ET to pass door D1 by all people from R1, t_{11} (s)									
Run 5	A2	C2	B1	10.8					
Run 6	B2	A1	C2	15.1					

Physical data were obtained from the evacuation test. This comparison showed that the total evacuation time for Runs 1 to 4 ranged from t_1 = 84 s - 95 s. The average evacuation time of all four runs is $t_{1, avg}$ = 88.75 s. Runs 5 and 6 were $t_{1, 5}$ = 53 s and $t_{1,6}$ = 55 s. Slight variations of time were probably caused by a change in the number or nature of persons located in different rooms. Divergence times are also a natural phenomenon since no person is able to behave naturally whilst performing the same, absolutely identical action.

3.2 General characteristics of the evacuation

Evacuation started immediately after the announcement. Response times were zero. Increased activity was evident throughout the group, as well as striving for the fastest and most efficient movement and exit from the building. No specific activities or problems were reported from the start of the evacuation until reaching door D4. Here an increased concentration of people was recorded before continuing to the staircase, which was smooth and again without any problems. Movement through the door D4, the movement in the rooms and the movement on the stair are the most significant parts of the evacuation, which influence the evacuation time.

Tables and chairs caused the greatest obstruction to the flow of movement. The space between tables caused people to queue, which reduced the tendency of bottlenecking at the door. However, the rooms were not fully occupied and it is necessary to state that the answer to the movement and behaviour in the room when fully occupied or over-occupied is unknown. The answer to the movement and behaviour in the room with variable table and equipment layouts is also unknown. In Table 2, labelled t_2 (s) is presented with respect to time needed to empty room R1.

Movement of persons down the stairs had a large influence on the evacuation during Runs 1 – 4. During the descent, the group was spread out across the full length of the staircase. The first ten to twelve people were ordered in a row with significant distances between them. These people reached the highest values of staircase movement speed (Fig. 2a). Increasing time gradually increased the number of people on the same flight of stairs, while decreasing the rate of descent. The analogy to the speed of descent can be observed in terms of the number of persons on the staircase. However, places where movement was slowed down by one person resulted in an increase in the number of people on the flight of stairs. When people were arranged one after another, a maximum of three persons were found on each flight of stairs. It was necessary to arrange people next to each other as well as one after another where group sizes exceeded four persons on the flight of stairs. However, during all test runs never more than six people were recorded on a flight of stairs. The movement characteristics comply with the results of the work [11], especially in terms of sorting of people on the staircase.

3.3 Speed of stair movement, stair flow

Movement speed of persons is based on the general movement described above. Movement speeds of persons are presented as a speed over one flight of stairs. Speed is always referred to as the speed on the real length of the flight of stairs. To determine the descent, Run 1, Run 2 and Run 3 were analysed. The times to traverse one flight of stairs vary from 1.563 s to 2.953 s. The average value is 2.14 s.

The descent of persons is based on the measured time of the descent of a flight of stairs, which lead to the following range of 1.03 - 1.91 m/s. The speeds of selected individuals are presented in Fig. 2a. The average speed was 1.33 m/s (median 1.26 m/s; mode 1.19 m/s). Probability distribution is presented in Fig. 2b. Average values are higher than commonly used values in evacuation models [12], or those available in the literature [7]. Moreover, these values are significantly higher than those for the examples presented in [8] or [13]. Also, the values are higher than those in a national prescriptive regulation [14], which is required for the evacuation calculation speed of movement down the stairs (0.42 m/s). However, this value is expressed as the horizontal speed on the staircase.

The flow of people has been reported in Run 1 to 4 by the following values 1.25 p/s, 1.34 p/s, 1.51 p/s, 1.19 p/s. The average flow of all runs is 1.32 p/s, or 0.88 p/s/m as the flow in one flight of stairs. The average flow of the escape route is described in the literature as a value of 1 p/s for a staircase width of 1100 mm. This value is particularly valid for high-rise buildings. National prescriptive regulation [14] has a requirement of 0.5 p/s for a single evacuation unit 0.55 m wide. Multiplying this requirement by the width of the staircase provides a maximum value equal to 1.25 p/s. The average flow of the evacuation test was closer to the requirement for prescriptive regulation than for the speed of movement.

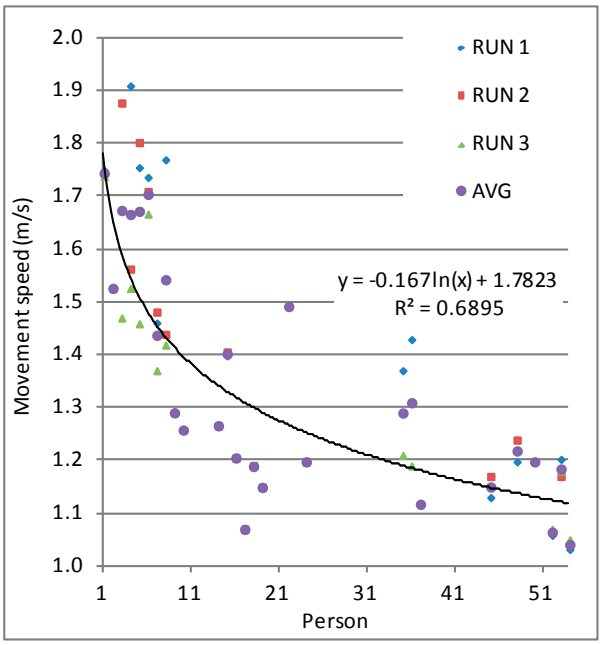

a)

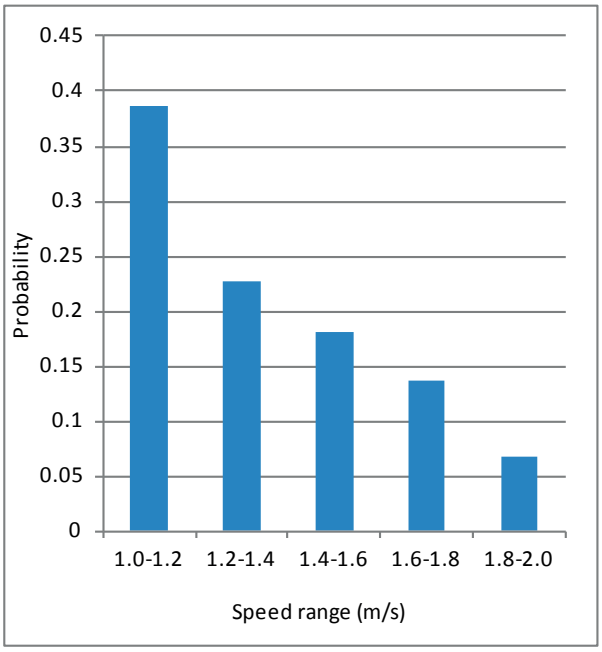

b)

Fig. 2 a) Speed of people on the flight of stairs in m/s b) Probability distribution

3.4 Movement through the door, flow through the door

Door D4 was selected to determine the flow through the door, because it directly accesses the staircase area and the protected area. Door transit time is shown in Table 2 as time t_5 and t_6. At this time, the flow was calculated to be between 1.5 and 1.67 p/s, with respective unit flows of 1.88 to 2.09 p/m/s. Door flow is fixed at a population density of 4 p/m^2. The details of the door transit are shown in Fig. 4 (marked as RUN 2). The highest flow of people in a short time interval (t = 5s) was 1.8 p/s (Fig. 4b; F RUN2). In contrast to the speed on the stairs, these data are consistent with the literature where the range for unit flow rate was reported to be from 1.25 to 2.0 p/m/s according to its corresponding density [2], [15] and [16].

As far as the queuing and transition through the door are concerned, it was observed that people exited the door predominantly in a row (Fig. 3a). In a few cases two persons exited the door simultaneously. In such cases mutual coordination had to be facilitated (Fig. 3b). Such coordination was necessary even in the case of two women (Fig. 3c). A simultaneous exit of two men did not occur.

The door transit was the most significant factor of the test. From the point of view of evacuation modelling, an appropriate solution of this passage is a critical step. Comparison of various solutions of door transit of model buildingExodus (BE) [17] and the actual door transit during the test can serve as an example. BE allows two solutions in case of 800-mm door. Either one node (1*0.5m) or two nodes (2*0.5m) are considered. None of

a) b) c)

Fig. 3 Movement through the door D4 a) in a row man-man; b) man-woman; c) woman-woman

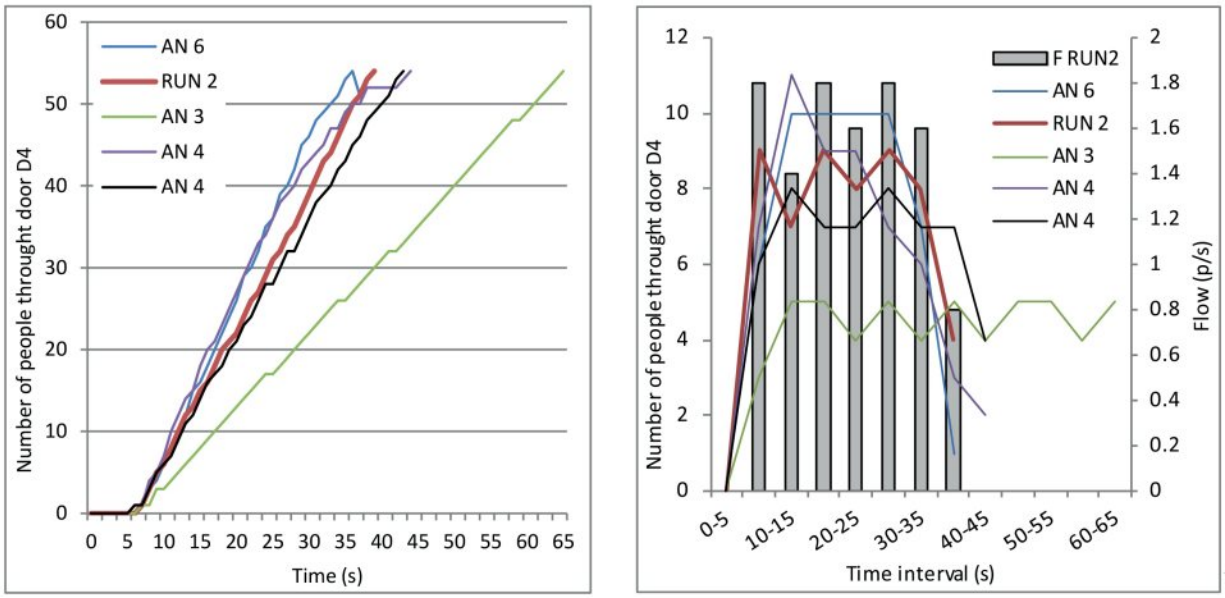

a) b)

Fig. 4 a) Cumulative course of the door flow b) The time interval door flow

the solutions corresponds to the actual width of the door, which is 800mm. The adjustment of the flow is therefore necessary in order to reach coherence between the test and the evacuation. Accurately designed door showed coherence in the course and the cumulative representation of the transit time. As can be seen from results (Fig. 4a), a single-node solution does not correspond to reality (green line – AN4). Two nodes with incorrectly assigned flow also do not show coherence with the course of the door transit (blue – AN 6 and violet – AN 4). Correct solution is represented by the black line – AN 4, which is coherent to the actual course of the door transit during evacuation.

If the flow parameters are chosen correctly, people are ordered in front of the staircase in a way corresponding to the test. Ordering of people in front of the staircase in three different situations is illustrated in Fig. 5. In Fig. 5a, the ordering is the result of the course of door transit as represented by the green line (AN3). The number of people at the staircase is low and does not correspond to the test. Figure 5b represents the blue line (AN6). The number of people is too high and also does not correspond to the test. Figure 5c represents the black line (AN4) and does correspond to the test.

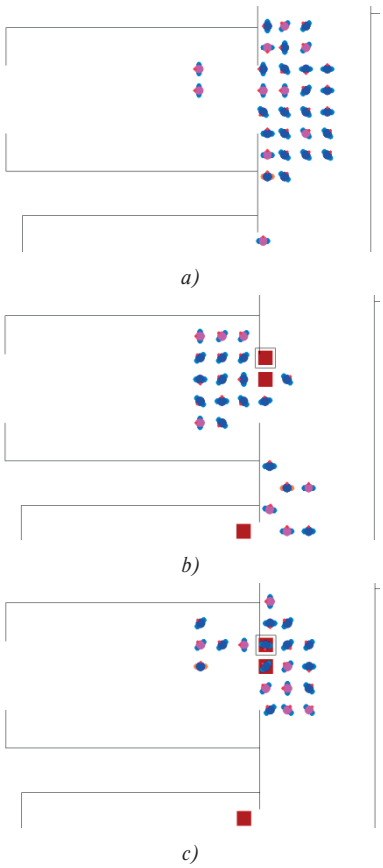

a)

b)

c)

Fig. 5 Concentration of people in front of the staircase for different model solutions
a) green AN3; b) blue AN6; c) black AN4

3.5 Level movement

Level movement was measured over a 3.6 m long section. The section is shown in Fig. 1. Values range from 1.45 to 1.97 m/s. The average value is 1.56 m/s. According to Ando [18], the maximum walking speed is 1.6 m/s for males and 1.4 m/s for women. The test results are within this range. During the runs, the corridor flow was 1.66 p/s, which is consistent with the flow through door D4. The maximum population density was 1.92 p/m^2. The average concentration of people was in accordance with the Fruin density of C or D [2]. At this level there is no restriction to the movement of persons, hence the value for the speed of flat movement is high. During Run 6 an interesting situation occurred. The first 18 people ran to door D5. Their action was voluntary. The average speed of movement was 3.22 m/s.

4. Discussion

Evacuation modelling allows the usage of various input data. Movement parameters and flow capacities belong among the most significant. Peacock [7] recommends the use of a wider range of movement parameters rather than a narrow range or one average value. The evacuation model will therefore be more realistic.

The test results and the derived movement parameters and flow capacities have to be perceived as the upper limit values when used in evacuation scenarios and simulation calculations. The results of the test were influenced especially by the following facts: evacuation had been announced; participants were familiar with the environment; participants had no mental load (knowing that nothing was actually happening, which promoted a smooth and orderly evacuation); no other burdens (personal items, handbags, notebooks); physiological parameters, and health (the optimum age, weight, movement ability). The achieved results correspond with the data in literature describing the movement of people and flow capacity for similar groups of people, their composition and familiarity with the environment.

The test results do not implement the evacuation of people with disabilities. It is very difficult kind of evacuation tests. People with disabilities need to be included in the evacuation models but their movement characteristics have to be included correctly. For this purpose it is necessary to perform this kind of test in the future.

The results suggest the need of the update of movement parameters in the national prescriptive regulation. The values used for calculation are too low not only when compared to the test results but also in comparison to data used in other literature.

In any case, it is highly recommended to implement evacuation tests. Attention should be paid to different local constraints, which may inhibit movement or cause unexpected

reactions. During evacuation tests, it is important to create conditions which would encourage the natural behaviour of people. The execution of small scale tests for specific activities such as corridor congestion, movement in densely populated rooms, movement in rooms with differing furniture layouts, and movement in overloaded rooms with people moving in opposite directions, is important for future analysis. Special attention is needed for preschool children, people with disabilities and the movement of emergency units going against the direction of the mainstream, and so on. In those areas, data has already been presented but the quantity is significantly smaller than data for a dominant population group.

5. Conclusion

The paper presents the results of an evacuation test focused on movement and flow parameters. The achieved results were compared to data presented in literature and prescriptive regulations. The values of movement parameters and flow capacities have to be perceived as upper limit values when used in evacuation scenarios and simulation calculations. The results are valid for persons up to 30 years of age, familiar with the environment. Mutual comparison of results showed that the movement speeds listed in the national technical standard are low and need to be updated.

References

[1] BRYAN, J. L.: A Selected Historical Review of Human Behaviour in Fire, *J. of Fire Protection Engineering*, 16, 4-10, 2002.

[2] FRUIN, J. J.: *Pedestrian Planning and Design*, Metropolitan Association of Urban Designers and Environmental Planners, New York, 1971.

[3] PAULS, J.: A Personal Perspective on Research, Consulting and Codes/Standards Development in Fire-related Human Behavior, 1969-1999, with an Emphasis on Space and Time Factors, *Fire and Materials*, 23(6), 265-272, 1999.

[4] PREDTECHENSKII, V. M., MILINSKII, A. I.: *Planning for Foot Traffic Flow in Buildings*, Amerind Publishing: New Delhi, 1978.

[5] WECKMAN, H., LEHTIMAKI, S., MANNIKKO, S.: Evacuation of a Theatre: Exercise vs. Calculations, *Fire and Materials*, 23(6), 357-361, 1999.

[6] WAS, J., ROBERT, L., MYSLIWIEC, W.: The Role of Proxemics in Pedestrian Evacuation: Comparison of Simulation and Experiment, *Emergency Evacuation of People from Buildings*, 377-384, 2011.

[7] PEACOCK, R. D, HOSKINS, B. L., KULIGOWSKI, E. D.: Overall and Local Movement Speeds During Fire Drill Evacuations in Buildings up to 31 Stories, *Safety Science*, 50 (8), 1655-1664, 2012.

[8] GALEA, E. R., HULSE, L., DAY, R., SIDDIQUI, A., SHARP, G., BOYCE, K., SUMMERFIELD, L., CANTER, D. D., MARSELLE, M., GREENALL, P. V.: The UK WTC 9/11 Evacuation Study: An Overview of the Methodologies Employed and Some Preliminary Analysis, *Pedestrian and Evacuation Dynamics*, 3-24, 2008.

[9] AVERILL, J. D., PEACOCK, R. D. & KULIGOWSKI, E. D.: Analysis of the Evacuation of the World Trade Center Towers on September 11, 2001, *Fire Technology*, vol. 49, No. 1, 37-63, 2013.

[10] GWYNNE, S., GALEA, E. R., LAWRENCE, P. J., OWEN, M., FILIPPIDIS, L.: A Review of the Methodologies Used in the Computer Simulation of Evacuation from the Built Environment, *Building and Environment*, 34(6), 741-749, 1999.

[11] PAULS, J.: *The SFPE Handbook of Fire Protection Engineering,* National Fire Protection Association (NFPA), Quinci, 1995, 3-285.

[12] GALEA, E. R.: *Principles and Practise of Evacuation Modelling,* CMS Press, London, 2009.

[13] GALEA, E. R., BLAKE, S.: *Collection and Analysis of Human Behaviour Data Appearing in the Mass Media Relating to the Evacuation of the World Trade Centre Towers of 11 September 2001,* Building Disaster Assessment Ground (BDAG), London, 2004.

[14] STN 920201-3. *Fire Protection of Buildings: Escape Routes and Evacuation of Occupants*, SUTN : Bratislava, 2000.

[15] HANKIN, B. D., WRIGHT, R. A.: Passenger Flows in Subways, *Operational Research Quarterly*, 9, 81-88, 1958.

[16] DAAMEN, W., HOOGENDOORN, S. P.: Emergency Door Capacity: Influence of Door Width, Population Composition and Stress Level, *Fire Technology*, 46, 1-17, 2010.

[17] FSEG. *Building EXODUS*. Version V5.0. FSEG, November, 2012.

[18] ANDO, K., OTA, H., OKI, T.: Forecasting the Flow of People, *Railway Research Review*, 45(8), 8-14, 1988.

Jozef Futo - Lenka Landryova - Vladena Baranova *

TECHNICAL IMPROVEMENT IN REVOLUTION CONTROL EXPRESSED THROUGH PROCESS CAPABILITY INDICES

In today's competitive environment, it is essential that the company has a set of key indicators reflecting its credible performance. Modern concepts of measuring corporate performance emphasize the need for not only financial but also non-financial indicators that allow us to create a dynamic picture of the competitive situation on the market and help us to link the short-term performance to the long-term strategic vision of the company. This area can also include the issue of the numerical evaluation of the benefits brought about by using new technology in the enterprise when compared with the previously used technology. As an example, we show the modernization of equipment and the possibility of expressing the quality of a design change described on an experimental stand used for the research of the disintegration process.

The stability of the input variables crucially affects the course of the experiment, the results and the subsequent models formation. To assess the quality of the measured values a suitable method searched for their numerical evaluation. It was found that this can be done through a process capability index, as a measure of the quality of the monitored process, and an application of the process capability index is one of the possibilities for such evaluation.

Keywords: *Input and output variables of the system, process capability index, evaluation of measurements.*

1. Introduction

An application of high voltage semiconductor devices (diodes, thyristors, diacs, triacs, transistors) in the late seventies and early eighties of the last century in the industry meant a qualitative change in the technical solutions in many areas of industry and in mostly it had significant economic consequences. However, the most significant impact it had was in the field of control technology and automatic control. For decades the technical solutions as well as the parameters of these devices were suitable. They worked accurately, reliably and for the operation were satisfactory. But the current economic and environmental conditions and new technologies require advanced technical solutions often based on industrial PCs and the hardware and software. They almost ensure a step change in quality control. The technical changes often have large capital requirements for funding projects, producing documentation and commissioning it. The more complex a new technology is, the more difficult it is to express the benefits and it is often missing the appropriate means for the exact (sophisticated) expression. One solution may be a new level of quality representation using process capability indices (PCI).

Examples of their use can be calculating the PCI before and after the structural change of control of the experimental stand in a laboratory of the Institute of Geotechnics of the Slovak Academy of Science (UGT SAV in Kosice). The experimental stand is used to study the process of disintegration of rock by drilling tools used in practice, up to a diameter of 54 mm. A detailed description of the stand is in [1]. In this paper we pay particular attention to the control of revolutions as the input variable of the system indentor-rock before and after the technology stand reconstruction, which should have ensured the greater stability of the input variables. Given the complexity of the experimental stand (Fig. 1) and the experiment itself, we will show examples of using capability indices to control the revolutions by the original method based on high-voltage semiconductor devices and after the stand reconstruction.

2. A system to ensure controllable revolutions

The original manual control or continuous revolution control of a DC electric motor with the drive type Ward Leonard was replaced by a revolution control with a frequency converter. The original DC electric motor with a power of 12.5 kW was replaced by a new asynchronous motor with an output of 22 kW. The initial revolution control range 0-24 s^{-1} was replaced by a control with a unistor range from 0 to 33.3 s^{-1}.The drilling tool (indentor)

* [1]Jozef Futo, [2]Lenka Landryova, [2]Vladena Baranova
[1]Institute of Control and Informatization of Production Processes, Faculty of Mining, Ecology, Process Control and Geotechnology, Technical University of Kosice, Slovakia
[2]Department of Control Systems and Instrumentation, VSB - Technical University of Ostrava, Ostrava, Czech Republic
E-mail: jozef.futo@tuke.sk

is driven by an asynchronous motor with a belt and V-belt system. Measurement revolution is provided by a tachodynamo which is on the common axis with a disconnecting tool. According to the values of the output voltage of the tachodynamo, which is in the range of 0 to 10 V, we can determine the instantaneous revolutions of a disconnecting tool. The output of the tachodynamo is calibrated with a stroboscope tachometer with an accuracy of 0.5% +2 digits. The control of the revolution variable of the disconnecting tool spindle is provided by the control computer using a control algorithm which compares the desired revolution input to the system with the real revolution. By the feedback system the frequency converter provides the stable spindle revolution of the disconnecting tool during the experiment.

Fig. 1 Experimental stand

For qualitative assessment of input or output process variables it is possible to proceed in several ways. One is the evaluation by Process Capability Index (PCI) which compares the prescribed maximum permissible variability of values given by tolerance limits to the actual variability of the observed character achieved by a statistically controlled process. Without proper measuring equipment and methodology we are not in a position to determine the capability of processes adequately. This fact was proven as particularly important in the case of the non-standard identification of complex systems when the useful signal represented only a small fraction of the total monitored signal. Statistical control is based on the fact that the specified measured value (revolution) is controlled at appropriate intervals within a selected set of a number of values. Measurement procedure is implemented by a measuring process. By taking into account the specific effects we set the final measured value in the specific range. The size of a range, thus the rate of distraction, expresses a measurement error. If this error is acceptable, measurement uncertainty is low, then we conclude that the measurement process has the capability for those conditions. The aim of research of measurement system capability is a statistical estimate of the rate at which the repeatability and reproducibility misrepresent the evaluated reality [2, 3, 4, 5, 6, 7, 8, 9 and 10].

3. Theoretical analysis of the statistical evaluation of the quality of the measurement process

Statistical control of the measuring process can be understood as the maintenance of its statistically controlled status. This would ensure the consistency of measurement results with specific requirements for measurement. We assume that the behavior of the measuring process describes the behavior of multiple output values, compared with the established criteria. The basic statistical control tool for measuring processes is the control chart [1, 11 and 12].

The theory of control charts is based on differentiating between two types of variability. The first type is a random variability due to random causes. This type produces a wide range of unidentified causes. Each contributes with a small component of the total variability, but none of them contribute significantly to it. The second type of variability is a real change in the measuring process. Such a change may be caused by some identifiable causes which are not a part of the internal measuring process and can be, at least in theory, removed. These causes can be systemic and can be attributed to the use of measuring devices, the methods and procedures of measurement, measurement conditions, measuring staff, and similar.

For the experiment of rock disintegration in the laboratory of UGT SAV in Kosice the previous control of revolution was replaced by an automatic control. Then, it was necessary to find a suitable (mathematical) tool for a quantitative assessment of the structural changes and for the numerical evaluation. One option seems to be the use of the process capability index. Data from control charts are available to calculate the necessary PCI. It is necessary to take into account the specific use of relationships, since the calculated indices change values according to the input process parameters.

4. Process capability

The role of the PCI is simply to express the relationship between the target setpoint-T (Target Value), specified limits LSL and USL (Lower/Upper Specification Limit) and the actual process value expressed by the mean μ and standard deviation σ of the measured values of the selected quality parameter of the process. The target value T is the desired mean of the quality parameter that needs to be achieved, or approximately achieved.

The lower and upper specific limits LSL and USL are the limits set for the quality parameter with respect to the required variability in order to ensure the desired functionality of the process [2, 3, 9, 10, 11 and 12].

To evaluate the processes various indices were gradually developed. According to the number of monitored quality parameters they can be divided into:

- single parameter indices,
- several simultaneously monitored quality parameter indices.

5. Using capability indices to determine the quality of the measured values

For practical interpretation it is important to accurately select a combination of indices, therefore, not consider those, for which the conditions are not met, and complete them with graphical representation of the distribution of the monitored quality parameter, a target value and specific limits. In Fig. 2 - 7 we can observe the courses of revolution with the changing target value n = 1000 min^{-1}, and n=1500 min^{-1} respectively, and the required tolerance range with the range of values ± 1%, and ± 5% respectively. These courses were obtained experimentally at various monitored process modes and simulations. When compared they vary in the random variable characteristics (mean, standard deviation, covariance function), but they do not give an adequate overview of the correlation of the required (target) value, mean, the required tolerance and standard deviation.

Assessment of the characteristic of monitored signals (values) is based on the assumption that the input variable - revolution must be constant. However, such an assumption cannot be reached under real conditions (the experimental stand), so determination of the stability of the observed variable is based on the theory of control charts.

The basis of a control chart is to display data in a two-dimensional coordinate system. The figures show three criteria: Center Line (CL), Upper/Lower Control Limits (UCL and LCL), and it is recommended that the so-called Upper/Lower Warning Limits (LWL/UWL) are also shown. These limits are calculated as three or two multiplications of the standard deviation of the observed value [13].

In Fig. 2, 3, 5 and 6 we can monitor the revolution with the original control method applied and in Fig. 4 and 7 the revolution with the automatic control after the design change. Control charts are completed by a Target Value - the required revolution value T, and the required tolerance range LSL/USL, which has a range of values of T ± 1%, ± 5% respectively.

A common feature of the control chart is that all the courses are in the range of CL ± 3 σ, so taking these criteria into account; revolution was statistically stable and suitable for further processing. The tolerance range of 1%, 5% respectively, was exceeded several times; therefore, the original experimental stand did not meet the demands of further experiments. This problem was solved by a change in constructional design, as it can be observed in Fig. 4 and 6. Comparison of required and output values of each characteristic can be observed in Table 1 which, however, does not give an overview of the quality achieved (the quality of measured values), and based on these values it does not show whether or not the input signal of the system is suitable for further use.

6. C_{pm} Capability Index

Capability index C_{pm}, called Taguchi capability index, removes some of the problems of C_p and C_{pk} indices and keeps their good properties. Index C_p characterizes the variability of the process, but does not say how it was actually used. Its disadvantage is that it does not take into account the center of the distribution of measured values with respect to the desired target value T and requires both tolerance limits to be entered. Index C_{pk}, unlike C_p index, considers not only variability, but also the location of the monitored values of the quality parameter in the tolerance field. Thus, it characterizes the true process capability to follow the prescribed tolerance limits.

Index C_{pm} was designed in relation to the loss function used in the Taguchi approach for a quality assessment. It compares the maximum permissible variability of observed quality parameter specified by a tolerance range width and the actual variability around the target value T:

$$C_{pm} = \frac{USL - LSL}{6 \cdot \sqrt{\sigma^2 + (\mu - T)^2}} \qquad (1)$$

The term $\{\sigma^2 + (\mu - T)^2\}$ is a measure of the average quadratic loss caused by a failure to comply with the terms of production quality. If the standard deviation increases and/or the mean moves away from the Target value, the denominator of an index increases and C_{pm} index value decreases. The advantage of this index is its ability to record the changes of a mean that are "compensated" in the index C_{pk} by changing the standard deviation. This index is used for two-sided tolerances and a target located in the center of the tolerance range, as is the case in our application [14 and 15].

After calculation of capability indeces C_{pmt1} a C_{pmt5} (tolerance of input variable is 1, resp. 5%) these factors are taken into account, capability indices are calculated and the increasing value of the coefficient is representing the increasing quality of the input variable as well (Table 1).

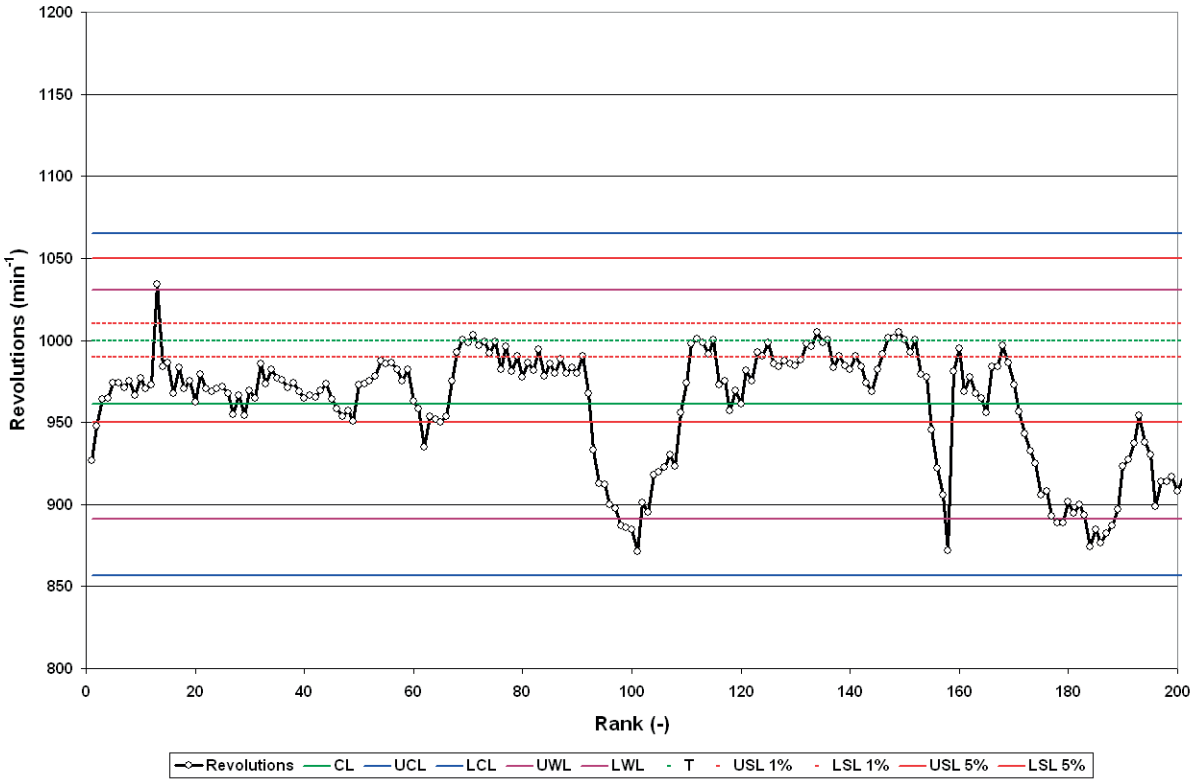

Fig. 2 Revolution course for the previous stand design with manual control and higher pressure (2004)

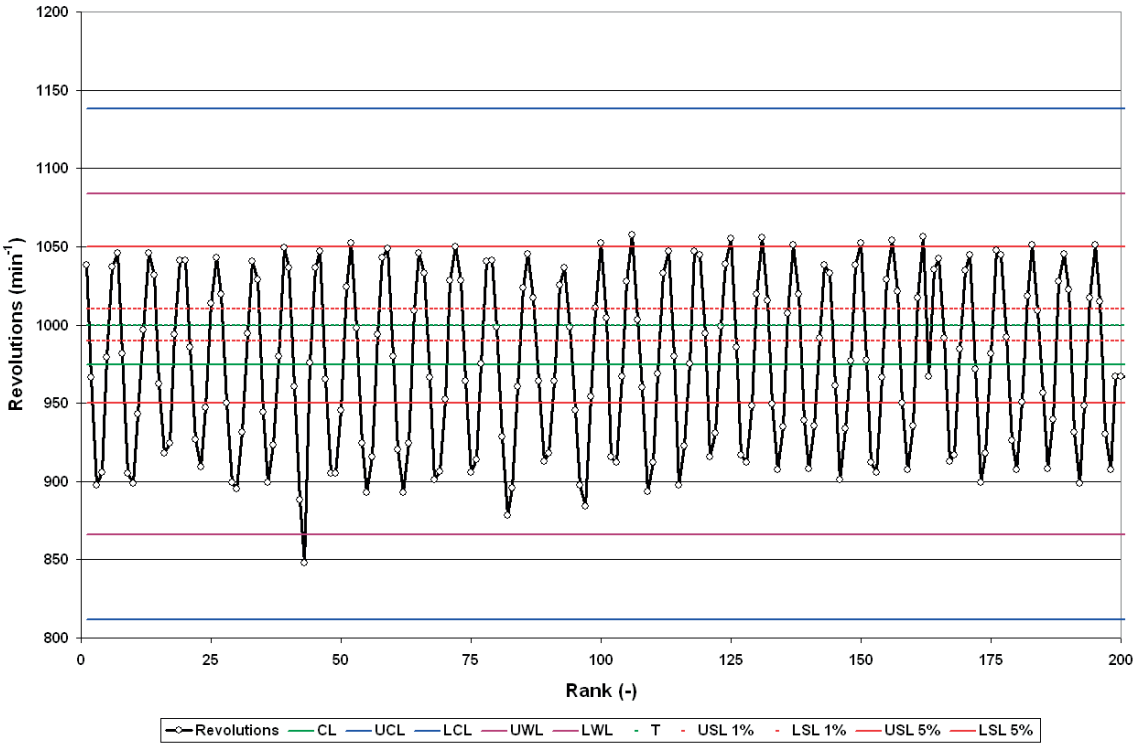

Fig. 3 Revolution course for the previous stand design with manual control and lower pressure (2004)

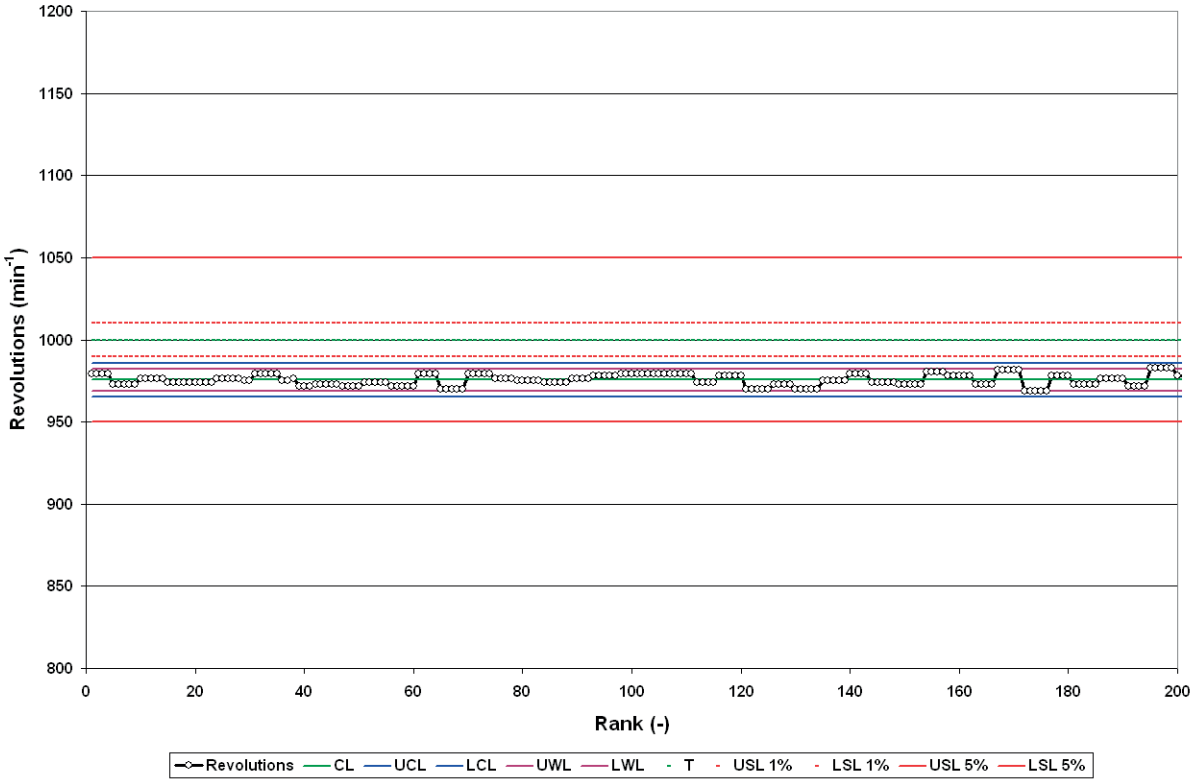

Fig. 4 Revolution after the constructional change of design with automatic control (2012)

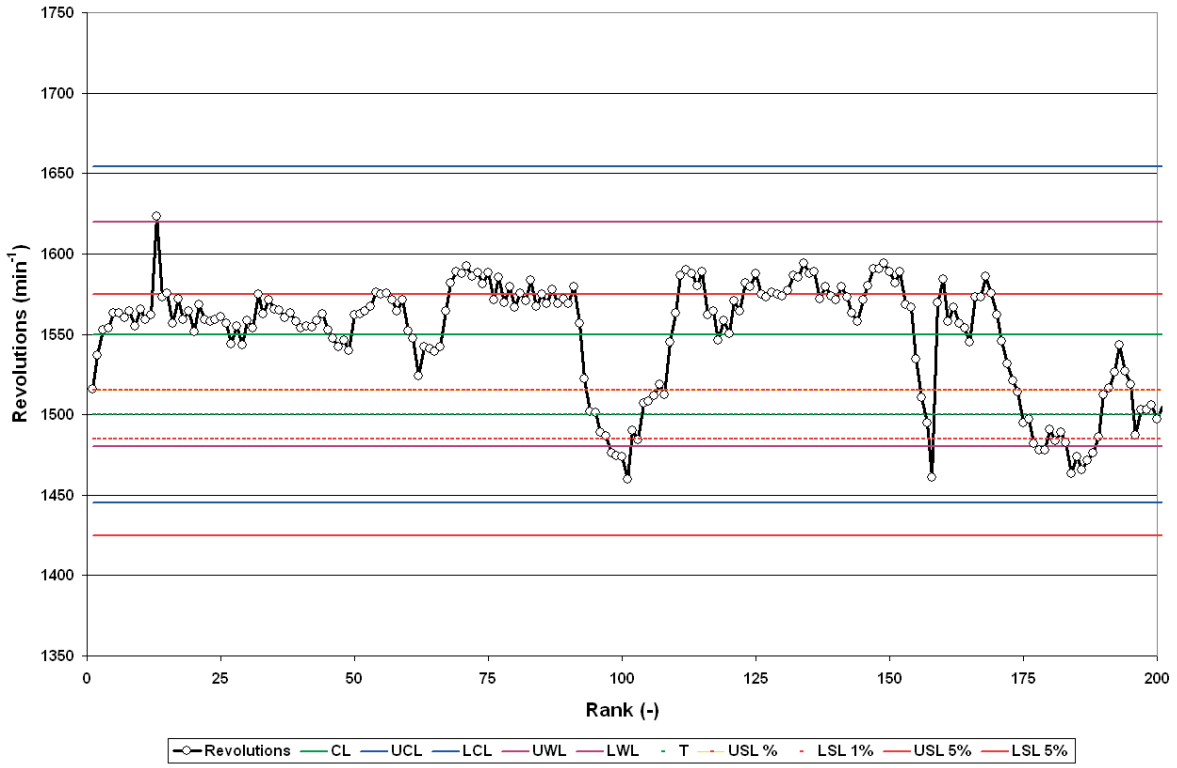

Fig. 5 Simulated revolution course for the previous control and higher pressure (2004)

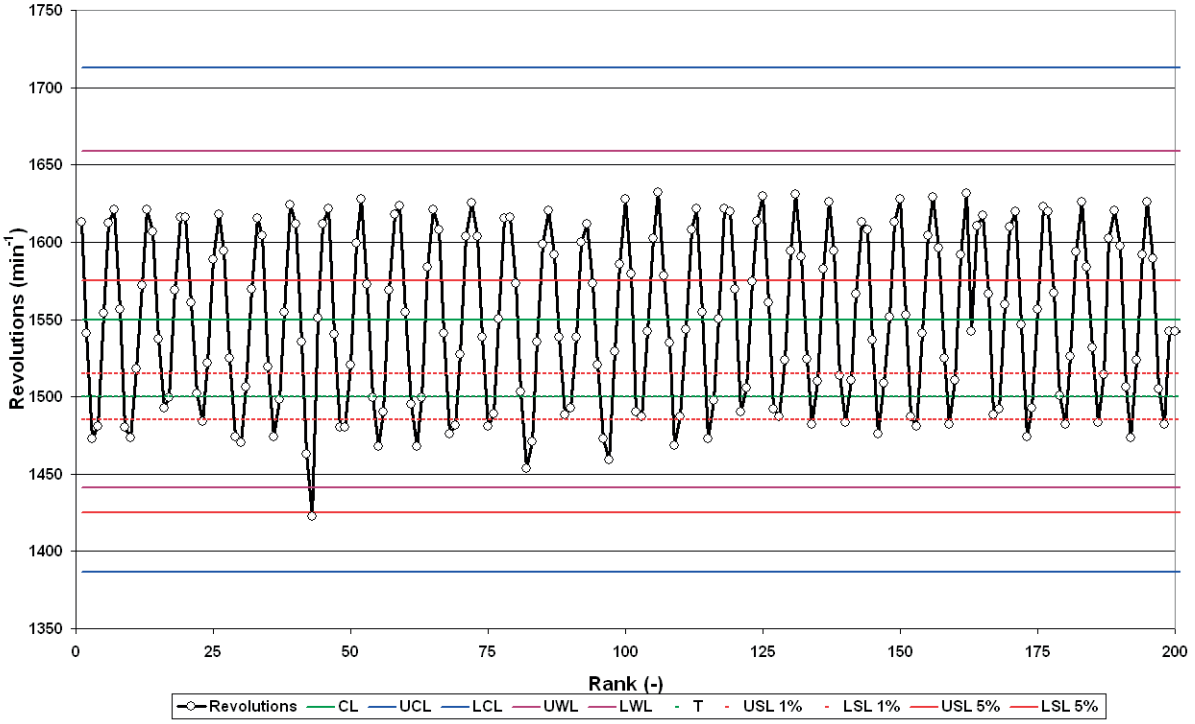

Fig. 6 Simulated revolution course for the previous control and lower pressure (2004)

Fig. 7 Revolution course after the constructional change of design with automatic control (2012)

Characteristics and quality criteria of measured variable - revolution Table 1

Criteria	Revolution (min^{-1}) (Fig. 2)	Revolution (min^{-1}) (Fig. 3)	Revolution (min^{-1}) (Fig. 4)	Revolution (min^{-1}) (Fig.5)	Revolution (min^{-1}) (Fig. 6)	Revolution (min^{-1}) (Fig. 7)
CL	961	975	975	1550	1550	1551
UCL	1065	1138	986	1654	1654	1561
LCL	856	812	965	1445	1445	1540
UWL	1031	1084	982	1620	1620	1557
LWL	891	866	969	1480	1480	1544
T	1000	1000	1000	1500	1500	1500
SIGMA	34.82	54.36	3.41	34.82	54.36	3.41
USL 1%	1010	1010	1010	1515	1515	1566
LSL 1%	990	990	990	1485	1485	1534
USL 5%	1050	1050	1050	1575	1575	1628
LSL 5%	950	950	950	1425	1425	1473
C_{pmt1}	**0.0334**	**0.0224**	**0.1348**	**0.0822**	**0.0678**	**0.0988**
C_{pmt5}	**0.3183**	**0.2782**	**0.6739**	**0.4109**	**0.3389**	**0.4939**

7. Conclusion

The results we have obtained by monitoring data from the original measurement and measurement after reconstruction can be formulated as follows:

1. Construction of control charts with the currently used hardware and software is relatively simple, quick and easy,
2. The course of the measured values and their limits based on control characteristics UCL and LCL give a sufficiently accurate picture about the variability of the measured values and the tolerance limits USL and LSL,
3. If corrective action (structural changes) are taken it is possible to see in Figures 4 and 6 a positive expected change in the variability of the monitored quality parameter, or process tolerance limits, which the parameter meets respectively,
4. The Taguchi capability index application in the process of the disintegration of rocks on one of the input parameters of monitored system has served as an example to determine the quality of the process, its use also points to the possibility of a numerical expression of a number of parameters of the evaluated variables,
5. Process capability indices for the reconstructed experimental stand are generally increased more than ten times,
6. This method can also be used for complex processes, technology, such as models of MISO types, determining the Key Performance Indicators whose role is to define and quantify progress towards meeting the objectives of the company.

Acknowledgement

This contribution was written within the framework of VEGA 1/0729/12, VEGA 1/0295/14 project and specific research project of VSB-TUO No. SP2013/85.

References:

[1] FUTO, J., IVANICOVA, L., KREPELKA, F.: *Hydraulics and Pneumatics - Parts 1-2 (in Slovak)*, 2010, pp. 9-13.
[2] BENKOVA, M.: *Quality Assurance Processes (in Slovak)],* Kosice : Technicka univerzita : F BERG, 2007.
[3] BENKOVA, M., FLOREKOVA, L., BOGDANOVSKA, G.: Variability of Quality Parameters and the Loss Function (in Slovak), *Acta Montanistica Slovaca*, vol. 10, No. 1, 2005, 57-61.
[4] FLOREKOVA, L.: Statistical Methods for Quality Assessment (in Slovak), *Acta Montanistica Slovaca*, vol. 1, 1998, 1-20.
[5] HANZELOVA, M., FLOREKOVA, L.: *Environmental Performance Evaluation.* 5th intern. Control Conference 2004, Zakopane, May 2004, 915-918, ISBN 83-89772-00-0.
[6] HANZELOVA, M., FLOREKOVA, L., BENKOVA, M.: *A Protection of Air from the Point of View of Local Producer of Polluting Substances/Emissions*, 3rd intern. Control Conference 2002, Malenovice, May 2002, 569-574, ISBN 80-248-0089-6.

[7] MALINDZAKOVA, M.: Significance Evaluation of Environmental Aspects, *Communications - Scientific Letters of the University of Zilina*, vol. 13, No. 3, 2011, 48-51, ISSN 1335-4205.
[8] LESSO, I., FLEGNER, P.: *Specifications Symptoms of Rock Disintegration Process of Rotary Drilling Control Process (in Slovak)*, Sbornik vedeckych praci Vysoke skoly banske - Technicke univerzity Ostrava : Rada stavebni, vol. 9, No. 2, 2009, 155-165, ISSN 1213-1962.
[9] LESSO, I. et al.: Research of the Possibility of Application of Vector Quantisation Method for Effective Process Control of Rocks Disintegration by Rotary Drilling, *Metalurgija*, vol. 49, No. 1, 2010, 61-65, ISSN 0543-5846.
[10] LESSO, I. et al.: New Principles of Process Control in Geotechnics by Acoustic Methods. *Metalurgija*. vol. 46, No. 3, 200), 165-168, ISSN 0543-5846.
[11] PAVLICKOVA, M.: *Methodology for Assessing the Quality Parameters of Selected Products*, *(in Slovak)*, Dissertation work, Kosice, 2007, TUKE : F BERG.
[12] STN ISO 8258:1995: *Shewhart Control Charts, Slovak Technical Standard (in Slovak)*, Slovenska technicka norma, 1995.
[13] SMITH, D., J.: *Reliability Maintainability and Risk*, Rochester : Kent, 1997
[14] SMITH, J.: *The KPI Book*, Insight Training & Development, 2001, ISBN 978-0-954-02590-8.
[15] PARMENTER, D.: *Key Performance Indicators: Implementing*, *and Using Winning KPIs*, John Wiley & Sons : Inc., Hoboken : New Jersey, 2010, ISBN 978-0-470-54515-7.

Jan Plachy - Jana Vysoka - Radek Vejmelka - Zdenek Caha *

CORRELATION OF WATER ABSORPTION VALUES OF BITUMEN WATERPROOFING SHEETS OBTAINED ACCORDING TO CSN EN 14223 AND CSN 503602

The article deals with the issue of weight water absorption of bitumen waterproofing sheets. It compares two methodologies applicable to examination of water absorption of bitumen waterproofing sheets from the point of view of testing procedures. It compares the results of both the methods for individual bitumen sheets upon experimental measurement and examines mutual relation between the individual results. The experimental measurement was performed on bitumen sheets used for waterproofing of bridge deck [1].

Keywords: *Bitumen waterproofing sheets (BWS), carrier, coarse gritting, fine gritting, water absorption.*

1. Introduction

Water in liquid or gaseous state in bridge deck waterproofing system can be a source of a defect and consequent damage to the whole system of layers. It leads, e.g., to buckling of the carriageway that appears up to the carriageway surface course, see Fig. 1.

Apart from further numerous sources water may get into the waterproofing system even in the form of water contained in bitumen waterproofing sheets (BWSs). Water may penetrate into the BWS structure during manufacturing process, but also during storing before application. There are two test procedures dealing with water content in a complete BWS. An older one is presented in CSN 503602 [2] and a newer one in CSN EN 14223 [3]. General requirements for BWSs are presented in Table 1. Our aim is to define mutual dependence between the weight absorption set by the methodologies of CSN EN 14223 [3] a CSN 503602 [2] standards. At present we can still meet both the testing procedures and it is advantageous to know their mutual relation to be able to find quickly what values of weight absorption a particular BWS reaches. The term weight absorption is hereinafter referred to as absorption.

Fig. 1 Buckling under milled protective layer and surface course. Source: own

Quality requirements for bitumen waterproofing sheets as per [4], [5], [3] and [2] Table 1

Requirement name	Size	Value	Testing method	Testing procedure applicability
Water absorption after 28 days at 23+3°C	%	max. 1.5	CSN 736242:2010 CSN EN 14223	Yes
Water absorption after 30 days at 20+2°C	%	max. 2¨.5	CSN 736242:1995, CSN 50 3602:1967	No

* **Jan Plachy, Jana Vysoka, Radek Vejmelka, Zdenek Caha**
Institute of Technology and Business in Ceske Budejovice, Czech Republic
E-mail: plachy@mail.vstecb.cz

2. Methodology and material

20 BWSs used for single-layer application to waterproofing of concrete bridge decks in the Czech Republic and Slovakia were chosen for the testing in total. BWS used for waterproofing of bridges and roads on motorways and class 1 roads must belong to the waterproofing systems approved by the Ministry of Transport in the Czech Republic. In Slovakia approval of waterproofing system is directly subject to the particular investor after meeting legislation requirements.

The following group of BWSs is divided according to requirements of CSN 736242:2010 [4]. There are eleven BWSs with coarse gritting, five with fine gritting and four BWSs are without gritting. There are fifteen BWSs with plastomeric type substance and five with elastomeric type substance. The basic characteristics for the water absorption test are described in Table 2. All the BWSs had polyester carriers impregnated with bitumen substance.

Correlation is examined between two water absorption tests after 28 days according to CSN 736242:2010 [4], CSN EN 14223 [3] and for water absorption after 30 days according to CSN 736242:1995[5], CSN 503602 [2].

2.1 Water absorption after 30 days

Water absorption is determined by a testing procedure according to SN 503602 [2]. The testing specimen is immersed in water bath (20 ± 2) °C warm for 30 days. Three specimens of 100 x 100 mm are used for the test, see Fig. 2. Before immersion all loose gritting is removed by delicate wiping and the specimens are weighed with accuracy of 0.01 g. The specimens are removed from the water bath after 24 hours and dried between sheets of filter paper (80 – 100 g/m^2) so as their surfaces are free of wet glossy stains and they are kept between the sheets. The testing specimens have to be weighed within 8 minutes from removal from the water at air temperature 20 ± 2°C and relative humidity 60 ± 5%.

Water absorption of bitumen sheets is expressed as percentage, namely as the ratio of the difference of the weight of the testing specimen after immersion – the weight of the testing specimen before immersion to the weight of the testing specimen before immersion. BWS water absorption is the ratio of the weight difference to the weight of the testing specimen before immersion expressed as a percentage. The arithmetic average of five individual values is the test result.

Selected characteristics of the specimens. KEY: CG - Coarse gritting, FG - Fine gritting, N - geotextile surfacing (approx. 20g/m^2), PES - polyester fleece, P - plastomeric character, E - elastomeric character. Source: own. Table 2

Specimen characteristics /specimen number	**2**	**3**	**6**	**7**	**8**	**9**	**10**	**11**	**12**	**13**
Top surfacing	CG	N	N	FG	CG	FG	CG	CG	CG	CG
Bitumen substance type	P	P	P	E	P	P	P	P	P	P
Carrier – areal weight (g/m2)	230	200	200	250	220	230	230	230	230	230
BWS thickness (mm)	5.20	5.24	4.83	5.10	5.47	4.85	5.16	4.95	5.54	5.15
Place of BWS application (state)	SK	SK	SK	SK	SK	SK	CZ	CZ	CZ	CZ
Specimen characteristics /specimen number	**14**	**15**	**16**	**17**	**18**	**19**	**20**	**21**	**22**	**25**
Top surfacing	FG	CG	FG	CG	CG	N	FG	N	CG	CG
Bitumen substance type	P	E	E	P	E	P	E	P	P	P
Carrier – areal weight (g/m2)	230	230	230	230	250	250	250	250	250	280
BWS thickness (mm)	6.25	5.46	4.80	5.67	5.05	4.15	4.15	4.06	5.22	5.18
Place of BWS application (state)	CZ	CZ	CZ	CZ	SK	CZ	CZ	CZ	SK	SK

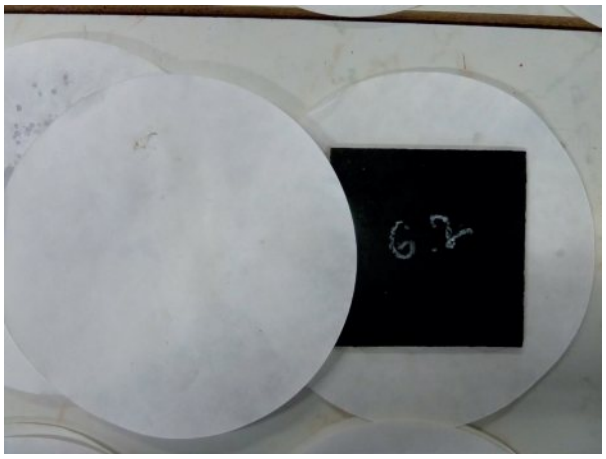

Fig. 2 Testing specimen between filter paper sheets for the water absorption test according to [2]. Source: own

Fig. 3 Water bath according to [2], [3] for the specimens. Source: own

2.2 Water absorption after 28 days

Water absorption is determined by a testing procedure according to CSN EN 14223 [3]. The testing specimen is immersed in water bath (23 ± 3) °C warm for 28 days ± 4 hours, see Fig. 3. Weight is measured before and after immersion. Five test specimens 200 x 200 mm are used for the test. All loose gritting has to be removed before weighing the test specimens and they are dried for 24 h ± 30 min. at temperature (50 ± 3) °C. Then they are tempered for 1h ± 5min at temperature (23 ± 3) °C and relative humidity (50 ± 5) %. After removal from water the specimens are dried in the air for 5h ± 5min at temperature (23 ± 3) °C and relative humidity (50 ± 5) %. After expiry of this period they are weighed.

Water absorption of bitumen sheets is expressed as percentage, namely as the ratio of the difference of the weight of the testing specimen after immersion – the weight of the testing specimen before immersion to the weight of the testing specimen before immersion. BWS water absorption is the ratio of the weight difference to the weight of the testing specimen before immersion expressed as a percentage. The arithmetic average of five individual values is the test result.

2.3 Correlation of the testing procedures

Our aim is to determine mutual dependence between the absorption values according to the mentioned standards. We expect existence of direct linear dependence or more precisely direct proportion between the two standards. First we are going to calculate the value of Pearson correlation coefficient, which is the most suitable for determination of linear dependence. After that we will perform a correlation coefficient test to confirm the statistical significance. Then we will prepare a linear regression model representing the relation between the two standards and perform a test of its significance and evaluate its suitability.

For comparison we will also perform a different method of examination of mutual dependence of the water absorption values according to both the standards. As the absorption values differ in different BWSs we will apply a straight line to the absorption values of the individual specimens in order of size for both the standards. We will get two straight lines this way, which we expect to be nearly parallel, and the relation between the two standards will then be given by mutual position of the straight lines.

3. Test results

3.1 Water absorption after 28 and 30 days

Absorption test results after 28 days according to [3] and after 30 days according to [2] for the individual specimens. Source: own Table 3

Specimen characteristic /specimen number	2	3	6	7	8	9	10	11	12	13
Absorption according to CSN 503602, 30 days in (%)	1.59	1.49	1.54	1.51	2.03	1.22	1.30	7.79	1.82	6.54
Absorption according to EN 14 223, 28 days in (%)	0.80	1.30	0.80	0.40	0.60	0.70	1.30	4.40	0.70	4.10
Specimen characteristic /specimen number	14	15	16	17	18	19	20	21	22	25
Absorption according to CSN 503602, 30 days in (%)	0.94	2.71	0.84	1.55	1.05	1.79	0.95	1.28	1.76	1.30
Absorption according to EN 14 223, 28 days in (%)	0.40	1.60	0.40	0.60	0.20	0.50	0.50	0.80	0.90	1.30

3.2 Correlation of the testing procedures

3.2.1 Correlation coefficient and direct regression model

The value of Pearson correlation coefficient between standards CSN EN 14223 [3] and CSN 503602 [2] is $r = 0.929$. The value of the testing statistics in the correlation coefficient test is t = 11.245 at 20 degrees of freedom. P-value of the test is approximately $2.124 \cdot 10^{-10}$, one-side confidence interval at the level of 95% for the correlation coefficient is (0.855; 1). The linear regression model expressing dependence of the absorption values according to CSN EN 14223 [3] on the values according to CSN 503602 [2] is CSN EN 14223 = 0.5785 · CSN 503602.

Model determination coefficient $R^2 = 0.86$ · 95% both side confidence interval for regression coefficient is (0.4712; 0.6858).

3.2.2 Method of two regression lines

After performing the procedure described in 2.3 we got two straight lines with equations $y = 0.182x + 0.131$ and $y = 0.144x - 0.4$. The achieved results are graphically interpreted and described in Fig. 4.

4. Discussion

4.1 Water absorption after 28 and 30 days

The obtained absorption results, see Table 3, allow us to say that all the specimens except for two have met the requirements of the standards [2] a [3]. In the instance of the two specimens they were BWSs in which the carrier was insufficiently impregnated. BWSs with coarse gritting and with plastometric character had the highest absorption even in the case when the two above mentioned specimens had been removed from the examined group.

4.2 Correlation of the testing procedures

4.2.1 Correlation coefficient and direct regression model

The obtained value of the correlation coefficient between CSN EN 14223 [3] and CSN 503602 [1] is 0.929. This value shows strong direct linear dependence. This conclusion is also confirmed by the correlation coefficient test which confirms at the significance level of 5% that the correlation coefficient value is not zero. The interval estimation then shows that this value is with 95 % liability higher than 0.855. The created regression model of

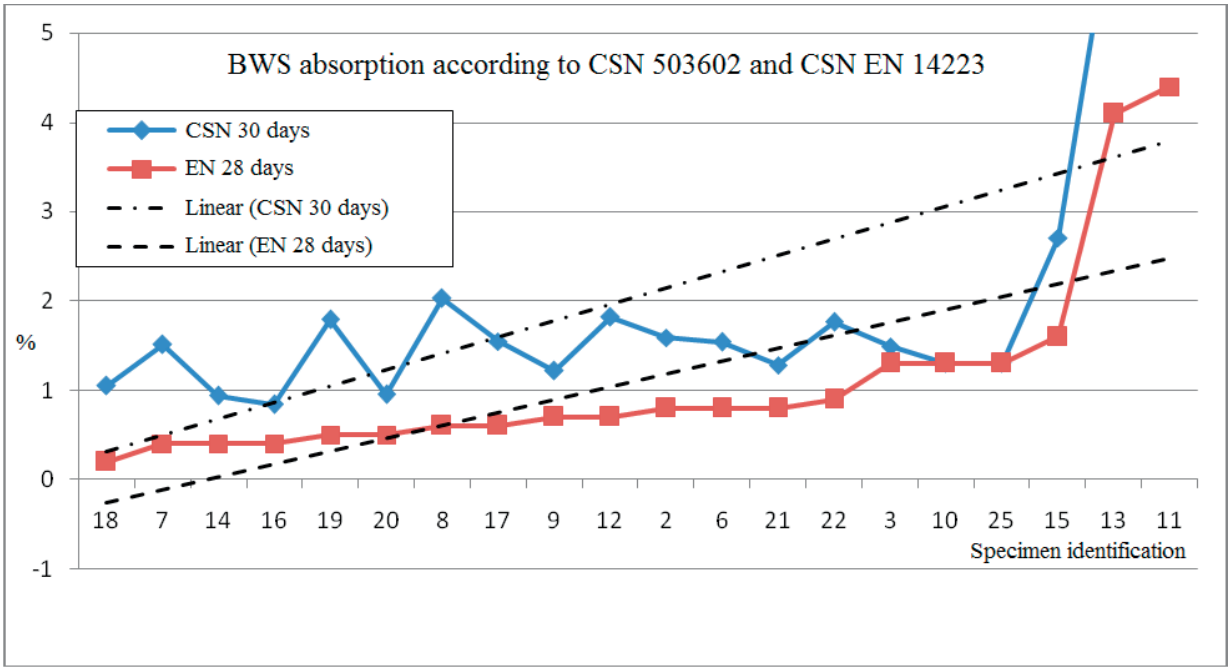

Fig. 4 Results of the BWS weight absorption test according to [2] and [3]. Source: own

dependence of absorption values according to CSN EN 14223 [3] on the values of CSN 503602 [2] is statistically significant and the determination coefficient whose value approximates to 90% shows that suitability of this direct proportion model has been confirmed as the absolute member of the equation of the line is statistically insignificant so it can be considered zero.

4.2.2 Method of two regression lines

The hypothesis set in 2.3 was confirmed even by the second approach. The directions of both the regression lines are very close so they can be considered approximately parallel with the given range. Their distance is then given by the absolute value of the difference of the absolute members of the lines and it is 0.531, while this value falls into the interval estimation of the regression coefficient determined by the previous procedure.

5. Conclusion

We have managed to derive the mutual relation between the values of the examined data files by means of two different approaches. Both the methods led to the conclusion that this relation can be considered direct proportion, which corresponds with the original assumptions.

References

[1] CSN EN 14695:2010. *Flexible Sheets for Waterproofing - Reinforced Bitumen Sheets for Waterproofing of Concrete Bridge Decks and other Trafficked Areas of Concrete - Definitions and Characteristics.* Prague : Czech Standards Institution. 2010-05-01. Classification mark 727605.

[2] CSN 503602:1967. *Testing Roofing and Waterproofing Materials in Roles.* Prague : Czech Standards Institution. 2010-02-22. Classification mark 503602.

[3] CSN EN 14223:2006 *Flexible Sheets for Waterproofing - Reinforced Bitumen Sheets for Waterproofing of Concrete Bridge Decks and other Trafficked Areas of Concrete - Determination of Water Absorption.* 1st ed., Prague : Czech Standards Institution, 2006-07-01. Classification mark 727677.

[4] CSN 736242:2010. *Design and Construction of Pavements on Road Bridges.* Prague : Czech Standards Institution. 2010-04-01. Classification mark 736242.

[5] CSN 736242:1995. *Design and Construction of Pavements on Bridges and Roads.* Prague : Czech Standards Institution. 1995-03-01. Classification mark 736242.

Jaroslav Smutny – Daniela Sadlekova *

THE VIBRATION ANALYSIS BY MARGENAU-HILL TRANSFORMATION METHOD

The paper is devoted to the description and application of Margenau Hill transformation for vibration analysis. This is a transformation belonging to the large group of non-linear time-frequency transformations. The properties predestinated it to a successful use in the area of non-stationary and transitional signal analysis describing various natural processes. A very interesting application area of this transformation is its use for the vibration analysis of signals from railway traffic. The paper contains mathematical analysis of the transformation, case study and gained practical experience and recommendations for practice.

Keywords: *Vibration, signal analysis, time frequency transformation, railway transport, crossing construction.*

1. Introduction

The information on any engineering, physical, or other phenomenon is represented in the signal by the changes over time of the current value of the quantity described by the signal. In many applications, direct evaluation of the time-amplitude representation is neither easy nor advantageous. For this reason, at first, the signal is transformed from the time-domain into another one. In some cases, important information can be obtained from the frequency domain. For the transformation from time to frequency area the most used and known method is the Fourier's transformation and their modifications. The Fourier transform, or its modification and some of the parametric methods are well suited techniques to processing stationary signals.

For determination of time localization of frequency components within non-stationary signals it is not possible to use classical proceedings of frequency analyses but it is necessary to apply some other transformation procedures and other calculation methods.

2. Time frequency analysis

If the information sources from the time and frequency domains are to be combined, we can use what is called time-frequency transformations. This enables us to determine the frequency as a function of time. So, one of the possible procedures is the application of so called time-frequency transformations. They can be divided according to calculating methods into two basic classes [1]:

- linear (including especially short-time Fourier's transformation, transformation Wavelet etc.)
- non-linear (including especially quadratic Cohen's, affinity and hyperbolical transformations, or other special proceedings).

The main disadvantage of all linear and time-frequency transformations is the fact that the resulting determination within the time and frequency is limited by so called Heisenberg's principle of indefinitely. The frequency signal component can be presented only inside the rectangle $\Delta t \times \Delta f$ given in time-frequency area (Δt represents minimal time interval – time step, Δf represents minimal frequency interval – frequency step). This fact may be limited in many applications. That is the reason why it is necessary to look for more precious proceedings in some cases. Especially, the non linear time-frequency transformation belongs to them.

Within non-linear procedures the most suitable are especially quadratic methods. From the point of view of mathematical features there is a very important group of quadratic transformations represented by so called Cohen's transformations. These include Margenau-Hill transformation too.

The mathematical definition of this time-frequency transformation is given by the following relation [2],

$$MHT(t,f) = \int_{-\infty}^{\infty} \frac{1}{2}\left[\begin{matrix} x(t+\tau)\cdot x(t)^{*} \\ +x(t)\cdot x^{*}(t-\tau) \end{matrix}\right]\cdot e^{-j\cdot\omega\cdot\tau}\cdot d\tau, \quad (1)$$

* **Jaroslav Smutny, Daniela Sadlekova**
Institute of Railway Structures and Constructions, Faculty of Civil Engineering, Brno University of Technology, Czech Republic
E-mail: smutny.j@fce.vutbr.cz

where t is time, τ is the time transition, f is the frequency, $x(t)$ represents the time signal, symbol '*' represents the complex conjunction, j imaginary unit, $\omega=2\cdot\pi\cdot f$ is angular frequency, and $MHT(t,f)$ is the time frequency representation of the signal. Let us note that this refers to a complex transformation which, from the viewpoint of processing the measured signals has many suitable properties, offers an excellent resolution both in the time and in the frequency regions.

Generally, theory of non-linear time-frequency transformations is based on quantity mechanics and for derivation and calculation there can be used operator´s theory. The theory assumes that every quadratic, time and frequency invariant transformations can be expressed by the relation

$$CT_x(t,f)=\int_{-\infty}^{\infty}\int_{-\infty}^{\infty}A_x(\theta,\tau)\cdot\psi(\theta,\tau)\cdot \cdot e^{-j\cdot\theta\cdot t}\cdot e^{-j\cdot\tau\cdot\omega}\cdot d\theta\cdot d\tau, \quad (2)$$

where $CT_x(t,f)$ is the time frequency representation of the signal, the symbol τ represents time-shifting, j imaginary unit, ω is angular frequency, θ is frequency shifting, $\psi(\theta,\tau)$ is the kernel function of particular time-frequency transformation and $A(\theta,\tau)$ represents time-frequency autocorrelation function. This function is given by the equation

$$A_x(\theta,\tau)=\int_{-\infty}^{\infty}x\left(t+\frac{\tau}{2}\right)\cdot x^*\left(t-\frac{\tau}{2}\right)\cdot e^{j\cdot\theta\cdot t}\cdot dt. \quad (3)$$

It is worth noting that this „narrow-band" function is complex and represents measure of time-frequency correlation of signal, or expresses the degree of similarity between the signal and its shifted version in time-frequency plane. In essence it represents the time-frequency autocorrelation function.

Kernel function $\psi(\theta,\tau)$ at the same time unambiguously determines the features of given transformation and in this way also determines the suitability of particular transformations for particular applications. It should be remarked that the kernel function of the Margenau-Hill transformation has got the form

$$\psi(\theta,\tau)=\cos\left(\frac{\theta\cdot\tau}{2}\right). \quad (4)$$

Multiplication of $A_x(\theta,\tau).\psi(\theta,\tau)$ is also known under the name characteristic function. Because function $A_x(\theta,\tau)$ represents a bilinear operation on the processed signal and calculating the contributions arising from the above-mentioned cross-components which, in turn, deteriorate the resolution of the given transformation. This effect can be reduced by a suitable choice of kernel function. The kernel function then explicitly determines the properties of the transformation. In practice, the coefficients of the transformation from Cohen's class for discrete signals may be calculated by fast two-dimensional discrete Fourier transformation of the characteristic function $A_x(n,k).\psi(n,k)$.

To remove disturbing interference contributions (if their existence may significantly affect the analysis) their smoothed („pseudo") version can also be defined by application of window function according to equation [1 and 3]

$$PMHT(t,f)=\int_{-\infty}^{\infty}\frac{h(\tau)}{2}\cdot\begin{bmatrix}x(t+\tau)\cdot x(t)^*+\\ x(t)\cdot x^*(t-\tau)\end{bmatrix}\cdot e^{-j.\omega.\tau}\cdot d\tau, \quad (5)$$

where function $h(\tau)$ represents suitable window function, t time, τ the time transition, ω is angular frequency, $x(t)$ represents the time signal, symbol '*' represents the complex conjunction, j is imaginary unit, and $PMHT(t,f)$ is the time frequency representation of the signal.

The spectrograms are gained by the representation of the calculated values of Margenaau-Hill transformation or of the amplitude time-frequency spectrum in the graph. These spectrograms can also be represented in the three-dimensional space (frequency, time, amplitude or the spectral output density etc.). Alternatively, a two-dimensional representation by means of density spectrograms is also used in which an amplitude or a value of the spectral function of a certain shade is added to. When analysing some complex signals, it is appropriate to supplement the time frequency representation of spectrum with possible frequency and time sections. Then, these sections offer a distinctive graphic support in the analysis of the results of the time frequency analysis.

3. Case study

The next part of this paper describes the application of Margenau Hill transformation on the railway engineering issue. The maintenance and its cost minimization is one of the most discussed problems of the railway track nowadays. That is the reason why it is necessary to pay attention to diagnostics of the railway tracks and to assess steps which will lead to cost minimization. The effective diagnostic tools include analysis of the dynamic effects acting on the railway superstructure during train passing [4].

This is related mainly to the parts of aborted continuity and the parts where stiffness of the single-phase railway is changed as these are the parts where the advanced dynamic effects occur. As a result an uneven ballast settlement, gravel crushing and defects on the running surface occur. The common crossings are constructions with interrupted running surface; as a consequence they belong to the most stressed parts of the railway transport corridor from the point of view of dynamic effects. Their correct function and on-time maintenance have the principal impact on the safety of railway traffic. The most stressed point of crossing construction is the frog part consisting of wing rails and crossing nose followed by crossing rails (Fig. 1).

The most important place of this part from the point of view of dynamic effects is the area of transmission from the wing rail to the crossing nose where the dynamic impact occurs. This impact is transmitted through the sleeper to the ballast which is thereby extremely stressed; which leads to grinding of ballast under the sleeper. As a consequence there is a degradation of the ballast shape and following weak support of the crossing. If the crossing is not supported enough, the geometry of the transmission from the wing rail to crossing nose collapses and the whole process of degradation continues very fast. That is the reason why it is necessary to pay extra attention to these parts of the railway track.

The measurement and the evaluation of the dynamic effects acting on the common crossings introduce the issue which has not been complexly solved in the Czech Republic yet. Therefore, the team of authors has compiled a comprehensive methodology of the measurement and evaluation of the dynamic effects acting on the crossings. This methodology (as Fig. 1 shows) consists of three parts. The measurement of moving behaviour is included in the first part. The measurement of moving behaviour represents the analysis of the shifts of particular parts of the crossing (vertical displacement of the sleeper under the crossing part and mainly the vertical shifts along the crossing part) under the load. For this the induction sensors are used. The second part of the methodology consists of measurement of vibrations spreading around the crossing part and especially the effects of vibrations on the ballast. The third part involves the measurement of the loading of rail. A part of the methodology is also the application of time-frequency analysis of the measured data.

Fig. 1 General view of a frog including distributed sensors

The most important part of the methodology is devoted to the analysis of transmission of vibrations from the rail through the sleeper to the ballast caused by running wheelset of the railway vehicle. For measurement of parameters characterizing the dynamic effects the piezoelectric vibration acceleration sensors were used. The sensors are placed in such a manner that it's possible to follow up spread of vibration energy through the whole system. Three-axis accelerometer placed on flange of the wing rail detects the magnitude of dynamic impact which is acting on crossing part (Fig. 2, sensor A4ZA5XA6Y). Vertical dynamic impact posed on crossing part is detected in vertical direction, or the part which is transmitted to flange of the wing rail. According to the condition of transmission geometry there is also a part of dynamic impact carried out in longitudinal direction. In transversal direction the wheelset is led by the check rail, so the side impact is very small. Nevertheless, it is interesting to monitor this branch from the perspective of the fluency of unit train passage through the crossing, therefore, it is also a part of the suggested methodology.

The other sensors are one-axis sensors and are placed on such positions to best detect spreading of dynamic impact from the rail through the sleeper and into the ballast. Sensor A3Z is placed on the bearer nearest to the crossing nose and sensor A0Z is on the measure bar embedded to the ballast close to crossing nose.

The chosen crossings for measurement and analysis of dynamic effects were the fix common crossings of turnout number 59 (crossing inserted in 2009) and number 63 (crossing inserted in 2012) in station head of the railway station Chocen. The turnouts track systems are the same and both of them are a part of one common crossover. In addition to this, they are run by the same type of trains in trailing direction. These constructions were chosen with the aim to compare the dynamic effects in the crossing in various stages of wear.

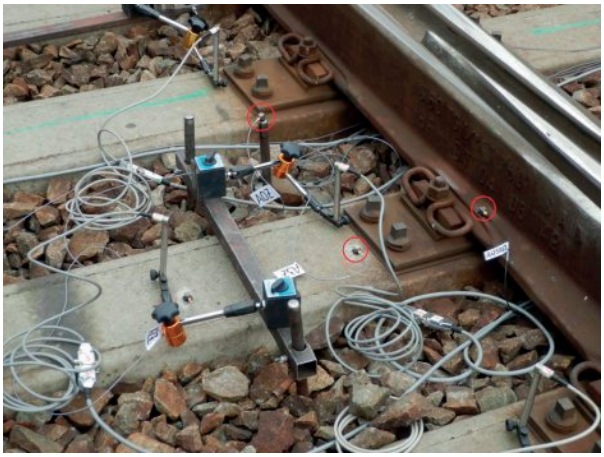

Fig. 2 Detail of a crossing part with vibration and shift sensors

For presentation of comparison of the dynamic loading on crossings the authors chose the unit train Pendolino with travel speed of 160 km/h^{-1}. Due to scope of this paper we will show only the evaluation from the sensor A3Z installed on the bearer under the crossing nose.

For the illustration of the analysis, figures which consist of a triplet of graphs were used. The upper graph represents time course of vibration acceleration. The left graph shows the amplitude spectrum of the vibration response calculated by

direct application of the Fourier transform on the measured signal. The middle graph is a 3D display of time-frequency amplitude spectrum of vibration response. The values of vibration acceleration in the decibel scale are shown in the middle graph as different colour areas while the maximum value is black.

Graphs in Fig. 3 represent analysis of passing of unit train Pendolino through turnout number 59 and graphs in Fig. 4 turnout number 63. Using the graphs of time courses (Figs. 3 and 4, the upper graph) we are able to find out that the maximal and minimal values of vibration acceleration measured on turnout No.59 are higher than values on turnout No.63. These parameters provide information about unroundness of wheels, defective or overloaded axle or defect on the running surface of the rail. In our case they indicate a higher wear of the crossing nose of turnout 59 and thus also its worse transition geometry.

The left graph in Figs. 3 and 4 presents the amplitude spectrum of the vibration acceleration calculated from the measured signals by application of the Fourier transform. Amplitude spectra are presented in the frequency range of 1 Hz to 1000 Hz. It is also important to say that for dynamic loading of structural components of the railway superstructure are significant frequencies up to 600 Hz. From comparison of the both left graphs in Figs. 3 and 4 it is evident that vibration actions at the turnout No.59 occur in the wider frequency spectrum than at the turnout No.63. The crossing No.63 has its important components of the amplitude spectrum in frequency of up to 200 Hz while the crossing No.59 has significant frequency components in up to 600 Hz, divided into more significant frequency clusters. This fact reflects the more complicated vibrational actions in the transition area of this crossing and also their higher energy. Within the analysis a decibel scale in the range 200-240 dB with a threshold value $1e^{-6}$ m/s^{-2}was used.

To evaluate the vibration acceleration in the time-frequency area density spectrograms calculated by Margenau-Hill transformation were used (Figs. 3 and 4, the middle graph). Extreme values of vibration amplitude spectrum are shown in the graph in the form of red areas corresponding to the time intervals of wheel (wheelset) passing over the sensors. Both middle graphs in Figs. 3 and 4 show that the time occurrences of significant frequency components in the spectrum are different from each other. It is, therefore, well possible to identify at which moment there was an action (which wheel or axle caused it) and which frequency components correspond to this action. Time-frequency analysis therefore very well and accurately complements the conclusions derived from the time and frequency analysis.

4. Conclusion

The permanent pressure on increasing the transport speed and the operational loading of tracks causes a magnificent development of new technologies in the railway traffic. The development and the application of new experimental procedures for the evaluation of the quality and usefulness of particular structural solutions must be in accordance with this trend.

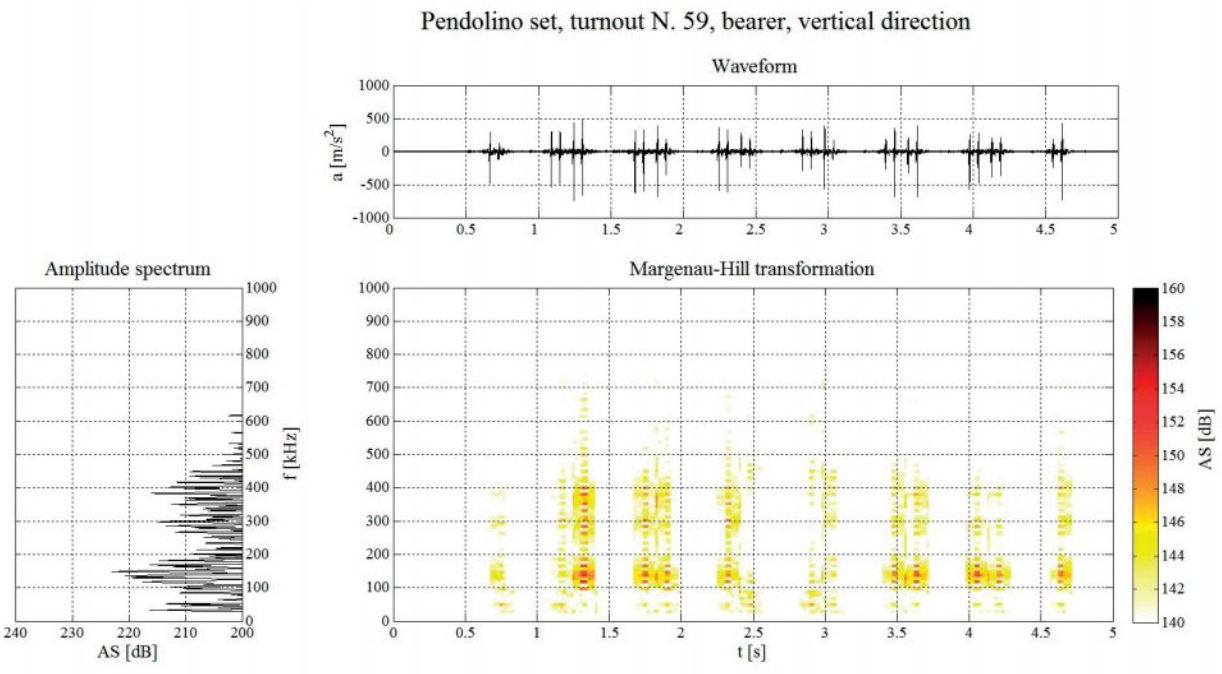

Fig. 3 Time history of acceleration, amplitude spectrum and jointed time-frequency spectrum in vertical direction for turnout No. 59

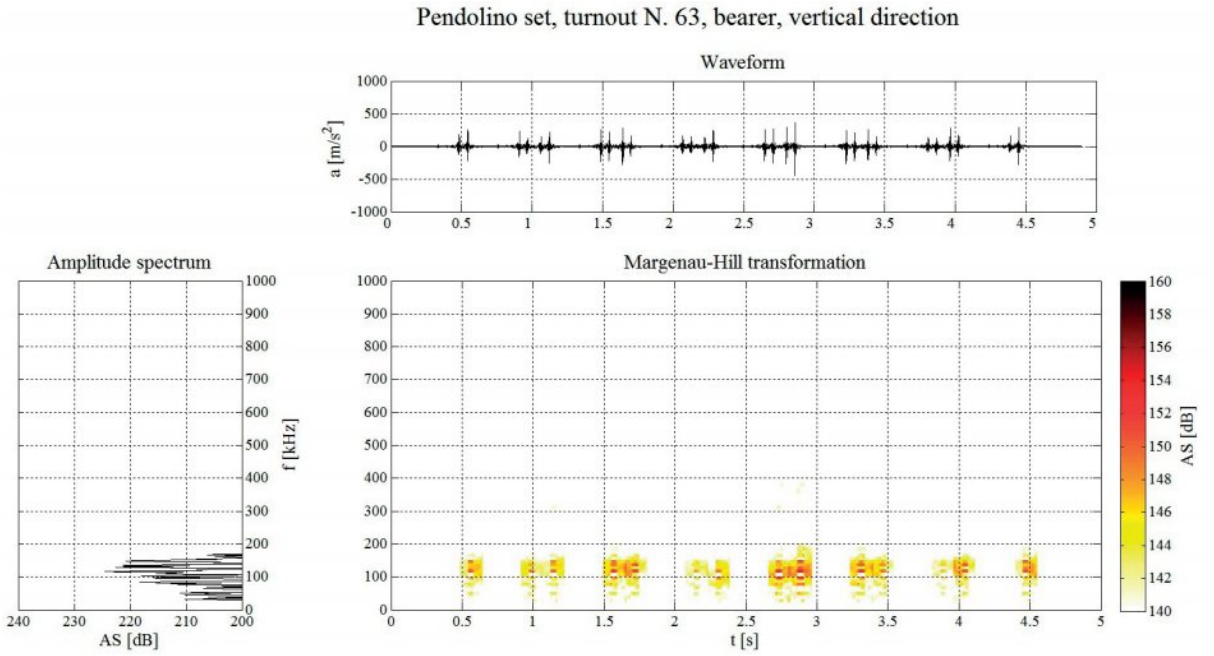

Fig. 4 Time history of acceleration, amplitude spectrum and jointed time-frequency spectrum in vertical direction for turnout No. 63

Especially methods of time-frequency analyses comparing to other methods distinguish information about the given technical activity so that they determine the time localization of frequency components, i.e. they determine the size of amplitude spectra on individual frequencies in respective time moment. It is, therefore, possible to state that the measurement and analysis of technical signals with the use of time-frequency methods provides mainly a new view to transition and non-stationary characteristics of measured structures.

Based upon the analyses made it is possible to say that the used methods offer good results and conclusions. The measured and calculated values prove to be sufficiently accurate and have testing capabilities. In conclusion, it should be stated that modern means of the time and frequency signal analyses (especially then Margenau-Hill transformation), perfectly contributed to the high-quality processing of the data measured.

Generally, characteristic feature of presented non-linear transformations (including Margenau-Hill transformation) is the fact that their resulting resolution in time and frequency is not limited by Heisenberg principle of indefiniteness. This fact includes the high resolution ability in time-frequency level, which results in "precise" localization of important frequency components in time. The elaboration and generalization of the theory of non-linear time-frequency transformations contributed and will contribute to formation of further procedures with more advantageous properties.

Acknowledgments

This article was supported by the project FAST-S-14-2452, "The study of dynamic effect taking place in the switches by Margenau-Hill distribution".

References

[1] POULARIKAS, A. D.: *The Transform and Applications Handbook*, IEEE Press, 1996.

[2] SMUTNY, *J.: Measurement and Analysis of Dynamic and Acoustic Parameters of Rail Fastening,* NDT & E International - Independent Nondestructive Testing and Evaluation, ISSN 0963-8695, Elsevier, 2004.

[3] SMUTNY, J.; PAZDERA, L.: Jointed Time and Frequency Transforms in Testing Material Defects, *Engineering Mechanics*, ISSN 1802-1484, Engineering Academy : Brno, 2007.

[4] MORAVCIK, M.: Analysis of Vehicle Bogie Effects on Track Structure-nonstationary Analysis of Dynamic Response, *Communications - Scientific Letters of the University of Zilina*, vol. 13, No. 3, 2011, ISSN 1335-4205.

Peter Dorcak - Frantisek Pollak - Martin Mudrik - Ludovit Nastisin *

SLOVAK VIRTUAL MARKET IN THE LIGHT OF ANALYSIS OF POSSIBILITIES OF DETECTING ON-LINE REPUTATION FOR SELECTED SUBJECTS

The main aim of this article is to analyze the theoretical possibilities of detecting an On-Line reputation of selected subjects functioning on Slovak virtual market. The purpose of article is also to present selected method of measuring on-line reputation of selected subjects based on newest knowledge in the field of managerial sciences. For purposes of this article, subjects are represented by on-line presence of Slovak towns in a virtual market place. In particular, cultural and anthropological context, and the resulting specificities and peculiarities typical of the post-communist block of countries will be taken into account in relation to the chosen market. The target group is narrowed to 20 biggest Slovak towns as the best representation of subjects which officially presented themselves to internet users on the specific type of market.

Keywords: *Reputation, On-Line reputation, SME, Market, Entrepreneurship, Competition, Image, Internet, Social Networks, Virtual Social Networks.*

1. Introduction

The issue of the use of internet tools in marketing is in itself still very young. However, we may definitely conclude that any new techniques and media used within the portfolio of marketing tools can help distinguish an entity from the competition [1]. The competition is huge for both commercial and non-commercial entities. Times when the „only" thing necessary for market prosperity was a quality product are long gone [2]. It is becoming increasingly difficult to reach the target audience. Overcapacity of advertising messages on the market is a problem the marketing managers worldwide must deal with on a daily basis [3]. Regardless of the resources and effort it is often the case that the advertising message disappears, or simply ceases to exist in the context of other more or less important information of various kinds. An appropriate solution in marketing practice is especially reduction of communication paths through the use of the internet and its tools. The internet offers us the possibility of a clear and precise message targeting of selected market, often to the individuals themselves. It also significantly reduces the communication path when the entities are allowed to communicate directly with their customers. Customers, in this case internet users, demand themselves the information, thereby significantly increasing the rate of adoption of communicated message. Thanks to its nature the internet allows for easy sharing and transfer of information and creates space for entities whose motives may not always be ethical [4]. The issue of reputation is therefore highly relevant issue in the context of virtual identity of entities using the internet to communicate. Undoubtedly, companies with a high reputation have at present a competitive advantage in terms of customer acquisition [5]. It has been shown that 80 % of customers prefer the company with a high reputation rather than an average company or a company with a dubious reputation. In Slovakia, this area has been examined to some extent in relation to banking entities [6]. Such factors have been analyzed as value, quality of products or social activities of companies. Subsequently, it has been examined how these factors are perceived and evaluated by the consumers, customers, business partners, the public and so on.

2. The issue of reputation in the times of the internet and modern technology

New technologies, forms of communication, as well as the internet itself, are on the one hand positive aspects of this age but, on the other hand, they entail a risk. Dissemination of negative information, rumors or false information through these media is very quick and uncontrollable. Based on the above arguments a study has been carried out in Washington [7], which has examined the relationship of reputation management and current social media. A similar survey regarding online communication

* [1]Peter Dorcak, [2]Frantisek Pollak, [2]Martin Mudrik, [2]Ludovit Nastisin
[1]Goethe UNI, Bratislava, Slovakia
[2]Department of Marketing and International Trade, Faculty of Management, University of Presov, Slovakia
E-mail: peter@dorcak.com

has been conducted at the University of Singapore [8] and it has provided a clear view of the relationship between these poles. In the context of scientific literature focusing on e-marketing, specifically on the field of online reputation, conceptual or rather empirical studies are available in limited quantities. The claim in question is referred to by the author [9] who states that despite the lack of analyses many authors believe that reputation is much more important in online than in offline context because factors determining trust in offline context are absent and are not yet known [10]. Reference [11] defines online social media as open interactive online applications which support the development of informal user networks. Users create and share various contents in these networks, such as personal experience, opinions, videos, music and photos. The most important online social media include online social networks, blogs, forums and other online communities. However, this division is somehow problematic because, in practice, the media overlap.

In our territory, we can currently see an enormous increase in the use of social media services. A good example is the largest social network in the world, Facebook, which is with its more than 500 million registered and more than 50% of daily active users successful also in Slovakia. 1.5 million registered people in Slovakia prove it. The age group which is most represented are the users aged between 18 and 24 years (32 %), followed by a group aged between 25 and 34 years (29%) [12]. The importance of social media has been indicated in the works of foreign scientists and scientific teams published in the Journal of Marketing Research, under the auspices of the American Marketing Association - AMA. Their research has been in particular focused on the perception of the value of social networks by consumers [13], the analysis of marketing strategies and social media [14], the potential of social networks for the development of e-business [15], the impact of social networks on consumer decisions [16]. Virtual social networks are currently the focus of several authors. From all of these authors we may mention Robert Cross and Robert Thomas who in their writings explore the perception of the value of social networks by consumers [17]. American professor Wehr, for example, has been working on the analysis of marketing strategies of social media for three years.

2.1 Reputation and the possibility of its measurement, various methodologies used in determining reputation

Worldwide research in the area of reputation which has been conducted at the University of Oxford [18] shows that reputation is made up of two elements: customer opinion of the respective company and the real truth about the company and its commercial policy, procedures, management system and financial performance. Other research shows that reputation may be responsible for 8 to 15% of the value of company shares in business sector. Authors [19] concluded that a company has a good reputation if it always meets or exceeds the expectations of its customers and vice versa, a company has a bad reputation if it does not meet these expectations. Consequently, they proposed the following formula for reputation: Reputation = experience - expectations. At any moment, customers measure reputation by comparing current experience in contrast to their expectations [20]. This formula for the evaluation of reputation can be complemented by the trust evaluation model presented by [21] in 2005. They claim that Trust = 0.5* Reputation + 0.5* Cooperation.

Particularly important is the process of identification of the most important factors that determine the reputation of a company. Fombrun prepared a methodology to measure the perception of the company through the prism of its major shareholders. He introduced 20 factors that affect reputation based on 6 criteria [22]. These factors include, for example, emotional factors, products and services, vision and leadership or social responsibility of the company. Some of the most complex structures of reputation factors are specified by Turner. Not only he defines eight main reputation factors, but for each of them he also provides sources of information that affect them. In addition, these factors may be divided into rational and emotional [23]. It should be noted that the above factors may help to improve the company's reputation but, at the same time, they may also severely worsen it. Their initial identification is a very important point in building the reputation of management in the company. It's a long, time consuming process, and actual results are only achieved from a long-term perspective. That is why it is appropriate to use the research and experience of the company which analyse the impact of individual factors on the level of reputation.

In 2006, an interesting study was carried out by [24] entitled "Protection of reputation". The study included 950 managers and directors representing companies from 11 countries. The results were divided into four regions: World, North America, Europe and Asia. The most important factors that are able to destroy reputation identified by the executives include: financial fraud, unethical behaviour, illegal data collection, irresponsibility towards environment and violations of safety and health regulations.

3. Analysis of reputation of selected entities on Slovak virtual market

Managing a virtual reputation, or in other words, On-line Reputation Management (ORM) is neither new nor unknown term in Slovakia. ORM has been applied in many industries such as banking or insurance. The results of these surveys have provided a realistic and current view on the virtual presentation of organization as well as the image of their virtual identities.

The level of positive on-line reputation is not only a source of information for the organizations themselves, but also an important factor influencing decision-making of consumers.

For the purpose of this analysis the online reputation of twenty largest Slovak towns as the best representatives of entities officially presenting themselves directly to target customers and internet users in the environment of specific virtual market was established by a selected methodology. The used methodology is called „sentiment analysis" [25]. The presented methodology can be subsequently used for the purposes of the on-line reputation survey of the various entities, for example SME´s, public institutions, or even individuals using the internet for personal branding. The sequence of the process of measuring reputation begins with defining the representatives of investigated segment, in this case, chosen specific Slovak towns. Consequently, virtual identity of these entities is investigated by means of Google search. When analyzing sentiment, the first 10 search results are taken into consideration. To ensure the objectivity of results, which may be distorted by the tendency of search engines to personalize the search based on the history of the internet activity,

Sentiment of results / position of results [25] Table 1

Sentiment/Position of the result	1	2	3	4	5	6	7	8	9	10
Positive sentiment +	20	19	18	17	16	15	14	13	12	11
Own Website of the town X	10	9	8	7	6	5	4	3	2	1
Neutral sentiment ±	2	2	2	2	2	2	2	2	2	2
Negative sentiment -	-20	-19	-18	-17	-16	-15	-14	-13	-12	-11

Overall rating of sentiments of twenty largest Slovak towns [own elaboration according to 25] Table 2

Town / Sentiment result position	1	2	3	4	5	6	7	8	9	10	Result
Komarno	x	x	±	+	±	+	±	x	±	+	**73**
Bardejov	x	±	+	+	±	x	±	+	±	x	**72**
Nitra	x	±	±	+	+	+	±	±	±	±	**70**
Michalovce	x	x	x	±	±	±	+	+	±	±	**64**
Kosice	x	+	±	±	±	+	+	±	±	±	**60**
Martin	x	±	±	±	+	+	±	±	±	±	**55**
Trencin	x	±	±	±	+	±	+	±	±	±	**54**
Poprad	x	±	+	±	±	±	±	±	+	±	**54**
Prievidza	x	±	±	±	+	±	±	±	±	±	**42**
Spisska Nova Ves	x	±	±	±	+	±	±	±	±	±	**42**
Zvolen	x	±	±	±	±	+	±	±	±	±	**41**
Bratislava	x	±	±	±	±	±	+	±	±	±	**40**
Presov	x	±	±	±	±	±	+	±	±	±	**40**
Levice	x	x	±	±	±	±	±	±	±	±	**35**
Nove Zamky	x	±	±	±	x	±	±	±	±	±	**32**
Humenne	x	±	±	±	x	±	±	±	±	±	**32**
Zilina	x	±	±	±	±	±	±	±	±	±	**28**
Banska Bystrica	x	±	±	±	±	±	±	±	±	±	**28**
Trnava	x	±	±	±	±	±	±	±	±	±	**28**
Povazska Bystrica	x	±	-	±	±	±	±	-	±	±	**-7**

Note: In determining the sentiment the numbers of positive reviews on social networks were not taken into account. Only the fact that the town owns a profile on any of the virtual social networks was taken into account. The nature of the town descriptions on the Wikipedia portal was also not taken into account. Only the fact that Wikipedia mentions the town was taken into account. In both cases, these results were assigned neutral sentiment. If the search engine found, besides an official town's web site, web pages of entities associated with such town on other places in a search, these results were assigned neutral sentiments. If the town's web site occurred in several places within the search, only the first occurrence was taken into account, where the following occurrences of town's web site were assigned neutral character.

proxy anonymizers were used to ensure the greatest possible relevance of the findings. Only organic results were included in the survey. The search phrase was always a well-known and well established town name, regardless of the homepage. One of the main factors in the evaluation process is the sentiment of results. It may be broadly defined as a nature of found results after entering key words. The results may include positive, neutral, as well as negative feedback. These sentiments, as well as the position in which they appear, provide a picture of researched entity, and thus ultimately determine its online reputation. Sentiment of individual results in Top 10 is shown in the table below with a brief commentary. At the same time, each position is assigned a score based on the sentiment according to the following Table 1.

The table shows chronological sequence of awarding points to the analyzed entities. Positive response or sentiment results in the increase of the score. The higher the position of this sentiment in the search result, the more points are awarded. Similarly, but with the opposite effect, it works in identifying the negative sentiment. Points are deducted, the higher the position of the display, the bigger the deduction of points, and this significantly deteriorates the reputation. Next, individual sentiments are counted as a part of the overall evaluation and the resulting number indicates the strength of the sentiment of all ten search results for the town / entity. The resulting number of sentiments stands for the overall level (power) of the online reputation. The entities are then listed for comparison in ascending order based on their overall level of online reputation in a virtual environment of the Slovak internet. Table 2 of the overall evaluation of sentiments of twenty largest Slovak towns (and, therefore, the overall level of their online reputation) looks as follows.

4. Evaluation of the analysis and discussion

The above analysis of virtual identity of researched entities – twenty biggest Slovak towns – clearly shows that the first search results are dominated by the towns'own websites or the websites managed by the towns. Search results of neutral sentiment formed the largest group of sentiments. Only one entity showed negative sentiment, and even two negative sentiments, on the third and the eighth place in the search results (town of Povazska Bystrica had a negative evaluation due to the transport infrastructure of the city). In respect to virtual reputation among internet users, entities in the leading positions have an advantage as their complex virtual identity is perceived more positively.

In case the user is searching for information on a particular town and comes across some negative references, it may ultimately affect his/her overall perception of the destination. Especially if the user is a tourist who personally never visited the town or the area and forms his/her view strictly on the basis of the information from the virtual environment. The same applies to potential investors. Towns should therefore make sure that the necessary information available to potential visitors is as clear as possible. It is in their interest to eliminate negative publicity (and enhance positive publicity), at least in the first ten search results. This can be achieved by active internet communication policy, i.e. spreading positive information on renowned internet portals, such as electronic forms of major Slovak newspapers or virtual social networks. The best way to eliminate negative or neutral publicity in the first ten search results is literally a displacement of such publicity by active work (for example, by means of a coherent marketing communication policy) on the internet. As mentioned above, the presented methodology is one of many methodologies used for the determination and measurement of online reputation. However, the complexity of this methodology, its transparency and the fact that it is less time consuming, makes it ideal for identifying online reputation of different entities, such as SMEs, public institutions and even individuals using the internet for their personal branding.

5. Conclusion

In today´s post-industrial society, power elites come to the fore through the use of new technologies. There is a general willingness when applying marketing tools to build quality and strong brand and its presentation for wider area. It does not matter whether it is a city or town, product, service, or organization. This study pointed out the importance of reputation in the online world that can harm the brand or damage its image within a millisecond when searching information on the internet. For the purpose of this paper a ranking of levels of online reputation for biggest Slovak cities was processed and it showed great differences. The result of the perception of reputation, on the basis of this paper, may be correct and targeted communication, which is part of the marketing mix. Positive reputation, especially in the online environment of immediate decisions is often a critical factor in the realization of customer products purchase, city or town visit, or ordering service. In addition to a long built positive image it is therefore important to regularly verify the level of reputation and eliminate negative news.

Acknowledgement

This article is one of the partial outputs of the current research grant VEGA No. 1/0145/14 entitled "Online Reputation Management (ORM) as a Tool to Increase Competitiveness of Slovak SMEs and its Utilization in Conditions of Central European Virtual Market".

References

[1] ZGODAVOVA, K. BOBER, P.: An Innovative Approach to the Integrated Management System Development: SIMPRO-IMS Web Based Environment. *Quality Innovation Prosperity*, vol. 16, No. 2, 59-70, 2012.

[2] BACIK, R.: *Increase of the Competitiveness of Small and Medium Businesses in Presov with the Assistance of Specific Marketing Instrumentation.* Management 2008, 181-190. ISBN 978-80-8068-849-3.

[3] SOVIAR, J.: Simplification of Marketing Scheme for Business Start-Ups. *Communications - Scientific Letters of the University of Zilina*, vol. 13, No. 4, 2011, 55-57. ISSN 1335-4205.

[4] SOVIAR, J., VODAK, J.: Value Network as Part of New Trends in Communication. *Communications - Scientific Letters of the University of Zilina*, vol. 14, No. 2, 2012. ISSN 1335-4205.

[5] HORVAT, M., MICHALKOVA. A.: Monitoring Customer Satisfaction in Service Industry: A Cluster Analysis Approach. *Quality Innovation Prosperity*, vol. 16, No. 1, 49-54, 2012.

[6] RAJZAK, P. et al.: *System for Evaluation of Online Reputation of Banks (in Slovak)*. Faculty of Electrical Engineering and Informatics of the Technical University of Kosice, 652-657, 2010. ISBN 978-80-553-0460-1.

[7] MADDEN, M., SMITH, A.: *Reputation Management and Social Media*. [online]. [cit. 2013-03-03]. Available on the internet: <http://www.pewinternet.org/Reports/2010/ Reputation-Management/Summary-of-Findings.aspx>.

[8] ZHIGI, S. et al.: *A Survey of Trust and Reputation Management Systems in Wireless Communications*. University Singapore, 1755-1772, 2010. ISSN 0018-9219.

[9] ARGRYIOU, E., KITCHEN, P. J., MELEWAR, T. C.: The Relationship between Corporate Websites and Brand Equity: A Conceptual Framework and Research Agenda. *Intern. J. of Market Research*, vol. 48, No. 5, 559-575, 2006.

[10] LAJCIN, D., FRANKOVSKY, M., STEFKO, R.: Possibilities of Predicting the Behavior of Managers When Coping with Demanding Situations in Managerial Work. *Ekonomicky casopis,* vol. 60, No. 8, 835-853, 2012. ISSN 0013-3035.

[11] KRALICEK, J.: *The Position of Consumer in Relationship Containing and International Element.* Masarykova Univerzita, 2011, [online]. [cit. 2013-03-05]. Available on the internet: <http://is.muni.cz/th/170265/?lang=en>.

[12] SOCIALBAKERS.COM. *Slovakia Facebook Statistics.* [online]. [cit. 2013-03-04]. Available on the internet: <http://www.socialbakers.com/facebook-statistics/slovakia>.

[13] STEPHEN, A.T., TOUBIA, O.: Deriving Value from Social Commerce Networks, *J. of Marketing Research*, 2010, 215-228, ISSN 0022-2437.

[14] WEHR, L.: *An Eye Tracking Analysis on Social Networking Sites.* [online]. [cit. 2013-03-09]. Available on the internet: <http://www.ergophile.com/wp-content/uploads/2009/08/oneupweb_ eye_tracking_study_ 2009.pdf>.

[15] ZEISSER, M.: *Unlocking the Exclusive Potential of Social Networks*. [online]. [cit. 2013-02-25]. Available on the internet: <http://www.mckinseyquarterly.com/ Unlocking_the_elusive_ potential _of_social_networks_2623>.

[16] BULMER, D., DIMAURO, V.: *The New Symbiosis of Professional Networks: Social Media's Impact on Business and Decision-Making.* Palo Alto : Society for New Communications Research, 2010, 32 pp. ISBN 978-0982700402.

[17] CROSS, R. L., THOMAS, J.: *Driving Results through Social Networks: How Top Organizations Leverage Networks for Performance and Growth.* Hoboken : John Wiley & Sons, 2009, p. 240, ISBN 978-0470481189.

[18] SCHULZ, H. B., WERNER, A.: *Reputation Management, Human Resources Management.* [online]. [cit. 2013-02-19]. Available on the internet: <http://www.oxford.co.za/download_ files/cws/Reputation.pdf>.

[19] LUISOM, J. P., RAYNER, J., GAULTIER-GAILLARD, S.: *Managing Risks in Reputation - From Theory to Practice, Reputation Capital.* Springer-Verlag : Berlin : Heidelberg, 2009

[20] DELINA, R.: Trust Building Electronic Services as Crucial Self-Regulation Feature of Digital Business Ecosystems. *IDIMT 2011: Schriftenreihe Informatik*, vol. 36, 315-327, 2011.

[21] LAVARAC, N., LJUBIC, P., JERMOL, M., BOLHALTER, S.: *A Decision Support Approach to Trust Modeling in Networked Organizations, Collaborative Networks and Breeding Environments.* Norwell : Camarinha-Matos L. M. (ed.), the Kluwer Academic Publishers - Springer, 2005, p. 170.

[22] FOMBRUN, C. J., VEIL VAN, C. B. M.: *How Successful Companies Build Winning Reputations.* New Jersey : FT Press, 2003

[23] TURNER, M.: Reputation, Risks and Governance. *Effective Risk and Business Management Topic Paper,* No. 6, The Housing Corporation, 2004, p. 3.

[24] SHANDWICK, W., KRC, R.: *Safeguarding Reputation.* [online]. [cit. 2013-02-27]. Available on the internet: <http://www.reputationrx.com/>.

[25] ROHAL, R., SASKO, J.: *Sentiment Analysis of Results of Slovak Companies (in Slovak)*. [online]. cit. 2013-03-10]. Available on the internet: <http://www.reputation.sk/ whitepapers/Analyza_sentimentu_reputation_sk.pdf>.

Milan Mikolas - Jana Bartonova - Jana Magnuskova - Dagmar Letavkova *

PRICE OF ELECTRICITY VS DIFFERENT HEATING TECHNOLOGIES IN CZECH REPUBLIC

This paper analyses both individual components of the price of electricity and the electricity rates as related to individual modes of heating. The price development has been monitored and assessed since July 1, 2001, i.e. the date on which the 'Price Decree of the Energy Regulation Office, No. 5/2001' entered into force concerning introduction of new rates and prices of electricity for households and businesses. Primarily, the rate, D 02d, was chosen for assessment. This rate is used by the majority of households as they use gas or solid fuels for heating. Further, the rate, D45 d, for direct electric heating, and rates, D55 d and D 56 d, for heating by thermal pumps were also subject of assessment. Both the development trends and the comparison of the investigated rates of electricity make it obvious that prices of electricity will continue to be rising in the long-term perspective.

Keywords: *Electricity market, price of electricity, electricity rate.*

1. Introduction

The current economic situation implies ever increasing need to take into account savings concerning all aspects of human existence. No doubt, one of the substantial things we cannot ignore in our lives is keeping appropriate temperatures of our homes. Due to climatic conditions we live in, household heating must be provided for periods often in excess of eight months yearly.

After the revolution of 1989, there was a new kind of boom concerning alternatives of household heating away from traditional ways of ensuring comfortable temperature conditions in our homes. The environmental protection priorities of the nineties of the past century made it essential to concentrate on wider use of environment friendlier household heating technologies, which meant using natural gas and electricity, the latter either directly or by ways of accumulation heaters.

The electric heating belongs among the most comfortable ways of home heating plan implementation from the point of view of the usage, readiness, service and maintenance, but also as regards aspects of environmental protection. It is readily accessible anywhere where there has been electric power of sufficient wattage installed. But due to steep rise in prices of electricity, usage of electric heaters represents the most expensive ways of providing comfortable home temperatures. Away from this advantageous mode of heating, as it was the case of the nineties of the last century, the electricity, because of the continuing rises in its prices, has become the most expensive option of ensuring household or home comfortable temperature. Nevertheless, it should be highlighted that costs of direct or accumulation electricity usage in contrast to using electrically powered heat pumps differ to the advantage of the latter.

The objective of this paper has been to provide a review of the components which the electric energy price consists of, as implication of electric energy market liberalisation, and then to analyse development trends of some electric power rates as related to specific heater usage.

2. Electric energy market liberalisation

The *Energeticky regulacni urad* (Energy Regulatory Office) was established on January 1, 2001 as decreed by the Act No. 458/2000, Coll. Its principal role has consisted in regulating energy prices; supporting utilisation of renewable and secondary energy sources and combined heat and power generation; protecting customers and consumers' interests; protecting licence holders' vested interests; leading inquiries into conditions for competition; co-operating with the Office for the Protection of Competition (*UOHS*); supporting competition of energy industries; and providing supervision of energy markets.

On January 1, 2002 started the process of the electric energy market liberalisation in the Czech Republic. In practical terms, the former 'protected consumers of electricity' have transformed

* [1]Milan Mikolas, [2]Jana Bartonova, [2]Jana Magnuskova, [2]Dagmar Letavkova
[1]Institute of Mining Engineering and Safety, Faculty of Mining and Geology, VSB - TU Ostrava, Czech Republic
[2]Institute of Economics and Control Systems, Faculty of Mining and Geology, VSB - TU Ostrava, Czech Republic
E-mail: milan.mikolas@vsb.cz

into 'rightful consumers' for whom electric energy prices are no longer subject of annual decrees of the Energy Regulatory Office and who have the right to choose electricity suppliers of their own. These rightful electric power consumers have only part of their final electricity prices regulated [1].

The electric energy market was liberalised in stages concerning specific categories of consumers:

- Since Jan. 1, 2002 – End-users consuming more than 40 GWh,
- Since Jan. 1, 2003 – End-users consuming more than 9 GWh;
- Since Jan. 1, 2004 – All end-users who have their consumption continually measured apart from households,
- Since Jan. 1, 2005 – All end-users apart from households,
- Since Jan. 1, 2006 - All end-users inclusive households [1].

3. Electricity price structure

The liberal market price of electricity basically consists of two components: delivery and production.

The former component is regulated as electric energy transmission and distribution providers are natural monopolies. The latter component of electricity production per se is determined by the producers themselves and is subject of negotiation between producers and their customers. This component is not regulated by the Energy Regulatory Office. The two-component structure of the electricity reflects situation of the electric power free market. [2]

Table 1 specifies items that electricity final prices comprise, inclusive electric power taxes and VAT.

To the regulated items of the price of the electric power delivered belong [3]:

a) *Distribution costs:* Payments of distribution services are divided into floating and fixed constituents. The floating constituent concerns electric energy delivery volumes, CZK/MWh, and covers costs of distribution network losses that are directly proportional to the volumes of electric energy transferred, i.e. delivered. The fixed constituent (a monthly fee relative to the voltage class of the main circuit breaker) concerns fixed costs of the distribution provider who guarantees continuing deliveries of electricity in the quality defined. For example, the costs cover maintenance and renewal of electricity distribution networks, measurement costs, back readings, etc.

b) *System service costs:* These cover all allowable expenses of the distribution provider, *ČEPS a.s.* The company, apart from the distribution of the high voltage electricity, also regulates production and consumption within the distribution network so that production is in direct proportion to specific consumption. Some of the services are out-sourced. These costs also embody transmission and distribution losses, as well as network maintenance and development expenses.

c) Costs of additional expenses related to support of renewable source electricity production, combined heat and power generation, and secondary resources: Costs of renewable and non-traditional electric energy generation are generally higher than those of thermal and nuclear power stations. All end-users participate in covering these additional costs (i.e. difference between the electricity price subsidised by *OZE, KVET* and *DZ*, and the average market price) in the form of a regulated contribution. The support of renewable and non-traditional energy generation has been assisted by the Act No. 180/2005 Coll. on Support of Renewable Resources, and the Act No. 458/2000 Coll., on Entrepreneurial Activities and Public Administration in the Field of Energy Industries, and some Energy Act Amendments.

d) Market operator costs: They cover services of the company, *OTE a.s*. This company provides balances concerning supply and demand of electric power, differences between the planned and realised deliveries, as well as balances of long-term electricity consumption in the Czech Republic. All end-users participate in paying these costs.

The amount of the regulated payments is decreed annually by the Energy Regulatory Office that takes into account wishes of the subjects involved.

End-user electricity price structure — Table 1

Regulated Items	Electricity Distribution	Wattage Fee
		Price per volume of distributed electricity
	Concurrent services	System services
		Accountant service provider fee
		Electricity sale support by *OZE, KVET*, and *DZ*
Non-regulated items	Electricenergy delivery	Fixed fee
		Price for delivered electricity volume
Taxes	Electricity tax	
	VAT	

Among the non-regulated constituents of the price of electricity are:

a) *F*ixed fee for the specific circuit breaker installed.
b) P*rice of electricity deliveries.*

The non-regulated constituents of the electricity price are determined by individual providers who are oriented by market principles. The price of electric power derives from the price of the energy stock exchange.

The last constituent of the electricity price are taxes:

a) Electricity tax rates the amount of electric power consumed. Since 2008, the electricity price also includes a new, so called ecological tax that is incumbent on the members of the European Union. The electrical power provider pays the tax, as a total for all his customers, to the Duty Office. The rate, 28.30 CZK/MWh, is universal for all consumers. The provider does not collect this tax if the electric energy delivered has been from renewable sources.
b) The value added tax (VAT) rates the sum of all the price constituents mentioned. Until December 31, 1997, the VAT had been 5%. On 1st of January, 1998, it increased to 22%, which then decreased to 19% on May 1, 2005. On 1st of January, 2006, the electricity VAT increased again and since then the rate has been 20%.

The individual constituent percentages, as related to household consumption of electric energy, are illustrated by Fig. 1. The ratios given are without taxes and VAT.

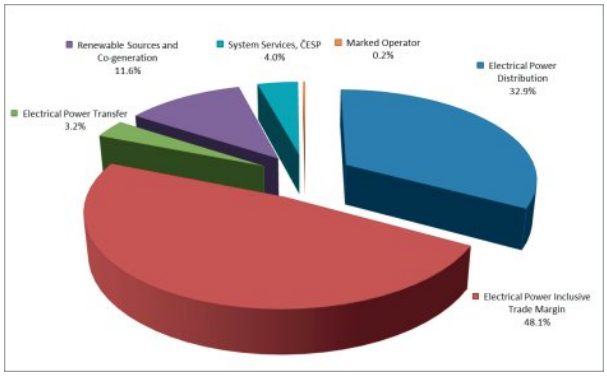

Fig. 1 Price constituent percentages as regards household electricity consumption in 2012 [4]

4. Electric energy rates

The electric energy rate depends on the consumption and utilisation of the electric power by household end-users. Usually, it is a fixed rate as specified by the mode of the heating utilised. The rate is designated by a symbol, *D-rate number-d*, for example, *D 02d*. Currently, nine rates are valid for the households.

The households that do not use electric power for heating of the rooms and water but only utilise it for lighting and running of electric appliances (refrigerators, wash-machines, washers, microwave ovens, computers, etc.) usually have a single tariff rate, *D 02d*, which is valid all day through for one kW per hour. The overall majority of household fall within this standard class.

If a household end-user uses electric power for heating, it is of advantage to negotiate a double tariff rate, *NT-VT*. The *NT* means a low tariff rate, the latter a higher one as they depend on the specific hour interval of the day. The low tariff rate interval is decided by the electricity provider in respect of the Energy Regulatory Office decrees.

Concerning the household heating, this paper has focused on these double-tariff rates:

- Low tariff rate of the operative interval, *D 45d*, for households that use electricity for direct running of electric heaters of rooms and water. The rate is valid for minimum of 20 hours daily. [5]
- Low tariff rate of the operative intervals, *D 55d* and *D 56d*, for households that run a thermal pump heating appliance which had been put into operation until 31. 3. 2005 (rate, *D 55d*) or until 1. 4. 2005 (rate, *D 56d*). The rate is valid for minimum of 22 hours daily [6].

The double-tariff options are of advantage if electric energy savings are taken into account.

5. Development of electric energy prices

The decisions and decrees of the Energy Regulatory Office and the price lists of some suppliers provided the input data for assessing development trends of electric energy [7]. For comparison's sake, in view of the fact that there are very many suppliers of electric power, the suppliers were chosen according to the criterion of their specific distribution area, namely *E.ON Energie, a.s.* (the former *JCE*, *JME*), *Prazska energetika, a.s.*, and *CEZ Prodej, s.r.o.* (the former *SCE, SME, STE, VCE, ZCE*) because they offer distribution services for three areas. The major part of the Czech Republic is being supplied by the *CEZ Distribuce*, the South of the country is served by *E.ON Distribuce*, and Prague by *PREdistribuce*, see Fig. 2.

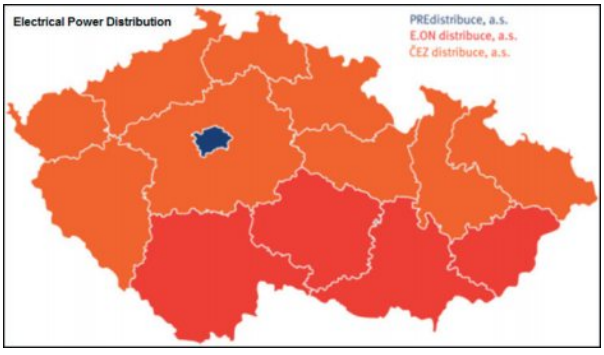

Fig. 2 Survey of distribution areas [8]

This paper investigation started in July 2001 as on 1st of July, 2001 new rates and prices of electric energy for households and entrepreneurs were decided by the Energy Regulatory Office (*Cenove rozhodnuti ERU c. 5/2001*). As noted above, the price of electricity for households depends on the heating technology utilised. That is why the rate, *D 02d,* (used by the majority of households that use solid fuels or natural gas for heating), the rate, D45d, (specific for direct electric heater usage), and rates, *D55d* and *D 56d*, (specific for thermal pump heater usage), were taken into account so that to asses development trends of prices of electricity. A common type of the circuit breaker for households, 3x25 A, was considered when comparing development trends of fixed fees.

Figure 3 illustrates the price development of the single tariff rate, *D 02d* which applies to the majority of households in the Czech Republic. Until 2006 a more or less steady development can be seen. It is also obvious from this figure that prices started to rise steeply after the liberalization of the electric power market on 1st of January, 2006, in an effort to adjust prices of electric energy in the Czech Republic to those of the European Union, which concerned all end-users inclusive households. After 2009, this trend of steady increase was interrupted by the world economic recession. In future years, the anticipated economic revival will most probably restore the former, maybe less steeply rising trend than it had been the case for the period, 2006-2009.

Fig. 3 Rate, D 02d - Price development, CZK/MWh

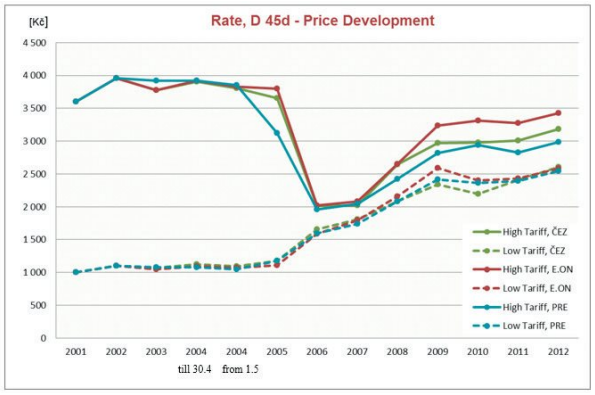

Fig. 4 Rate, D 45d - Price development

The development of the double-tariff rate, *D 45d,* is illustrated by Fig. 4. Before the electric energy market liberalization in 2006, the low-tariff prices were increasing slightly, and the high-tariff prices slightly decreased. After 2006, ale electric energy prices started to rise steeply. The electricity producers, in greedy quest for ever increasing profit, ingeniously increased the low-tariff prices as this tariff applies to the rate, *D 45d* that the households use for a 20hour minimum daily. In contrast to this, the high-tariff, whose operational maximum is 4 hours per day, increased in 2006 but it has started to be rising again since 2007. Both the tariff increases abated due to the world economic recession, and the low-tariff prices even slightly decreased in 2010. Currently, further rise of both tariffs has been noted.

Figure 5 informs on another double-tariff rate, *D 55d*. This rate applies to the majority of households that utilize thermal pump for heating; the equipment which had been put in operation until March 31, 2006. In comparison to the foregoing rate, *D 45d*, for direct electric heater usage, *D 55d* differs in the limits of time when low- or high-tariff rate applies. For the rate, *D 55d*, the low-tariff minimum limit is 22 hours per day. In the past few years if costs of 1 MWH are considered, the differences between the rates D *55d* and D *45d* have been rather small in amount. The principal difference between these two rates consists in lower fixed fee as related to usage of the specific circuit breaker where the costs of *D 55d* application are half of those when *D 45d* is applied - see Table 2.

Fig. 5 Rate, D 55d - Price development, CZK/MWh

Fig 6 Rate, D 56d - Price development

Fixed fee development for circuit breaker, 3x25 A, CEZ Comp., figures mean CZK Table 2

Rate	2001	2002	2003	2004 until 30.4.	2004 since 1.5.	2005	2006	2007	2008	2009	2010	2011	2012
D 45d	438	498	482	502	490	490	269	281	351	374	390	408	420
D 55d	178	215	211	217	211	232	95	113	119	148	157	167	179

Since April 1, 2005, a double-tariff rate, *D 56d*, has been applied for thermal pump usage as decreed by the Energy Regulatory Office. The development of this rate is illustrated by the Fig. 6. Step by step, the price level of the rate, *D 55d*, for thermal pumps put into operation until March 31, 2005, is approaching the level of the rate, *D 56d*. Currently, there is no difference between consumption at low- or high-tariff rates but the fees for specific circuit breakers only. The reason for the introduction of the two rates was in the effort to minimise impact of the electricity market liberalization on consumers who opted for usage of thermal pumps whose usage was promoted and strongly supported then. The rate, *D 56d*, is a clear signal for the electric energy market which way the price levels of distribution rates for thermal pumps will be taking in future [8].

To make the arrangement of Fig. 7 clear, price development for rates, D 55d and 56d, are given only for the company, *CEZ*, at which point, the 1 MWh prices of low- and high-tariff rates have been identical since 2009. The figure also illustrates the fixed fee payments for the circuit breaker, 3x25 A as they represent the only difference between the rates, *D 55d* and *D 56d*.

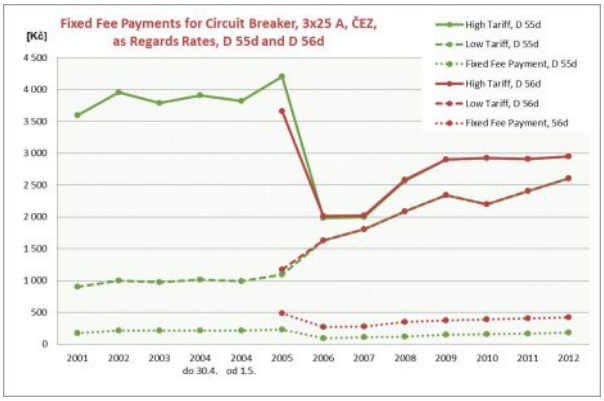

Fig. 7 Rates, D 55d and D 56d, CZK per 1 MWh and monthly fees for circuit breaker 3x25 A in CZK

Figure 8 provides details of fixed fee payment as regards the circuit breaker, 3x25 A, and the rates, *D55 d* and *D56 d,* concerning all supplier companies investigated. Since 2007, there has been a trend of increasing fixed fee payments. Only in 2012, the companies, *E.ON* and *Prazska energetika* slightly lowered their circuit breaker fees. The company, *CEZ*, has been constantly increasing the fixed fees of their circuit breakers.

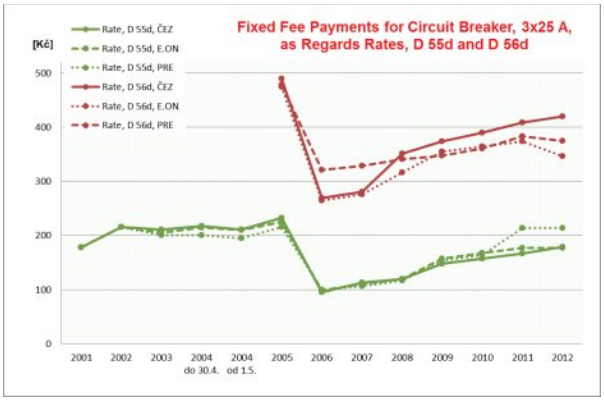

Fig. 8 Fixed fee payments for circuit breaker, 3x25 A, in CZK as regards rates, D 55d and D 56d

6. Conclusion

It has been within the scope of this paper to provide assessment of electric energy price developments vis-à-vis usage of different household heating technologies since 2002 when new rates were introduced. The focus has been only on those rates that concern heating by solid fuels, natural gas, and electricity. For the electricity, more detailed investigations have been performed, namely concerning alternatives of using direct electric heaters or thermal pumps. The investigation results can attest to the fact that electric market liberalisation started the trend of soaring prices for all rates investigated. The Energy Regulatory Office has substantiated this steep rise in electric energy prices as implication of the rising electric energy prices on the European market, and the necessity of increasing efforts to support utilisation of renewable energy sources. In 2010, the electric power prices slightly decreased due to economic recession. The household started to economise, and the firms, because of the economic slump, needed less electric energy, which meant that the total electricity consumption went down. It might have been presumed that prices would be decreasing fast because of the market mechanism of supply and demand. Nevertheless, in our country, there is practically no competition as regards distribution of electric power and, consequently, the prices of electricity distribution rose again in 2010. What´s more, also the VAT increased from 19% to 20%, and the contribution to the support of alternative energy resources tripled in contrast to 2009

[9]. Since 2011, the electricity prices have been steadily rising but the increase has been less steep than it was the case of the past period, 2006-2009. The presented Figs. 3 - 8 make the long-term development trends obvious. Stagnation or even decrease of electric power prices can hardly be anticipated.

References

[1] Eru.cz.: *Electrical Energy Prices and Conditions Related (in Czech).* [online]. [30-8-2012]. Available on internet: http://www.eru.cz/dias-read_article.php?articleId=172#1, 2010.

[2] Eru.cz .: *Economic and Activity Report (in Czech).* [online]. [27-9-2012]. Available on internet: http://www.eru.cz/user_data/files/vyrocka06.pdf , 2006.

[3] Eru.cz .: *How to Read an Electrical Energy Invoice).* [online]. [20-8-2012]. Available on internet: http://www.eru.cz/dias-read_article.php?articleId=172#4, 2012.

[4] Eru.cz.: *Press Release Concerning Regulated Electrical Price Decrees (in Czech).* [online]. [20-10-2012]. Available on internet: http://eru.cz/user_data/files/tiskove%20zpravy/2011/TZelektro22%2011%202011.pdf , 2011.

[5] Cenyenergie.cz.: *Direct Electrical Heaters (in Czech).* [online]. [18-10-2012]. Available on internet: http://www.cenyenergie.cz/elektrina/clanky/d45d-primotop-a-ohrev-vody-elektrinou.aspx, 2010.

[6] Cenyenergie.cz.: *Thermal Pump Rate (in Czech).* [online]. [18-10-2012]. Available on internet: http://www.cenyenergie.cz/elektrina/clanky/d55d-a-d56d-sazba-pro-tepelne-cerpadlo.aspx, 2010.

[7] Tzb/info.cz.: *Price Lists of Electrical Energy as Valid From 1. 1. 2012 (in Czech).* [online]. [1-10-2012]. Available on internet: http://www.tzb-info.cz/prehled-cen-elektricke-energie, 2011.

[8] BLAZICEK, J.: *Electrical Prices in 2011 (in Czech).* [online]. [30-10-2012]. Available on internet: http://www.tzb-info.cz/ceny-paliv-a-energii/7131-ceny-elektriny-na-rok-2011, 2011.

[9] BECHNIK, B.: *Support Renewable Sources and Electrical Prices (in Czech).* [online]. [02-11-2012]. Available on internet: http://www.tzb-info.cz/ceny-paliv-a-energii/6184-podpora-obnovitelnych-zdroju-a-cena-elektriny, 2010.

COMMUNICATIONS – Scientific Letters of the University of Zilina
Writer's Guidelines

1. Submitted papers must be unpublished and must not be currently under review for any other publication.
2. Submitted manuscripts should not exceed 8 pages including figures and graphs (in Microsoft WORD – format A4, Times Roman size 12, page margins 2.5 cm).
3. Manuscripts written in good English must include abstract and keywords also written in English. The abstract should not exceed 10 lines.
4. Submission should be sent: By e-mail – as an attachment – to one of the following addresses: komunikacie@uniza.sk or holesa@uniza.sk (or on CD to the following address: Zilinska univerzita, OVaV – Komunikacie, Univerzitna 1, SK-10 26 Zilina, Slovakia).
5. Uncommon abbreviations must be defined the first time they are used in the text.
6. Figures, graphs and diagrams, if not processed in Microsoft WORD, must be sent in electronic form (as JPG, GIF, TIF, TTF or BMP files) or drawn in high contrast on white paper. Photographs for publication must be either contrastive or on a slide.
7. The numbered reference citation within text should be enclosed in square brackets. The reference list should appear at the end of the article (in compliance with ISO 690).
8. The numbered references (in square brackets), figures, tables and graphs must be also included in text – in numerical order.
9. The author's exact mailing address, full names, E-mail address, telephone or fax number, the name and address of the organization and workplace (also written in English) must be enclosed.
10. The editorial board will assess the submitted paper in its following session. If the manuscript is accepted for publication, it will be sent to peer review and language correction. After reviewing and incorporating the editor's comments, the final draft (before printing) will be sent to authors for final review and minor adjustments
11. Submission deadlines are: September 30, December 31, March 31 and June 30.

Errata: Communications – Scientific Letters of the Zilina, No. 3, 2014, "The System of Transitivity in the War on Terror Discourse", pp. 46-51. The proper wording of paragraph 7 on p. 49 should be formulated as follows:

In the clauses within which enemies are presented, the speaker employs "a number of words" which "have affective connotations" and most of these words have "negative evaluations of the activity to which they refer. Therefore, the negative evaluation" [16] can be observed in clauses with Material processes such as "kill", "violate", as they are usually negatively perceived in "most contexts. Thus the actors" in the clauses are "evaluated negatively in the processes that they perform" [16].

References:

[16] MATU, P.: Transitivity as a Tool for Ideological Analysis. *J. of Third World Studies*, vol. 25, No. 1, 2008, p. 199. 10.

COMMUNICATIONS

SCIENTIFIC LETTERS OF THE UNIVERSITY OF ZILINA
VOLUME 16

Address of the editorial office:
Zilinská univerzita
Office for Science and Research
(OVaV)
Univerzitna 1
SK 010 26 Zilina
Slovakia

E-mail: komunikacie@uniza.sk

Each paper was reviewed by two reviewers.

Journal is excerpted in Compendex and Scopus.

It is published by the University of Zilina in
EDIS – Publishing Institution of Zilina University
Registered No: EV 3672/09
ISSN 1335-4205

Published quarterly

Single issues of the journal can be found on:
http://www.uniza.sk/komunikacie

ICO 00397 563
December 2014